Axonal mRNA localisation and the development of peripheral sensitisation *in vitro*

Asta Arendt-Tranholm, BSc

School of Pharmacy

University of Nottingham

June 2022

Thesis submitted to the University of Nottingham for the degree of Doctor of Philosophy

Abstract

Sensory neuronal cells of the dorsal root ganglia (DRG) are highly polarised cells, which receive and relay noxious signals from the periphery to the spinal cord. These sensory neuronal cells are capable of remarkable plasticity to adapt to the local environment and external stimuli. During periods of inflammation and in chronic pain states, the nociceptors are sensitised and consequently activated by lower thresholds of stimuli, in addition to firing of action potentials at a higher frequency. Multiple mechanisms have been shown to contribute to these events, including inflammatory mediators such as prostaglandin E_2 (PGE_2), which has been shown to be crucial in inducing a sensitised state. The neuroplasticity of sensory neurons is likely mediated by local regulation of translation which drives changes to the local proteome and neuronal function. *In vitro* studies have characterised a distinct neurite transcriptome unique to that of the cell body of the sensory neuronal cell. Changes to the local transcriptome, and local translation regulation in the axon, are hypothesised to facilitate quick adaptation in the periphery of sensory neuronal cells. The aim of this thesis was to characterise the local axonal transcriptome and to assess the changes in the axonal transcriptome in a PGE_2-induced model of sensitisation of DRG-neurones.

Embryonic (16.5) DRG-cells were exposed to 24-hours (H) 10µM PGE_2, to create an *in vitro* model of sensitisation of peripheral nociceptors. The PGE_2-protocol induced a significant increase in excitability to subsequent exposure to capsaicin, measured as calcium (Ca^{2+}) transients, compared to vehicle-treated control DRG-cells. Additionally, the PGE_2-protocol resulted in significantly higher expression of *Ngf* mRNA in the cell body, compared to control DRG-cells. The model was successfully replicated with adult (8WO) DRG cells, with an adjusted protocol of exposure to PGE_2 for 12H. The data demonstrated a suitable *in vitro* model of sensitisation had been established.

Porous membrane chambers were used to allow the separate extraction of RNA from the cell body or the axons of PGE_2-exposed and control DRG-cells. This RNA

was used for sequencing (RNAseq) to explore potential changes in the axonal transcriptome induced by PGE_2. Comparison of the axonal transcriptome revealed considerable overlap in expression patterns between the control DRG-cells from embryonic and adult mice. Pathways associated with local translation, such as eIF2- and oxidative phosphorylation-signalling, characterised the axonal transcriptome of control E16.5 and 8WO DRG-cells. These results provide evidence for a compartmentalised transcriptome playing a key role in the functional adaptation of DRG-cells, possibly through local regulation of translation. The PGE_2-sensitisation protocol induced significant changes to the local axonal transcriptome of DRG-cells from both embryonic and adult mice. Pathways previously associated with hyperalgesic priming of sensory neuronal cells, including IL-6- and cyclic AMP (cAMP)-mediated signalling, were identified as characteristic of the axonal transcriptome following PGE_2-sensitisation. Overall, 23 RNAs were significantly increased in the axon following PGE_2-sensitisation for both embryonic and adult mice.

Bioinformatic analysis of the axonal transcriptome identified 3 RNAs, *Arid5a*, *Cebpb*, and *Tnfrsf12a*, associated with the sensitisation by PGE_2 and predicted as potential localised therapeutic targets. *Arid5a*, AT-rich interactive domain-containing protein 5a, is an RNA-binding protein which has been identified to play a role in stabilising mRNAs associated with an inflammatory response through NF-κB and CREB. *Cebpb,* the transcription factor C/EBPβ, has been linked to the development of sensitisation in the central nervous system through cAMP-signalling and increased expression of nociceptive channels including the capsaicin receptor, transient receptor potential cation channel subfamily V member 1 (TRPV1). *Tnfrsf12a* mRNA encodes the tumour necrosis-like weak inducer of apoptosis (TWEAK) receptor, also known as Fibroblast growth factor inducible 14 (Fn14), associated with neurite regeneration following axotomy through NF-κB pathway activation. In the final study, the identified RNAs were knocked down in E16.5 DRG-cells with 24H siRNA treatment prior to induction of the model of PGE_2 sensitisation. Knockdown of *Tnfrsf12a* RNA prevented PGE_2-induced hyperexcitability to capsaicin. While

underpowered, knockdown of *Arid5a* also reduced the PGE_2-induced sensitisation of the capsaicin response.

The results presented in this thesis characterise the similarities and differences in the axonal transcriptome of DRG-cells from embryonic and adult mice. The identified changes in the axonal transcriptome of nociceptors in the model of sensitisation, and the subsequent knockdown of specific RNAs successfully reducing excitability, support the further investigation of the local transcriptome and translation regulation for the development of novel analgesics.

Acknowledgements

I feel incredibly fortunate to have so many people to acknowledge and thank for their support throughout my PhD.

First, I want to express my sincerest gratitude to my supervisors. My primary supervisor Dr Cornelia de Moor has been a bottomless source of encouragement and guidance both academically and personally. Dr Federico Dajas-Bailador has supervised with patience and understanding. Professor Victoria Chapman has supported and guided me from undergrad, through this PhD and onwards, and provided me with incredible scientific opportunities for me to pursue and grow to take on. I am endlessly thankful to my supervisors for believing in me enough to push me to become a better researcher.

I owe great thanks to many previous and current members of the CdM group and the whole GRRB lab, but especially Dr Sadaf Ashraf and Steven Lawrence, both of whom were particularly supportive and helpful in and outside of the lab. I am thankful to members of the FDB group who have taught and assisted me, particularly Dr Alice Rockliffe. I am similarly grateful to members of the VC group at the Versus Arthritis Pain Centre, particularly Dr Li Li. Additionally, I would like to thank Professor Theodore Price for allowing me to visit and train at his facilities at the University of Texas at Dallas, as well as Dr Pradipta Ray for significant help with the bioinformatic analysis of RNAseq data.

My deepest gratitude is to my family and friends. My family, particularly my parents Mikael and Christel, Sten, and my brother Osvald, as well as my friends, specifically Yiota, Ann-Katrine and Carmen, have always provided endless support, encouragement, and motivation. Particular thanks go to the people who helped me with office-spaces when writing required additional motivation.

Finally, I would like to acknowledge and thank Versus Arthritis for funding this research (Grant reference: 21586). I have been proud to work on this project with them as a sponsor.

List of Figures

List of Tables

Table of Contents

Chapter 1: General Introduction

1.1 Defining pain

Pain is an essential biological warning mechanism, existing to protect the body from physical injury, however, the corruption of the mechanism can induce detrimental abnormal pain sensation. It is estimated that up to 10% of the global population suffers from prolonged abnormal pain sensations characterised as chronic pain (Scholz et al., 2019; van Hecke et al., 2014). The majority of patients experience suboptimal relief from the currently available treatments.

1.1.1 Pain with or without a purpose

The International Association for the Study of Pain (IASP) has defined 3 characteristic types of pain according to the physical presentation and genesis: nociceptive pain, inflammatory pain, and neuropathic pain ('Classification of Chronic Pain, Second Edition (Revised)', 2011). Nociceptive pain is the essential protective mechanism. Acute inflammation following injury or lesion is associated with inflammatory pain, and characterises increased activation of pain pathways for the specific purpose of protecting the site of injury during healing (R.-R. Ji et al., 2016; Yam et al., 2018). Nociceptive and acute inflammatory pain are contrasted with chronic inflammation and neuropathic pain. Chronic inflammation is associated with pathologies such as arthritis, while neuropathic pain is associated with damage or trauma to the nervous system either by lesion or disease (Colloca et al., 2017). While distinct differences characterise chronic pain as either inflammatory or neuropathic pain depending on the genesis, they are found to share common mechanisms of modulating pain pathways (Q. Xu & Yaksh, 2011).

1.2 The somatosensory nervous system

The somatosensory nervous system detects tactile sensation of the physical environment through pressure and temperature, as well as pain. As illustrated in Figure 1.1, the somatosensory system detects stimuli which are relayed via the peripheral nervous system (PNS) to the spinal cord and then to the brain.

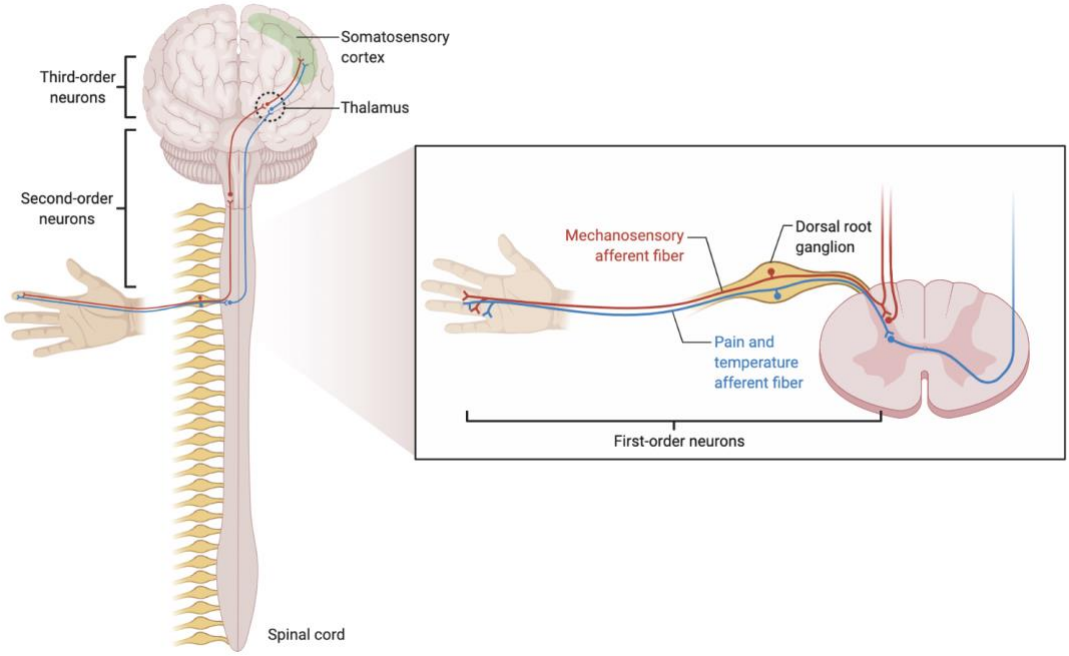

Figure 1.1: *Somatosensory nervous system pathways from peripheral input to central processing. Adapted from "Somatosensory Afferents Convey Information from Periphery to Central Circuits", by BioRender.com (2022). Retrieved from https://app.biorender.com/biorender-templates*

1.2.1 Signalling of sensory neuronal cells

Signals of neuronal cells are transmitted as action potentials along axons in nerve fibres. An action potential is a transient reversal of the polarity of the membrane potential of neuronal cells, initiated through stimulus capable of raising the polarity to a minimum threshold that induces a chain reaction causing the temporary permeability of the cell to select ions including Na^+ and K^+ (Barnett & Larkman, 2007). An action potential is initiated by electrical, temperature, chemical or mechanical stimulation and it is commonly characterised through 3 distinct phases: depolarisation, repolarisation and hyperpolarisation (Figure 1.2) (Barnett & Larkman, 2007; Raghavan et al., 2019).

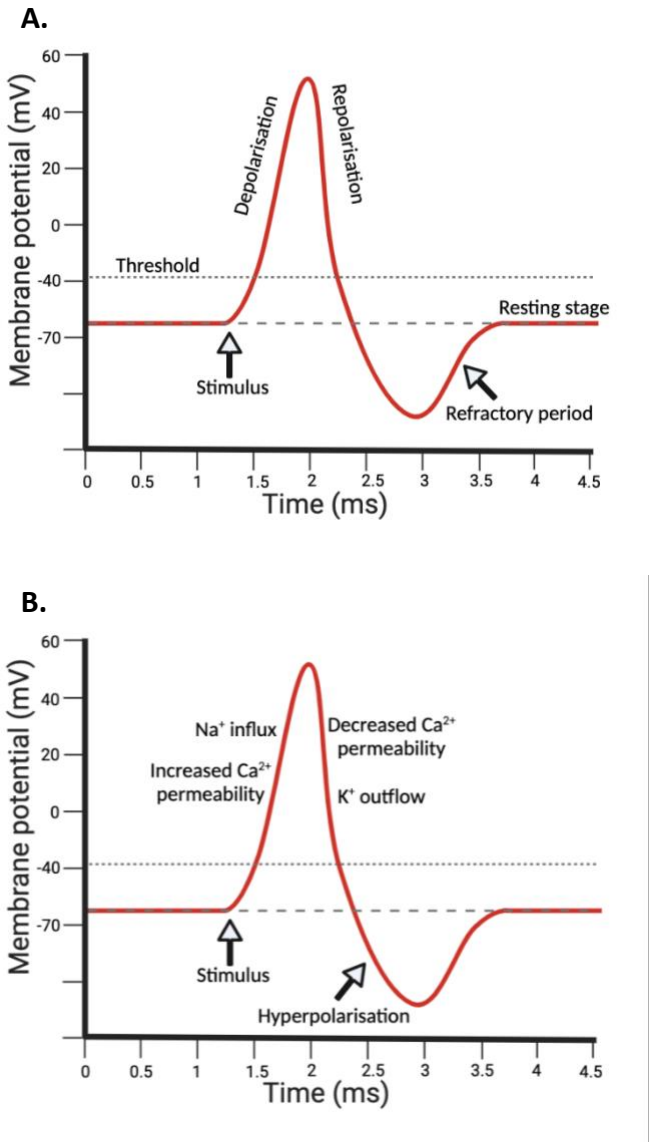

Figure 1.2: *The fluctuations of the membrane potential throughout an action potential are defined by the movement of ions across the membrane. Figure adapted from (Bahar et al., 2016) created in BioRender.* ***A.*** *The stages of an action potential following exposure to a stimulus.* ***B.*** *The ion movements driving the changes to the membrane potential identified on the membrane potential trace*

An initial stimulus causes the membrane potential to rise to the threshold which triggers the opening of sodium (Na^+) and calcium (Ca^{2+}) channels, causing an influx of Na^+ into the cell driving depolarisation (Barnett & Larkman, 2007; Bean, 2007). Depolarisation facilitates increased permeability of the membrane to Ca^{2+} along with a release of Ca^{2+} from intracellular stores in the endoplasmic reticulum (ER) (Bahar et al., 2016; Bean, 2007). The depolarisation phase is terminated due to

spontaneous inactivation of the Na^+ channels and opening of K^+ channels (Bahar et al., 2016; Tsantoulas & McMahon, 2014). During the repolarisation phase K^+ rapidly exits the cells. K^+ channels start to close upon reaching an electrical threshold, however the K^+ are slow to close, thus an undershoot occurs manifesting as hyperpolarisation. Hyperpolarisation is resolved through the inward current I_h, which serves to return the membrane potential to the resting stage and allow subsequent action potential initiation (Momin et al., 2008; Momin & McNaughton, 2009).

Signals are transmitted from the free nerve endings of first-order sensory neuronal cells in the periphery. Peripheral nerves terminate in the dorsal horn of the spinal cord, synapsing on both interneurons and projection neurones. The spinal cord is divided into 10 cytoarchitectonic layers, the Rexed laminae (Rexed, 1952). Nociceptive first-order neurons primarily terminate in the upper superficial laminae (I and II) or in lamina V (Bourne et al., 2014). Second-order neurons are divided into nociceptive-specific (NS) which selectively transmit noxious stimulus from the upper laminae, or wide-dynamic-range (WDR) neurons in lamina V, which respond to both noxious and innocuous stimuli (G. I. Lee & Neumeister, 2020). The second-order neurons transmit the signal via the spinothalamic tract to the thalamus where somatosensory information is primarily processed (Finnerup et al., 2021; G. I. Lee & Neumeister, 2020). The central nociceptive pathways are beyond the scope of this thesis, however, the following reviews are recommended for further information (Bourne et al., 2014; Heinricher and Fields, 2013; Kuner & Kuner, 2021; Yam et al., 2018).

1.3 Cellular anatomy of the peripheral sensory nervous system

The peripheral nervous system (PNS) is broadly characterised as consisting of neuronal cell bodies grouped in ganglia, and nerve fibres consisting of axons encapsulated in myelin sheaths and connective tissue (Catala & Kubis, 2013; Goldstein, 2001). The sensory neuronal cells of the PNS, which relay messages of innocuous and noxious tactile sensation, are supported by non-neuronal cells within the periphery including immune cells (macrophages and T-lymphocytes) and

glial cells (Schwann cells and satellite glial cells) as well as fibroblasts, which play crucial roles in the stabilisation of neuronal cells, as well as the transmission of sensory signals (Bhatheja & Field, 2006; R.-R. Ji et al., 2016; Scholz & Woolf, 2007; Shinotsuka & Denk, 2022).

First-order sensory neuronal cells are pseudo-unipolar cells, where the cell body (the soma) is located in a dorsal root ganglion (DRG). A single axon extends from the soma and divides into two branches, one extending toward the periphery, and the other into the dorsal horn of the spinal cord. The DRG are bilateral structures situated at every vertebrae adjacent to the spinal cord (Esposito et al., 2019; Sleigh et al., 2016). Humans possess 31 pairs of DRG, while mice contain 30 or 31 pairs of DRG depending on the genetic variant. DRGs are characterised according to their level along the spinal column, divided into cervical, thoracic, lumbar, or sacral (Haberberger et al., 2019; Sleigh et al., 2016) (Figure 1.3). A majority of the research on DRG-cells have been carried out in mice, as the availability of viable human tissues and broadly accessible experimental techniques has been limited until very recently (Haberberger et al., 2019; Nguyen et al., 2021; Ray et al., 2021). The research discussed should therefore be assumed to be applicable to mice, unless otherwise stated.

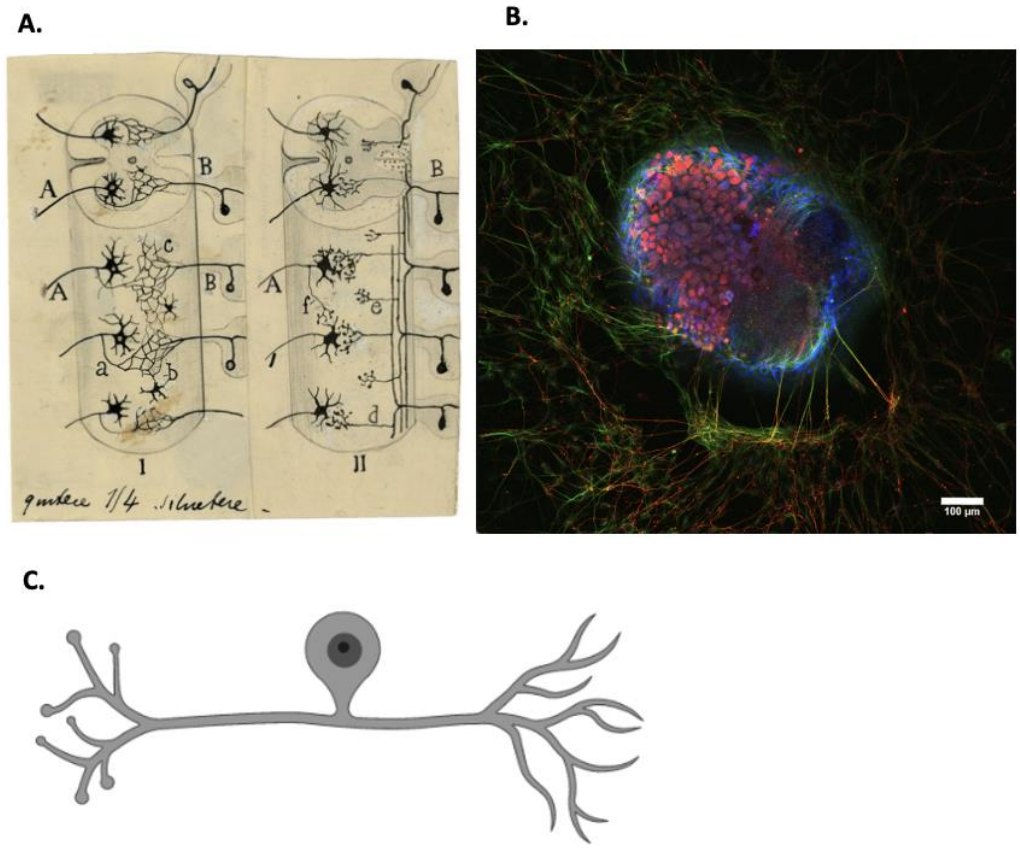

Figure 1.3: *Characterisation of neuronal cells of the DRG.* ***A:*** *A drawing of the spinal cord with DRGs clearly illustrated by Cajal, 1917, originally from Recuerdos de mi vida-Historia de mi labor cientı´fica ("Recollections of my life—The story of my scientific work"), published by (DeFelipe, 2013).* ***B:*** *A DRG-explant stained to visualise the neurites (anti-β-Tubulin in green and anti-peripherin in red) and cell bodies (nuclei stained with Hoechst stain in blue), through immunofluorescence, published by (Fornaro et al., 2018).* ***C.*** *Illustration of a pseudo-unipolar sensory neuron, the primary neuronal type of the DRG, with one axonal branch extending to the periphery and another towards the spinal cord (Figure from Biorender.com)*

A heterogeneous population of neuronal and non-neuronal cells collectively function to mediate sensory and nociceptive signalling in the periphery. The peripheral sensory neuronal cells are similarly characterised as a heterogenous population of subtypes, facilitating the sensation of noxious input of different modalities.

1.3.1 Functional and structural characterisation of peripheral sensory neuronal cells

Peripheral sensory neuronal cells have been characterised according to the speed of transmission, the expression of select proteins, and the input stimulus inducing transmission.

Nerve fibre subtypes

Neuronal cell-types in the periphery are subdivided based on the nature of the nerve fibres, or the axonal branches, including the diameter and the myelination (Table 1.1).

	Aβ-fibre (A-beta)	**Aδ-fibre (A-delta)**	**C-fibre**
Myelinated	Yes	Yes	No
Diameter	6-12µm	1-5µm	0.02-1.5µm
Conduction speed	>20 m/s	2-10 m/s	<2 m/s
Thermal sensitivity	No	Yes/No	Yes/No
Function	Proprioceptor/ mechanoreceptor	Nociception/ Touch	Nociception/ Touch
Modality	Touch and pressure from skin	Mechano-thermal and touch from skin	Polymodal (mechanical, thermal, chemical)

Table 1.1: *Nerve fibre subtypes of the DRG. Table adapted from (G. I. Lee & Neumeister, 2020)*

A functional distinction is made by further dividing neurons into low-threshold mechanoreceptors (LTMR) and high-threshold mechanoreceptors (HTMR), the latter of which respond to noxious stimuli (Abraira & Ginty, 2013; Basbaum et al., 2009). Non-nociceptive cells of the somatosensory nervous system can broadly be characterised as LTMR cells. The majority of LTMR cells have Aβ- and Aδ-fibres with large-diameter axons which transmit signals quickly, however, Aα-fibres and unmyelinated C-LTMRs are also observed (Abraira & Ginty, 2013; L. Li et al., 2011; Meltzer et al., 2021). In contrast, the majority of HTMR cells, nociceptors, are unmyelinated C-fibre neurons, however, cell subtypes with Aδ- and Aβ-fibres

additionally fall within this categorisation (Djouhri & Lawson, 2004; Dubin & Patapoutian, 2010).

Aβ-fibre neurons: Aβ-fibres are large, myelinated fibres with fast conduction speed, which primarily transmit innocuous signals (Table 1.1). The existence of nociceptive Aβ-fibres has been a topic of controversy, however, research indicates that a small number of Aβ-fibres transmit noxious signals in nociceptive signalling, presenting with high heat thresholds and moderate pressure threshold (Crawford & Caterina, 2020; Djouhri & Lawson, 2004).

Aδ-fibre neurons: Aδ-fibres are medium-sized, myelinated fibres with moderate conduction speed, which transmit both innocuous and noxious signals (Table 1.1). Aδ-fibre cells have been further divided into 2: A-mechano-heat (AMH) Type I and Type II. AMH Type I is characterised by high heat threshold and lower mechanical threshold and additionally responds to lower heat threshold after prolonged stimulus, while AMH Type II presents with high mechanical threshold and lower heat threshold (Basbaum et al., 2009; Djouhri & Lawson, 2004). Furthermore, AMH Type I is insensitive to capsaicin, while AMH Type II is readily stimulated by capsaicin. Nonpeptidergic nociceptors with Aδ-fibres are specifically associated with cold temperature sensation (Crawford & Caterina, 2020).

C-fibre neurons: C-fibres are small-diameter, unmyelinated fibres, which primarily transmit noxious signals (Table 1.1). HTMR C-fibres respond solely to mechanical stimuli and are distinct from thermal-responsive C-fibre nociceptors (Abraira & Ginty, 2013). Thermal-responsive C-fibres are divided into peptidergic or non-peptidergic nociceptors (Abraira & Ginty, 2013; Basbaum et al., 2009). Peptidergic C-fibres innervate the basal regions of the epidermis and mediate temperature nociception, while nonpeptidergic C-fibres innervate superficial layers of the epidermis and transmit noxious cold sensation, as well as noxious mechanical stimuli (Abraira & Ginty, 2013; Cavanaugh et al., 2009; Crawford & Caterina, 2020).

1.3.2 Markers of peripheral sensory neuronal subtypes

Neuronal subtypes are preliminarily identified as peptidergic or nonpeptidergic. Peptidergic neurons express the neuropeptides calcitonin gene-related peptide

(CGRP, encoded by *Calca* mRNA) or substance P (SP, encoded by *Tac1* mRNA), along with broad expression of the NGF receptor TrkA (encoded by *Ntrk1* mRNA) (Abraira & Ginty, 2013; Basbaum et al., 2009; Cranfill & Luo, 2021). Nonpeptidergic neurons, despite the nomenclature, in some cases still express neuropeptides, however, they are primarily identified through isolectin B4 (IB4)-binding, as well as expression of the GDNF-receptor c-RET (encoded by *Ret* mRNA), the Mas-related G protein-coupled receptors (Mrg-family of GPCRs, encoded by *Mrgpr* mRNAs) and the purinergic ion-channel Piezo2 (encoded by mRNA of the same name) (Basbaum et al., 2009; Cranfill & Luo, 2021; M. Zhang et al., 2019) (Figure 1.4).

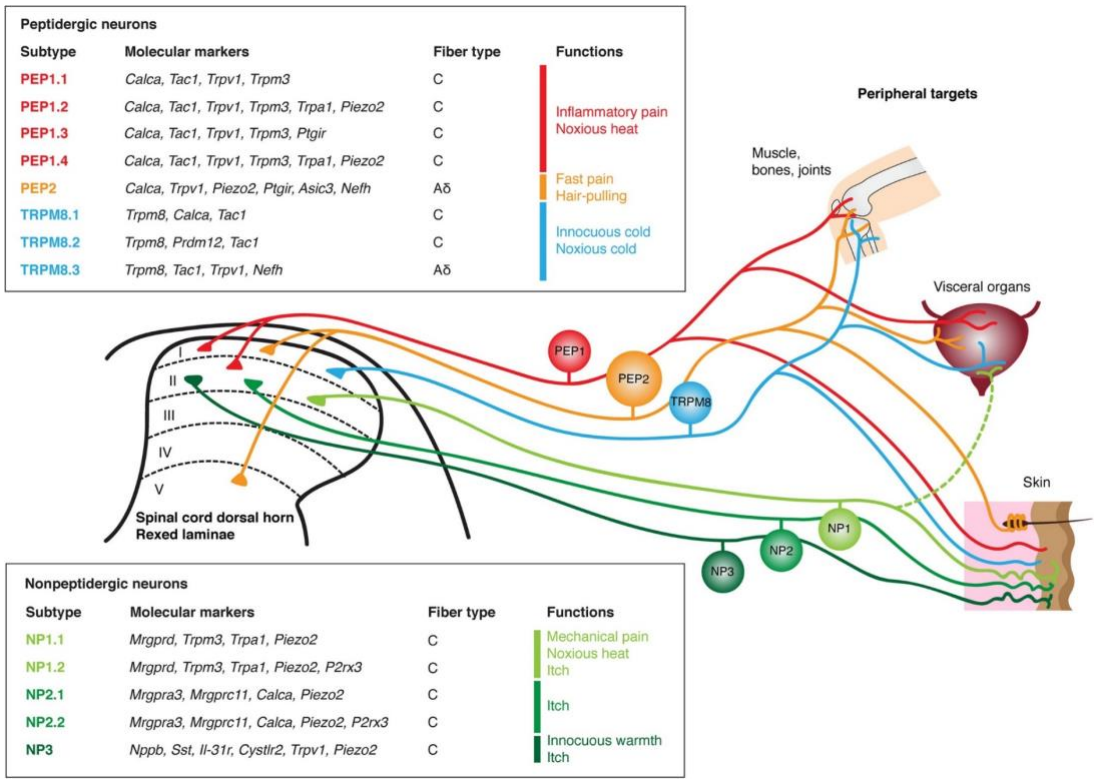

Figure 1.4: *The functional significance of expression of molecular markers and receptors of peptidergic and nonpeptidergic neurons of the PNS. Figure from (Cranfill & Luo, 2021)*

Consequently, neuronal cells are further classified through functional roles defined by receptor-expression. Specific receptors have been identified as playing key roles in sensory transmission through the stimulus-specific response such as TRPV1 (heat), TRPM8 (cold) and acid-sensing ion channels (ASICs, pH) (Basbaum et al., 2009; Dubin & Patapoutian, 2010).

1.4 Nociceptive signalling

Nociceptive signalling is characterised by binding or activation of receptors or channels attuned to specific sensory modalities. These receptors or channels increase the membrane potential sufficiently to trigger the opening of voltage-gated channels, thereby inducing an action potential.

1.4.1 Receptors of the nociceptor

TRP-channels

TRP-channels are cationic channels with non-selective pores facilitating the movement of Na^+, K^+, and Ca^{2+} across the cell membrane (Patapoutian et al., 2009). The TRP vanilloid (V1) channel plays a key role in nociceptive signalling (Caterina et al., 1997; J. Huang et al., 2006; Van Buren et al., 2005). The TRPV1 channel is formed by 4 subunits, each of which consists of the 6 transmembrane domains that characterise all TRP-channels and form a polymodal sensor of physical and chemical noxious stimuli. The cation channel is activated by capsaicin, noxious heat (>42°C) and pH<6, which triggers opening of the pore to allow ions, predominantly Ca^{2+}, to move through the channel (Touska et al., 2011). TRPV1 is colocalised with the TrkA receptor, as well as SP and IB4, consequently appearing on both peptidergic and nonpeptidergic neurons of the DRG (J. Huang et al., 2006).

TRP ankyrin 1 (A1) is involved with chemical and cold noxious sensation, activated by <15°C, isothiocyanates (found in mustard, horseradish and wasabi), cinnamaldehyde (cinnamon), allicin (garlic), bradykinin (BK), and ROS (Berta et al., 2017; O. Chen et al., 2020; Hjerling-Leffler et al., 2007). BK activates TRPA1 through a phospholipase C (PLC)-mediated pathway (Bandell et al., 2004; García-Añoveros & Nagata, 2007). Additionally, the TRPA1 is activated by microRNA *let-7b*, which is released from proinflammatory macrophages and nociceptors, as *let-7b* binds to TRPA1 and induces coupling to TLR7 which triggers an action potential (O. Chen et al., 2020; Lehmann et al., 2012). TRPA1 is particularly highly expressed in small-diameter nociceptors and often colocalises with TRPV1, as well as CGRP, SP and TrkA (García-Añoveros & Nagata, 2007).

TRP melastatin 8 (M8) is associated with cold innocuous and noxious sensation, activated by <25°C, menthol and icilin, exposure to which predominantly drives Ca^{2+} movement (Liu et al., 2020; Xing et al., 2007). TRPM8 is expressed by ~10% of DRG-neurons, however, generally does not colocalise with IB4, TRPV1, and TRPA1 (Hjerling-Leffler et al., 2007; Liu et al., 2020; Patapoutian et al., 2009).

ASICs

Acid-sensing ionic channels (ASICs) are broadly expressed in the DRG (Deval & Lingueglia, 2015). The extracellular binding of protons on ASIC channels facilitate the movement of Na^+ across the membrane (Yam et al., 2018). Injury-sites and subsequent inflammatory states are characterised by an increase in protons measured as low pH (Deval & Lingueglia, 2015; Yam et al., 2018).

Purinergic receptors

Purines, adenine triphosphate (ATP) and adenosine are released locally following lesion or in inflammatory states, activating distinct pathways mediating nociceptive pain through two receptor groups: P2X and P2Y. There are 7 ionotropic P2X receptors (ligand-gated ion channels) identified. P2X1-6 are expressed in neuronal cells and P2X2 and P2X3 show preferential expression in small neurons of the periphery in both murines and humans (Hamilton & McMahon, 2000). Binding of ATP triggers the opening of the P2X-channels, facilitating Na^+ mediated depolarisation, and Ca^{2+} intracellular signalling (Dawes et al., 2013; Hamilton & McMahon, 2000; J. Huang et al., 2006; Yam et al., 2018).

Voltage-gated channels

Voltage-gated ion channels are activated by membrane depolarisation induced by TRP-channels, ASICs or purinergic receptors, and allow ion movements across the cell-membrane thereby mediating action potentials (Dib-Hajj et al., 2009; Yang & Zheng, 2014). Voltage-gated Na^+ and K^+ channels (NaV and KV channels) are broadly expressed in sensory neuronal cells, with a select few showing preferential expression in nociceptors. NaV1.7, NaV1.8 and NaV1.9 (encoded by *Scn9a*, *Scn10a*, and *Scn11a* mRNA respectively) are preferentially expressed in peripheral nociceptors (Dib-Hajj et al., 2009; R. S. Y. Ma et al., 2019). KV channels are widely

expressed in neuronal cells and, as previously described, play a key role in action potentials by facilitating rapid efflux of K^+ driving repolarisation and thereby affecting the threshold and frequency of action potentials in humans and murines (Tsantoulas & McMahon, 2014).

Consequently, specialised neuronal subtypes emerge, with unique physical attributes and biomolecular profiles attributed to receptor expression patterns. The sensory modality of nociceptors is defined by the expression patterns of stimulus-specific receptors within the periphery, while the signalling transmission is characterised by the nerve-fibre morphology. Following trauma or disease, distinct neuroplastic changes to nociceptive signalling mediators and pathways are associated with hyperexcitability of nociceptors.

1.4.2 Inflammatory mechanisms induce hyperalgesic priming

Exposure to inflammatory mediators drives long-lasting neuroplastic changes to nociceptors manifesting as a state of sensitisation. This process of hyperalgesic priming is established through activation of several protein kinases, inducing increased nociceptive signalling (Ferrari et al., 2010). Key inflammatory mediators, that drive hyperalgesic priming, are discussed below.

Prostaglandins

Prostaglandins (PGE_2, PGI_2, PGE_1 and PGD_2) are metabolites of arachidonic acid produced by cyclooxygenases (COX-1 and COX-2), released by non-neuronal cells, including macrophages and keratinocytes, in response to inflammation (L. Chen et al., 2013; W. Ma & Eisenach, 2003; Sugimoto & Narumiya, 2007; C. Wang et al., 2007). G protein-coupled receptors (GPCRs) for PGE_2 (EP1-4) are broadly expressed in DRG-neurons, however, EP1 and EP4 are particularly relevant in the development of peripheral sensitisation (L. Chen et al., 2013; L.-Y. M. Huang & Gu, 2017). Activation of EP receptors cause increased cAMP, synthesised from ATP, which triggers protein kinase A (PKA) to induce phosphorylation of TRPV1, thereby sensitising TRPV1 (J. Huang et al., 2006; L.-Y. M. Huang & Gu, 2017; Hucho & Levine, 2007; W. Ma & St-Jacques, 2018). PGE_2 has additionally been indicated to cause increased expression of the nociceptor-specific NaV1.8 through a nitric oxide (NO)

mediated pathway (Hucho & Levine, 2007). PGE_2-induced increase of cAMP additionally activates exchange proteins activated by cAMP (Epacs), an intracellular protein, which in turn increases protein kinase Cε (PKCε) and have been associated with sensitisation of P2X3-receptors (Cheng et al., 2008; L.-Y. M. Huang & Gu, 2017; St-Jacques & Ma, 2011; C. Wang et al., 2007). Furthermore, prolonged exposure to PGE_2 has been shown to increase EP4 receptors in the axon of nociceptors (St-Jacques & Ma, 2014). The activation of the EP4 receptor in nociceptors is shown to mediate an increase in hyperpolarisation-activated current I_h causing faster refractory period (Kasai & Mizumura, 2001).

Cytokines

Cytokines, such as interleukins (ILs), tumour necrosis factors (TNFs), and neurotrophins (including NGF) are released from non-neuronal cells, including macrophages, mast cells and Schwann cells, in an inflammatory state. NGF binds both TrkA and pan-neurotrophin $p75^{NTR}$ receptor, with TrkA primarily mediating the effect of heat sensation and lower affinity for the $p75^{NTR}$ receptor (Denk et al., 2017). Binding of NGF to TrkA causes endocytosis of the ligand-receptor complex and subsequent retrograde transport, which leads to increased expression of not only TRPV1 but also P2X3 and ASIC3 receptors in peripheral neurons, along with SP and CGRP (Denk et al., 2017; Hucho & Levine, 2007; R.-R. Ji et al., 2002; Van Buren et al., 2005). Additionally, NGF binding of the $p75^{NTR}$ in DRG-neurons induces increased CGRP expression and drives heat hyperalgesia in the periphery, demonstrating a role for the low-affinity NGF-receptor in peripheral sensitisation (Watanabe et al., 2008). Exposure to NGF is associated with increased transcript and protein level of the voltage-gated channel NaV1.7 (Dib-Hajj et al., 2009; R. S. Y. Ma et al., 2019). Interestingly, expression of NaV1.8 and NaV1.9 is diminished in peripheral neurons following injury, however, exposure to inflammatory mediators including NGF and PGE_2 induces increased expression of the voltage-gated ion channels in uninjured unmyelinated cells, facilitating a sensitised state in inflammatory states (Gold et al., 2003; Rush & Waxman, 2004). Exposure to NGF and IL-6 has additionally shown increased hyperexcitability of NaV1.7 and NaV1.8 in DRG-neurons, independently of transcript and protein changes, hypothesised to

instead be driven by extracellular signal-regulated kinase (ERK) and p38 mitogen-activated protein kinase (MAPK) pathways of phosphorylation (Atmaramani et al., 2020). Specifically, NGF exposure triggers Src kinase, PI3 kinase (PI3K), as well as p38 and ERK MAPK activity, which induces increased expression of TRPV1 in the membrane, through increased transport and translation of *Trpv1* mRNA (Denk et al., 2017; J. Huang et al., 2006; R.-R. Ji et al., 2002).

Interleukins including IL-1β and IL-6 are released from macrophages and monocytes in inflammatory conditions (J.-M. Zhang & An, 2007) They are shown to bind to IL-1 and IL-6 receptors (IL-1R, IL-6R), driving increases in PGE_2, SP and CGRP in DRGs (Ebbinghaus et al., 2015; J.-M. Zhang & An, 2007). IL-1β increases the excitability of NaV currents through a pathway with p38 MAPK activation (Dawes et al., 2013). The activation of IL-6R or soluble IL-6R (sIL-6R) is mediated through glycoprotein 130 (gp130) and has been associated with several downstream pathways. IL-6 has been indicated to mediate a pathway of axonal growth and regeneration through Janus kinase/signal transducers and activators of transcription (Jak-STAT)/ERK MAPK pathway in sensory neurons (Kummer et al., 2021; Melemedjian et al., 2010; Moy et al., 2017). Increased action potential firing of nociceptors has been shown to be mediated through the MNK1/2-eIF4E signalling pathway of translation, which is additionally activated through IL-6R/ERK MAPK activation, regulating expression of voltage-gated channels, as well as probable increases in membrane trafficking of PGE_2-receptors (Kummer et al., 2021; Moy et al., 2017).

Inflammatory mediator TNF-α binds the TNF receptor (TNFR) and activates PKCε which phosphorylates TRPV1, thereby sensitising the receptor (Hucho & Levine, 2007; J.-M. Zhang & An, 2007). Additionally, TNF-α is found to induce sensitisation, measured as an increase in action potentials, through increased activity of ASICs in a pathway mediated by p38 MAPK activity (Wei et al., 2021). TNF-α is additionally capable of increasing NaV currents through a pathway with p38 MAPK, similar to that of IL-1β (Dawes et al., 2013).

Neurotransmitters

SP and CGRP are neuropeptides which characterise the peptidergic class of nociceptors, however, additionally mediate sensitisation. SP is increased in the axon following prolonged exposure to inflammatory mediator IL-1β, and is released from afferent fibres of nociceptors in inflammatory states (Jeanjean et al., 1995; J.-M. Zhang & An, 2007). SP binds the GPCR NK_1 receptor to induce release of PGE_2 and NO as well as enhance cAMP/PKA activity, thereby mediating excitatory effects and the development of sensitisation (R.-R. Ji et al., 2014; Yam et al., 2018). CGRP is released from axonal terminals in the periphery in states of inflammation, however, it also activates a GPCR (CLR) on nociceptors, which is associated with Ca^{2+}-mediated depolarisation, as well as sensitisation of peripheral neurons (Schou et al., 2017; Segond von Banchet et al., 2002).

Neurotransmitter ATP is released from damaged tissues and activates purinergic receptors including the metabotropic P2Y GPCRs on nociceptors, which is associated with PLC-β/PKC and cAMP/PKA pathways of TRPV1 phosphorylation (J. Huang et al., 2006; Yam et al., 2018). P2Ys have additionally been associated with phosphorylation of cAMP response element-binding protein (CREB), a key mediator of neuroplasticity in nociceptors (Melemedjian et al., 2014; Molliver et al., 2002). Inflammatory mediators including PGE_2 have been observed to induce increased ATP-responses of P2X3-receptors through cAMP/PKA signalling pathway (C. Wang et al., 2007). Furthermore, the P2X7-receptor is preferentially expressed in non-neuronal cells, specifically satellite glial cells, and activated by higher concentrations of ATP which triggers release of inflammatory mediators IL-1β and TNF-α, thereby triggering additional inflammatory pathways (R.-R. Ji et al., 2013; Toulme et al., 2010).

Collectively, neuroplastic changes to nociceptors are induced following exposure to inflammatory mediators, including PGE_2 and NGF, which manifest as a state of sensitisation.

1.5 The transcriptome of sensory neuronal cells

The transcriptomic profile reveals the genomic phenotype of a cell, which mediates the protein expression-patterns for functional differences, such as receptor-expression patterns (Chambers et al., 2019; Z. Wang et al., 2009). The transcriptomes of different cell-types are highly variable, and additionally adaptable to facilitate both natural physiological processes such as maturation, as well as adverse external cues, inducing changes to protein expression. Neuronal cells contain thousands of mRNAs which collectively make up the transcriptome of the cell. The transcriptome encompasses both coding RNAs (messenger RNAs, mRNAs), which can be translated into proteins, and noncoding RNAs, ncRNAs, of various subtypes with a wide array of functions including post-transcriptional roles. Microarray is a technique which allows quantification of several thousand mRNAs in parallel from at least two contrasting sources through the presence of oligonucleotides corresponding to gene transcripts in catalogued locations on a glass "chip" (Schena et al., 1995). More recently, the developments within next generation sequencing (NGS) protocols, such as RNA sequencing (RNAseq) allow for the collection of short sequences of bases, collectively characterising all the RNAs present in a sample including novel transcripts and isoforms. RNAseq techniques have significantly increased the understanding of the unique transcriptomic profile of cells, and neuronal subtype classification has been presented in several studies using sequencing protocols (Usoskin et al., 2015; Zeisel et al., 2018). The use of RNAseq techniques to study the transcriptome of DRG-cells and the changes observed in the manifestation of chronic pain, has similarly been initiated by several research groups (Starobova et al., 2018).

1.5.1 Categorising neuronal cell-types of the DRG based on the transcriptomic profile

Sequencing studies of sensory neuronal cells have largely been carried out with aims that can divided into two groups: 1. Studies exploring the differences between different types of cells, and 2. Studies exploring the differences induced by exposure to various insults or mediators of pain pathways. Studies comparing the differences in cell-types have demonstrated the unique profiles of different cell-

types. Single-cell RNAseq has been utilised to create categories for cell-types of the DRG (Hockley et al., 2019; C.-L. Li et al., 2016; Usoskin et al., 2015; Zeisel et al., 2018; Y. Zheng et al., 2019). Interestingly, while there are common categories which are generally agreed upon, sub-categories are found to differ between research groups. In some cases this is due to the focus of the study, such as tissue-specific innervation (Hockley et al., 2019) or innate preliminary characterisations within the study design (Y. Zheng et al., 2019). The most comprehensive characterisation is thus found to be carried out through single-cell RNAseq of cells from both the peripheral and central nervous system (Zeisel et al., 2018), suggesting updates to the sub-divisions previously presented (C.-L. Li et al., 2016; Usoskin et al., 2015). Three primary groups of sensory neurons are suggested; peptidergic (eight subtypes), nonpeptidergic (seven subtypes), and neurofilament (three subtypes).

Recently, data has been published attempting to similarly categorise cell-types from human DRGs demonstrating that while some cell-types appear to correspond to murine cell-types, there are novel cell-type with no clear transcriptomic equivalent in murine models (Nguyen et al., 2021). This follows a number of papers which comparatively characterise the transcriptomes of DRG-tissues from humans to mice DRGs, indicating distinct differences, although meaningful features are conserved between the human and mouse DRG-transcriptome (Ray et al., 2018; Wangzhou et al., 2020). An additional valuable library of transcriptomic data is the toolbox developed by the Denk laboratory; characterising non-neuronal cell-types of the periphery, specifically macrophages of nerves and DRGs (Liang et al., 2020). Over 20 studies have explored the transcriptome of sensory neuronal cells through sequencing techniques including microarray, whole- and single cell-RNAseq (Table 1.2).

Tissue	**Organism**	**Comments**	**Ref.**
DRGs	M	Comprehensive characterisation of neuronal cell-types of both the central	(Zeisel et al., 2018)

		and peripheral nervous system through single-cell RNAseq	
DRGs	M	Large scale classification of RNA expression in sensory neurons of lumbar DRGs through single-cell RNAseq	(Usoskin et al., 2015)
DRGs	M & H	Comparative transcriptome profiling of human and mouse DRG cells	(Ray et al., 2018)
DRGs	M & H	An exploration of changes between native and cultured mouse and human DRGs with a focus on potential pharmacological targets	(Wangzhou et al., 2020)
DRGs	M	Bulk RNAseq of labelled sensory neuronal subtypes focused on ion-channel expression	(Y. Zheng et al., 2019)
DRGs	M	Characterisation of subpopulations of sensory neurons of the DRG in cells from embryonic and adult mice	(N. Sharma et al., 2020)
DRGs	M	Characterisation of mechanosensory properties and molecular profiles of sensory neurons from the DRG using patch-seq and single-cell RNAseq	(Parpaite et al., 2021)
DRGs	M	Transcriptomic profile of MRGPRD-expressing C-fibres and C-low threshold mechanoreceptors through RNAseq of fluorescence activated cell sorting (FACS) of DRG-cells	(Reynders et al., 2015)
DRGs	M	Insight into the gene expression profile of $Na_V1.8$-expressing nociceptors	(Thakur et al., 2014)

		through magnetic cell sorting (MACS) and RNAseq	
DRGs	M	Identification of gene sets expressed in TRPV1-positive DRG neurons based on FACS and RNAseq	(Goswami et al., 2014)
DRGs	M	Microarray shows that KO of SCN9A ($Na_V1.7$) gene leads to upregulation of *PENK* mRNA in DRG	(Minett et al., 2015)
DRGs	M	Clarification of genes enriched in TRPM8 neurons of the DRG using microarray analysis to explore cold nociception	(Lippoldt et al., 2013)
DRGs	M	Identification of seven subtypes of colonic sensory neurons by single-cell RNAseq of retrogradely traced mouse colonic sensory neurons in the DRG	(Hockley et al., 2019)
DRGs	M	Identification of subtypes of somatosensory neurons by transcriptomic, morphological, and functional characteristics using single-cell RNAseq	(C.-L. Li et al., 2016)
DRGs	M	Characterisation of lymph-node innervating nociceptors of the DRG through single-cell RNAseq	(S. Huang et al., 2021)
DRGs	M	Characterisation of sacral and lumbar sensory neurons in embryonic and adult mice considering sex differences using RNAseq	(Smith-Anttila et al., 2020)
DRGs and TGs	M	Comparison of transcriptomic profiles of dorsal root and trigeminal ganglia with	(Manteniotis et al., 2013)

		focus on ion channels and GPCRs through RNAseq	
DRGs and TGs	M	Comparison of gene expression of dorsal root and trigeminal ganglion neurons through FACS and RNAseq	(Lopes et al., 2017)
DRGs	M	Sex differences in murine Nav1.8 expressing nociceptor cells of the DRG are characterised through Translating Ribosome Affinity Purification sequencing	(Tavares-Ferreira, Ray, et al., 2022)
DRGs and TGs	M	RNAseq of whole DRG and purified sensory neuronal cultures from male and female mice demonstrate sex differences of the transcriptome	(Mecklenburg et al., 2020)
DRGs	H	Comprehensive characterisation of neuronal cell-types within the human DRG through single nucleus RNAseq	(Nguyen et al., 2021)

Table 1.2: *Transcriptomic studies exploring molecular physiology and characterisation of sensory neuronal cells. DRGs: dorsal root ganglia, SN: sciatic nerve, TGs: trigeminal ganglia, H: human, M: mouse. Table adapted and progressed from (Starobova et al., 2018)*

Transcriptomic methods have been used to explore specific targets, or diseases of interest, in subpopulations of cells within the DRG. Distinct differences to RNA expression patterns are revealed, demonstrating transcriptomic profiles of sensory neuronal subtypes within the DRG, which may facilitate adaptability to changing environments.

1.5.2 Changes to the transcriptome of sensory neuronal cells induced by noxious stimulus

Comparative assessments of the transcriptome of sensory neuronal cells have shown differences attributed to maturity, tissue specificity and gender (Hjerling-Leffler et al., 2007; N. Sharma et al., 2020; Smith-Anttila et al., 2020). While it was

found that cells from embryonic mice were sufficiently developed to study pain pathways (Hjerling-Leffler et al., 2007), more comprehensive assessments of the transcriptome found distinct differences between cells from mice of different age-groups (N. Sharma et al., 2020; Smith-Anttila et al., 2020). Mediators of pain pathways, such as transcription factor Prdm12, play different roles depending on the maturity of the nociceptor (Landy et al., 2021).

Changes to the transcriptome have additionally been studied in sensory neuronal cells in states of chronic pain. DRG-cells from mice have been sequenced following induction of a pain state, which is most commonly been done by inducing a model of pain *in vivo* and subsequently isolating cells for RNA sequencing (Table 1.3).

Pain type	**Org.**	**Tissue**	**Comments**	**Ref.**
Burns pain	M	DRGs	RNAseq shows genes involved in neuropeptide signalling, axon guidance, and glutamatergic synaptic transmission increased following burns injury in mice	(Yin et al., 2016)
Spared nerve injury (SNI)	M	DRGs and spinal cord	Transcriptional and translational changes are explored in the DRG through RNAseq and ribosome profiling following SNI injury including changes to the ERK signalling pathway	(Uttam et al., 2018)
Spinal nerve ligation (SNL)	M	DRGs	RNAseq shows genes of the DRG following SNL in male mice are characterised by increased expression of ion	(Wu et al., 2016)

			channels and GPCRs and mediators of GnRH signalling, as well as alternative splicing	
Peripheral diabetic neuropathy	M	DRGs	RNAseq of sensory neuronal cells from an *in vivo* model of diabetic neuropathy show increased expression of mediators of inflammatory pathways	(J. Ma et al., 2015)
Radicular/ neuropathic pain ass. with malignant tumours within or adjacent to the spine	H	DRGs	Electrophysiological measurements were correlated with RNAseq to show significant sexual dimorphisms characterising neuropathic pain development	(North et al., 2019)
Charcot Marie Tooth (mutation)	R & H	DRGs	Comparison of gene expression profile in sciatic nerve and DRGs from humans and rats comparing the transcriptomic profile of neuronal and Schwann cells using RNAseq	(Sapio et al., 2016)
Spinal nerve transection, sciatic nerve transection	M	DRG	Significant changes to the transcriptome of neuronal cells are established through scRNAseq following axotomy, directly reliant on	(Renthal et al., 2020)

or sciatic nerve crush			the activity of transcription factor Atf3	
Partial sciatic nerve ligation	M	Isolated satellite glial cells and nociceptors from DRG	RNAseq following peripheral nerve injury illustrates SGCs exhibit increased immune profile distinct to the transcriptional changes of nociceptors	(Jager et al., 2020)

Table 1.3: *Studies exploring changes to the transcriptomic of DRG sensory neuronal cells in pain pathology. Table adapted from (Starobova et al., 2018)*

RNAseq confirms the flexibility of the transcriptomic profile of DRG-neurons during chronic pain states, showing plasticity of sensory neuronal cells in the manifestation of sensitisation. Assessments of transcriptome patterns in models of chronic pain showed distinct cell-subtype differences including increased expression of RNAs encoding mediators of axon guidance, neuropeptide and extracellular signalling, as well as inflammatory and ERK signalling, collectively pointing towards neuroplastic pathways inducing a hyperexcitable state in inflammatory and neuropathic pain (J. Ma et al., 2015; Sapio et al., 2016; Uttam et al., 2018; Wu et al., 2016; Yin et al., 2016). Interestingly, pathway analysis shows the ERK signalling pathway as an upstream regulator of both transcriptional and translational changes of the SNI induced chronic pain model, hypothesised to be mediated through mitogen-activated protein kinase interacting kinase (MNK1/2)-dependent translation regulation, which has previously been associated with sensitisation of sensory neuronal cells (Moy et al., 2017; Uttam et al., 2018). The study of the transcriptome is therefore of key importance to further characterise the changes of sensory neuronal cells in the development of sensitisation.

Consequently, the transcriptome of sensory neuronal cells is found to characterise cell-subtypes, and changes thereof are suggested to drive sensitisation in chronic pain states.

1.6 Compartmentalised functional genomics of sensory neuronal cells

Neurons are highly polarised cell structures which extend axons that can reach hundreds of times the diameter of the cell body to innervate the outer periphery. The cell body contains the nucleus and the DNA of the cell, while the axons contain 99% of the cytoplasm (Holt et al., 2019). Local mechanisms are consequently necessary to facilitate axonal guidance and growth, adaptation to synaptic inputs and extrinsic stimulus, and maintain functionality (Glock et al., 2017; Holt et al., 2019).

1.6.1 Translation of mRNAs

Functional genomics is the study of the transcriptome (the RNAs present in the compartment), the translatome (the RNAs in the process of translation) and the proteome (the proteins within the compartment). The process of translation characterises the expression of genetic information to produce proteins, which ultimately facilitates the classification, functioning, and purpose of the cell. The process of translation is divided into 3 steps: initiation, elongation, and termination (Gkogkas et al., 2010; Hellen, 2018; Knight et al., 2020). Although it is now clear that translation can be controlled by modulating both the initiation and the elongation rates, the majority of regulatory mechanisms identified in neurons involve regulation of the initiation of translation (Klann et al., 2004; Malone & Kaczmarek, 2022). During initiation, the Met-tRNA$_i$ complex is formed, in which the tRNA combines with eukaryotic initiation factor 2 (eIF2) and guanosine triphosphate (GTP) to form the ternary eIF2-Met-tRNA$_i$-GTP complex (Bhat et al., 2015; Jung et al., 2014; Klann et al., 2004). The 43S preinitiation complex is formed as the 40S ribosomal subunit is recruited, and the ternary complex associated with the small subunit of the ribosome (Bhat et al., 2015; Jung et al., 2014). The eIF4F cap-binding complex, consisting of eIF4E (cap-binding protein), eIF4A (ATP-dependent helicase) and eIF4G facilitates binding of the 43S preinitiation complex to the 5’ end of the mRNA (Bhat et al., 2015; Jung et al., 2014). The small ribosomal subunit scans the 5’UTR until the start codon (AUG) of the mRNA is identified by base-pairing to the Met-tRNA$_i$. Upon locating the start codon, the complexes form

the 48S initiation complex through binding of eIF3. The 60S ribosomal unit is recruited through GTP hydrolysis and the 40S and 60S ribosomal subunits form the 80S complex completing the initiation process and facilitating the progression to the elongation phase for protein synthesis (Bhat et al., 2015; Knight et al., 2020; Passmore & Coller, 2022).

1.6.2 Localised translation regulation

The process of translation is characterised by mechanisms facilitating regulation of both localisation and timing of translation. Localised translation, inducing increased protein expression in the axon, has been found to drive axonal growth and branching in both murines and humans (Bigler et al., 2017; Donnelly et al., 2013; Vogelaar et al., 2009).

Translating ribosomes were reported to be important in dendrites in early research (Autilio et al., 1968; Steward and Levy, 1981). The field suffered from initial contradictory information, as the existence of axonal ribosomes was challenged, however, multiple studies have since confirmed and validated their existence and consequently their role in axonal translation (Hafner et al., 2018; Lasek et al., 1973; Shigeoka et al., 2016; Tennyson, 1970). Local protein translation within the axon was hypothesised following studies showing proteomic changes at a time-scale which excluded trafficking in both murine cells and the squid giant axon (Eng et al., 1999; Giuditta et al., 1968, 1991; Holt et al., 2019). The transport of proteins produced in the cell body would require several days to reach the distal axon (Holt et al., 2019; Maday et al., 2014). Additionally, studies following axonal transection confirmed the continued emergence of newly synthesized proteins, despite the divorce from the somal compartment, providing a convincing argument for a localised mechanism (Giuditta et al., 1968).

Interestingly, axotomy was additionally reported to trigger the transfer of ribosomal proteins from glial cells to the axon (Rangaraju et al., 2017). The transfer of polyribosomes from Schwann cells was observed in a process not unlike endocytosis, where vesicles from Schwann cells were absorbed into the axon the contents of which were subsequently released into the axoplasm (Court et al.,

2008; Rangaraju et al., 2017). While minimal expression of polyribosomes was detected, the presence of which can perhaps be attributed to Schwann cells, monosomes are found more readily expressed within the axon, associated with a surprisingly large expression of ribosomal RNA (rRNA) within the axon, the presence of which introduces the possibility of locally synthesised ribosomal RNAs contributing to the translation capacity of axons (Holt et al., 2019; Rangaraju et al., 2017).

Regulation of translation is mediated through numerous mechanisms, facilitating control of the specific localisation and timing of protein translation. It is generally well accepted that RNAs can be transported in a repressed state, mediated through targeted inhibition of initiation, and subsequently translated following specific local signalling mechanisms (Moine & Vitale, 2019). The structure and sequence of both the 3'UTR and the 5'UTR of the transcript contribute to the localisation and the translation-state of specific mRNAs (Di Liegro et al., 2014; Moine & Vitale, 2019). Translation initiation can be regulated through several mechanisms including activation of multiple receptors such as mGluRs, particularly mGluR1 and mGluR5, NMDA receptors and TrkA/TrkB receptors (Khoutorsky & Price, 2018; Moine & Vitale, 2019). Collectively, downstream effects include activation of ERK, mTOR, S6K1 and eukaryotic translation initiation factors, inducing differential translation initiation (Figure 1.5).

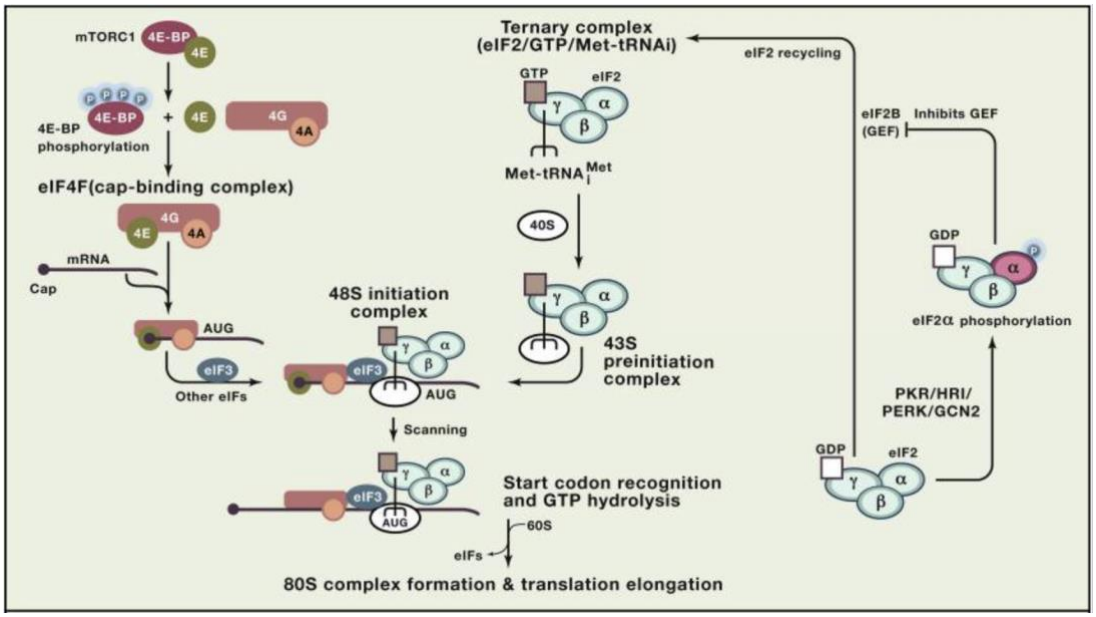

Figure 1.5: *Key signalling pathways of translation initiation. Translation initiation factors eIFs and initiation complexes play key roles in translation and are targeted for translation regulation. Figure from (Jung et al., 2014)*

Translation regulation by eIF2

Phosphorylation of key mediators of the eukaryotic initiation complexes regulates translation of specific mRNAs. Phosphorylation of eIF2α is mediated by 4 kinases: heme-regulated eIF2α kinase (HRI), the RNA-dependent eIF2α kinase (PKR), the amino acid-regulated eIF2α kinase (GCN2), and the PKR-like endoplasmic reticulum eIF2α kinase (PERK) (Jung et al., 2014; Klann et al., 2004). Phosphorylated eIF2α prevents the formation of the ternary complex necessary for translation initiation, thereby inducing global decreases in translation. However, interestingly, certain mRNAs containing an upstream open reading frames (μORF) in the 5'UTR exhibit increased expression following eIF2α phosphorylation (Jung et al., 2014; Moine & Vitale, 2019). An example of this is *Atf4* mRNA, which is localised to dendrites in neurons and for which increased expression is associated with neuroplasticity in long-term potentiation (LTP) and memory formation (Costa-Mattioli et al., 2007; Jung et al., 2014). Additionally, axon branching and guidance are associated with alternative regulation of eIF2 translation initiation pathway (Cagnetta et al., 2019; Pacheco et al., 2020). At the peripheral terminal, exposure to the extracellular cue Sema3a induces phosphorylation of eIF2α by PERK, which mediates noncanonical eIF2B-driven increased translation of 75 specific RNAs in the axon driving axon

guidance and neuronal wiring (Cagnetta et al., 2019). Furthermore, axonal injury induces eIF2α phosphorylation by PERK, which instigates an increase in Ca^{2+}-binding protein calreticulin, despite global decreases in translation, in a pathway mediated by eIF2B, and found to promote axonal regeneration (Pacheco et al., 2020).

Translation regulation by 4E-BPs

eIF4E-binding proteins (4E-BPs) bind to eIF4E, thereby preventing the formation of the eIF4F complex. Phosphorylation of 4E-BPs prevents binding to eIF4E, and eIF4E is free to form the eIF4F complex, which locates the 5'cap thereby stimulation translation initiation (Price & Géranton, 2009). Phosphorylation of 4E-BPs is predominantly mediated by mTOR (Klann et al., 2004).

Two variants of mTOR exist, mTOR complex 1 (mTORC1, where mTOR binds the regulatory protein Raptor), and complex 2 (mTORC2, where mTOR binds the regulatory protein Rictor). mTORC1 is a downstream target of the receptor coupled lipid kinase PI3K (Obara et al., 2012). mTORC1 is additionally distinct from mTORC2 as it is susceptible to inhibition by rapamycin. It has been extensively studied and shown to induce protein translation in dendrites when phosphorylated through TrkB-activation, which triggers the late phase of LTP (L-LTP) (Jung et al., 2014; Kelleher et al., 2004). mTORC1 induces changes to translation through phosphorylation of 4E-BPs and kinase p70 S6 (S6K1) (Khoutorsky & Price, 2018; Nandagopal & Roux, 2015). S6K1 phosphorylates S6 protein which mediates translation of mRNAs through eIF4A interaction (Nandagopal & Roux, 2015). mTOR additionally regulates translation of RNAs with a specific 5' terminal oligopyrimidine tracts (5'TOP) sequence through mTOR phosphorylation of LARP proteins (Berman et al., 2021; Nandagopal & Roux, 2015). RNAs with the 5'TOP sequence are commonly mRNAs localised in dendrites and encode ribosomal proteins and other translational machinery, and may therefore contribute to the generation and regeneration of axonal ribosomes (Kelleher et al., 2004; Khoutorsky & Price, 2018; Klann et al., 2004). The phosphorylation of mTORC1 is shown to be indirectly limited or inhibited by ERK (Gobert et al., 2008; Klann et al., 2004; Obara et al., 2012; Roux et al., 2007). ERK MAPK additionally phosphorylates protein kinase MNK1 which, along with p38 MAPK, selectively phosphorylates eIF4E to induce

translation initiation in axons of neuronal cells mediating L-LTP (Kelleher et al., 2004; Obara et al., 2012; Price & Géranton, 2009).

Translation regulation by cytoplasmic polyadenylation

Cytoplasmic polyadenylation facilitates translation regulation by the 3'UTR in contrast to eIF2 and 4E-BPs which target the 5'UTR (Klann et al., 2004; Sutton & Schuman, 2005). The cytoplasmic polyadenylation element-binding protein (CPEB), binds mRNAs with U-rich sequences, termed cytoplasmic polyadenylation elements (CPE), and can block the recruitment of the eIF4F complex thereby preventing translation initiation (Y.-S. Huang & Richter, 2004; Kelleher et al., 2004). Phosphorylation of CPEB is suggested to induce translation in the cytoplasm (Charlesworth et al., 2013). During translation in the cytoplasm, poly(A) polymerase (PAP) is recruited to lengthen the poly(A)-tail and the poly(A)-tail is bound by polyadenylate-binding proteins (PABPCs) (Passmore & Coller, 2022; Sutton & Schuman, 2005). PABPCs are theorised to bind the eIF4E translation initiation complex and collectively recruit the 40s ribosomal complex to induce the closed-loop translation initiation complex (Charlesworth et al., 2013; Passmore & Coller, 2022). Additionally, although the focus has been on CPEB, several other RNA elements and RBPs are suggested to mediate cytoplasmic polyadenylation and thereby localised translation, including Pumilio and ELAV-like proteins (Charlesworth et al., 2013; Vicario et al., 2015).

Translation regulation by FMRP and miRNA

Fragile X mental-retardation protein (FMRP), encoded by the *Fmr1* RNA in mice, is an RNA-binding protein which mediates translation regulation of specific RNAs by direct binding to a G-quadruplex structure or indirectly through recruitment of the *BC1* RNA (Kindler & Kreienkamp, 2012; Klann et al., 2004; Liu-Yesucevitz et al., 2011). A granule is formed of FMRP-proteins, mRNAs, microRNAs (miRNAs), ribosomes and RBPs, which additionally includes the RNA-induced silencing complex (RISC), facilitating trafficking of transcripts in a repressed state. Phosphorylation of FMRP subsequently facilitates localised translation initiation following mGluR activation, through a pathway mediated by mTOR (Kindler & Kreienkamp, 2012; Price et al., 2007).

Short noncoding RNA sequences, miRNAs, are well-known for their role in translational control, mediated through binding of specific sequences in the 3'UTR to inhibit translation of a given transcript (Lucci et al., 2020; Price & Géranton, 2009). The inhibition is mediated through miRNA, bound to specific RNAs, attaching to RISC, leading to shortening of the poly(A) tail and inhibition of translation initiation (Andersen et al., 2014).

1.6.3 Axonal translation drives sensitisation

The presence of ribosomes, RBPs and eukaryotic translation initiation factors has been shown in the axon of sensory neuronal cells both *in vivo* and *in vitro,* and explored to assess the association of mRNAs with ribosomes in the neurite compartment (Shigeoka et al., 2016, 2018; J.-Q. Zheng et al., 2001). The process of localised translation in axons of sensory neuronal cells is suggested to drive the development of sensitisation through neuroplastic pathways similar to LTP and L-LTP (E. Kim & Jung, 2020).

Translation regulation by 4E-BPs

mTOR and ERK are activated following stimulation of cells through exposure to NGF and IL-6 in axons of nociceptors (Kandasamy & Price, 2015; Melemedjian et al., 2010; Moy et al., 2017; Obara et al., 2012). Both mTORC1 and mTORC2 have been associated with axonal plasticity in nociceptor in chronic pain states (Khoutorsky et al., 2015; Obara et al., 2012; Wong et al., 2022). mTORC2 has specifically been associated with hyperexcitability of $NaV1.8^{+}$-nociceptors, as ablation of the regulatory protein Rictor of the mTORC2 complex inhibited specific structural changes localised to the peripheral terminal (Price & Géranton, 2009; Wong et al., 2022). Additionally, mTORC2 induces phosphorylation of Akt, which acts as an upstream regulator of mTORC1, however, mTORC2 activation is capable of bypassing direct mTORC1 inhibition to induce neuroplastic changes (Price & Géranton, 2009; Wong et al., 2022). Interestingly, ERK translation mediation is indicated to primarily affect heat hyperalgesia in C-fibres, while mTOR signalling predominantly induces mechanical hypersensitivity in A-fibre nociceptors (Obara et al., 2012; Price & Géranton, 2009).

Translation regulation by cytoplasmic polyadenylation

Activation of PKC by inflammatory mediators in states of chronic pain, as has been previously shown, induces increased CPEB-mediated polyadenylation in axons of select mRNAs, including the mRNA encoding α-CaMKII, which has 2 CPE sites (Ferrari et al., 2013; Sutton & Schuman, 2005). Neuroplastic changes characterising hyperalgesic priming has been directly linked to activation of CPEB and increased α-CaMKII expression in the axonal terminals of $IB4^{+}$-nociceptors (Bogen et al., 2012; Ferrari et al., 2013).

Translation regulation by FMRP and miRNAs

miRNAs have been found to play a key role in mediating neuroplasticity of sensitisation through compartmentalised localisation of specific miRNAs, mediated localised regulation of RNA translation (Jung et al., 2014; Kress et al., 2013; Sasaki et al., 2014). Inflammation is associated with repression of a number of miRNAs causing increased expression of IL-1β (miR-124), as well as TNF-α and IL-6 (miR-146a) (Andersen et al., 2014; X. Li et al., 2011).

Phosphorylation of FMRP stimulates the dissociation from target RNAs, driving translation initiation, and is observed following mGluR1/5 activation in peripheral nociceptor sensitisation in a pathway associated with mTOR (Price & Géranton, 2009). Interestingly, expression of α-CaMKII in the axon appears to be mediated through FMRP-pathways as well as CPEB-activity (Kindler & Kreienkamp, 2012).

1.6.4 Trafficking of mRNAs in neuronal cells

Local RNA translation relies on the subcellular localisation of specific RNA transcripts relevant for neuroplastic changes. Localisation and translation of key RNAs is well known to rely on both retrograde and anterograde trafficking of RNAs and proteins (Di Liegro et al., 2014; C. González & Couve, 2014; Sinnamon & Czaplinski, 2011). The anterograde transport of RNAs and retrograde transport locally synthesised proteins has been shown to be mediated through a number of pathways (C. González & Couve, 2014; Sinnamon & Czaplinski, 2011). The primary mechanism is through movement along microtubules by molecular motors such as the kinesin or dynein complex (C. González & Couve, 2014; Kanai et al., 2004). A

complex is formed by RNA binding proteins (RBPs) binding RNAs and forming larger RNA transport granules (Sinnamon & Czaplinski, 2011). The RNA granules are trafficked with translation repressors (such as FMRP, Pum2 and ZBP1), as well as miRNAs, to prevent continuous translation (Klann et al., 2004; Van Driesche & Martin, 2018). Dynein and kinesin mediate the retrograde and anterograde trafficking of the RNA granules along microtubules (Kanai et al., 2004).

1.6.5 The significance of the 3'UTR in localisation of mRNAs

Sequences within the 3'UTR are found to serve as binding sites for RBPs (Martin & Ephrussi, 2009). Exploration of isoforms within the neurite transcriptome are found to exhibit alternative polyadenylation with site usage downstream of the ones used in proliferating cells, leading to 3'UTR sequences with increased RBP motifs and RNA modification sites (Martin & Ephrussi, 2009; Mayr, 2016; Taliaferro et al., 2016; Van Driesche & Martin, 2018). Alternative distal exon splice-variant isoforms have been observed to be predominantly located in neurites from cortical neuronal cells using MISO (Mixture-of-Isoforms) bioinformatic analysis of RNAseq data (Taliaferro et al., 2016). Additionally, targeted deletion of the 3'UTR sequence of *mTOR* is shown to prevent axonal localisation of the RNA in sensory neuronal cells, which consequently reduces mTOR protein expression following nerve injury (Terenzio et al., 2018). In DRG-neurons, 2 isoforms of the nuclear transport regulator *Importin-β1* are observed, and the isoform with the longer 3'UTR exhibits axonal localisation, while the shorter 3'UTR isoform of *Importin-β1* exhibits somal localisation (Perry et al., 2012). Interestingly, following injury, the axonal isoform was shown to be increased and inhibition thereof was found to disrupt transcriptional responses in the soma of sensory neuronal cells following axonal injury, indicating both anterograde and retrograde trafficking of the axonal isoform as a signalling mechanism (Korsak et al., 2016; Perry et al., 2012).

Extracellular stimuli, including NGF exposure, are found to alter local levels of specific mRNAs, including *β-actin*, *Gap43*, and *Prph* (encoding peripherin), indicating activated transport mechanisms (Willis et al., 2007). It is suggested that trafficking of specific transcripts is triggered by stimulation of pathways similar to translation initiation regulation. Pathways of PI3K and MAPK activation, as well as

phosphorylation of kinases including ERK and p38 MAPK, c-Jun N-terminal kinases (JNKs), and Akt, are associated with phosphorylation of kinesin and dynein to induce select RNA transport mediating changes to the local transcriptome (Gibbs et al., 2015; Sahoo et al., 2018; Vuppalanchi et al., 2009; Willis et al., 2007).

1.7 The distinct localised transcriptome of neurites of neuronal cells

The significance of localised RNAs in mediating neuroplastic changes in neuronal cells is apparent (Cajigas et al., 2012; Lucci et al., 2020; Shigeoka et al., 2016; Van Driesche & Martin, 2018). A particularly elegant study by Zappulo et al. provided data for the comparative study of the transcriptome (RNA abundance through RNAseq), the translatome (ribosomal RNA association of mRNAs through Ribo-seq), and the proteome (protein abundance by mass spectrometry, LC-MS) of neurites from sensory neuronal cells (Zappulo et al., 2017). RNAs enriched in neurites were found to account for upwards of 50% of the localised proteome (Zappulo et al., 2017). However, the neurite transcriptome was additionally found to be enriched in markers of non-neuronal cells, indicating a possible contamination in the neurite compartment utilised to extract RNA localised to the axons. Despite this, the local transcriptome is suggested to characterise a "functional fingerprint" of the axon.

Sequencing techniques have significantly increased our knowledge of localised mRNAs, facilitating the development of a unique compartmentalised transcriptome profile (Cajigas et al., 2012; Van Driesche & Martin, 2018). 18 studies are considered, which have directly assessed the transcriptomic profile of neurites (either axons, dendrites, or both) of neuronal cells (Table 1.4).

Organism	**Tissue/Cell type**	**Findings**	**Ref.**
Rat	Hippocampal neurons from post-natal day 0 rats	Microarray characterised over 100 mRNAs localised to the dendrites largely associated with translation, however, axonal RNAs could not be confirmed	(Poon et al., 2006)
Rat	Embryonic cortical and	Microarray of axonal RNA shows transcriptional profile optimised	(Taylor et al., 2009)

	hippocampal neurons	for translational machinery and transport	
Mouse	DRG neurons	Microarray of axonal RNA from DRG-cells from embryonic and adult mice shows differential expression profiles according to maturity	(Gumy et al., 2011)
Rat	Hippocampal neurons (pups)	Through RNAseq of neuropil (neurite network and associated glial cells) from hippocampal cells transcriptome profiling was presented, showing thousands of localised transcripts encoding a heterogenous localised proteome	(Cajigas et al., 2012)
Mouse	Embryonic DRG (sensory neurons)	RNAseq of axons from NGF-dependent sensory neurons showed enriched expressions of mRNAs encoding transcription factors and translation machinery	(Minis et al., 2014)
Mouse/ Human	Sciatic nerve, primary afferent fibre	RNAseq was used to characterise sciatic nerve fibre, identifying specific targets of Charcot Marie Tooth neuropathy in the periphery	(Sapio et al., 2016)
Mouse	Differentiated embryonic stem cells (iNeurons)	Comparative exploration of the transcriptome, translatome and proteome of neurites, attributing the localised proteome profile	(Zappulo et al., 2017)

		largely to the localised transcriptome	
Mouse	Neuronal cell-lines (CAD and N2A) and primary cortical cells	Transcriptome characterisation at the isoform-level was carried out through RNAseq showing key role of 3'UTR in localisation of mRNAs to neurites	(Taliaferro et al., 2016)
Mouse	Primary motoneuron cultures from embryonic mice	RNAseq of the axonal compartment of motoneurons shows transcriptional profile optimised for translation including rRNAs	(Briese et al., 2016)
Human	Differentiated human embryonic stem cells (hESC-neurons)	Transcriptional profile of neurite projections favours translational and ribosomal expression mimicking results from the axon of embryonic primary rat cortical neurons	(Bigler et al., 2017)
Mouse	Primary embryonic motoneurons	Microarray data shows a transcriptomic profile optimised for protein synthesis, identifying *Smn* mRNA, deficient in spinal muscular atrophy, as key in axonal growth and synaptic plasticity	(Saal et al., 2014)
Mouse	Differentiated mouse embryonic stem cells (iNeurons)	Alternative 3'UTR characterises the transcriptomes localising to the axon	(Ciolli Mattioli et al., 2019)
Mouse	Primary hippocampal	RNAseq was used to show distinct subregional profiles of	(Farris et al., 2019)

	CA2 and CA1 pyramidal neurons	dendritic transcriptomes with long distinct 3'UTR	
Human	Differentiated human pluripotent stem cells (spinal motoneurons)	RNAseq was used to characterise the axonal motoneuron transcriptome showing roles associated with transport and ER-associated protein catabolism	(Maciel et al., 2018)
Mouse	Embryonic motoneurons	Transcriptomic profile of the axon of motoneurons is found to correlate ca 60% with the axonal transcriptome of sensory neurons and characterised by mRNAs facilitating RNA translation and transport as well as receptor activity	(Rotem et al., 2017)
Mouse	Embryonic hippocampal neurons	Single cell RNAseq characterisation of the dendritic transcriptome of hippocampal neurons shows 3'UTR isoform variation to dictate localisation patterns with enriched RNAs associated with translation and mitochondrial function	(Middleton et al., 2019)
Human	Differentiated human pluripotent stem cells (iCell neurons)	Single cell sequencing of neurite compartment obtained through nanobiopsy protocol with enriched RNAs associated with protein synthesis and ribosome biogenesis facilitating response to extracellular stimuli	(Tóth et al., 2018)

Rat	Mature myelinated motor axon	Microdissection and sequencing of contents of axonal cytoplasm from ventral root shows depletion of glial markers, while enrichment of neuronal markers and RNAs associated with translation and mitochondrial proteins are observed	(Farias et al., 2020)

Table 1.4: *Transcriptomic studies exploring the neurite compartments of primary neuronal cells and cell-lines from mice, rats, and humans*

The transcriptomic profiles of neurites from neuronal cells of a heterogenous population of neurons from both CNS and PNS have been explored (Table 1.4). The localised transcriptome of neurites are expected to exhibit subtype specific profiles, however, despite this, a comparative analysis demonstrated a group of 61 RNAs defined as the core transcriptome of neurites, which was retained across the majority of addressed studies (von Kügelgen & Chekulaeva, 2020). The core transcriptome of neurites contains RNAs associated with ribosomal proteins, translational machinery, signalling pathways, synaptic function and interestingly, nuclear RNAs. These data support an inducible mechanism of retrograde transport of locally translated proteins from the axonal to somal compartment (Korsak et al., 2016; Rangaraju et al., 2017).

The first comprehensive assessment of the transcriptome of the axon of sensory neuronal cells is believed to be published in 2014 (Kar et al., 2018; Minis et al., 2014). A large and distinct transcriptome was observed specifically in the axon of DRG-neurons, characterised by enrichment of mRNAs encoding transcription factors and translational machinery, using RNAseq of DRG-cells from E13.5 mice grown in porous membrane chambers (Minis et al., 2014).

1.7.1 The changes to the localised transcriptome in sensitisation

Previous research has indicated a key role for localised translation in the development of a chronic pain state (Melemedjian et al., 2010, 2014; Obara et al.,

2012; Price & Géranton, 2009). Studies have demonstrated how peripheral administration of modulators of translation, including rapamycin (inhibiting mTORC1), anisomycin (inhibiting 80S), and cordycepin (inhibiting polyadenylation), were capable of both preventing and reversing hyperalgesia *in vivo* in rats (Bogen et al., 2012; Ferrari et al., 2013; Jiménez-Díaz et al., 2008). This data suggests a role for localised translation, but it is insufficient to definitively conclude that translation in axons is involved, as the peripheral injection will also have affected translation in the surrounding tissue. However, transcriptome analysis of sensory neurons following burn injury shows differential expression of mediators of axonal guidance, strongly suggesting local translation and consequently identifying a largely unexplored area of interest (Yin et al., 2016). Despite the evidence suggesting a role for localised translation in chronic pain and sensitisation, limited research has, as of yet, been done to comprehensively assess changes to the localised transcriptome in the axon in chronic pain states. A semi-static transcriptome profile of the axon is hypothesised, with a fixed core transcriptome, and varied elements induced by trafficking of RNAs, inducing functional differences.

1.8 Aim of Thesis

The aim of this thesis is to characterise the change in the axonal transcriptome of sensory neuronal DRG-cells from embryonic and adult mice and to identify potential changes to the localised transcriptome which may drive sensitisation of nociceptors.

To address this aim, I developed an *in vitro* model with DRG-cells grown in porous membrane chambers which allowed the separate extraction of axonal and somal RNA (Chapter 3). Nociceptor sensitisation was induced via prolonged exposure to prostaglandin E2 (PGE_2) (Chapter 4). I used RNA sequencing to characterise the axonal transcriptome of embryonic (E16.5) and adult (8WO) mice and explored the changes to the axonal transcriptome induced by PGE_2-induced sensitisation (Chapter 5). Finally, I investigated the role of 3 RNAs, identified in the analysis in Chapter 5, through targeted siRNA knockdown, as potential mediators of peripheral sensitisation in the axon (Chapter 6).

Chapter 2: Materials and Methods

2.1 Animals

Animals (C57BL6/J mice) were bred, housed, and treated according to ethics and welfare regulations of the *Animal (Scientific Procedures) Act 1986*. Schedule 1 procedures were performed under the ethical guidelines of the NC3Rs in accordance with the age and species used (Kilkenny et al., 2010). In accordance with NC3R principles, all dissections were designed and planned to optimise the use of each animal, with cells extracted from tissues from both the pregnant female and embryos.

2.2 Cell culture techniques

2.2.1 Preparation of dishes for cell-culturing

All protocols for cell-culturing and preparation for cell-culturing was carried out in a class II cabinet using sterile equipment.

Dishes were obtained sterile or soaked in 70% ethanol for 24H and airdried to sterilise. Poly-L-Lysine (PLL)-coating (Sigma P1524) was carried out 24H prior to seeding. PLL was diluted to 0.02mg/ml for nunclon dishes (nunc 35mm, Thermo Fisher Scientific 153710) in sterile water (dH_2O) and 1ml was added to dishes. 1mg/ml for porous membrane chambers (Corning 353102) in sterile water (dH_2O) and 500ul both above and below the chamber-insert for porous membrane chambers. Plates were incubated at room temperature for 1 hour, then washed once in dH_2O. Plates were dried overnight in class II cabinet.

Laminin-coating (Sigma L2020) was carried out 1H prior to seeding. Laminin was diluted to 20ug/ml in Dulbecco's Modified Eagle's Medium (DMEM D6546, Sigma). 200µl was added to nunc dishes in the centre of the dish, and 500µl above and below the porous membrane chamber to coat the membrane. Laminin was removed following 1H incubation at 37°C, and cells immediately seeded without allowing the dish to dry.

2.2.2 *In vitro* culturing of DRG-cells from embryonic mice

Dissection

Embryos were obtained on day 16.5 (E16.5) from C57/BL6 mice for extraction of dorsal root ganglia (DRGs). DRGs were individually isolated using forceps and placed in Leibovitz-15 (Sigma) media on ice (Figure 2.1).

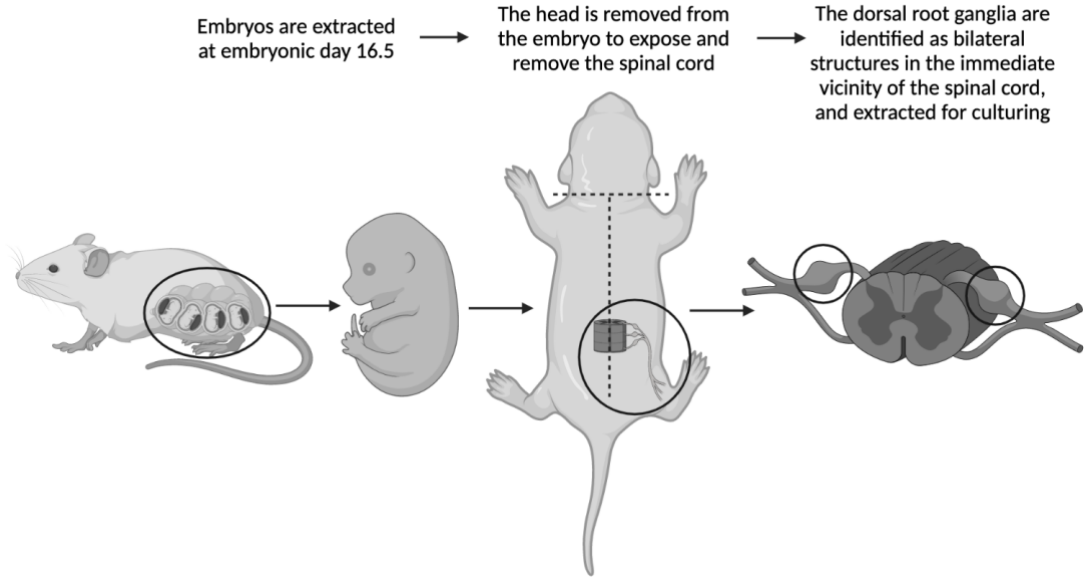

Figure 2.1: *An illustrated timeline of DRG extraction from E16.5 embryos of C57/BL6 mice. Figure created with BioRender.com.*

Explant seeding

Explants were moved from ice directly to an eppendorf tube with of complete media (Complete media: 48ml DMEM (Sigma D6546 or Sigma D5546), 1ml (2%) B27 supplement 50x (Gibco, 17504-044), 500µl (1%) penicillin-streptomycin (Pen/Strep, Invitrogen), 500µl (1%) GlutaMax (Gibco), 4µM Aphidicolin (APH, Sigma A4487), 4µM (final concentration 50ng/ml) GDNF (Sigma SRP3200, resuspended in DMEM + 2% BSA), 2mM (final concentration 50ng/ml) NGF 2.5S (Thermo Fisher Scientific 13257019)). Complete media was supplemented with APH, NGF, and GDNF to reduce proliferation of non-neuronal cells and promote axonal growth (E. J. Huang & Reichardt, 2001; LoPresti et al., 1992; Markus et al., 2002; Mundy et al., 2010). Explants were seeded in PLL- and laminin-coated dishes in complete media with 2 explants per dish. Explants were grown for a total of 7 days with media changes every 2-3 days.

Dissociation and seeding of dissociated cells

Eppendorf tubes were prepared containing 1ml 0.025 mg/ml Trypsin (Sigma T9201) in Dulbecco's Phosphate Buffered Saline (PBS without $MgCl_2$ and $CaCl_2$, Sigma-Aldrich) and 10-15 DRGs added per tube. They were incubated in 37°C waterbath for 10min. 0.2%(w/v) collagenase type II (Gibco 17101-015) was prepared in falcon tube with 5ml PBS and filtered using 0.2µm filter syringe to sterilise. Trypsin was replaced by 1ml collagenase solution and explants incubated for 20 min at 37°C. Collagenase solution was removed and 1ml dissociation media added (Dissociation media: 44ml DMEM media, 5ml (10%) Fetal Bovine Serum (FBS, Gibco F7524), 500µl (1%) Pen/Strep, 500µl (1%) GlutaMax). Explants were dissociated by gently pipetting against the side of the eppendorf tube up to 15 times. The dissociated cells were centrifuged at 4000g for 5 min and supernatant discarded. The cell pellet was resuspended in complete media for seeding.

Culturing in dishes

Dissociated DRG-cells were seeded in PLL- and laminin-coated dishes at a concentration of 2-3 dissociated DRG-explants/dish ($1.22x10^5$ cells/ml) in 100µl complete media in the centre of the dish. Media was topped up to 1ml after 24H. DRG-cells were allowed to grow for up to 8 days with media changes every 2-3 days. DRG-cells were grown in incubators at stable conditions of 37°C and 5% CO_2.

Culturing in porous membrane chambers

The protocol for seeding and culturing in porous membrane chambers was adapted from previous experimental protocols (Unsain et al., 2014). The porous membrane chamber was prepared by adding 2ml complete media below the chamber-insert. 25 dissociated DRG-explants ($6.39x10^5$ cells/ml) were seeded above membrane in 100µl complete media in the centre of the chamber. Media was topped up to 1ml after 24H. DRG-cells were allowed to grow for up to 7 days to facilitate the development of an axonal network below the membrane, with media changes every 2-3 days. DRG-cells were grown in incubators at stable conditions of 37°C and 5% CO_2.

Culturing in custom PDMS-rings

Custom polydimethylsiloxane (PDMS) rings with a diameter of 11mm were produced for minimising media-use when culturing in nunc dishes. Dishes were PLL- and laminin-coated as previously describes and PDMS-rings sterilised in 70% ethanol. PDMS-rings were placed in the centre of laminin-coated dishes and attached through gentle pressure to the rim of the ring. 1 dissociated DRG-explant was used to seed 2 dishes. DRG-cells were grown for a total of 7 days with media changes every 2 days. DRG-cells were grown in incubators at stable conditions of 37°C and 5% CO_2.

2.2.3 *In vitro* culturing of DRG-cells from adult mice

Dissection and dissociation

DRG explants were isolated from adult 8-week-old (8WO) C57/BL6 mice. The DRG-explants were stored in a falcon-tube with Hank's Balanced Saline Solution (HBSS, Sigma-Aldrich) on ice. The tube was centrifuged at 440rpm for 30seconds to collect tissue at the bottom. Following aspiration of supernatant, collagenase A solution (50mg collagenase A (Roche), 50ml HBSS) was added. The tissue was gently loosened and incubated in 37°C waterbath for 25min. The tube was once again centrifuged at 440rpm for 30seconds to facilitate the aspiration of supernatant. Collagenase D solution (50mg collagenase D (Roche), 5ml (10%) Papain (Roche), 45ml HBSS) was added. The tissue was gently loosened by swirling tube, and the tube subsequently incubated in a 37°C waterbath for 20min. The falcon-tube was centrifuged at 440rpm for 2min and supernatant aspirated. Enzyme T solution (50mg Trypsin inhibitor (Roche), 50mg Bovine Serum Albumin, 50ml TG media (TG media: DMEM with F12 and GlutaMax (Gibco), 10 %FBS, 1% Pen/Strep) was added to falcon-tube and dissociation commenced by pipetting up and down repeatedly. To minimise debris, the tissue was strained through cell strainer (70µm nylon). The filter was washed with TG media to obtain optimal number of neurons in strained solution. A cell pellet was obtained by centrifuging the tube at 440rpm for 4min. Dissociated DRG-cells were diluted in L-15 media (L-15 media, FBS, Pen/Strep, FRDU, NGF). FRDU is an anti-mitotic agent which minimises the growth of non-neuronal cells, while NGF (final concentration 5ng/ml) is added to promote the

axonal growth. Dissociated DRG-cells were seeded in porous membrane chambers as previously described.

2.3 DRG sensitisation protocol

2.3.1 PGE_2

Dissociated DRG-cells were exposed to prolonged incubation with Prostaglandin E_2 (PGE_2, Cayman Chemical) to induce an *in vitro* model of sensitisation. PGE_2 was purged with nitrogen and stock solution made through dilution in PBS to 10mM stock. Final working concentration of 10µM was obtained by adding directly into complete media every 2H for 24H for E16.5 DRG-cells (Figure 2.2). PBS (vehicle) was added to control DRG-cells every 2H for 24H.

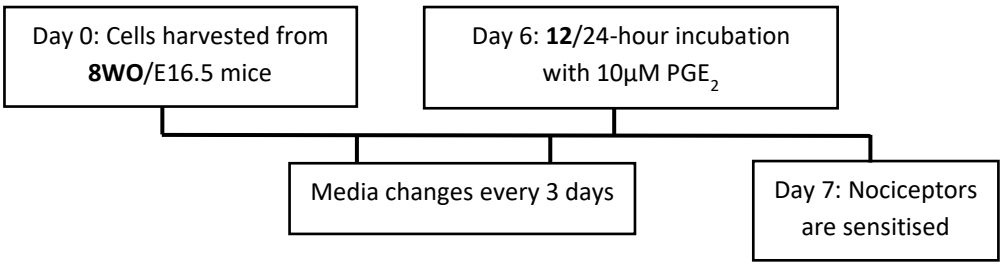

Figure 2.2: *A timeline of treatments of dissociated DRG cells with 10µM PGE_2*

Due to laboratory constraints, the 24H incubation could not be maintained for 8WO DRG-cells. Consequently, a 12H incubation was imposed for 8WO DRG-cells with treatments every 2H for 12H.

2.3.2 16,16-PGE_2

Prolonged PGE_2-exposure was found to successfully induce a functional *in vitro* model of sensitisation, however, the manual addition of PGE_2 every 2H was challenging in the long term. Stabilised 16,16-dimethyl PGE_2 (16,16-PGE_2, Tocris) has in previous research been used in place of PGE_2, making it a promising candidate to optimise the PGE_2-model of sensitisation (W. Ma, 2010). 16,16-PGE_2 has a prolonged half-life of 12H, compared to 2H for PGE_2, due to resistance to metabolism by 15-hydroxy PGDH, thereby necessitating fewer additions to maintain concentration in culture. 16,16-PGE_2 was purged with nitrogen prior to dilution in dimethyl sulfoxide (DMSO, Sigma-Aldrich) to 100mM stock. It was

subsequently diluted directly into culture medium of dissociated DRG-cells every 12H for 24H to maintain a final concentration of 10µM according to previously described timeline (Figure 2.2). For the control protocol 0.01% (v/v) DMSO (vehicle) was added to DRG-cells every 12H for 24H.

2.4 siRNA silencing of target RNAs

To evaluate the role of the RNAs of interest in the model of hyperalgesia, select siRNAs were introduced for the RNAs into our PGE_2-model. siRNAs are short non-coding RNA sequences which silence the target RNA through RNAi. RNAi strategies are most commonly facilitated using shRNA or siRNA, which utilise different mechanisms to reach the same results: post-transcriptional gene silencing through silencing of target RNA. siRNAs are synthetic sequences which, upon entry into cells associates with the RNA-Induced Silencing Complex (RISC), facilitating the binding of innate mRNA to the guide-strand of the siRNA in the RISC (Y. Dong et al., 2019; Rao et al., 2009). Upon binding the siRNA/RISC complex, the mRNA is cleaved and subsequently degraded. In the present study, I used Accell SMARTpool siRNA which contains a mix of 4 siRNAs collectively targeting all transcripts of the target RNA and has been validated as effective in murine neuronal cells (Dolga et al., 2008; Vagnoni et al., 2012).

2.4.1 siRNA silencing protocol

siRNAs for target RNAs *Arid5a*, *Cebpb* and *Tnfrsf12a*, as well as a non-targeting control, were obtained from Horizon Discovery Biosciences Limited (Table 2.1).

Name	**Accession hits**
Accell Mouse *Arid5a* (214855) siRNA - SMARTpool	Transcript variant 1 (NCBI Reference Sequence: NM_001172205.1), Transcript variant 2 (NCBI Reference Sequence: NM_001172206.1), Transcript variant 3 (NCBI Reference Sequence: NM_145996.4), Transcript variant 4 (NCBI Reference Sequence: NR_033310.1), Transcript variant 5 (NCBI Reference Sequence: NM_001290726.1),

	Transcript variant 6 (NCBI Reference Sequence: NM_001290727.1), Transcript variant X1 (NCBI Reference Sequence: XM_017319751.3)
Accell Mouse *Cebpb* (12608) siRNA - SMARTpool	Transcript variant 1 (NCBI Reference Sequence: NM_001287738.1), Transcript variant 1 (NCBI Reference Sequence: NM_001287739.1), Transcript variant 1 (NCBI Reference Sequence: NM_009883.4)
Accell Mouse *Tnfrsf12a* (27279) siRNA - SMARTpool	Transcript variant 1 (NCBI Reference Sequence: NM_013749.2), Transcript variant 2 (NCBI Reference Sequence: NM_001161746.1
Accell Non-targeting Pool	None

Table 2.1: *Accell siRNA details of targets and accession hits*

5nmol of siRNA was dissolved in 50µl HyClone water (Fisher Scientific) by gently spinning for 30min at room temperature. Target siRNAs were further diluted directly into cell media for a working concentration of 1µM. Dissociated DRG-cultures were exposed to siRNA for a total of 48H, with incubation commenced 24H prior to 16,16-PGE_2, to ensure silencing of target RNA (Figure 2.3).

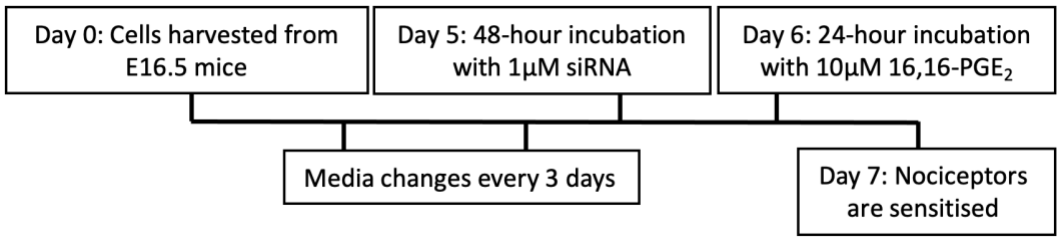

Figure 2.3: *A timeline of incubations with 48hour 1µM siRNA and 24hour 10µM 16,16-PGE_2*

2.5 Imaging of DRG explants using brightfield microscopy

Axonal growth was assessed to evaluate the effect of glucose concentration in the growth media. E16.5 DRG explants were seeded in nunc dishes with 2 explants/dish. Three dishes were seeded per condition: low glucose media (Sigma D5546) or high glucose media (Sigma D6546).

2.5.1 Axon length

Axons were imaged at day 3, 5 and 7 using phase contrast/brightfield microscopy using an Axiovert Zeiss 200M with a 10x objective coupled to a CCD Photometrics CoolSnap MYO camera and Micro-Manager software v2.0 (Edelstein et al., 2010). An axon was identified and followed from the edge of the explant to the end of the axon and images stitched together for a complete image. 2 complete images were obtained per explant with 6 technical replicates for a total of 12 complete images per condition each day.

2.5.2 Axonal network density

Axons were imaged at day 6 and 8 through phase contrast/brightfield microscopy using an Axiovert Zeiss 200M with a 20x objective coupled to a CCD Photometrics CoolSnap MYO camera and Micro-Manager software v2.0 (Edelstein et al., 2010). Images were taken mid-way between the end of the axon network and the edge of the explant-body. An average of 15 photos/dish were taken, providing ~45 images per condition for each day. Axonal network density was measured using an ImageJ plugin, which calculated the total axonal area through binarisation of the images and subtraction of the background, thereby measuring the coverage of the dish (Sasaki et al., 2009; Schneider et al., 2012).

2.6 Immunocytochemistry

Immunocytochemistry was utilised to visualise the growth of dissociated E16.5 DRG-cells in porous membrane chambers. Following 7 days of growth, the growth-media was removed, and cells washed in 1x PBS. Porous membrane chambers were incubated with 4% paraformaldehyde (1.6g PFA, 34ml 4% sucrose in H_2O, 80µl 10mM NaOH, dissolved for 30min in waterbath at 50°C, followed by 4ml 10x PBS, 200ul 1M $MgCL_2$, ~60µl HCl) 1ml above and below chamber for 30min at room temperature. Cells were subsequently washed twice with PBS (1x)/Glycine (10mM) 1ml above and below chamber and incubated in Glycine (10mM)/0.2%Triton/PBS (1x) for 30min at 4°C. Chambers were washed twice in PBS/Triton and either stored in 1xPBS overnight or immediately incubated in 3% BSA for 30min at 4°C to. The

membrane was subsequently cut out of the porous membrane chamber using a scalpel. Primary antibody was prepared in 3% BSA according to Table 2.2.

Target and dilution	Host	ID	2°antibodies
Acetylated tubulin, 1:300	Mouse	Sigma T7451	Anti-mouse 563

Table 2.2: *Antibodies used for immunocytochemistry with fixed DRG cultures*

Membrane was incubated overnight with primary antibody in darkened humidified chamber at 4°C. Membrane was gently washed twice for 5min in PBS/Triton to remove unbound primary antibody. Secondary antibody (anti-mouse 563) was diluted in 3% BSA. DAPI nuclear was added directly with secondary antibodies for a final concentration of 300nM. Membrane was incubated in 100µl of secondary antibody in humidified chamber for 2hours at room temperature or overnight at 4°C. Membrane was washed twice in PBS/Triton and lastly washed in PBS, before gently dried. Imaging slide was prepared by adding hardset Vectashield (Vector laboratories) or fluorogel mounting medium (~20µl) and membrane placed onto slide. Another drop of Vecta shield or mounting gel was added prior to coverslip, which was pressed down to remove bubbles. Imaging was performed using the Zeiss LSM 880 confocal microscopy at 20x or 63x.

2.7 RNA extraction from porous membrane chambers

2.7.1 RNA extraction from E16.5 DRG-cells

RNA extraction from E16.5 DRG-cells grown in porous membrane chambers was carried out according to an experimental protocol from (Garcez et al., 2017) with TRIzol™ Reagent (Invitrogen 15596018). RNase-free DNA LoBind® Tubes (Eppendorf) tubes were used to minimise surface-binding of nucleic acids and consequently maximise RNA product.

Lysing

Prior to lysing, growth media was aspirated, and the cells gently washed with PBS. 1ml of TRIzol™ Reagent was used to remove the somal or axonal contents from porous membrane chambers by gently scraping the membrane to promote

detachment and pipetting onto each side of the porous membrane. The contents of the somal or axonal compartment were added into separate 1.5ml eppendorf tubes. 0.2ml chloroform was added and the tube vigorously shook for 15 seconds, followed by a 2-3min incubation at room temperature. Tubes were centrifuged at 12,000g for 15min at 4°C allowing for three distinct layers to form. The upper aqueous phase was removed and placed in new eppendorf tubes, discarding remaining liquid.

RNA isolation

10ng GlycoBlue (Invitrogen AM9516) was added followed by 0.5ml 100% isopropanol. The tube was incubated at room temperature for 10min or overnight at -20°C and subsequently centrifuged at 12,000g for 10min at 4°C, causing a blue cell-pellet to become visible.

RNA wash

The supernatant was removed, leaving the cell-pellet, to which GTC mastermix (GTC solution, 300µl; 2M Sodium Acetate, 35µl; Isopropanol, 500µl) was added. The tube was briefly vortexed, followed by a 30min incubation at -20°C. Subsequently the eppendorfs were centrifuged at 12,000g for 30min at 4°C. The supernatant was removed and 1ml of 75% ethanol added. Following a brief vortex, the eppendorfs were centrifuged at 7500g for 5min at 4°C. The ethanol wash was carried out 3 times. Lastly the ethanol was removed, and the RNA pellet was dried for 10-15min.

RNA suspension

RNA pellet was dissolved in 30µl RNase-free H_2O by pipetting cell pellet up and down gently against side of eppendorf followed by an incubation in a heat block for 15min at 55-60°C. RNA samples were immediately moved to -20°C for short-term storage or -80°C for long-term storage.

2.7.2 RNA extraction from 8WO DRG-cells

RNA extraction from 8WO DRG-cells grown in porous membrane chambers was carried out using TRIzol-based Direct-zol™ RNA Miniprep Plus (Zymo Research) according to manufacturer instructions. All reagents and tubes were provided in the

kit apart from TRIzol™ Reagent and RNase-free DNA LoBind® Tubes for lysing cells in TRIzol™ Reagent. All centrifuge steps were carried out at 14,000g.

Lysing

Lysing was carried out as previously characterised for E16.5 DRG-cells grown in porous membrane chambers (see chapter 2.6.1).

RNA purification

1ml 100% ethanol was added to tube with TRIzol™ Reagent and cells, and thoroughly mixed. The total contents were subsequently added to a Zymo-Spin column in a Collection tube and centrifuged for 30sec. The column was moved to a new Collection tube and the previous discarded along with the flow-through. For DNase I treatment, 400µl RNA Wash Buffer was added to the column and the tubes were centrifuged for 30sec. The flow-through was discarded and DNase I treatment (5µl DNase I and 75µl DNA Digestion Buffer) added to column. The samples were incubated at room temperature for 15min. 400µl Direct-zol™ RNA PreWash was added to column and samples centrifuged. The flow-through was discarded and the PreWash step repeated once. 700µl RNA Wash Buffer was then added to the column and the tubes centrifuged for 1min. The column was then transferred into the final tube for RNA elution. Somal samples were eluted in 30µl and axonal samples in 20µl RNase-free H_2O. RNA samples were immediately moved to -80°C for storage.

2.7.3 RNA quantity and quality assessments

The amount of RNA in all samples was assessed through measurements of UV absorbance at 260nm using a NanoDrop 2000 spectrophotometer (Thermo Scientific, USA) (Becker et al., 2010). A yield of >25ng/µl was considered acceptable for axonal samples and >100ng/µl for somal samples.

The quality of the RNA extracted from E16.5 DRG-cells was evaluated through electrophoresis to ensure sufficient quality for RNAseq.

Automated Electrophoresis

The Agilent RNA Screentype System was used with Agilent 2200 TapeStation instrumentation according to manufacturer instruction. The RNA Screentype Sample Buffer (5067-5577) and RNA Screentype Ladder (5067-5578) was equilibrated to room temperature over 30min, then vortexed to ensure sufficient mix of samples. Meanwhile RNA samples were thawed on ice. 5µl RNA sample-buffer was mixed with 1µl RNA sample or ladder. The sample was spun down, vortexed at 2000rpm for 1 min to mix, then spun down again. A denaturation cycle was carried out where samples were heated to 72°C for 3min, then placed on ice for 2min, and finally spun down. Samples were then run on the Agilent 2200 TapeStation instrument. The ratio of 28s to 18s RNA is a widely accepted and utilised indicators of RNA integrity (Imbeaud et al., 2005). 28S and 18S are the most widely distributed ribosomal RNAs and a ratio of 2 is considered great quality, while >1 is generally accepted as good. Additionally, the RNA integrity number (RIN) are obtained for all samples. The RIN gives an estimate of RNA quality through automated and standardised assessment of RNA degradation, by assigning a RIN value from 1 (totally degraded) to 10 (intact) (Schroeder et al., 2006).

2.8 RT-qPCR

2.8.1 Reverse transcription (cDNA synthesis)

cDNA synthesis was carried out to facilitate subsequent qPCR. Invitrogen SuperScript III CellsDirect cDNA synthesis kit was used for cDNA synthesis according to manufacturer instructions (Thermo Fisher Scientific). 3µl of mastermix 1 (2µl 200ng/µl random hexamers and 1µl 10mM dNTPs per sample) was added to each small eppendorf. Xµl RNA equivalent to 500ng and 11.5-Xµl of RNase-free H_2O was added. Eppendorf was placed in heat-block at 70°C for 5min, then moved to ice for 1min. 5µl of mastermix 2 (4µl 5x First Strand Buffer and 1µl 100mM DTT per sample) was added per sample. Eppendorf was briefly vortexed and spun down. 0.5µl Superscript III was added, followed by brief vortex and spin, and tubes were subsequently incubated at room temperature for 5min. The tubes were then placed in a waterbath for 1hour at 50°C, followed by 10min in a 70°C heating block. The contents of the tubes were spun briefly to collect any condensation. For qPCRs a

1:20 dilution was performed by adding 180ul of RNase-free H_2O. cDNA was stored at -20°C.

2.8.2 qPCR

qPCR was carried out to measure the expression level of select RNAs of interest. Mastermix was made according to the following quantifications per sample: 0.5µl forward primer, 0.5µl reverse primer, 5µl GoTaq qPCR mastermix (Promega A6002) and 2µl RNase-free H_2O. Primer sequences are listed in table 2.3.

Target	**Forward primer**	**Reverse primer**
Gapdh	5' - AAGAAGGTGGTGAAGCAGGC	5' - ATCGAAGGTGGAAGAGTGGG
Ngf	5' - ACACTCTGATCACTGCGTTTTTG	5' - CCTTCTGGGACATTGCTATCTGT
Hprt	5' - GGTGTTCTAGTCCTGTGGCC	5' - AGTGCAAATCAAAAGTCTGGGG
Arid5a	5' - ATCTTGGCTTCAAGCAGATTAAC	5' - TTGCTTCCTGGGCTTGGTAG
Tnfrsf12a	5' - CATGGACTGCGCTTCTTGTC	5' - CAGTCTCCTCTATGGGGGTAGT

Table 2.3: *Primer sequences for qPCR*

Primers were checked for efficiency and specificity.
8µl of mastermix was added to each qPCR tube followed by 2µl of cDNA sample (previously diluted). 3 technical replicates were always run per sample. Samples were loaded to QIAGEN Rotor-Gene Q and exposed to the following thermal profile (40-50 cycles): Hold for 5min at 95°C. Cycle at 95°C (10sec), 60°C (20sec), 72°C (20sec). Melt at 72-95°C.

2.8.3 Analysis of qPCR data

qPCR results in the form of Ct values were imported into Microsoft Excel for analysis. Expression patterns of *Ngf, Hprt, Tnfrsf12a and Arid5a* mRNA were normalised to *Gapdh* as an internal housekeeper, or reference gene, and compared for E16.5 DRG-cells exposed to control-protocol or PGE_2-protocol through the

comparative Ct method ($2^{-\Delta\Delta Ct}$) (Livak & Schmittgen, 2001). The output of the comparative Ct method is the fold change of expression of an RNA of interest (ROI) in the target sample compared to the control. It is defined by the following equation:

$$\Delta\Delta Ct = (Ct_{ROI} - Ct_{\textit{Gapdh}})_{Target} - (Ct_{ROI} - Ct_{\textit{Gapdh}})_{Control}$$

The expression of the ROI (*Ngf*, *Arid5a*, *Tnfrsf12a*) is consequently normalised to the expression of the reference gene (*Gapdh*) and the expression pattern of the ROI in the target sample (PGE_2-protocol) is compared to the expression pattern of the control sample. As $2^0 = 1$ the expression of the ROI in control conditions is close to one.

2.9 Ca^{2+} imaging

2.9.1 Ca^{2+} imaging protocol

The measurement of Ca^{2+} transients using fluorescence imaging was carried out as a measure of neuron excitability of E16.5 DRG-cells following activation. Each dish of cells was only imaged once.

After 7 days of culturing, growth media was removed, and DRG-cells were loaded with the fluorescent dye, Fluo-5 AM (Thermo Fisher) for a total of 30min at room temperature. Fluo-5 AM is a single wave-length fluorescent dye, which binds to Ca^{2+} and renders the cell-membrane permeable through acetoxymethyl (AM) ester-forms. Fluo-5 AM binds at a lower affinity compared to other fluorescent Ca^{2+} dyes, making it the optimal choice for intracellular measurements which ranges within 1µM-1mM. This range which would result in saturation with the use of dyes with higher affinity such as Fluo-4 (Paredes et al., 2008; Thomas et al., 2000). Fluo-5 AM was diluted in Pluronic F127 20% solution in DMSO (Sigma-Aldrich) for a 10mM stock, which was stored at -20°C. Fluo-5 AM is extremely light-sensitive and all subsequent work with the compound was carried out in red light conditions. Fluo-5 AM was diluted in complete imaging buffer to a final concentration of 100nM (Imaging buffer: 500ml autoclaved sterile water, 3.9447g (135mM) NaCl, 0.1118g (3mM KCl), 1.191506g (10mM) HEPES, 1.35117 (15mM) glucose (all Sigma-Aldrich).

Imaging buffer was made every 4 weeks and complete imaging buffer was made for every experiment by adding 1mM $MgSO_4$ and 2mM $CaCl_2$.

Following loading with Fluo-5, a gentle wash with complete imaging buffer was used to remove unbound or nonspecifically associated dye. Subsequently, a de-esterification period of 30min was imposed where cells were incubated with complete imaging buffer at room temperature to cleave the AM-group from intracellular Fluo-5 to allow fluorescence upon activation (Lock et al., 2015). Imaging buffer was removed from the cells immediately prior to imaging.

Imaging was carried out using an Olympus IX70 Inverted tissue culture microscope connected to a CCD camera (Photometrics CoolSnap MYO). Image recording was carried out through multi-acquisition in ImageJ, with 1200 frames recorded (one frame every 500ms for 10min) per measurement. Image settings were selected for 10x magnification, as 2x2 image binning of 470nM wavelength filter. Dissociated DRG-cells were imaged for 20seconds prior to stimulation to establish baseline fluorescence signaling. Stimulus (30µl 200nM capsaicin or 25mM KCl) was gently added directly to cells following baseline recording of 30 sec.

2.9.2 Analysis of Ca^{2+} imaging data

All analysis of Ca^{2+} imaging data was completed using ImageJ software (FIJI) V. 2.0.0 and Microsoft Excel (Schindelin et al., 2012). The image-files were recalibrated to account for pixel to µm ratio (110 pixels = 150µm). Cells were manually selected in the ImageJ software (Figure 2.4), and the fluorescent intensity collectively measured using the multimeasure feature.

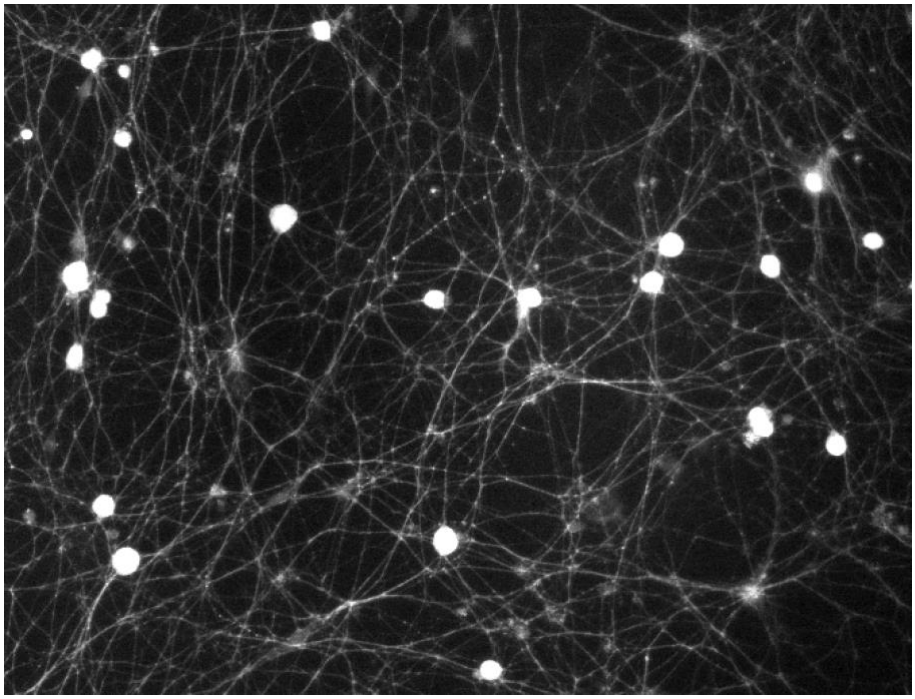

Figure 2.4: *Representative image of the axonal network of DRG neurons following 7 days of in vitro growth*

The cell-size (µm) and fluorescence (F) for each selected cell over 1200 frames were obtained and exported into Excel for further analysis. To normalise the fluorescent intensity, the baseline fluorescence, F_0, for each selected cell was calculated, as the average fluorescent intensity for the first 30sec prior to stimulation. The baseline fluorescence was subtracted from the fluorescent intensity at every time point (F_t) for each selected cell. The change in fluorescence over time was consequently defined by the equation $\Delta F=(F_t - F_0)/F_0$. The average change in fluorescence for all cells in 1 dish (up to 20 cells) was obtained and considered 1 technical replicate. At least 2 technical replicates were included in each biological replicate. For each experiment a minimum of 3 independent repeats (biological replicates) was obtained for statistical analysis. The fluorescent intensity was converted to % for graphical representation of time-course analysis, thereby showing the change in excitability in response to stimulus over time. The peak fluorescent intensity (PFI) was calculated as the increase in % between the baseline and the normalised maximum fluorescent intensity defined by the equation $PFI=\Delta F - F_0$.

2.10 Statistical analysis

All image analysis, including bright field microscopy of axon growth, immunocytochemistry of membranes from porous membrane chambers, and Ca^{2+} imaging was carried out using ImageJ Fiji. qPCR and Ca^{2+} imaging data files were organised in Microsoft Excel for Mac. Statistical analysis and most graphical presentation were carried out using Graphpad Prism V. 7.0 for Mac. Additional graphical presentation was indicated where applicable. For all statistical tests "n" indicated independent experimental repeats. When less than n=3 was obtained the data was considered preliminary and statistical significance was not assessed. Statistical significance was considered when p-value<0.05.

Axon network density: The effect of low or high glucose concentration in media on axon network density was assessed following 6 and 8 days of growth (n=3 for each group) using two-way analysis of variance (ANOVA) with Sidak's multiple comparisons test.

Ca^{2+} imaging: The difference in PFI between DRG-cells exposed to control-protocol (n>3) or PGE_2/16,16-PGE_2-protocol (n>3) was assessed using paired two-tailed t-test. The effect of siRNA silencing of key RNAs *Cebpb, Arid5a* or *Tnfrsf12a* on 16,16-PGE_2-induced hyperexcitability was analysed by first normalising all PFI values to the PFI of DRG-cells exposed to the 16,16-PGE_2 protocol to obtain %PFI of PGE_2-sensitised PFI. The %PFI of PGE_2-sensitised PFI of untreated control-cells, siRNA control+16,16-PGE_2, *Arid5a* siRNA+16,16-PGE_2, *Cebpb* siRNA+16,16-PGE_2, or *Tnfrsf12a* siRNA+16,16-PGE_2 were compared using matched one-way (mixed effects) ANOVA with Geisser-Greenhouse correction and Tukey's multiple comparisons test.

qPCR: The effect of the PGE_2-protocol compared to the control-protocol on *Ngf*, *Hprt*, *Tnfrsf12a* and *Arid5a* RNA expression in E16.5 DRG-cells was assessed using paired two-tailed t-test of $2^{-\Delta\Delta Ct}$ values (n>3).

2.11 RNAsequencing

RNA sequencing (RNAseq) is a next generation sequencing technique where the expression patterns of all RNAs in a sample are measured. Total or fractionated RNA is converted to a library of cDNA fragments with adapters attached to either one or both ends, facilitating single-end sequencing or paired-end sequencing respectively (Kukurba & Montgomery, 2015; Z. Wang et al., 2009). The output reads from sequencing are 30-400bp depending on the sequencing equipment and protocol. Sequenced reads are mapped to a reference genome/transcriptome to identify known RNAs or the reads are assembled de novo if a reference genome does not exist (Grabherr et al., 2011).

2.11.1 Library preparation and sequencing

Library preparation can be carried out in several ways the most common of which include poly-A selection (polyA+) or rRNA depletion (Kukurba & Montgomery, 2015; Z. Wang et al., 2009) to remove the highly abundant ribosomal RNAs from the samples, which would otherwise interfere with measurements of lowly expressed RNAs (Kukurba & Montgomery, 2015). rRNA depletion selectively circumvents rRNA through tagging with oligo(dT) primers for depletion during reverse transcription (Kraus et al., 2019), while polyA+ works by tagging polyadenylated RNAs with poly-T oligos for sequencing and thereby excludes not only rRNA but also other RNA lacking a poly-A tail, such as long non-coding RNAs (Bush et al., 2017; Z. Wang et al., 2009). Subsequent consideration must be given to the details of the sequencing protocol itself, which includes the length of reads, whether it is carried out as single-end or paired-end sequencing, and finally the depth of sequencing, all of which could create biases within the final outputs (Freedman et al., 2020). Paired-end is commonly preferred to optimise sensitivity and specificity, however, has been shown to only be imperative for transcriptomic assembly, while single-end sequencing has been shown to be perfectly satisfactory to quantify gene expression (E. González & Joly, 2013).

RNA from E16.5 mice: DNase treatment was carried out by followed by library preparation with rRNA depletion in preparation for Illumina HiSeq paired-end 150bp sequencing by GeneWiz (Azenta Life Sciences).

RNA from 8WO mice: polyA-selected library preparation and single-end 75bp sequencing at the University of Texas at Dallas sequencing core.

2.11.2 Bioinformatic analysis

The bioinformatic analysis pipelines of RNAseq data can vary greatly with rapid developments of new tool-packages (Conesa et al., 2016; Koch et al., 2018). RNAseq data needs to be aligned and mapped to a genome or transcriptome with annotations in order to produce the quantification of the transcriptome in the form of counts for genes/RNAs. Subsequently, the raw counts can either be inputted directly into a tool-package for differential expression analysis or alternatively the raw counts can be transformed through normalisation calculations prior to comparable analysis. Additionally, filtering can be carried out to explore changes to select subtypes of RNAs. Quality control can and should be utilised at several steps throughout the final bioinformatic pipeline. A thorough discussion of the bioinformatic tools used for analysis will follow.

All bioinformatic analysis was carried out in the Terminal coding operating system on MacOS and graphical presentation was created in Graphpad Prism V 9.3.1 or in an online instance of MathWorks MATLAB.

Quality control and mapping

Upon obtaining RNAseq datafiles quality control was carried out using FastQC which assesses the read quality and gives a quality score per base. Commonly it is observed that the quality drops towards the 3’ end of reads and may be clipped to discard sequences of poor quality or possibly contamination with adapter sequences (Conesa et al., 2016; Kukurba & Montgomery, 2015). The initial length of the read should however be considered as shorter reads are at risk of multi-mapping shorter reads to multiple loci (Raghupathy et al., 2018)

Alignment and mapping of the sequences to a reference genome/transcriptome is subsequently carried out. The selection of the same reference genome for mapping libraries to be compared is of importance to avoid introducing innate bias (Frankish et al., 2015). Several different tools can be used for this process, one of the most common is STAR (Conesa et al., 2016; Dobin & Gingeras, 2015). STAR is found to be not only faster, but indicated to produce more uniquely mapped reads (Sahraeian et al., 2017; Schaarschmidt et al., 2020). STAR is additionally preferable for mapping particularly long reads, and is capable identifying both canonical and non-canonical splice junctions (Dobin & Gingeras, 2015).

Having obtained mapped reads, various packages can similarly be used to process, quality-check and transform data to obtain formatted files of gene or transcript counts for significance testing. Samtools allows for sorting and merging of alignment files as well as removal of PCR duplicates (H. Li et al., 2009). HTSeq is a large tool-package for sequence manipulation, such as quality evaluation and trimming of reads, as well as creation of counts tables specifically for differential expression analysis (Anders et al., 2015).

Quality checks of the RNAseq data was carried out using FastQC in a local instance of Galaxy and FastQC files obtained (See Appendix). E16.5 and 8WO axonal and somal samples were mapped to the GENCODE GRCm38 genome using the GENCODE vM25 reference annotation through the STAR mapping tool-package (Dobin & Gingeras, 2015; Frankish et al., 2015, 2019). Clipping was carried out in STAR for RNA from embryonic mice to 5pN 5 and 3pN 94 based on FastQC results (See Appendix). Clipping was not carried out on RNA from adult mice as FastQC results showed it was unnecessary.

Duplicates were not attempted to be removed due to indication of low rate of duplication, and the risk of removing real reads. Filtering was carried out to only consider protein-coding, non-mitochondrial genes. HTSeq was subsequently used to obtain counts tables for further analysis.

Normalisation

Differential expression (DE) analysis is often the primary exploratory output of an RNAseq experiment. DE provides an initial insight into defining features of the datasets of interest. An important aspect for meaningful DE analysis is found within the mapping and counting, however, further consideration must be given to transformations and normalisation of datasets. Visualisation of datasets is used to assess similarities and comparability, such as principle component analysis (PCA) and Kernel density plots (Koch et al., 2018; Lever et al., 2017; Van den Berge et al., 2019). Distribution plots such as Kernel density plots are used to assess the comparability of samples through graphical representation of the distribution of RNA expression in samples. PCA is utilised to explore the overall groupings of samples, however, important consideration must be taken regarding the effect of normalisation techniques on results (Lever et al., 2017).

Normalisation is an essential part of analysis to ensure reliability of findings. Normalisation of data can be incorporated within DE analysis tool-packages, as is seen within DESeq2, or it can be imposed on raw counts following filtering. Normalisation can be divided into three types; 1. normalisation for gene/transcript length length, 2. normalisation for library size or sequencing depth, 3. normalisation for technical artifacts across samples.

Normalisation for transcript length is particularly important as gene-length can create bias towards more reads for longer transcripts (Conesa et al., 2016; Oshlack & Wakefield, 2009). It is carried out using transcripts per kilobase million mapped reads (TPM) based on normalisation for length of the gene/transcript and the number of reads in the sample (Conesa et al., 2016). TPM is calculated by dividing reads by the length of the transcript, followed by normalising to the number of reads in the sample through a per million scaling-factor.

Samples with different library-sizes are normalised to facilitate comparison between heterogenous transcript expression by calculating a scaling factor (Abbas-Aghababazadeh et al., 2018; Conesa et al., 2016). The most utilised methods Upper Quartile (UQ) and Relative Log Expression (RLE), the latter of which is included

within the DESeq2 DE analysis package. RLE normalisation is based on calculating a transformation factor to satisfy the assumption that most genes are not differentially expressed when comparing two samples. The RLE correction factor is calculated by dividing the median of the ratio of reads for each gene in a sample, by the geometric mean across all samples (Abbas-Aghababazadeh et al., 2018). This normalisation is based on negative binomial distribution and applied to all read counts to strengthen the reliability of findings of differential expression analysis (Anders & Huber, 2010). UQ normalisation does not contain an assumption within the statistical framework. For UQ normalisation only RNAs with reads in at least one sample are considered. Each read-count in a given sample is divided by the 75th percentile of reads with counts within that sample and subsequently all read-counts are multiplied by the mean upper quartile across all samples (Abbas-Aghababazadeh et al., 2018; Dillies et al., 2013; Glusman et al., 2013).

Normalisation was optimised to address the experimental objectives: To analyse the differences between somal and axonal samples from E16.5 and 8WO DRG-cells, counts were transformed to TPMs, and UQ normalisation was subsequently carried out to obtain uqTPM values. Normalising for known or unknown technical artifacts was not carried out due to the risk of removing real biological effects (Abbas-Aghababazadeh et al., 2018). To assess the effect of the PGE_2-protocol compared to the control-protocol on axonal samples the counts obtained from HTSeq were imported into the DESeq2 analysis package and consequently underwent RLE normalisation. Kernel plots were created in a local instance of MathWorks MATLAB to assess comparability of axonal and somal samples from E16.5 and 8WO mice. Principle component analysis (PCA) was additionally carried out in MathWorks to assess similarity of axonal and somal control samples from both E16.5 and 8WO mice.

Differential expression analysis

Differential expression analysis is commonly used for finding targets or markers of pathologies or following pharmacological interventions. DESeq2 was used for differential expression analysis. DESeq2 utilises a negative binomial distribution as the probabilistic model and a modified empirical Bayes method to estimate

shrinkage for distribution based on calculations of width of prior distribution of data assessed (Costa-Silva et al., 2017; Lamarre et al., 2018; Love et al., 2014). As previously described, RLE normalisation is an inherent part of DESeq2 analysis, which asserts that most genes are not differentially expressed in the analysis. Depending on the research hypothesis DESeq2 may not be appropriate to explore certain experimental designs (Kukurba & Montgomery, 2015).

To analyse the differences between somal and axonal samples from E16.5 and 8WO DRG-cells DESeq2 was not an appropriate analysis tool due to the expected large differences between the cell compartments, thus increasing the risk of false negatives. uqTPM values for axonal and somal samples were compared using GraphPad Prism V. 7.0 for Mac. Unpaired multiple t-tests with two-stage linear setup procedure of Benjamini, Krieger and Yekuteili to control the false discovery rate. To assess the effect of the PGE_2-protocol compared to the control-protocol on axonal samples the counts obtained from HTSeq were analysed using DESeq2. All coding scripts are included in the Appendix (See A.2).

2.12 Qiagen Ingenuity Pathway Analysis

Pathway analysis of results from differential expression analysis facilitates the interpretation of RNAseq results in the context of previous knowledge of molecular, cellular, and biological functions. Ingenuity Pathway Analysis (IPA) is an advanced tool package allowing for in depth analysis of pathways, not only in comparison to publicly available pathways and ontology databases, but additionally, by comparing to an extensive library of high-throughput datasets (Krämer et al., 2014). IPA contains analytical tools which allow for explorations of predicted Upstream Regulators, Mechanistic Networks, Causal Network Analysis, and Downstream Effects Analysis.

Outputs of DESeq2 and multiple t-tests were uploaded to IPA with regular p-value and log_2 fold change values for pathway analysis (QIAGEN Inc., https://www.qiagenbioinformatics.com/products/ingenuitypathway-analysis) (Krämer et al., 2014). For the assessment of the effect of the PGE_2-protocol compared to the control-protocol in the axon, cut-offs were imposed of regular p-

value<0.05, and log_2 fold-change for downregulated RNAs<-0.5 and log_2 fold-change for upregulated RNAs>0.5. For exploration of changes between the axon and the soma, cut-offs were imposed of regular p-value<0.05 and log_2 fold change for downregulated RNAs<-1 and upregulated RNAs>0.6. Comparative analysis was carried out for results from E16.5 and 8WO DRG-cells to assess the similarities of canonical pathways and upstream regulators.

Chapter 3: Compartmentalised culturing of DRG-cells for studies of axonal growth and *in vitro* modelling

3.1 Introduction

Modelling disease is a key aspect of preclinical research, allowing researchers to explore fundamental aspects of pathophysiological progression, which are otherwise elusive in a clinical setting. Animal models have been used widely to explore pathophysiological changes of chronic pain states, with a plethora of different methods used to induce and explore different types of pain such as neuropathic pain and inflammatory pain (Burma et al., 2017; Kaliyaperumal et al., 2020; Muley et al., 2015). The use of cell-based, or *in vitro*, models provide a unique opportunity to explore basic preclinical research aims, while adhering closer to NC3R principles for animal research (reduction, replacement, and refinement) (*The 3Rs | NC3Rs*, n.d.). The use of *in vitro* models facilitates studies of individual tissues or cell-types through a broad range of experimental tools to manipulate and quantify changes. *In vitro* models are a valuable preclinical tool found particularly well suited to explore nociception, as it allows for the study of sensory hyperexcitability without exposing animals to undue stress. As previously discussed (See Chapter 1), dorsal root ganglion (DRG) cultures contain sensory neuronal cells which innervate peripheral tissues including skin and muscle, responding to tactile and noxious stimuli. It is generally accepted that changes to DRG-cells, specifically changes affecting the responses to stimuli, play a key role in the manifestation of chronic pain (Berta et al., 2017). The isolation and culturing of DRG-cell cultures are therefore well-suited to study nociception and the development of sensitisation (Fornaro et al., 2018; Lin & Chen, 2018; Unsain et al., 2014).

3.1.1 Compartmentalised chambers facilitate the study of axonal growth

Mice and rats are the most commonly used animals in both *in vivo* and *in vitro* models (Ellenbroek & Youn, 2016). While rats were previously more common in *in vivo* models, the use of mice has significantly increased over recent years. This is at least partially due to developments in tools for genetic manipulation in mice, allowing for further manipulation of both *in vivo* and *in vitro* models. Primary cell cultures from isolated DRGs of murines have proven particularly useful to study neurite and axonal networks. Several labs have specialised in cell culture methods

that allow for the exploration of changes localised to the periphery of sensory neurons through the use of compartmentalised chambers (Gumy et al., 2011; Taylor et al., 2005; Unsain et al., 2014; Willis & Twiss, 2011). These chambers are designed with the purpose of facilitating axonal projections to develop and grow, either through pores in a membrane or microgrooves in microfluidic chambers and into a separated compartment (Figure 3.1).

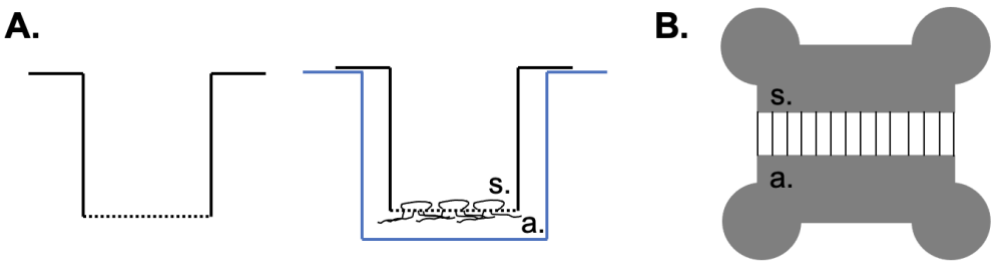

Figure 3.1: *Compartmentalised chambers facilitate the growth of an axonal network in a separate compartment.* ***A.*** *Porous membrane chambers are inserts for wells which contain a porous membrane, shown to separate the growth of cell bodies in the upper compartment (somal, s.), while axons pass through the pores to the lower compartment (axonal, a.).* ***B.*** *Microfluidic chambers facilitate compartmentalisation with fluidic isolation as two compartments are connected through microgrooves which only axons pass through*

Microfluidic chambers allow for fluidic separation, thereby facilitating localised stimulation/treatments to specific cellular compartments (axon or cell body, Figure 3.1B) (Taylor et al., 2005). In porous membrane chambers, also known as modified Boyden chambers, the separation is facilitated by a membrane which only axons pass through, however, in this case there is no fluidic separation (Figure 3.1A) (Willis & Twiss, 2011). Porous membrane chambers are utilised despite this disadvantage, as many more cells can be seeded within these chambers. This makes porous membrane chambers ideal for compartmentalised extraction of cellular material for further studies of molecular biology (Taylor et al., 2005; Willis & Twiss, 2011). Consequently, the porous membrane chambers facilitate compartmentalised extraction of RNA from the axons and the soma, allowing the study of changes localised to one compartment of neuronal cells.

3.1.2 Maturity affects the transcriptome of sensory neuronal cells

DRG-cells can be isolated from both adult and embryonic mice, each with advantages and disadvantages. Protocols using DRG-cells from mice have been in use since the 1970's, initially presented with cells from adult animals (Scott, 1977), clearly demonstrating the benefits of a culture with neurite outgrowth. DRG-cells from adult animals additionally allow for the preceding initiation of *in vivo* models of disease, the effects of which can subsequently be studied *in vitro*. However, the maturity of the cell upon harvest has been indicated to inversely correlate with the rate of regeneration of axons in culture (Chierzi et al., 2005; Verma et al., 2005). Axon regeneration is dependent on the development of a new growth cone, a process which is driven by localised protein translation. An intrinsic decrease in protein translation and synthesis machinery in mature sensory neuronal cells is found to decrease, but not inhibit, successful axonal regeneration (Chierzi et al., 2005; Verma et al., 2005).

Using compartmentalised chambers, the differences in the transcriptome of DRG-cells from rats of different maturity has been explored (Gumy et al., 2011; Vogelaar et al., 2009). qPCR results showed stable expression of β-*actin* mRNA in axons, a known component of processes leading to axonal guidance and growth, despite the maturity of the cells (Vogelaar et al., 2009). However, a look at broader transcriptomic changes through microarray analysis showed differences in core cell cycle RNAs and RNAs associated with axonal growth (Gumy et al., 2011). Interestingly, RNAs associated with cellular assembly and, more specifically trafficking, were found predominantly expressed in embryonic axons. These results correlate with embryonic neuronal cells inherently showing enhanced regeneration of axons compared to adult neuronal cells (Chierzi et al., 2005). Cells from adult rats were conversely found to retain mRNA levels in the axon to an extent indicating ongoing localised translation, suggesting that while decreased, localised translation remains a retained mechanism (Vogelaar et al., 2009). Collectively, the studies show that while axonal regeneration is maintained in sensory neuronal cells of the PNS, the maturity of the cell does affects the axonal growth through changes to trafficking and translation of local RNAs (Chierzi et al., 2005; Vogelaar et al., 2009).

In contrast with RNAs associated with axonal growth, RNAs associated with inflammation and immune response have in microarray experiments been shown to be increased in the axons of mature cells (Gumy et al., 2011). These results were argued to support a novel role of mature sensory neuronal cells in nociceptive signalling and hyperalgesic priming mechanisms, compared to embryonic cells. However, RNAseq of DRGs from embryonic and adult mice has shown that while maturation of sensory cells introduces transcriptomic variation, a large proportion of differentially expressed genes are already present at embryonic day 18.5 (E18.5) (Smith-Anttila et al., 2020). Differences associated with the localisation of DRGs along the spinal cord (sacral and adjacent lumbar) were explored, from both embryonic and adult mice by sequencing DRG-cells. It was concluded that, despite variations, a unique phenotype of sensory neurons innervating differential areas, in this case the pelvic viscera, was already established by E18.5 (Smith-Anttila et al., 2020). Similarly, the development of TRP-channels has been shown to gradually progress from E12, with morphology as well as capsaicin responses equivalent to that of DRG-cells from adult mice, established at E14.5 (Hjerling-Leffler et al., 2007). Developmental changes from pre- to postnatal are additionally observed in the sensitivity to growth factors including NGF and GDNF, as NGF particularly has been shown to be crucial for the development of nociceptors and axon growth in pre- and early post-natal stages (Bracci-Laudiero & De Stefano, 2016; Denk et al., 2017; Koltzenburg, 1999). While all nociceptors express TrkA prenatally, requiring the growth factor for development, postnatally the non-peptidergic subpopulation of nociceptors lose the receptor, instead responding to GDNF through Ret expression (Denk et al., 2017; Koltzenburg, 1999). Collectively, the growth factors promote axonal growth and are essential for nociceptor development.

Consequently, while differences are clear, evidence shows that cells from embryonic mice exhibit a sensory neuronal phenotype, and are capable of facilitating regular axonal RNA transport, as well as respond to capsaicin activation.

3.1.3 Considerations for designing an *in vitro* model with sensory neuronal cells

To assess the changes induced by a specific model of disease, the environment considered the control conditions must be tightly regulated. As previously established, variations are naturally introduced, for example through maturity of the cells and following external stimulus. Therefore, all external factors such as media conditions, should be controlled and optimal for healthy normal growth. Extensive research has shown the role of neurotrophins on healthy neuronal and axonal growth of sensory neuronal cells of the PNS (E. J. Huang & Reichardt, 2001; Markus et al., 2002). Therefore, the cell culture medium used in these experiments was supplemented with nerve growth factor (NGF) and glial cell line-derived neurotrophic factor (GDNF), to optimise axonal regeneration. Furthermore, DRG-cultures are notoriously diverse cell-cultures, thus to explore changes specifically in sensory neuronal cells, aphidicolin (APH), a known antimitotic compound, was utilised to minimise proliferation of non-neuronal cells (LoPresti et al., 1992; Mundy et al., 2010).

Finally, glucose is a key nutrient in cell culture medium and is essential for neuronal growth. However, research has shown that even short periods of hyperglycaemia can induce abnormal axonal function, inhibit axonal regeneration and axonal degeneration, as well as cause neuronal death (Dewanjee et al., 2018; Feldman et al., 2019; Gumy et al., 2008; Vincent et al., 2005). It was therefore of particular importance to ensure that DRG-cells were not exposed to high glucose conditions in culture, mimicking a neuropathic condition. Diabetic neuropathy is the most common type of neuropathy, caused by hyperglycaemia which trigger a number of damaging pathways ultimately resulting in DNA damage, nerve dysfunction or even nerve death (Callaghan et al., 2012). Diabetic peripheral neuropathy (DPN) is observed in patients with type 1 diabetes where insulin production is inhibited as the beta-cells in the pancreas are broken down in an autoimmune reaction, thereby preventing regular breakdown of glucose (van Belle et al., 2011). It is generally accepted that imbalances of metabolic and physiological pathways in DPN cause damage to microvasculature supplying nerves in the periphery, inducing a toxic

environment. An increase in polyol and oxidative stress pathways is shown to play a key role, along with an increase of inflammatory mediators and advanced glycation end-products (AGEs). Additionally, activation of the JAK/STAT and mTOR pathways have been shown to play a role (Arora & Singh, 2013; Bestall et al., 2018; Dewanjee et al., 2018). These imbalances are caused by hyperglycaemia and associated with increased plasma glucose levels. Time-periods as low as 2 hours (H) of hyperglycaemia, are observed as sufficient to initiate destructive pathways of oxidative stress (Bestall et al., 2018; O'Brien et al., 2014; Vincent et al., 2005). It was of particular importance to avoid variations attributed to conditions mimicking diabetic neuropathy in the control environment, therefore glucose concentrations were of concern when establishing standard protocols.

3.2 Hypothesis and objectives

The hypothesis of this chapter was that growth of DRG-cells in compartmentalised chambers facilitates the development of an *in vitro* model to study changes localised to the cell body and axons of sensory neuronal cells.

The objectives were to:

- establish the optimal culturing-conditions for DRG-cells from embryonic mice to extend healthy neurite outgrowths *in vitro*
- establish the culture of DRG-cells in compartmentalised chambers to allow growth of axons into a membrane-separated compartment, facilitating RNA extraction from sub-cellular domains (axons vs cell body)

3.3 Methods

DRGs were surgically isolated from embryonic day 16.5 (E16.5) mice and either immediately placed in dishes for explant culturing or subjected to dissociation prior to culturing. Growth factors (NGF, GDNF and APH) were added to the culture medium to promote neuronal growth and inhibit growth of non-neuronal cells. DRG-explants were grown in dishes in medium containing either 1000mg/ml (low glucose, LG) or 4500mg/ml (high glucose, HG) of glucose (see detailed methods in Chapter 2.2).

The axonal length was assessed using brightfield microscopy on day 3, 5 and 7 of growth after seeding of DRG-explants. The axonal network was assessed as axon plate coverage on day 6 and day 8 of growth after seeding of dissociated DRG-cells. Through brightfield microscopy and Image J software, the percentage coverage of the dish was established (see detailed methods in Chapter 2.5).

The growth of DRG cultures in porous membrane chambers was assessed for separation of cell compartments using immunocytochemistry for DAPI and acetylated tubulin (see detailed methods Chapter 2.6). The quality of RNA from somal and axonal compartments was assessed to ensure satisfactory material was obtained. RNA quality was assessed through electrophoresis (see detailed methods Chapter in 2.7).

3.4 Results

3.4.1 DRG-cells grown *in vitro* developed axonal networks

E16.5 DRG-explants were grown for 7 days, and images of the axons were taken on day 3, 5 and 7 to assess the length of the axons. Representative images are shown (Figure 3.2).

A: Day 3

Axonal growth in LG media

Axonal growth in HG media

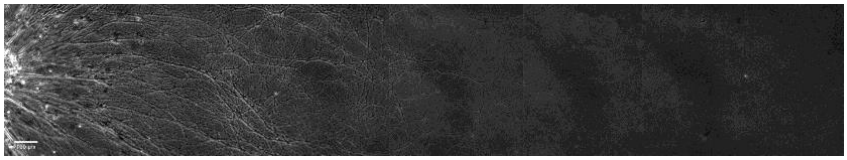

B: Day 5

Axonal growth in LG media

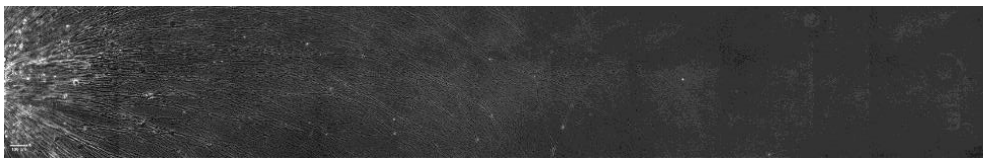

Axonal growth in HG media

C: Day 7

Axonal growth in LG media

Axonal growth in HG media

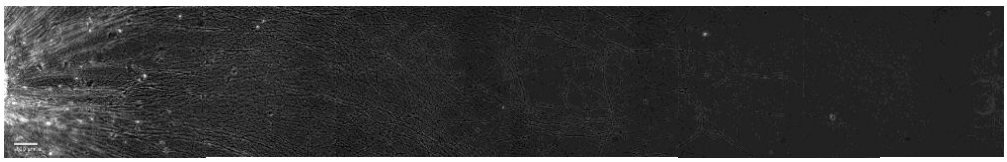

Figure 3.2: *Brightfield microscopy images show no effect of glucose concentration on axonal growth of DRG explants. Representative images are shown from* ***A.*** *day 3,* ***B.*** *day 5 and* ***C.*** *day 7. The growth of the axons is followed from the edge of the explant to the edge of the axonal network, allowing for a comparison of the growth between the glucose conditions over time. The photos displayed are randomly chosen from 3 dishes with 2 explants grown for each condition.*

Representative images show only minor effects of glucose concentration appeared to manifest on axonal length (Figure 3.2). A few particularly long axons were observed on day 3, which appeared to have disappeared by day 5 for both LG and HG conditions. An additional assessment of axon growth was carried out by measuring the density of the axonal network of dissociated DRG-cells.

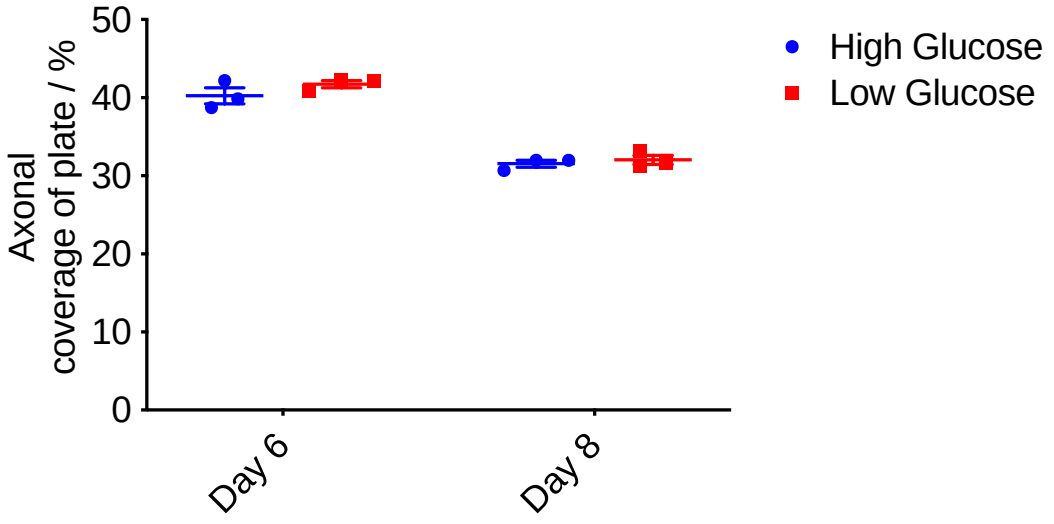

Figure 3.3: *The effect of glucose concentration on axonal network density. DRGs were grown in dishes in either low or high glucose media and the density of the axon network was measured as coverage of the plate (%) on day 6 and day 8 using Image J software. 3 dishes were evaluated with an average of 15 (n~15) images taken per dish. The average for each dish was plotted, as well as the mean and SEM for each condition. No significant difference was found between the density of the axonal networks grown in high or low glucose concentration using 2way ANOVA*

No difference in the axon coverage of the dish was found when comparing LG and HG media conditions (Figure 3.3). A consistent decline in coverage for both LG and HG media conditions was observed between day 6 and day 8, indicating a degeneration of the axonal network. This degeneration of the axonal network could be due to the extended period of culturing; therefore, the culturing period was limited to 7 days going forward.

Evaluations of axonal growth, measured as length of axons and density of axonal network, confirmed the successful culturing of E16.5 DRG-cells with healthy axonal networks. Glucose concentration in cell culture medium was found to not affect axon development, measured as both axonal length and network density. Consequently, LG media was used in all future experiments.

3.4.2 Porous membrane chambers allowed compartmentalised growth of DRG-cells

Having established healthy neurite outgrowths from DRG-cells *in vitro*, the use of porous membrane chambers for culturing was commenced. DRG-cells were stained

using immunocytochemistry to show the growth of the cell cultures across the membrane and to confirm the exclusive growth of axons below the membrane.

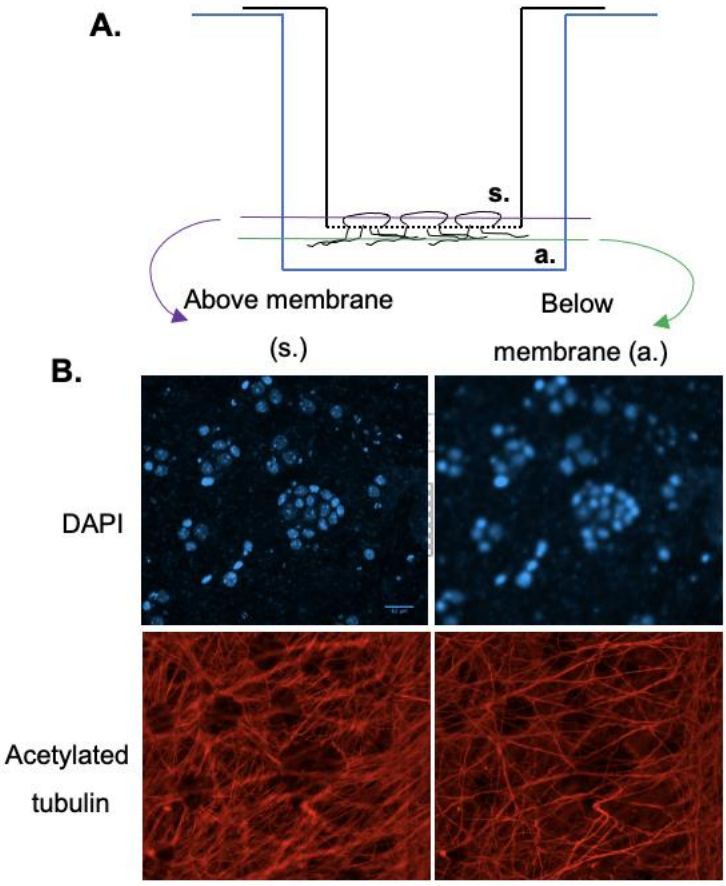

Figure 3.4: *Porous membrane chambers facilitate the development of a lower compartment with exclusively axonal growth.* ***A.*** *Diagram of a porous membrane chamber in a well with cells growing in the upper compartment and axons passing through the membrane to the lower compartment. Two sections are indicated corresponding to microscopy planes of immunocytochemistry stains* ***B.*** *Representative images of dissociated DRG-cells grown in a porous membrane chamber stained for DAPI (nuclei) and acetylated tubulin (axons), clearly showing the presence of an axonal compartment free of nuclei.*

The DAPI stain shows cell bodies in clear focus only in the focal plane above the membrane. Although fluorescence can be detected from the lower compartment, no nuclei are in focus within the lower plane. Acetylated tubulin stains separate axonal networks above and below the membrane with distinct demarcated areas in the upper compartment corresponding to the location of cell bodies. This data confirms that an axonal network developed below the membrane with no cell bodies moving through the pores.

3.4.3 Porous membrane chambers allowed separate extraction of RNA from axonal and somal compartment

To ensure the quality of the RNA extracted from the somal and axonal compartment of the porous membrane chambers, RNA was obtained from dissociated DRG cells. Several replicates were carried out with 25 DRGs dissociated and seeded in porous membrane chambers with LG media. RNA extracted from the somal and axonal compartments and the RNA quality was assessed through automated electrophoresis.

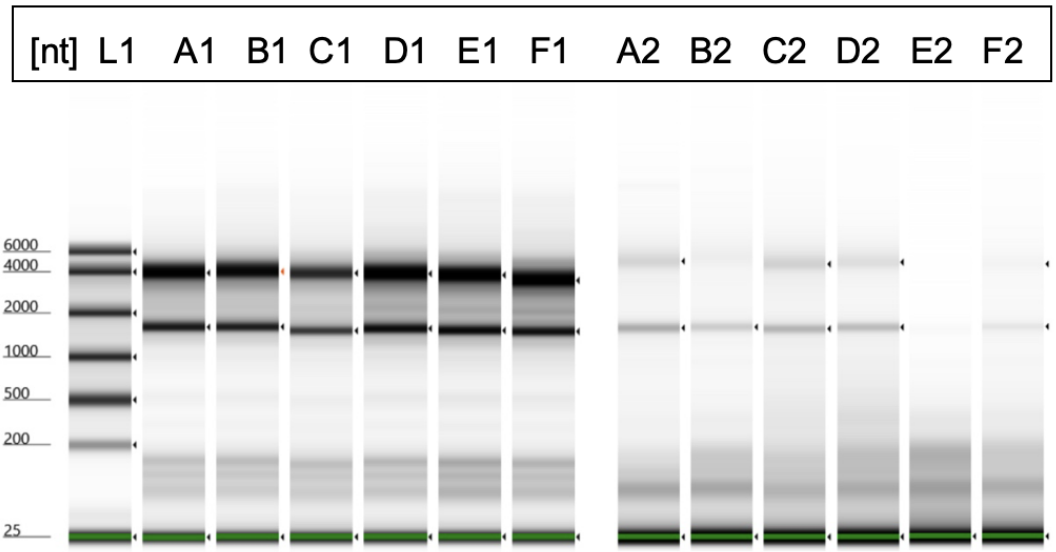

	A1	*B1*	*C1*	*D1*	*E1*	*F1*	*A2*	*B2*	*C2*	*D2*	*E2*	*F2*
RIN	10.0	9.9	9.8	9.9	9.9	9.8	9.1	8.4	8.1	8.0	2.3	6.4

Figure 3.5: *Automated electrophoresis confirms good quality RNA is extracted from the somal compartment, while the quality of axonal RNA varies. TapeStation results show quality of RNA extracted from somal (A1-F1) and axonal (A2-F2) samples showing bands for 28S (upper band) and 18S (lower band) ribosomal RNA. A1-F1 shows clear bands, with 28S appearing slightly stronger, as is expected for good quality RNA, which is supported by high RIN scores. A2-F2 show weaker bands, with two bands occurring in most but not all cases, corresponding to similarly varied RIN values*

Distinct bands were observed for both 28S and 18S ribosomal RNA from somal samples, with corresponding high RIN values. Less intense, but nonetheless mostly consistent, bands were visible for axonal samples. Despite the lower quantity, most axonal samples were assigned high RIN values as well, showing promising quality despite low abundance. For all subsequent experiments with porous membrane

chambers, 25 DRG explants from E16.5 mice were dissociated to obtain RNA of sufficient quantity and quality.

3.5 Discussion

3.5.1 Compartmentalised chambers facilitated separate extraction of axonal and somal RNA from DRG-cells

In this chapter, the culturing of DRG-cells from embryonic mice was assessed to optimise favourable conditions for growth of an axonal network, ultimately facilitating compartmentalised extraction of RNA. The effect of glucose concentration in media on axonal growth and development was assessed, by evaluating the length of axons as well as the density of the axonal network in a high (4500mg/ml, HG) and low (1000mg/ml, LG) concentration of glucose. High glucose concentration has been presented as *in vitro* models of diabetic neuropathy accompanied by abnormal axonal growth (Bestall et al., 2018; Dewanjee et al., 2018; Feldman et al., 2019; Gumy et al., 2008). As little as 2H of exposure to hyperglycaemic conditions has been found sufficient to induce changes to neuronal cells (Vincent et al., 2005). Despite this, no difference in axonal growth was established when comparing cells grown in LG and HG conditions. This could be due to the concentration in HG media being insufficient to induce a hyperglycaemic reaction. However, while the concentration was insufficient to induce structural changes to the axon, mechanistic or functional changes could not be refuted. Activation of oxidative stress pathways have been associated with short term exposure to hyperglycaemic conditions (Vincent et al., 2005). Consequently, all future experiments were carried out with LG media, to avoid any possible effect of HG media mimicking a model of DPN induced by hyperglycaemia *in vitro*. To further promote the development of an axonal network, growth factors NGF, GDNF, and APH were added to the media to promote neuronal growth and limit growth of non-neuronal cells. Following the validation of optimal culturing conditions, the use of porous membrane chambers was commenced. Porous membrane chambers were used for the separate extraction of RNA from the neurite compartment, facilitating the study of the axonal transcriptome (Unsain et al., 2014; Willis & Twiss, 2011). RNA samples were obtained from the axonal compartment, the

quality of which was assessed using automated electrophoresis. Two bands corresponding to 28S and 18S ribosomal RNA appeared for axonal RNA, which, despite being faint, was promising considering the smaller quantity of RNA collected. It is, however, worth considering whether RNA extracted from the axonal compartment would be expected to contain 28S and 18S ribosomal RNA in the same relative ratio as that of whole cells or somal RNA. Overall, in-depth exploration of the axonal transcriptome is needed to characterise what should be considered normal expression patterns in the axon.

3.5.2 Conclusions

Successful compartmentalised culturing of DRG-cells from E16.5 mice was established in porous membrane chambers exhibiting an axonal network in a compartment free of cell bodies. The establishment of a successful compartmentalised model of sensory neuronal cells allows for the study of local changes in the axon. This model is of particular interest to characterise the axonal transcriptome, as well as to explore the localised changes in the axon of an *in vitro* model of sensitisation.

Chapter 4: The development of an *in vitro* model of sensitisation

4.1 Introduction

Both *in vivo* and *in vitro* models have been developed to explore the defining pathways and functional genomics of sensitisation. *In vivo* models carry inherent benefits as behavioural symptoms can be directly measured revealing functional effects of physiological conditions (Burma et al., 2017; Kaliyaperumal et al., 2020; Miller & Malfait, 2017). However, the measurements of functional effects are vulnerable to human bias in scoring of behaviours, and often require additional measurements at cellular and molecular levels to infer conclusions. Moreover, the use of *in vivo* models is laborious and often time-consuming, with the development of models of chronic pain requiring weeks to months (Miller & Malfait, 2017). *In vitro* models of nociception and sensitisation are an attractive alternative, with inherent benefits regarding the availability of tissue, the timeframe of the experimental design, and the diversity of experimental protocols available to manipulate and analyse cell mechanisms and changes associated with pathological processes.

4.1.1 DRG-cultures utilised for *in vitro* models of hyperalgesia

Extraction and growth of DRG cells has been perfected in experimental protocols for the use in *in vitro* models (Fornaro et al., 2018; Lin & Chen, 2018). Primary DRG cultures are heterogenous cell cultures facilitating the study of biological processes and molecular pathways in single or multiple cells. *In vitro* models specifically allow the study of different compartments of cells as healthy neurite growth is established in culture due to glial cell support. Consequently, DRG-cells are a preferable alternative to single-cell-type cultures, due to translational advantages, in addition to a highly advantageous resource for the study of localised pathophysiological changes, including neurite physiology, functional genomics, neurotransmission, and biomolecular signalling pathways (Fornaro et al., 2018; Lin & Chen, 2018; Unsain et al., 2014).

In vivo models of chronic pain are commonly induced through either surgical procedures such as partial nerve ligation, constriction injury, tearing the medial meniscus or transecting the ACL, or chemical interventions; such as injections of

inflammatory mediators including monosodium iodoacetate, carrageenan or capsaicin (Burma et al., 2017; Kaliyaperumal et al., 2020). These variations are crucial to model different types of chronic pain, with each model presenting with unique timelines and symptoms. *In vitro* models of sensitisation are similarly induced in different ways to mimic varying aspects and modalities of chronic pain. DRGs can be isolated from naïve animals, as well as *in vivo* models of chronic pain, to study pathological changes at different stages *in vitro*. Numerous specific *in vitro* models of sensitisation with murine DRG-cells have been developed including inflammatory nociception, diabetic neuropathy, arthritic neuropathy and axonal injury (Chakrabarti et al., 2020; Gardiner & Freeman, 2016; J. Ma et al., 2021; Peeraer et al., 2011; Persson et al., 2013; Vyklický & Knotková-Urbancovä, 1996). Exposing sensory neuronal cells to inflammatory mediators or toxins capable of targeting relevant receptors known to activate nociceptive pathways, are common ways to initiate functional hyperalgesia in cell cultures (Atmaramani et al., 2020; J. Ma et al., 2021; Segond von Banchet et al., 2005). However, as previously discussed, specific conditions associated with a particular causal mechanism can additionally be modelled, such as increased glucose concentration for diabetic neuropathy (Gardiner & Freeman, 2016; Peeraer et al., 2011) (see also Chapter 3).

A review from 2016 discussed the most common *in vitro* models of osteoarthritis, one of the main causes of disability worldwide (Johnson et al., 2016). However, in doing so the paper demonstrated what is simultaneously the biggest strength and weakness of *in vitro* models: they are designed to assess a singular aspect of a given disease. In the most common *in vitro* models of osteoarthritis, the disease progression was modelled to explore tissue degradation of cartilage or the role of inflammatory pathways in synovial fluid, important aspects of pathology, however, failing to address the primary symptom of osteoarthritis: chronic pain or sensitisation. This stresses the importance of inducing experimental models to mimic specific pathways of the disease within specific cells of interest, in order to draw conclusions which can be applied beyond *in vitro* simulations.

DRG-cells are presented as an attractive option for an experimental model of sensitisation with inherent benefits for studying pathological progression of chronic

pain through induction of sensitisation mimicking that of inflammatory or neuropathic pain.

4.1.2 PGE_2-exposure induces sensitisation in DRG-cells

Prostaglandin E_2 (PGE_2) is a well-established mediator of pain pathways, associated with both nociceptive, inflammatory, and neuropathic pain (L. Chen et al., 2013; J. Huang et al., 2006; Kawabata, 2011; St-Jacques & Ma, 2014; Sugimoto & Narumiya, 2007) (see also Chapter 1). As previously discussed, PGE_2 is a known mediator of peripheral sensitisation (L. Chen et al., 2013; L.-Y. M. Huang & Gu, 2017). The effects within the peripheral nervous system (PNS) are mediated in part through direct interactions with receptors EP1, EP3, and EP4 in particular, triggering changes to the activity of ion channels including TRPV1-, and NaV-channels, as well as purinergic P2X3 receptors, ultimately inducing hyperexcitability of nociceptors (L. Chen et al., 2013; Kawabata, 2011; C. Wang et al., 2007). PGE_2 is a direct downstream product of COX-2 enzyme activity, a pathway targeted by nonsteroidal anti-inflammatory drugs (NSAIDs) used widely to treat inflammatory pain by inhibiting COX thereby preventing prostaglandin production (L. Chen et al., 2013).

Increases in PGE_2 have been linked to the development of chronic pain in osteoarthritis, through binding of the EP4 receptor in sensory neurons (Clark et al., 2008; A. S. Lee et al., 2013; Southall & Vasko, 2001). Activation of the EP4 receptor increases cAMP levels, which is known to activate three downstream pathways in particular; PKA (protein kinase A), PKC (protein kinase C) and Epac (exchange proteins activated by cAMP) (L.-Y. M. Huang & Gu, 2017; W. Ma & St-Jacques, 2018). PGE_2/EP4/cAMP/PKA, PGE_2/EP4/PKC, and PGE_2/EP4/Epac pathways are associated with increased IL-6, NGF, SP, and CGRP levels, as well as sensitisation of TRPV1- and P2X3R-receptors in DRGs, driving hyperalgesic priming of nociceptors (L.-Y. M. Huang & Gu, 2017; A. S. Lee et al., 2013; St-Jacques & Ma, 2011).

Consequently, PGE_2 is commonly used as an inducer of models of sensitisation, often in combination with other mediators of nociceptive neuroplastic pathways (Khomula et al., 2019; A. S. Lee et al., 2013; Segond von Banchet et al., 2005). The

specific effects of PGE_2, as well as the stabilised analogue 16,16-dimethyl PGE_2, on murine DRG-cells has been explored (Table 4.1).

Reference	**Cells**	**PGE_2 concentration**	**Experimental output**
(Southall & Vasko, 2001)	Dissociated DRG from rat	20min 100nM PGE_2 (acute)	- Significant increase in cAMP protein following acute PGE_2 exposure of DRG-cells
(Momin et al., 2008)	Dissociated DRG-cells from rat	4min 10µM PGE_2 (acute)	- Significantly increased excitability of small-diameter DRG-neurons measured as frequency of action potentials following depolarising current, along with an increased resting membrane potential (RMP)
(W. Ma, 2010)	DRG explants from rat	3-72 hour (H) 1, 10 or 100µM 16,16-dimethyl PGE_2 (prolonged)	- 6-48H of 100µM 16,16-PGE_2 significantly increased *pre-protachykinin* mRNA levels. 6-72H 100µM 16,16-PGE_2 significantly increased *CGRP* mRNA levels - 24H 10-100µM 16,16-PGE2 significantly increased SP peptide levels. 72H 1-10µM 16,16-PGE2 significantly increased CGRP peptide levels and 6-72H 100µM 16,16-PGE_2 significantly

			increased CGRP peptide levels. 3-48H 100µM 16,16-PGE_2 significantly increased SP peptide levels. 100µM 16,16-PGE_2 significantly increased NGF peptide levels - 24H 1, 10 and 100µM 16,16-PGE_2 significantly increased the expression of EP4. 24H 1, 10 and 100µM 16,16-PGE_2 significantly increased the protein levels of phosphorylated pan-PKC
(W. Ma & St-Jacques, 2018)	Dissociated DRG-cells from rat	1H 50µmol/L PGE_2 (acute)	- Significantly increased EP4 externalisation was observed following PGE_2 in a process reliant on both intracellular and extracellular Ca^{2+} as well as CaMKII signalling - Increased CGRP peptide following EP4 externalisation
(Segond von Banchet et al., 2005)	Dissociated DRG-cells from rat	10µM PGE_2 every 2H for 2days (prolonged)	- A significantly increased percentage of cells expressing NK1 receptor-like (a GPCR which binds SP) was observed following prolonged PGE_2 exposure

(Rush & Waxman, 2004)	Dissociated DRG-cells from mouse	1H 1 or 10µM PGE_2 (acute)	- NaV1.9 currents were significantly increased following PGE_2 exposure, measured in small C-fibre sensory neuronal cells
(St-Jacques & Ma, 2011)	DRG explants from naïve rats or rats with partial sciatic nerve ligation (PSNL)	3-72H 1, 10, 100µM dimethyl 16,16-PGE_2 (prolonged)	- *In vivo* induced PSNL induced increased expression of EP4 in DRG-cells - Significant increase in PGE_2 was observed in the ipsilateral sciatic nerve segment 48H after PSNL. Inhibitors of PKA, PKC and MAPK suppressed 100µM 16,16-PGE_2 induced IL-6 increase in DRG-cells - 10, 100µM 16,16-PGE_2 significantly increased *Il6* mRNA after 20H, through signalling with PKA, PKC and ERK/MAPK in DRG-cells - 8H 100µM 16,16-PGE_2 of DRG-cells significantly increased phosphorylation of PKA, ERK/MAPK, p65 of NF-κB and CREB

Table 4.1: *The effect of PGE_2, or stabilised PGE_2 analogue 16,16-dimethyl PGE_2, on murine DRG-cells explored through different experimental protocols assessing excitability, functional genetics, and inflammatory signalling pathways*

Acute (up to 1H) PGE_2 exposure induces increased externalisation of EP4 along with increased CGRP and cAMP expression in DRG-cells, while the activity of nociceptor

cells, measured as NaV1.9 currents and APs, is increased, showing neuroplastic mechanisms facilitating a sensitised state are triggered even following short exposure (W. Ma & St-Jacques, 2018; Momin et al., 2008; Rush & Waxman, 2004; Southall & Vasko, 2001). Prolonged PGE_2 exposure (>3H) is associated with increased expression of receptors of NK1 receptor-like IR and EP4, increased peptide levels of nociceptive mediators CGRP, SP, and NGF, and mRNAs *pre-protachykinin* and *CGRP*, showing effects on both transcriptional and translational level to collectively induce a sensitised state (W. Ma, 2010; Segond von Banchet et al., 2005; St-Jacques & Ma, 2011).

Consequently, prolonged exposure to PGE_2 is found to induce a sensitised state in nociceptors mediated through EP4 induced signalling pathways with PKA, PKC, and ERK MAPK, as well as increased levels of transcription factors p65 NF-κB and CREB, to increase externalisation of EP4 as well as drive increases to inflammatory mediators including SP, CGRP, and NGF, collectively presenting as increased excitability of sensory neuronal cells (St-Jacques & Ma, 2011).

4.1.3 Measuring hyperexcitability of nociceptors *in vitro*

Preclinical assessments of the effect of PGE_2 on *in vitro* cultured DRG-cells can be approached in numerous ways. PGE_2 is found to induce hyperexcitability in DRG-cells, measured as increased NaV1.9 currents (Rush & Waxman, 2004), as well as a reduced hyperpolarisation period (Kasai & Mizumura, 2001). As previously discussed, the excitability of sensory neuronal cells is a direct measurement of the state of the cell, with sensitisation manifesting as increased excitability, exhibiting lowered threshold to trigger an action potential, increased frequency of action potentials and shortened refractory period (see also Chapter 1). Additionally, an increase in intracellular Ca^{2+}, as well as evoked Ca^{2+} transients, have been shown to directly correlate with increased excitability of sensory neuronal cells following prolonged inflammation (Lu & Gold, 2008). To measure the excitability of neuronal cells, they are exposed to depolarising agents, which cause an increase in the membrane potential triggering an action potential. During an action potential the membrane permeability to Ca^{2+} rapidly increases (Bahar et al., 2016; Rienecker et al., 2020). Increased Ca^{2+} permeability, as well as release from intracellular stores,

induces increased cytosolic Ca^{2+} concentration, measured as Ca^{2+} transients. The Ca^{2+} transients consequently show the excitability of the neuronal cell.

As discussed previously, there is a large diversity of cell-types within DRGs, including both neuronal and non-neuronal cells (see also Chapter 1). With a focus on the development of sensitisation, there was a particular interest in measuring the activity level of cells following nociceptive stimulation. Therefore, it was of importance to find a method that allowed for the measure, specifically, of the excitability of nociceptors. Capsaicin depolarises nociceptors by binding the TRPV1 receptor, opening the cationic pore to Na^+, K^+ and Ca^{2+}, thus inducing depolarisation and an action potential (Caterina et al., 1997; Fattori et al., 2016; Hayes & Tyers, 1980; Touska et al., 2011; Wood et al., 1988). In contrast, an increase in the extracellular K^+ concentration, created through exposure to KCl, depolarises all cell-subtypes sufficiently to induce an action potential (Rienecker et al., 2020). Measurements of Ca^{2+} transients following exposure to specific depolarising agents can thereby provide an insight into the excitability of nociceptors of DRG-cultures.

The hyperexcitability induced by PGE_2 is shown to be mediated through transcriptional and translational changes following prolonged exposure. Specifically, PGE_2 has been shown to interact with NGF in inflammatory and neuropathic pain states to facilitate neuroplastic pathways of sensitisation (Kasai & Mizumura, 2001; W. Ma, 2010). Increases in NGF expression, as well as *Ngf* mRNA, has been found in several chronic disease states, both in pre-clinical and clinical settings, including osteoarthritis (Iannone et al., 2002; Schmelz et al., 2019). NGF has been linked to phosphorylation of receptors, including TRPV1 and P2X3, as well as increased expression of neurotransmitters, including SP and CGRP, ultimately inducing a sensitised state in nociceptors in inflammatory and neuropathic pain states (Denk et al., 2017; Wise et al., 2021). NGF is shown to be capable of directly increasing PGE_2 in mast cells, in addition to NGF driving intracellular mechanisms through cAMP and PKA and increases in CGRP in neuronal cells pathways closely linked to PGE_2 (Marshall et al., 1999; Stein et al., 2009). Consequently, an increase

in *Ngf* mRNA shows an increase in inflammatory and neuropathic pain pathways in DRG-cells, as are expected from prolonged exposure to PGE_2.

Within this chapter, the effect of prolonged exposure to PGE_2 on sensory neuronal cells was assessed by measuring excitability of nociceptors through Ca^{2+} transients and activation of neuroplastic inflammatory pathways through *Ngf* mRNA expression.

4.2 Hypothesis and objectives

The hypothesis of this chapter is that prolonged exposure to PGE_2 induces a sensitised state in DRG-cells established through neuroplastic changes.

The objective was to:

- induce a state of hyperexcitability in DRG-cells through prolonged exposure to PGE_2, thereby creating an *in vitro* model of sensitisation
- validate sensitisation of DRG-cells through measurements of somal *Ngf* mRNA and excitability of nociceptors

4.3 Methods

Dissociated DRG-cells from E16.5 mice were exposed to PGE_2 for 24 hours (H) every 2H to maintain a concentration of 10µM PGE_2, established based on previous studies for experimental framework, including concentration of PGE_2 and exposure-time (W. Ma, 2010; Rush & Waxman, 2004; Segond von Banchet et al., 2005). Control cells were treated with vehicle only (phosphate-buffered saline, PBS) every 2H to mimic the experimental design (see detailed methods in Chapter 2.3).

The functional validity of the model was assessed using two protocols: Ca^{2+} imaging and RT-qPCR.

4.3.1 Ca^{2+} imaging of capsaicin-induced excitability of nociceptors

Capsaicin-induced excitability of sensory neuronal cells was detected through measurements of Ca^{2+} transients using fluorescent Ca^{2+}-binding dyes (Bahar et al., 2016; Berridge et al., 2003). DRG-cells were loaded with fluorescent dye Fluo-5 and excitability was measured as Ca^{2+} transients during addition of stimuli inducing APs.

The excitability was presented as fluorescence intensity (ΔF) of responding cells only, which is normalised to baseline (see detailed methods in Chapter 2.9).

4.3.2 RT-qPCR of *Ngf* mRNA

RNA was extracted separately from the axon and the soma of E16.5 DRG-cells grown in porous membrane chambers. cDNA was obtained, and *Ngf* mRNA measured in the soma using qPCR with reference gene *Gapdh* (see detailed methods in Chapter 2.8). *Hprt* mRNA was measured as a housekeeper gene.

4.4 Results

4.4.1 Capsaicin induced activation of dissociated DRG-cells

The excitability of DRG-cells, and specifically nociceptors of the DRG, was assessed through measurements of Ca^{2+} transients using Ca^{2+} imaging. DRG-cells were preliminarily exposed to imaging buffer (IB) to assess whether the physical act of addition induced a response. Subsequently, cells were exposed to 200nM capsaicin to assess the excitability of nociceptors and successively 25mM KCl to activate the collective cells of the DRG, particularly those that had not responded to capsaicin-stimulation. Neuronal excitability was measured as changes to fluorescent signal (ΔF) (Figure 4.1).

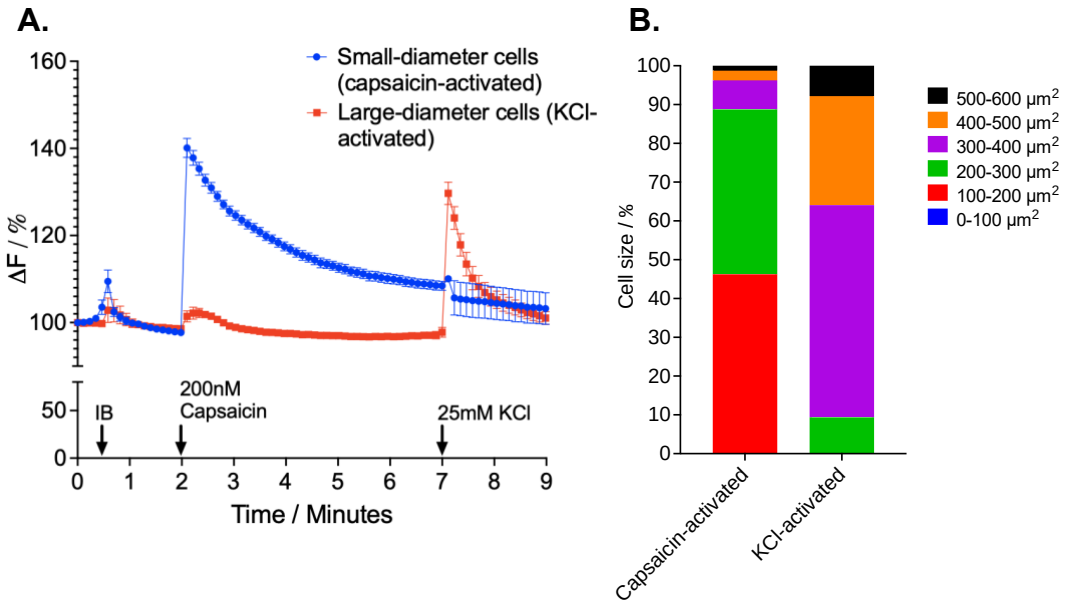

Figure 4.1: *The excitability of subtypes of sensory neuronal cells following stimulus. E16.5 DRG-cells (1 biological replicate with cells from a litter of an average of 6 embryos) exposed to imaging buffer (IB), 200nM capsaicin (n=6 dishes with an average of 13 cells imaged per dish) and 25mM KCl (n=5*

dishes with an average of 13 cells imaged per dish) shows that small-diameter cells predominantly react to capsaicin. ***A.*** *Exposure to IB induces an increase of 5-10% ΔF in responding cells, however this is dwarfed in comparison to exposure to depolarising agents; capsaicin (~40% ΔF) and KCl (~30% ΔF).* ***B.*** *The average size of cell bodies of cells activated by capsaicin fall in the range of 100-300µm^2, whereas cells activated by KCl are found to be 300-600µm^2 (n=5 dishes with an average of 13 cells imaged per dish)*

DRG-cells were measured for 30 seconds prior to addition of imaging buffer to establish baseline fluorescence. As observed in figure 4.1, the addition of imaging buffer alone produced a negligible response (~ 5% over baseline) in both small- and large-diameter DRG-cells. Subsequently, two populations of DRG-cells appear functionally distinct, as shown by excitability following stimulation with capsaicin (200nM). Small-diameter DRG-cells, with a soma of 100-300µm^2, exhibit an increase of ~40% ΔF to 200nM capsaicin, while large-diameter DRG-cells exhibit ~30% ΔF to 25mM KCl. KCl is expected to activate all cells, however, DRG-cells previously activated by capsaicin are likely depleted of intracellular Ca^{2+}, thus preventing a secondary activation in the time frame allocated. DRG-cells which were not activated by capsaicin are observed as large-diameter cells that respond to KCl-stimulation. Due to experimental limitations, cells could not be reloaded, therefore only responding cells were included in analysis and cell responses were normalised to baseline rather than to KCl response.

These results show small-diameter neurons are preferentially activated by capsaicin, demonstrating a distinct population of cells likely to be small C-fibre nociceptors (Caterina et al., 1997; Fattori et al., 2016; C.-L. Li et al., 2016). For all future experiments, DRG-cells were activated with 200nM capsaicin, unless otherwise stated, to measure the excitability of the nociceptors of the population.

4.4.2 24-hour treatment with PGE_2 induces increase in excitability of nociceptors of DRG-cultures

After PGE_2-exposure, the neuronal excitability following exposure to capsaicin was assessed using Ca^{2+} imaging. DRG-cells were exposed to 24H 10µM PGE_2 or control, and subsequently ΔF was measured during imaging buffer or capsaicin addition (Figure 4.2).

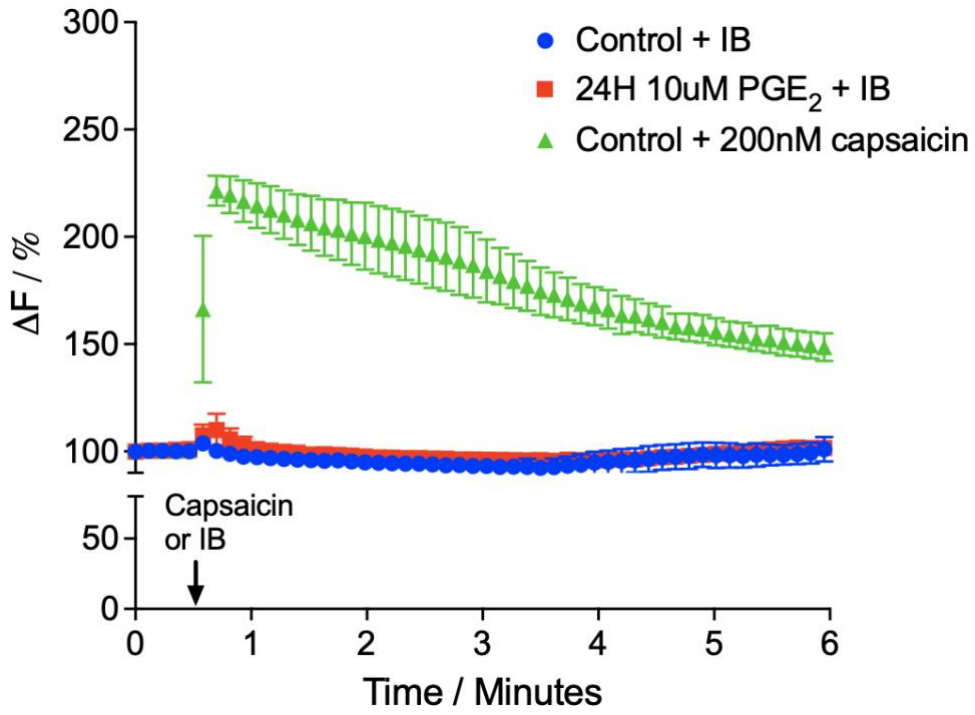

Figure 4.2: *The excitability of DRG-cells exposed to PGE_2- or control-protocol. Dissociated DRG-cells (1 biological replicate with cells from a litter of an average of 6 embryos) were exposed to prolonged PGE_2 and subsequently fluorescence intensity (ΔF) was measured during IB addition which showed an increase of 5-10% ΔF (n=3 dishes with an average of 16 cells imaged per dish), similar to that of control cells exposed to IB (n=3 with an average of 13 cells imaged per dish). Control DRG-cells activated with 200nM capsaicin exhibited an increased ΔF of ~120% (n=2 dishes with an average of 13 cells imaged per dish)*

DRG-cells were measured for 30 seconds prior to addition of imaging buffer or capsaicin to establish baseline fluorescence. DRG-cells exposed to prolonged PGE_2 showed comparable reaction to imaging to that of control DRG-cells of 5-10% increase in ΔF. Activation of DRG-cells with capsaicin shows the clear distinction in neuronal excitability, confirming that the physical act of addition is not sufficient to induce an increase in ΔF in DRG-cells, even in cells exposed to PGE_2.

Subsequently, PGE_2-induced sensitisation of DRG-cells was investigated through measurements of fluorescent activity following capsaicin-activation of nociceptors (Figure 4.3).

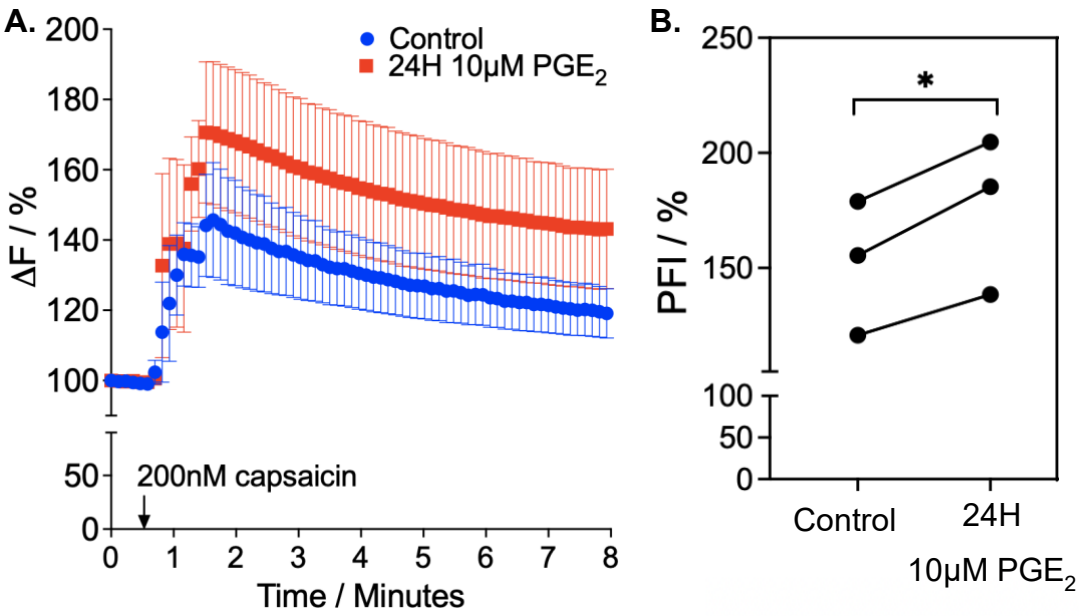

Figure 4.3: *DRG-cells pre-treated with PGE_2 and subsequently activated with capsaicin show a significant increase in excitability compared to control cells.* ***A****. The ΔF of cells, internally normalised to baseline, exposed to 10μM PGE_2 or control for 24H and subsequently stimulated with 200nM capsaicin (n=3 biological replicates).* ***B.*** *24H 10μM PGE_2 significantly increased (24.4±3.6%) the peak fluorescence intensity (PFI) following capsaicin stimulation compared to control cells (p-value=0.0210, n=3 biological replicates, paired t-test)*

The ΔF was normalised to the baseline intensity level and the percent increase analysed as the activity level of the nociceptors (Figure 4.3A). DRG-cells treated with 10μM PGE_2 for 24H showed a significant increase in peak fluorescent intensity (PFI) after 200nM capsaicin stimulation when comparing to control (Figure 4.3B). Overall, the increase in fluorescent intensity shows a hyperexcitable state of nociceptors of the DRG following prolonged PGE_2 exposure.

4.4.3 24-hour exposure to PGE_2 induces increased *Ngf* mRNA in the soma of dissociated DRG-cultures

To assess the effects of PGE_2 treatment on specific signalling mediators of nociceptive pathways, *Ngf* mRNA expression was measured in cells pre-treated with PGE_2 (Figure 4.4).

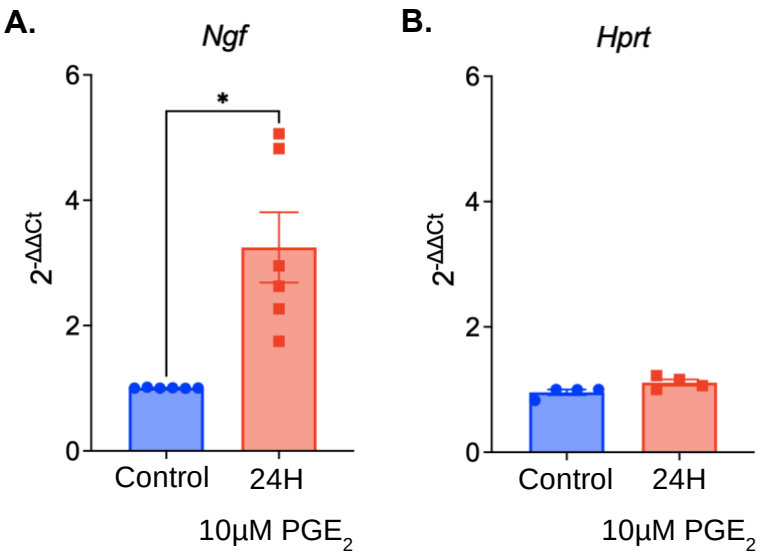

Figure 4.4: *RT-qPCR of **A.** target RNA Ngf and **B.** control RNA Hprt in the soma of DRG-cells exposed to 24H of 10µM PGE_2 compared to control cells. Ngf mRNA shows increased expression (24.2±3.6, p-value= 0.0232, n=5 biological replicates, paired two-tailed t-test) with reference gene Gapdh. Housekeeping gene Hprt mRNA shows no change in expression following PGE_2-protocol*

A significant increase in *Ngf* mRNA was measured in the soma of DRG-cells following 24H exposure to PGE_2 compared to control cells (Figure 4.4). The increase in *Ngf* mRNA shows an activation of neuroplastic pain pathways (Denk et al., 2017; Melemedjian et al., 2010).

4.4 Discussion

PGE_2 is a known key mediator of inflammatory and neuropathic pain pathways driving neuroplastic changes which induces a sensitised state in nociceptors, experienced as chronic pain (J. Huang et al., 2006; L.-Y. M. Huang & Gu, 2017; Hucho & Levine, 2007; A. S. Lee et al., 2013). The aim of this chapter was to develop an *in vitro* model of sensitisation with DRG-cells which was accomplished through prolonged exposure to PGE_2. E16.5 DRG-cells from mice were exposed to PGE_2 every 2H for 24H to maintain a concentration of 10µM, based on previous experimental protocols using PGE_2 on murine cells (W. Ma, 2010; Rush & Waxman, 2004; Segond von Banchet et al., 2005). The validity of the protocol as a functional model of sensitisation was verified through measurements of ΔF following capsaicin activation, as a measure of excitability of nociceptors, and expression of *Ngf* mRNA, a key mediator of inflammatory pain pathways.

4.4.1 Prolonged exposure of DRG-cells to PGE_2 induced sensitisation

Ca^{2+} imaging was used to measure the excitability of dissociated DRG-cells through fluorescence intensity of Ca^{2+} transients. The physical act of adding a stimulus was demonstrated to not affect excitability of DRG-cells through experiments with imaging buffer. Comparative assessments of neuronal excitability following addition of capsaicin and KCl revealed a distinct population of capsaicin-activated small-diameter DRG-cells. Large-diameter neurons exclusively showed increased Ca^{2+} transients to KCl, while small-diameter neurons showed no response. This is attributed to the small C-fibre nociceptors entering a state of insensitivity, due to depletion of intracellular Ca^{2+} stores (Hayes & Tyers, 1980; Touska et al., 2011). KCl would normally induce action potentials in all cells of the murine DRG through extracellular increases in K^+ manipulating the ion gradients of the cell-membrane, triggering influx of Na^+ into the cell (Rienecker et al., 2020), however, depletion of intracellular Ca^{2+} prevents the cell from producing an action potential (Hayes & Tyers, 1980; Wood et al., 1988). Consequently, capsaicin activation was, in our system, found to activate a distinct population of DRG-cells, presumed to be small C-fibre nociceptors, characterised through capsaicin and KCl stimulation (Caterina et al., 1997; C.-L. Li et al., 2016).

Subsequently, E16.5 DRG-cells were exposed to PGE_2 for 24H and the excitability of the sensory neuronal cells was measured as Ca^{2+} transients during capsaicin-activation. Increased excitability was confirmed in small C-fibre nociceptors of the DRG following PGE_2 exposure, compared to control cells. Additionally, a significantly higher expression of *Ngf* mRNA, a known mediator of inflammatory and neuropathic pain as well as priming, was established in the cell body of DRG-cells exposed to prolonged PGE_2 (Ferrari et al., 2010; Melemedjian et al., 2014).

Interestingly, localised injections of PGE_2 into the paw of rats has been found to induce a sensitised state *in vivo*, measured as behavioural changes such as paw withdrawal threshold, and driving neuroplastic changes to DRG-cells through a localised peripheral function of PGE_2 (Momin et al., 2008; St-Jacques & Ma, 2014). PGE_2 has been found to affect the action potential by modulating the I_h current in small-diameter neurons (Momin & McNaughton, 2009). I_h is a nonspecific cation

current, with the purpose of counteracting hyperpolarisation following action potentials (see also Chapter 1). PGE_2 injection in the paw induces an increase the hyperpolarisation-activated cyclic nucleotide-gated channel, HCN2, in DRG-cells in a pathway mediated by cAMP/PKA (Jansen et al., 2020; Weng et al., 2012). Increases of HCN1 and HCN2 are found to drive an increase in I_h which facilitates a shorter refractory period thereby increasing action potential firing (Jansen et al., 2020; Momin et al., 2008). Serial peripheral injections of PGE_2 additionally induces increased axonal expression of EP4 receptors through a pathway mediated by cAMP, PKA, PKC, PKCε, PLC a and IL-6, inducing tactile allodynia in rats (St-Jacques & Ma, 2014). Depletion of cytoplasmic polyadenylation element binding protein (*Cpeb*) mRNA, a known mediator of protein translation, was found to prevent the development of sensitisation by PGE_2 (Bogen et al., 2012). Collectively, PGE_2 is shown to induce a sensitised state in nociceptors, manifesting through increased inflammatory mediators, driving hyperexcitability of nociceptors through neuroplastic changes, which are likely mediated through localised mechanisms in the axon and free nerve ending.

4.4.2 Conclusions

These results show the successful establishment of an *in vitro* model of sensitisation and functional hyperalgesic priming. The model was established in porous membrane chambers, which were previously been validated as effective for the separative extraction of axonal and somal RNA (see Chapter 3). In summary, a compartmentalised *in vitro* model of sensitisation has been developed which facilitates the study of localised changes to the axon of sensitised sensory neuronal cells.

Chapter 5: Changes to the local transcriptome of the axon defines sensitisation

5.1 Introduction

5.1.1 Transcriptomic profile of sensory neuronal cells of the DRG

Cells from the DRG are a particularly heterogenous population. Studies have elucidated and defined the transcriptome of individual cell subtypes (Zeisel et al., 2018) (see also Chapter 1).The functional differentiation of cell subtypes has additionally been explored through comparative studies of transcriptomic characterisation and functional differences (C.-L. Li et al., 2016; Y. Zheng et al., 2019). Functional differences have been associated with the expression of individual mRNAs thereby classifying small sensory neuronal subtypes as thermo-nociceptive (*Trpv1*, *Trpv4*, *Trpm3*, *Trpm8*, *Trpa1*), mechano-nociceptive (*Kcnk2*, *Kcnk4*, *Asic3*), and chemo-nociceptive (*Ptger1*, *Ptger2*, *Ptgfr*, *P2rx2*, *P2rx3*) (C.-L. Li et al., 2016; Y. Zheng et al., 2019). Classification systems are presented according to transcriptomic profile (mRNA expression profile), cell and nerve-fibre size (small- or large-diameter neurons or Aβ-, Aδ- or C-fibre neurons), and functional role (stimulus modality) (C.-L. Li et al., 2016; Y. Zheng et al., 2019).

Previous studies have additionally explored transcriptomic changes to sensory neuronal cells in states of hyperalgesic priming (see also Chapter 1). Pathways characterising the changes to the transcriptome in sensitisation included broadly inflammatory signalling, as well as more specifically ERK- and neuropeptide-signalling (J. Ma et al., 2015; Uttam et al., 2018; Yin et al., 2016). Interestingly, mediators associated with axon guidance have been found significantly altered, despite the experimental design inherently lacking the capability to directly address changes to the axon (Yin et al., 2016). Due to the highly compartmentalised nature of neuronal cells, sequencing of DRGs directly extracted from animals without nerve fibre or axonal growth *in vitro*, cannot be assumed to reflect the transcriptomic profile of the axonal compartment. Consequently, the axonal transcriptome of sensory neuronal cells has been explored and characterised through the use of compartmentalised chambers and axon microdissection, followed by sequencing technologies (Farias et al., 2020; Minis et al., 2014; Nijssen et al., 2018). NGS technologies have exposed a unique transcriptomes of neurites of

sensory neuronal cells (Farias et al., 2020; Kar et al., 2018; Minis et al., 2014; Nijssen et al., 2018; von Kügelgen & Chekulaeva, 2020). 61 RNAs were found to characterise a core neurite transcriptome, with a high proportion (41 out of 61) encoding ribosome-binding proteins, however, RNAs encoding proteins with mitochondrial function and translation mediators were additionally enriched (von Kügelgen & Chekulaeva, 2020).

Local changes in the axon have separately been shown to play a key role in the manifestation of hyperalgesic states. Through the use of treatments which interfere with translation administered to the periphery, *in vivo* studies in rats have shown how local translation is essential for hyperalgesic priming (Bogen et al., 2012; Ferrari et al., 2013; Jiménez-Díaz et al., 2008). Peripheral depletion of mediator of protein translation CPEB through antisense oligodeoxynucleotides (ODNs, inducing degradation of *Cpeb* mRNA in IB4(+)-nociceptors) injected into the paw, prevented the development of mechanical hyperalgesia measured as withdrawal threshold, induced either through TNF-α/PGE_2 exposure or PKCε-agonist (Bogen et al., 2012). Mechanical hyperalgesia was shown to correlate with increased protein expression of CPEB in peripheral nerve, supporting the direct role of local protein translation in the periphery (Bogen et al., 2012). Peripheral inhibition of mTOR-mediated protein translation through rapamycin was found to prevent and reverse the mechanical hyperalgesia developed through both a surgical model of chronic pain (spared nerve injury, SNI) and a chemically induced model of chronic pain (peripheral carrageenan and PGE_2-injections), in a pathway localised to A-fibre nociceptors (Ferrari et al., 2013; Jiménez-Díaz et al., 2008). Peripheral inhibition of polyadenylation-mediated initiation of protein translation through cordycepin injections was found to prevent and reverse carrageenan/PGE_2-induced hyperalgesic priming within the paw (Ferrari et al., 2013). Additionally, peripheral administration of anisomycin, a protein translation inhibitor disrupting the ERK/p38 MAPK pathway prevented the development of mechanical hyperalgesia induced through peripheral carrageenan injections (Bogen et al., 2012; Radulovic & Tronson, 2008). Collectively, localised inhibition of protein translation pathways, including ERK/p38 MAPK signalling, mTOR-phosphorylation of 4E-BP1/2, PKCε/CPEB

signalling, and polyadenylation-induced translation initiation, is found to prevent and even reverse mechanical hypersensitivity through mechanisms mediated in the axon of nociceptors (Bogen et al., 2012; Ferrari et al., 2013; Jiménez-Díaz et al., 2008). As previously discussed, local translation is directly related to the local expression patterns of RNAs (see Chapter 1). Despite this, the changes induced by sensitisation to the local axonal transcriptome have, as of yet, not been comprehensively characterised.

5.1.2 Assessing the effect of the maturity of the cell upon the local transcriptome

As previously discussed, significant differences between results from cells of adult and embryonic mice have been shown (see Chapter 1). Transcriptomic variation in sensory neuronal cells attributed to maturation of the animal have been shown to include mediators of axonal growth and guidance, as well as mediators of inflammation and nociceptive processing (Landy et al., 2021; N. Sharma et al., 2020; Smith-Anttila et al., 2020). *Prdm12* mRNA, which encodes a transcription factor, plays a key role in nociceptive development, but subsequently becomes redundant for nociceptive processing in adult mice (Landy et al., 2021). Additionally, different expression of transcription factors, *Runx1* and *Runx3*, characterises cell-subtypes in adult mice, however on the contrary are broadly expressed in early embryonic cells (E11.5) (N. Sharma et al., 2020). Through simultaneous assessments of transcriptomic differences between lumbar and sacral DRG, and DRGs from embryonic and adult mice, a higher number of differentially expressed RNAs between spinal levels was shown in embryonic DRG-cells compared to adult DRG-cells, however, representation of most of 11 distinct subtypes of sensory neurons was established at E18.5 (Smith-Anttila et al., 2020). DRG-neurons from embryonic mice are additionally found to express unique sensory neuronal phenotypes, progressively developing functional subtypes defined by TRP-channel expression patterns, supporting the use of embryonic DRG-cells for *in vitro* models (Hjerling-Leffler et al., 2007; Smith-Anttila et al., 2020). Nevertheless, differences in the maturity of the cells are likely to contribute to differences to the core transcriptome of the axon. Similarly, pathways of neuroplasticity and sensitisation

may differ in the axon depending on the maturity of the cell, which should be addressed to confirm the clinical relevance of DRG-cells from embryonic mice. Consequently, the aim of this thesis was to characterise the local pathways facilitating the manifestation of sensitisation in the axon of sensory neuronal cells, and to characterise the similarities and differences in the pathways for DRG-cells from embryonic and adult mice.

5.2 Hypothesis and objectives

The hypothesis of this chapter is that PGE_2-induced sensitisation is mediated through changes to the axonal transcriptome of sensory neuronal cells from embryonic and adult mice.

The objectives were to:

- characterise the local transcriptome of the axon of sensory neuronal cells in comparison to the transcriptome of the cell body
- determine the differences in the local transcriptome of the axon driven by PGE_2-induced sensitisation
- compare the changes to the axonal transcriptome following sensitisation in DRG-cells from embryonic and adult mice

5.3 Methods

The PGE_2 model of sensitisation, developed using E16.5 DRGs, was replicated with dissociated DRG cultures from adult (8-week-old, 8WO) mice. 8WO DRG-cells were exposed to 12H PGE_2, rather than 24H PGE_2 as was used for E16.5 DRGs, due to laboratory time constraints (see detailed methods in Chapter 2.2 and 2.3). RNA was extracted from embryonic and adult axons and cell bodies after PGE_2-sensitisation protocol or control protocol and prepared for RNAseq (see detailed methods in Chapter 2.6). The comparisons explored in the present study are shown in Figure 5.1.

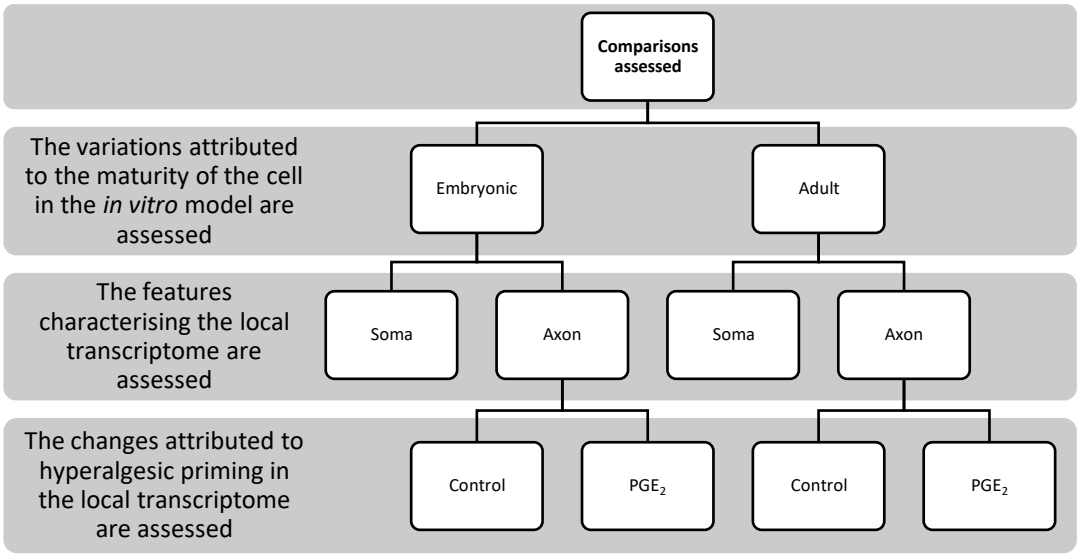

Figure 5.1: *A hierarchal tree listing the comparisons (embryonic vs adult, soma vs axon, control vs PGE_2) assessed through RNAseq in the present study*

Variation in the availability of equipment and technology caused differences in the RNA extraction protocol, library preparation and sequencing procedure for the E16.5 and 8WO samples (Table 5.1) (see detailed methods in Chapter 2.11).

	Embryonic samples	**Adult samples**
Sequencing core	GeneWiz	University of Texas at Dallas
Library prep	rRNA depletion	polyA selection
Fragment length	150bp	75bp
Paired-/single-end sequencing	Paired-end	Single-end

Table 5.1: *The differences to the experimental protocol defining the library preparation and sequencing design of the RNAseq experiments are listed*

Raw counts were obtained from RNAseq files using HTSeq. Filtering was carried out to only include protein-coding, non-mitochondrial genes in any downstream analysis, to avoid bias introduced through differing library preparations (Bush et al., 2017). Two bioinformatic pipelines were utilised to characterise the local axonal

transcriptome of embryonic and adult mice and to assess the changes to the local transcriptome induced by PGE_2:

- To characterise the localised transcriptome of the axon compared to the soma: STAR → Samtools → HTSeq → uqTPM normalisation → multiple t-tests
- To assess the effect of PGE_2-sensitisation in the axon: STAR → Samtools → HTSeq → DESeq2

To characterise the local transcriptome of the axon, the datasets were normalised according to transcript length, sequencing depth, and library size through calculations of transcripts per million and subsequent Upper Quartile normalisation to obtain uqTPM values. uqTPM values were then subjected to DE analysis through unpaired t-tests with corrections for multiple comparisons through Holm-Šídák multiple comparisons testing. The changes induced by PGE_2 were assessed through the use of the DESeq2 analysis tool-package, based on the assumption that a core axonal transcriptome exists and PGE_2-induced sensitisation manifests through differential expression of select mediators (von Kügelgen & Chekulaeva, 2020). Data from E16.5 and 8WO DRG-cells was analysed separately, subsequently allowing outputs to be indirectly compared. Pathway analysis was carried out using Qiagen Ingenuity Pathway Analysis (IPA). IPA is a software package which allows for the exploration of the profiles created by differentially expressed genes, by assessing similarities to known cellular and molecular pathways (QIAGEN Inc., https://www.qiagenbioinformatics.com/products/ingenuitypathway-analysis, (Krämer et al., 2014)). IPA is additionally capable of predicting upstream regulators to the given expression profiles (see detailed methods in Chapter 2.11 and 2.12).

5.3 Results

5.3.1 The axon and the soma of DRG-cells have different transcriptomic profiles

In this chapter the local axonal transcriptome of DRG-cells was characterised in comparison to the somal transcriptome. For E16.5 samples >15,000,000 counts were obtained for all axonal samples and >29,000,000 were obtained for somal

samples. For 8WO samples >25,000,000 counts were obtained for both axonal and somal samples. Filtering was carried out to exclude mitochondrial and non-protein-coding RNAs, to facilitate a comparison between the rRNA depleted and polyA-selected library preparations. After filtering E16.5 axonal samples had >10,000,000 counts distributed over an average of 16,411 genes and somal samples >23,000,000 counts distributed across an average of 17,536 genes (Table 5.2).

	Sample treatment group	*Label*	*Unique mapping percentage*	*Reads (post-filtering)*
E16.5	**V**ehicle **S**oma (VS)- Control soma	VS1	78.15%	35,810,572
		VSB	82.44%	41,143,662
		VSD	81.76%	36,636,274
	Vehicle **A**xon (VA) - Control axon	VA1	32.07%	10,725,681
		VA2	37.08%	17,529,951
		VAD	34.69%	14,425,396
	PGE_2-**T**reated **S**oma (TS)	TS1	59.63%	23,989,351
		TSB	78.88%	42,242,792
		TSD	81.20%	47,357,559
	PGE_2-**T**reated **A**xon (TA)	TA1	35.98%	16,486,693
		TA2	48.31%	19,896,401
		TAD	57.10%	35,060,885

Table 5.2: *Labelling and mapping statistics for RNA samples (n=3 per sample treatment group) from E16.5 mice. Labelling is defined by three characters; the first indicating treatment, the second indicating compartment of cell and the third is a unique identifier of the sample showing paired samples. The mapping percentage is 30-57% for axonal samples and 59-82% for somal samples*

The mapping percentage was comparatively lower for axonal samples, observed at >30% with an average of ~40%, which is attributed to low RNA obtained in the original samples. In contrast the mapping percentage was >59% for somal samples, with an average of ~75%.

After filtering 8WO axonal samples had >24,000,000 counts distributed across an average of 15,220 genes with counts, while somal samples had >25,000,000 counts distributed across an average of 15,927 genes with counts (Table 5.3). Filtering of samples from 8WO mice had less of an effect on the counts, due to the polyA-selected library limiting non-protein-coding RNAs.

	Sample treatment group	*Label*	*Unique mapping percentage*	*Reads (post-filtering)*
8WO	**V**ehicle **S**oma (VS)- Control soma	VS1	87.65%	40,090,424
		VS2	89.26%	39,505,184
		VS3	89.97%	31,123,382
	Vehicle **A**xon (VA) - Control axon	VA1	85.81%	31,348,467
		VA2	85.53%	29,020,651
		VA3	85.68%	32,862,783
	PGE_2-**T**reated **S**oma (TS)	TS1	86.90%	25,004,967
		TS2	87.88%	38,280,702
		TS3	86.03%	32,149,626
	PGE_2-**T**reated **A**xon (TA)	TA1	88.46%	39,107,465
		TA2	84.21%	24,867,269
		TA3	87.30%	32,006,126

Table 5.3: *Labelling and mapping statistics for RNA samples (n=3 per sample treatment group) from 8WO mice. Labelling is defined by three characters; the first indicating treatment, the second indicating compartment of cell and the third is a unique identifier of the sample showing paired samples. The mapping percentage is found to be >80% for both axonal and somal samples*

The mapping percentage was >80% for both axonal and somal samples from adult mice, correlating with similar RNA quantities extracted from the axonal and somal compartment.

Kernel density plots were created following filtering for E16.5 and 8WO samples separately. Kernel density plots of $\log_{10}$(filtered counts) are designed by creating a probability function for each sample conveying the probability that a given gene will have a given expression value. The probability function is drawn without making assumptions of the distribution and allows for a comparison of the expression pattern of the samples to evaluate how comparable samples are (Figure 5.2).

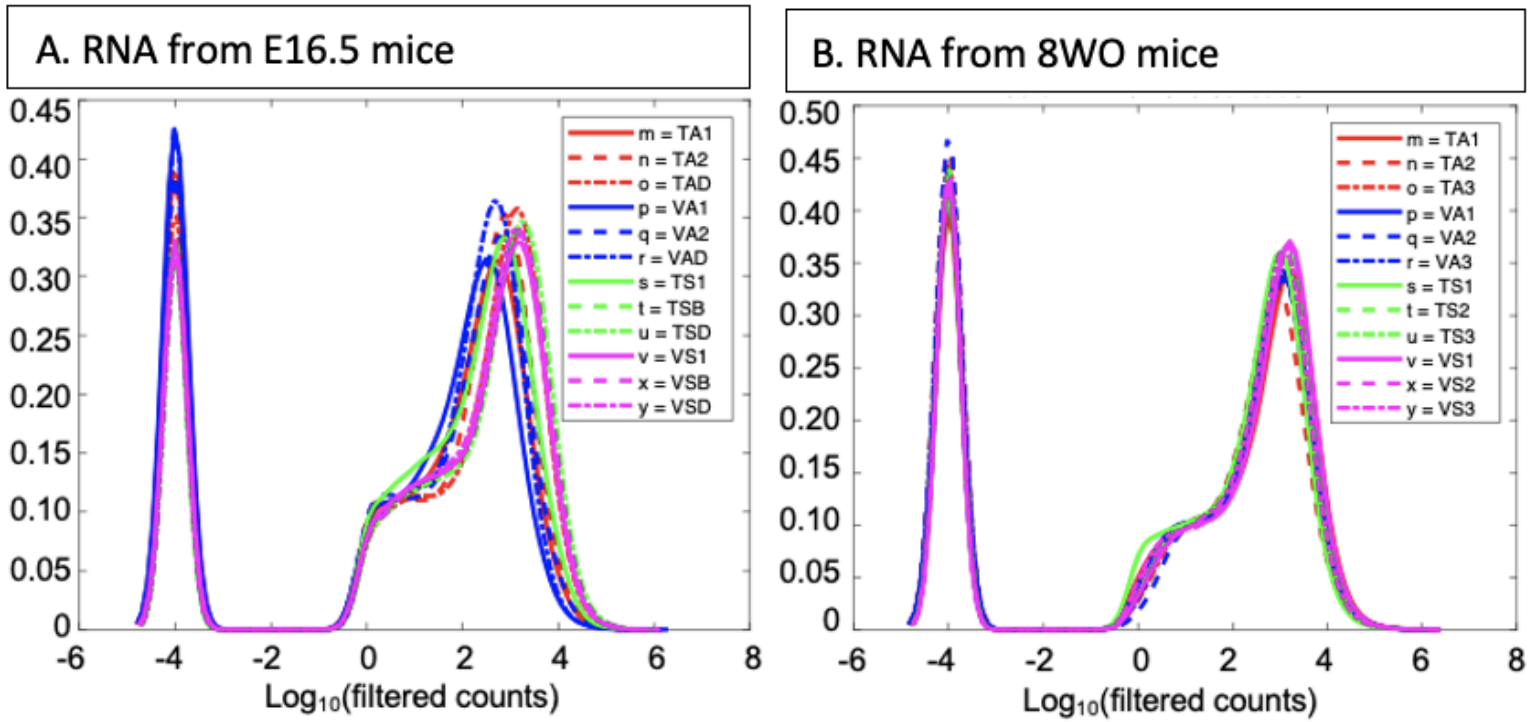

Figure 5.2: *Kernel density plots show the distribution of all samples from embryonic and adult mice. Kernel distribution of* ***A.*** *E16.5 mice and* ***B.*** *8WO mice of* log_{10}*(filtered counts) by plotting the probability that a given gene will have a given expression*

Kernel density plots confirmed that all samples had a satisfactory comparable expression profile, observed as similar shapes for the probability functions of samples from E16.5 and 8WO (Figure 5.2).

To allow further comparisons between the RNA expression patterns in the axon and the soma, as well as embryonic and adult mice, further normalisation was required of the raw counts. Transcripts per million (TPM) were calculated from the raw counts, and subsequently subjected to Upper Quartile normalisation to obtain uqTPM. This allowed for the subsequent comparable assessment of samples with principal component analysis (PCA). PCA shows the clustering of samples along axes indicating the weight of variation in a given direction, defined as Principal Components (PCs) (Lever et al., 2017) (Figure 5.3).

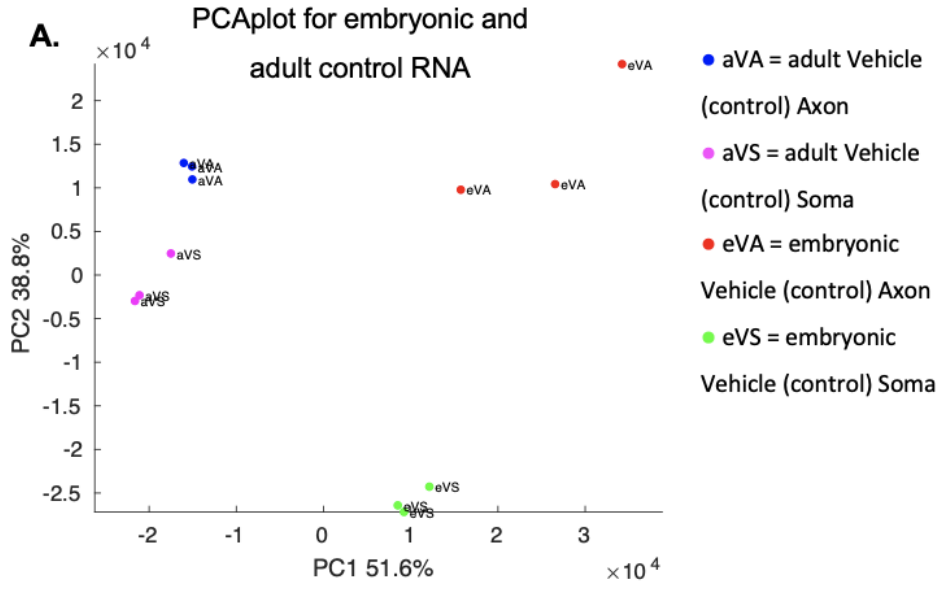

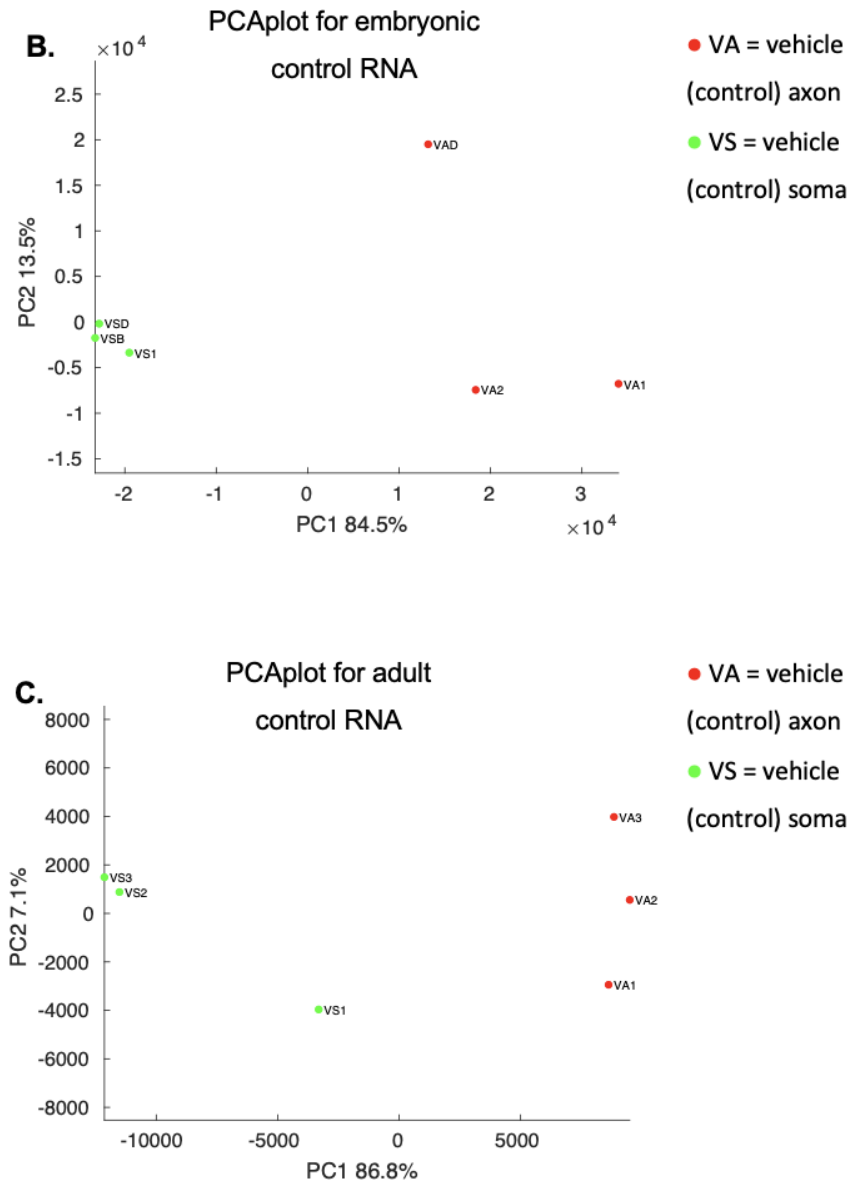

Figure 5.3: *PCA plots show the clustering of control samples.* ***A.*** *Control samples for both E16.5 and 8WO are characterised on the same graph demonstrating clear clustering according to fraction of the cell for both embryonic and adult mice. Any clustering attributed to age cannot be assumed due to possible batch effects. Subsequent plots show detailed clustering according to fraction of the cell for* ***B.*** *E16.5 and* ***C.*** *8WO. For all figures shown PC1+PC2>90% of the variance for the dataset*

Clustering of samples according to compartment of the porous membrane chamber (cell body vs axon) was established (Figure 5.3B, 5.3C). PCA showed significant differences, confirming the presence of a distinct transcriptome within the axonal compartment of the porous membrane chambers, indicative of a compartmentalised nature of the neuronal cell. The results are however not

excluding the possible presence of non-neuronal cells within the axonal compartment.

5.3.2 Analysis of cell-type distribution by transcriptome comparison

An assessment of the cell-types present in the DRG-cultures and contributing to the transcriptome profile from the somal and axonal compartments dataset was of interest, to add context to the results and weight to the conclusions. To assess the cell-subtypes present in the datasets, a comparative transcriptomic profiling was carried out using markers of different cell-types defined in previous studies. 5 markers for Schwann cells, 12 markers for satellite glial cells, 5 markers for immune cells (such as macrophages), and 11 markers for neuronal cells of the DRG were found based on previous studies characterising the cell sub-types of the DRG (Liang et al., 2020; Ray et al., 2018; Wangzhou et al., 2020; Zeisel et al., 2018). The expression of marker RNAs in control axonal and somal samples is listed as uqTPM, with colour-coding showing levels of expression for each gene in groups separating embryonic and adult samples (Table 5.4).

DRG neuronal markers

Gene ID	Gene name	E16.5						8WO					
		Axon			Soma			Axon			Soma		
ENSMUSG00000025576.17	Rbfox3	9.05	9.70	31.91	20.25	36.60	31.25	0.31	0.17	0.08	6.55	2.03	1.60
ENSMUSG00000030669.13	Calca	3434.41	3430.71	971.48	1173.87	1014.93	910.34	84.60	19.01	28.33	566.75	96.24	87.77
ENSMUSG00000030666.11	Calcb	194.77	112.26	60.98	120.92	68.61	83.04	4.48	2.09	0.53	32.99	7.87	7.29
ENSMUSG00000009292.18	Trpm2	40.79	35.77	21.90	66.26	76.06	75.78	0.05	0.10	0.09	0.34	0.19	0.21
ENSMUSG00000005952.15	Trpv1	95.42	87.50	32.94	167.96	139.03	107.33	0.55	1.40	0.64	37.25	8.16	7.72
ENSMUSG00000041482.17	Piezo2	191.71	208.20	395.51	1249.71	1613.79	1964.41	28.51	24.02	31.71	56.80	57.51	57.62
ENSMUSG00000020396.8	Nefh	51.37	35.90	80.81	157.82	289.97	189.39	3.63	0.35	0.48	38.61	12.72	11.27
ENSMUSG00000022055.7	Nefl	2914.18	2710.27	955.28	1758.87	1959.49	1537.49	9.72	1.89	4.54	112.81	38.00	32.46
ENSMUSG00000022054.11	Nefm	780.70	759.40	769.66	1057.90	1440.51	1152.67	11.83	11.72	7.71	41.92	18.45	17.32
ENSMUSG00000023484.14	Prph	3960.98	3320.06	1450.34	3065.25	2597.58	2409.41	31.78	24.49	16.02	424.21	143.49	121.66
ENSMUSG00000021675.4	F2rl2	18.41	15.87	30.44	50.89	50.06	42.74	0.68	0.55	1.75	15.60	3.58	3.23

Schwann cell markers

Gene ID	Gene name	E16.5						8WO					
		Axon			Soma			Axon			Soma		
ENSMUSG00000056569.11	Mpz	6.92	27.38	305.57	2.82	22.63	89.81	12.82	80.40	17.67	50.89	67.34	49.50
ENSMUSG00000041607.17	Mbp	12.55	35.65	80.76	11.84	12.26	16.12	10.43	28.92	14.23	8.10	15.96	14.38
ENSMUSG00000031740.8	Mmp2	41.27	154.71	845.84	29.86	57.92	152.18	186.02	331.77	277.11	174.82	401.27	412.58
ENSMUSG00000004655.5	Aqp1	300.18	245.85	117.17	321.78	225.55	188.53	39.53	28.82	34.41	115.66	57.02	55.40
ENSMUSG00000090125.3	Pou3f1	0.17	0.14	2.37	0.00	0.00	0.20	0.29	0.75	0.23	0.85	0.49	0.71

Satellite glial cells markers

Gene ID	Gene name	E16.5						8WO					
		Axon			Soma			Axon			Soma		
ENSMUSG00000006398.15	Cdc20	2.53	12.13	11.56	0.65	1.23	1.27	385.23	186.29	245.42	262.70	178.65	180.54
ENSMUSG00000022033.9	Pbk	3.17	10.29	10.66	0.17	0.54	0.89	172.63	127.22	137.46	123.99	88.58	88.69
ENSMUSG00000001403.13	Ube2c	0.96	2.43	5.01	0.17	0.31	0.38	227.77	148.76	155.82	126.96	103.67	105.26
ENSMUSG00000017716.15	Birc5	2.15	4.03	7.97	0.92	1.40	1.45	135.93	87.86	105.09	111.86	66.63	70.22
ENSMUSG00000050623.5	Catsperz	0.63	0.70	0.40	0.51	0.76	0.71	0.81	0.00	0.27	1.36	0.64	0.72
ENSMUSG00000064080.12	Fbln2	69.32	145.35	316.64	52.95	181.21	286.28	1135.90	1310.43	1310.94	1377.57	1920.69	2071.98
ENSMUSG00000005994.14	Tyrp1	0.36	0.39	0.11	0.32	0.08	0.11	0.16	0.00	0.00	0.00	0.00	0.08
ENSMUSG00000033491.13	Prss35	8.05	26.57	34.48	3.28	9.79	37.17	81.65	49.83	63.58	229.24	152.93	129.32
ENSMUSG00000019874.11	Fabp7	31.24	53.37	51.44	2.66	2.10	8.28	190.63	291.54	193.37	234.35	139.19	128.07
ENSMUSG00000036169.6	Sostdc1	5.05	25.56	69.23	2.35	4.11	18.03	2.03	6.70	3.77	15.66	11.17	9.77
ENSMUSG00000044708.5	Kcnj10	1.23	1.31	8.00	0.55	2.95	6.03	3.62	7.59	3.09	12.55	12.72	13.88
ENSMUSG00000005360.14	Slc1a3	6.29	4.46	11.04	1.56	8.78	8.95	2.43	2.00	2.14	5.13	4.26	3.90

Immune cells (macrophages) markers													
Gene ID	**Gene name**	**E16.5**						**8WO**					
		Axon			**Soma**			**Axon**			**Soma**		
ENSMUSG00000026395.16	Ptprc	0.00	0.12	0.80	0.21	0.40	0.69	0.95	1.00	1.51	1.02	2.17	1.83
ENSMUSG00000040747.9	Cd53	0.25	0.41	1.60	0.07	0.71	0.31	36.73	47.06	51.31	29.75	40.55	38.38
ENSMUSG00000059498.13	Fcgr3	1.00	0.60	0.37	0.53	0.81	0.72	42.80	57.34	87.55	48.98	77.61	76.11
ENSMUSG00000026656.15	Fcgr2b	0.00	0.13	0.62	0.00	0.51	0.11	3.97	1.15	3.04	4.18	3.64	4.06
ENSMUSG00000020044.13	Timp3	13.51	33.12	74.34	7.17	13.73	20.25	199.49	208.40	161.37	210.33	245.91	225.04

Table 5.4: *Expression profiles of non-neuronal and neuronal marker genes for control axonal and somal samples from E16.5 and 8WO mice. Expression listed in uqTPM for individual samples for markers for DRG neuronal cells, Schwann cells, satellite glial cells, and immune cells (including macrophages). Colour-coding according to low (blue) and high (red) expression for each gene comparatively between samples, separately for embryonic and adult mice. Markers from (Liang et al., 2020; Ray et al., 2018; Wangzhou et al., 2020; Zeisel et al., 2018)*

Broadly heterogeneous expression patterns were observed for neuronal and non-neuronal cell-types within both the axonal and somal RNA samples from embryonic and adult mice. In particular one E16.5 axonal sample appeared to have significant contamination of non-neuronal transcripts (sample VAD). When considering the PCA plot (Figure 5.3B), sample VAD was positioned slightly differently to the other two control axonal samples. The position of the VAD sample was however primarily defined by a shift along the PC2 axis compared to the other axonal samples, which only accounts for 13.5% of the variation in the dataset. Given that the clustering of the axonal samples remained distinctly separate from the somal samples, the VAD sample was still included in the differential expression analysis.

To provide comparative analysis, the dataset of Thakur et al. 2014 (GEO accession number: GSE62424) was obtained and the expression of the target genes was listed and similarly colour coded with expression listed in FPKM (Table 5.5). Two datasets from the study were assessed: Cells from DRG of male C57B1/6 mice lysed immediately after dissociation ("Dissociated") and nociceptor-enriched magnetic cell sorting (MACS)-sorted dissociated DRG from adult male C57B1/6 mice ("MACS").

DRG neuronal markers									
Gene ID	**Gene name**	**MACS**				**Dissociated**			
ENSMUSG00000025576.17	Rbfox3	87.10	89.44	69.58	66.45	66.93	67.51	63.47	59.02
ENSMUSG00000030669.13	Calca	1129.22	992.05	917.06	707.61	1066.24	1055.60	932.99	1003.16
ENSMUSG00000030666.11	Calcb	157.04	199.29	185.87	143.26	137.09	124.58	108.21	116.22
ENSMUSG00000009292.18	Trpm2	4.57	2.76	2.78	3.30	4.16	4.30	5.53	5.60
ENSMUSG00000005952.15	Trpv1	64.97	52.61	52.50	34.63	31.61	35.07	35.03	42.54
ENSMUSG00000041482.17	Piezo2	64.24	83.92	79.19	84.85	56.41	55.35	60.17	52.87
ENSMUSG00000020396.8	Nefh	101.54	54.21	81.94	68.15	618.98	609.74	745.31	690.45
ENSMUSG00000022055.7	Nefl	952.89	956.69	881.80	722.77	1883.01	1897.27	2208.05	2015.27
ENSMUSG00000022054.11	Nefm	399.86	325.71	338.10	271.22	1185.32	1173.91	1369.03	1237.61
ENSMUSG00000023484.14	Prph	1550.47	1817.15	1320.75	1343.28	888.99	847.82	875.92	854.86
ENSMUSG00000021675.4	F2rl2	67.47	60.12	54.25	38.15	33.96	33.57	32.68	35.09

Schwann cell markers									
Gene ID	**Gene name**	**MACS**				**Dissociated**			
ENSMUSG00000056569.11	Mpz	13.72	15.09	45.86	171.54	1336.06	1374.52	903.89	1535.84
ENSMUSG00000041607.17	Mbp	254.74	72.96	198.35	578.17	507.21	497.53	396.21	585.76
ENSMUSG00000031740.8	Mmp2	0.23	0.00	0.28	0.45	5.68	5.64	2.79	3.22
ENSMUSG00000004655.5	Aqp1	203.16	201.72	193.53	153.82	119.79	123.65	129.82	122.49
ENSMUSG00000090125.3	Pou3f1	0.15	0.16	0.02	0.24	3.28	3.68	2.46	3.41

Satellite glial cells markers									
Gene ID	**Gene name**	**MACS**				**Dissociated**			
ENSMUSG00000006398.15	Cdc20	0.00	0.00	0.00	2.33	0.00	0.00	0.00	0.00
ENSMUSG00000022033.9	Pbk	0.60	0.17	0.43	2.32	0.12	0.22	0.08	0.00
ENSMUSG00000001403.13	Ube2c	8.45	5.94	7.67	21.56	0.46	0.65	0.24	0.26
ENSMUSG00000017716.15	Birc5	5.63	3.26	3.44	13.07	1.54	1.30	1.53	1.86
ENSMUSG00000050623.5	Catsperz	Not expressed							
ENSMUSG00000064080.12	Fbln2	0.20	0.57	0.37	1.45	40.94	38.84	42.30	37.34
ENSMUSG00000005994.14	Tyrp1	0.00	0.00	0.09	0.24	7.42	7.05	4.83	5.08
ENSMUSG00000033491.13	Prss35	0.15	0.00	0.07	0.46	27.43	25.81	20.58	23.27
ENSMUSG00000019874.11	Fabp7	1.79	1.21	2.35	10.80	310.10	295.04	202.83	242.14
ENSMUSG00000036169.6	Sostdc1	0.14	0.20	0.44	0.48	30.37	27.98	20.51	28.37
ENSMUSG00000044708.5	Kcnj10	0.08	0.01	0.17	0.21	23.43	21.84	17.32	19.30
ENSMUSG00000005360.14	Slc1a3	0.02	0.05	0.01	0.07	4.62	5.34	4.50	4.87

Immune cells (macrophages) markers									
Gene ID	**Gene name**	**MACS**				**Dissociated**			
ENSMUSG00000026395.16	Ptprc	1.11	0.94	0.67	1.40	0.78	1.08	0.30	0.38
ENSMUSG00000040747.9	Cd53	0.80	0.12	0.20	0.90	1.04	1.07	0.39	0.50
ENSMUSG00000059498.13	Fcgr3	0.12	0.22	0.05	0.29	1.13	1.97	1.08	1.57
ENSMUSG00000026656.15	Fcgr2b	0.37	0.00	0.05	0.00	1.34	1.37	0.98	1.29
ENSMUSG00000020044.13	Timp3	9.23	1.82	9.57	15.17	81.48	80.55	61.97	78.39

Table 5.5: *Expression profiles of non-neuronal and neuronal marker genes for MACS and dissociated DRG samples from (Thakur et al., 2014). Expression listed in FPKM for individual samples for markers for DRG neuronal cells, Schwann cells, satellite glial cells, and immune cells (including macrophages). Colour-coding according to low (blue) and high (red) expression for each gene comparatively between samples. Markers from (Liang et al., 2020; Ray et al., 2018; Wangzhou et al., 2020; Zeisel et al., 2018)*

The nociceptor-enriched MACS-cells had a higher level of expression of neuronal markers. However, it is additionally observed that certain markers of non-neuronal cells (including *Aqp1*, *Ube2c* and *Ptprc*) were expressed at comparatively higher levels in MACS-cells, compared to dissociated cells. Whether this was due to mild contamination or biologically relevant differences in expression of marker genes within the nociceptor population is not clear. Further exploration of the cell-type distribution within the transcriptomic datasets obtained was carried out by comparing our samples to genes enriched in nociceptor cells (Thakur et al., 2014). A select number of marker genes were assessed of a total of 920 found transcriptionally over-represented in MACS-cells due to particularly high over-presentation.

Nociceptor enriched genes (Thakur et al., 2014)												
Gene ID	**Gene name**	**E16.5**						**8WO**				
		Axon			**Soma**			**Axon**			**Soma**	
ENSMUSG00000034115.10	Scn11a	106.28	105.67	198.64	424.76	457.13	576.16	0.52	0.19	0.09	5.56	1.93	1.82
ENSMUSG00000078698.3	Mrgpra3	23.06	15.29	29.22	29.74	17.49	37.02	0.00	0.00	0.00	0.00	0.00	0.18
ENSMUSG00000070551.3	Mrgprb5	0.57	0.15	0.05	0.87	0.61	1.18	0.00	0.00	0.00	0.00	0.00	0.22
ENSMUSG00000070552.2	Mrgprx1	857.82	514.57	488.73	873.69	707.14	926.21	0.00	0.00	0.00	1.16	0.23	0.29
ENSMUSG00000029503.16	P2rx2	1.11	0.46	0.08	0.78	0.22	0.47	0.00	0.24	0.00	0.20	0.10	0.00

Table 5.6: *Expression profile of nociceptor-marker genes for control axonal and somal samples from E16.5 and 8WO mice. Expression is listed in uqTPM of RNAs found to be enriched in nociceptor cells of the DRG by (Thakur et al., 2014). Colour-coding according to low (blue) and high (red) expression for each gene comparatively between samples, separately for embryonic and adult mice*

Interestingly, the E16.5 soma samples exhibit considerable expression of nociceptor enriched genes, while the 8WO samples had very low expression, with the axonal compartment largely devoid of expression of the marker genes (Table 5.6). For comparative assessment, the expression pattern of the nociceptor-enriched genes within the MACS-nociceptor cultures of Thakur et al. were obtain and compared to their dissociated cultures (Table 5.7).

Nociceptor enriched genes (Thakur et al., 2014)									
Gene ID	**Gene name**	**MACS**				**Dissociated**			
ENSMUSG00000034115.10	Scn11a	275.05	249.42	268.55	192.97	116.69	116.09	121.66	124.06
ENSMUSG00000078698.3	Mrgpra3	45.05	52.58	42.24	54.88	13.55	12.02	10.59	9.61
ENSMUSG00000070551.3	Mrgprb5	13.55	15.72	19.03	12.25	3.97	5.17	4.54	5.61
ENSMUSG00000070552.2	Mrgprx1	39.98	39.15	31.88	33.17	10.89	11.01	12.56	12.40
ENSMUSG00000029503.16	P2rx2	7.62	4.49	3.77	4.58	1.25	1.96	1.68	1.44

Table 5.7: *Expression profile of nociceptor-marker genes for MACS and dissociated DRG samples from (Thakur et al., 2014). Colour-coding according to low (blue) and high (red) expression for each gene comparatively between samples*

The expression of nociceptor-enriched genes was significantly higher within the MACS-population of cells, confirming the marker genes present a profile of nociceptors.

Characterising the RNA expression patterns of the axonal transcriptome by comparing to the transcriptome of non-neuronal and neuronal cells, including Schwann cells, STG cells, and nociceptors, showed heterogeneous expression patterns of marker genes within the axonal compartment (Table 5.4). This data was attributed to possible contamination of non-neuronal cells. However, as previously discussed, the axonal compartment is distinct compared to the somal, with a unique transcriptome profile (see also Chapter 1). Consequently, marker genes for specific cell-types may not retain their unique role within the axon compared to the soma, or even be expressed within the axonal compartment. In order to assess the purity of the axonal compartment for a representative axonal transcriptome, a comparative assessment was carried out of the expression pattern of select marker genes enriched in the neurite (axon and dendrite) transcriptome (von Kügelgen & Chekulaeva, 2020) (Table 5.8).

Neurite enriched genes (von Kügelgen & Chekulaeva, 2020)													
Gene ID	**Gene name**	**E16.5**						**8WO**					
		Axon			**Soma**			**Axon**			**Soma**		
ENSMUSG00000008668.15	Rps18	1018.02	816.18	502.02	235.53	168.50	154.62	1147.01	1161.88	1371.30	808.89	624.93	624.04
ENSMUSG00000038274.13	Fau	651.11	469.65	294.72	144.47	103.30	93.10	1819.49	1710.72	2017.73	1259.57	899.90	877.31
ENSMUSG00000061983.7	Rps12	590.16	372.22	287.11	50.69	38.49	37.38	3265.60	3474.28	3623.68	1574.74	1211.61	1235.18
ENSMUSG00000044533.15	Rps2	2836.92	1405.57	2093.80	313.37	238.47	242.48	3991.63	4088.11	4218.87	2172.77	2049.52	1910.38
ENSMUSG00000068220.6	Lgals1	973.63	955.86	823.49	555.87	298.20	357.02	13207.74	14860.51	16255.90	11164.73	8927.83	8803.26
ENSMUSG00000041697.8	Cox6a1	259.13	131.21	386.26	110.65	88.49	80.21	1316.30	1308.10	1382.52	1061.92	936.71	822.15
ENSMUSG00000058239.13	Usf2	14.41	14.41	19.37	10.81	11.88	12.21	42.81	52.99	54.00	39.81	44.29	50.18
ENSMUSG00000004891.16	Nes	16.06	39.85	173.72	4.76	9.60	18.51	434.15	873.89	384.13	241.81	286.34	293.31
ENSMUSG00000028333.10	Anp32b	13.64	10.75	41.86	7.22	6.91	8.93	776.74	772.01	826.66	462.02	463.48	481.24
ENSMUSG00000042312.10	S100a13	29.82	45.93	16.15	15.42	12.40	8.43	258.19	280.04	307.98	305.30	186.92	192.58
ENSMUSG00000002233.13	Rhoc	33.72	35.12	164.97	32.54	39.20	50.81	1036.72	1069.30	1109.74	790.48	729.99	718.05
ENSMUSG00000028639.14	Ybx1	575.81	273.96	447.48	114.86	92.55	112.46	1634.56	1731.15	1894.89	747.39	839.55	834.41
ENSMUSG00000031029.6	Eif3f	183.54	172.22	260.52	94.74	95.01	107.59	335.06	413.69	404.51	175.29	222.62	204.36
ENSMUSG00000007892.8	Rplp1	35424.13	21776.32	17023.89	3882.61	2656.63	2482.33	20420.28	21249.84	22365.37	13961.69	10822.02	10122.42

Table 5.8: *Expression profile of neurite-enriched genes for control axonal and somal samples from E16.5 and 8WO mice. Expression is listed in uqTPM of RNAs enriched in the neurite transcriptome by (von Kügelgen & Chekulaeva, 2020). Colour-coding according to low (blue) and high (red) expression for each gene comparatively between samples, separately for embryonic and adult mice*

Increased expression of nearly all selected marker genes of the neurite transcriptome was observed in the axonal samples from both embryonic and adult mice, clearly showing the RNA extracted from axonal compartment exhibits a transcriptome profile representative of the axonal transcriptome as previously characterised (Table 5.8). It should, however, be noted that non-neuronal markers appear within the neurite transcriptome, thus indicating the possible contamination of non-neuronal cells in all established axonal preparations.

In summary, a characterisation of the cell-type distribution in the somal and axonal compartment was attempted, through the comparative assessment of expression of marker genes for non-neuronal and neuronal cells. Expression of markers of non-neuronal cells in the axonal compartment of DRG-cells from both embryonic and adult mice was established, which may indicate a contamination within the axonal compartment. A comparative assessment of expression of RNAs previously established as enriched in the neurite compartment, showed RNA expression clearly representative of an axonal transcriptome in axonal samples from both embryonic and adult mice, thus the non-neuronal contamination would be present in all axonal preparations. The RNA extracted from the axonal compartment of DRGs is shown to contain a distinct transcriptomic profile, distinct from that of neuronal or nociceptor cells and is therefore considered an axonal transcriptome for the remainder of this thesis.

5.3.3 PGE_2-induced sensitisation causes distinct changes to the axonal transcriptome

The transcriptomic profile of the axon and the soma were broadly characterised as unique, however, the defining features thereof remain elusive. Additionally, the changes induced to the axonal transcriptome by PGE_2 are unknown. To evaluate the changes to the local transcriptome of the axon in a sensitised state, DESeq2 was utilised to compare PGE_2-treated axonal samples to control axonal samples for E16.5 (Figure 5.4A) and 8WO (Figure 5.4B).

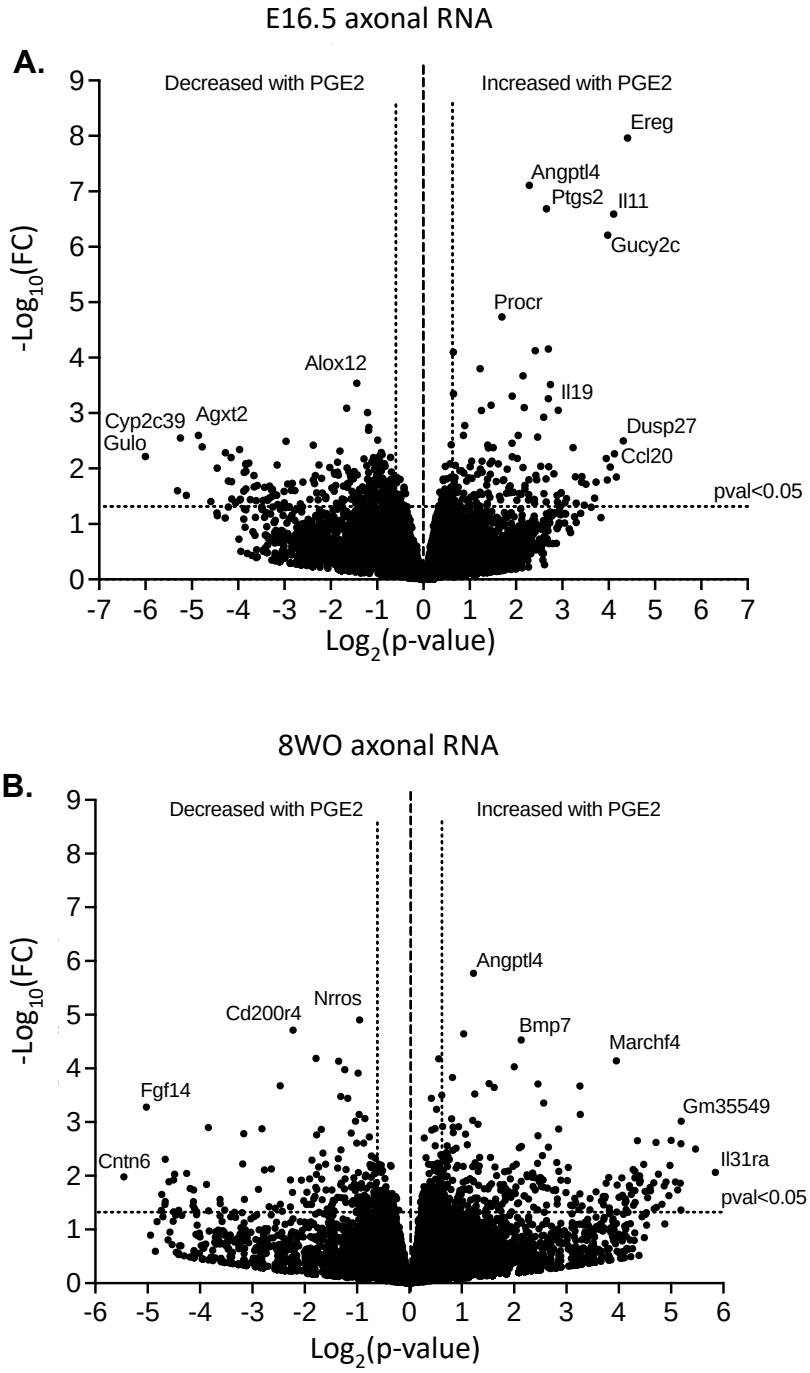

Figure 5.4: *Significantly changed RNAs in the axon of embryonic and adult DRG-cells following prolonged PGE_2. Volcano plot of the effect of PGE_2-treatment on RNAs localised to the axon of* ***A.*** *E16.5 and* ***B.*** *8WO mice evaluated using DESeq2 (n=3 for each condition). RNAs increased with PGE_2 measured as $-Log_{10}$(Fold Change) and Log_2(regular p-value) are found on the right and RNAs decreased with PGE_2 are observed on the left of the graph*

Statistically significant differences induced by incubation with PGE_2 in the axon were calculated by comparing PGE_2-treated axonal RNA to control axonal RNA individually for E16.5 DRG-cells (Figure 5.4A) and 8WO DRG-cells (Figure 5.4B) using

DESeq2. 155 and 496 RNAs and were significantly increased (with a regular p-value<0.05) with PGE_2-treatment for E16.5 and 8WO respectively, while 238 and 228 RNAs respectively were significantly decreased. A comparison of the overlap between results from E16.5 and 8WO mice was carried out and shown in a Venn diagram (Figure 5.5).

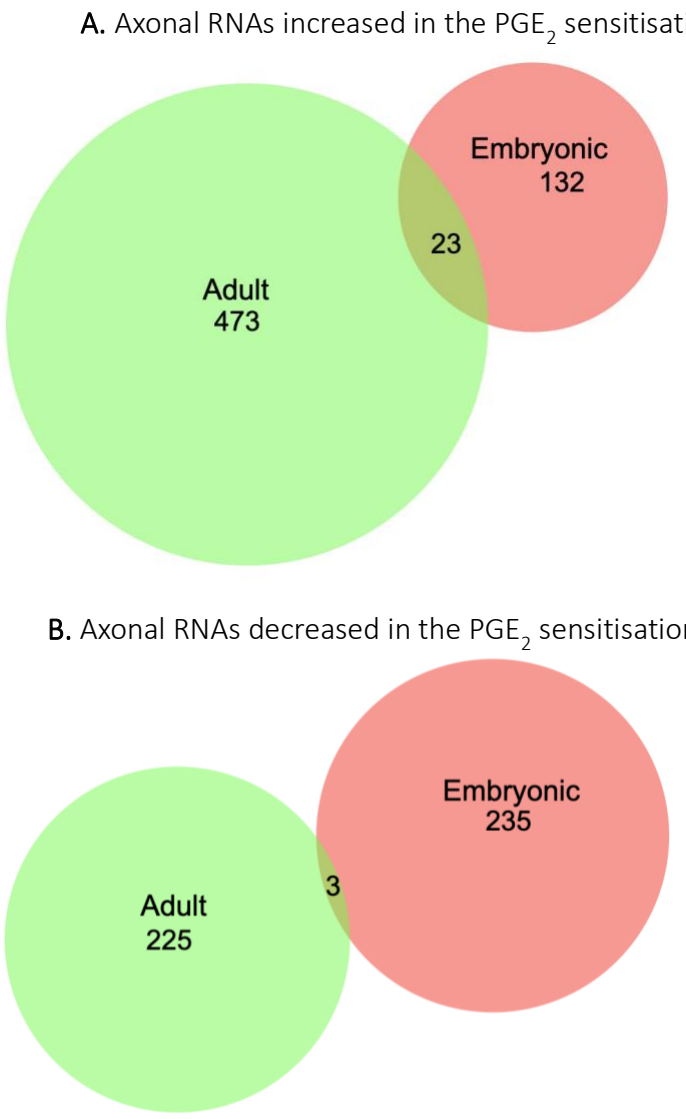

Figure 5.5: *Venn diagrams show the overlap of RNAs significantly changed in the axon of E16.5 and 8WO DRG-cells following prolonged incubation with PGE_2.* ***A.*** *23 RNAs significantly increased (p-value<0.05, DESeq2) in the axon of both E16.5 and 8WO DRG-cells following 24H 10µM PGE_2 incubation.* ***B.*** *3 RNAs significantly decreased (p-value<0.05, DESeq2) in the axon of both E16.5 and 8WO DRG-cells following 24H 10µM PGE_2 incubation. Venn diagrams were created through BioVenn (Hulsen et al., 2008)*

3 RNAs (*Mpped2*, *Slc22a1*, and *Myl2*) were significantly decreased following PGE_2 exposure, while 23 RNAs were significantly increased by PGE_2 in the axon for both

embryonic and adult mice (Figure 5.5). Interestingly, known markers of pain pathways such as *Ngf* and prokineticin receptor 2 (*Prokr2*) were included in the list of RNAs increased with PGE_2 (Table 5.9).

Gene ID	GeneSymbol	E16.5_FC	E16.5_pvalue	8WO_FC	8WO_pvalue
ENSMUSG00000040584.8	Abcb1a	3.734	6.32E-04	1.457	1.46E-02
ENSMUSG00000040396.12	Abhd13	1.317	3.10E-02	1.213	2.35E-02
ENSMUSG00000002289.16	Angptl4	4.835	2.56E-07	2.333	2.02E-06
ENSMUSG00000090698.2	Apold1	6.679	2.14E-04	2.025	1.59E-02
ENSMUSG00000037447.16	Arid5a	2.047	1.24E-02	1.405	1.45E-03
ENSMUSG00000036136.9	Fam110c	7.022	1.59E-02	1.769	1.32E-02
ENSMUSG00000003665.7	Has1	3.035	9.49E-03	2.143	3.08E-03
ENSMUSG00000020653.12	Klf11	1.343	4.35E-02	1.492	1.10E-02
ENSMUSG00000027859.10	Ngf	2.314	1.69E-04	1.430	4.94E-02
ENSMUSG00000028341.9	Nr4a3	6.414	8.67E-05	2.858	2.22E-04
ENSMUSG00000021684.17	Pde8b	1.576	2.84E-02	1.511	1.17E-02
ENSMUSG00000050558.13	Prokr2	2.585	3.68E-03	10.624	3.03E-02
ENSMUSG00000040511.14	Pvr	1.669	1.88E-02	1.482	1.38E-02
ENSMUSG00000026142.15	Rhbdd1	1.460	2.19E-02	1.274	3.63E-02
ENSMUSG00000022462.7	Slc38a2	1.376	2.37E-02	1.243	4.37E-02
ENSMUSG00000027737.10	Slc7a11	2.728	9.92E-04	1.295	1.89E-02
ENSMUSG00000032802.8	Srxn1	1.836	1.12E-03	1.337	1.55E-04
ENSMUSG00000032265.14	Tent5a	2.044	5.82E-03	1.474	2.88E-05
ENSMUSG00000040152.8	Thbs1	5.439	1.37E-02	1.528	3.51E-02
ENSMUSG00000024379.4	Tslp	9.257	5.98E-03	1.708	4.72E-02
ENSMUSG00000038172.14	Ttc39b	1.534	1.68E-02	1.253	1.50E-02
ENSMUSG00000020250.10	Txnrd1	1.668	4.00E-02	1.449	6.79E-03
ENSMUSG00000039646.5	Vasn	1.443	4.13E-02	1.277	4.82E-02

Table 5.9: *Significantly increased RNAs in the axon following PGE_2-sensitisation protocol for embryonic and adult mice showing the fold change, log_2(FC), and regular p-value*

5.3.4 The axonal transcriptome retains large proportion of expression patterns despite maturity of cells

Differences between the compartments of the cell were assessed through t-tests of uqTPMs separately for E16.5 and 8WO with Holm-Šídák correction for multiple testing. 1577 and 2141 RNAs were significantly enriched (p-value<0.05) in the axon compared to the soma for E16.5 and 8WO DRG-cells respectively. The similarities between results from embryonic and adult mice were assessed by comparing the lists of RNAs enriched in the axon (Figure 5.6).

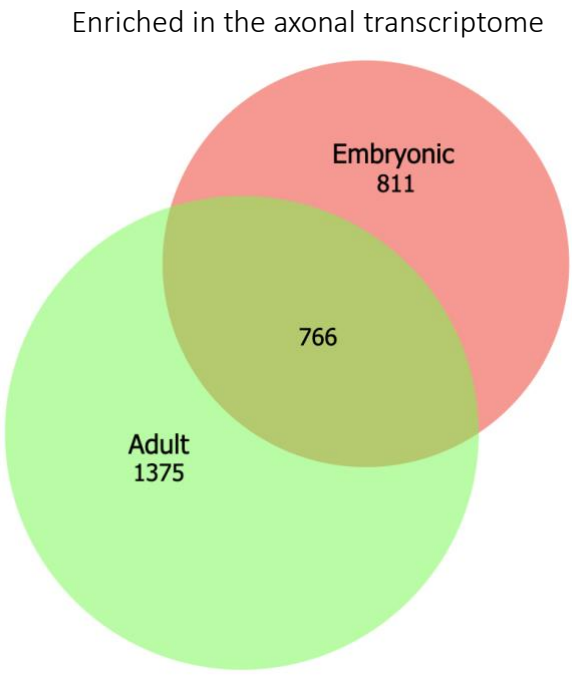

Figure 5.6: *Venn diagram shows 766 RNAs were enriched in the axon compared to the soma in both E16.5 and 8WO (p-value<0.05). Venn diagram was created through BioVenn (Hulsen et al., 2008)*

766 RNAs were significantly enriched in both E16.5 and 8WO (Figure 5.6), accounting for almost 50% of the genes enriched in the axonal E16.5 transcriptome. The *Ngf* mRNA encoding NGF was the only axonal RNA significantly increased with PGE_2 in the embryonic and adult mice, as well as being enriched in the axon for both embryonic and adult mice.

5.3.5 Canonical pathways defining the axon of DRG-cells are altered by PGE_2-sensitisation

To further explore the functional significance of the differential localisation of RNAs in the axon, as well as the changes evoked in our model of sensitisation, pathway analysis was carried out through Qiagen IPA software, characterising cellular and molecular pathways as well as upstream regulators.

The transcriptome of the control axon of embryonic and adult mice was explored using IPA. RNAs were included in the analysis if they were significantly increased or decreased (p-value<0.05) compared to the cell body with a $\log_2$ fold-change of

more than 0.6 and less than -1. Tighter restrictions were imposed for RNAs expressed comparatively lower in the axon to account for the high quantity of RNA in the cell body. The top 20 canonical pathways characterising the axonal compartment exhibit large overlap for embryonic and adult mice (Table 5.10).

Canonical Pathways of RNAs enriched in the axon	Embryonic Z-score	Adult Z-score
CREB Signalling in Neurons	-9.021	-5.126
EIF2 Signalling	5.689	6.325
Oxidative Phosphorylation	4.914	6.252
Phagosome Formation	-7.136	-3.571
Coronavirus Pathogenesis Pathway	-5.642	-4.902
Breast Cancer Regulation by Stathmin1	-6.869	-3.244
G-Protein Coupled Receptor Signalling	-5.824	-2.188
Gustation Pathway	-4.529	-2.84
Synaptogenesis Signalling Pathway	-3.91	-3.053
cAMP-mediated signalling	-4.116	-2.673
Calcium Signalling	-3.772	-2.53
Netrin Signalling	-4	-2.236
Dopamine-DARPP32 Feedback in cAMP Signalling	-3.545	-2.646
Synaptic Long Term Depression	-3.536	-2.5
IL-15 Production	-3.638	-2.309
Assembly of RNA Polymerase II Complex	3	2.828
GP6 Signalling Pathway	-1.606	-4.025
Neuropathic Pain Signaling In Dorsal Horn Neurons	-2.982	-2
Amyotrophic Lateral Sclerosis Signalling	-2.84	-2.111
Dilated Cardiomyopathy Signalling Pathway	-2.5	-2.333

Table 5.10: *Top 20 canonical pathways of RNAs enriched in the axon for both E16.5 and 8WO mice. Colour-coding indicates negative (blue) and positive (red) activation Z-score*

Activation of eIF2 and oxidative phosphorylation signalling pathways were observed as characteristic of the axonal transcriptome of both E16.5 and 8WO. The eIF2 signalling pathway was characterised by increased expression of translation initiation factor *Eif4a3* and RNAs encoding ribosomal proteins *Rps12* and *Rpl7a* in both E16.5 and 8WO. The oxidative phosphorylation signalling pathway was characterised by increased expression of mediators of mitochondrial function including *Cox6b1* and *Atp5md* in both E16.5 and 8WO. CREB signalling in neurons

had a negative activation score, indicating the repression of the pathway within the axonal compartment for both E16.5 and 8WO, compared to the somal compartment. Mediators of the CREB signalling pathway, which exhibited lowered expression in the axon compared to the soma, included *Ptgir* and *Cacna1h*, which encode the prostaglandin receptor I2, and the alpha-1H subunit of a voltage-gated Ca^{2+} channel.

IPA was subsequently used to evaluate statistically significant similarities of expression profiles of PGE_2-mediated sensitisation in the axon for embryonic and adult mice. RNAs which were significantly increased or decreased (p-value<0.05) with a $\log_2$ fold-change of more than 0.5 or less than -0.5 were considered for the analysis (Table 5.11)

Canonical Pathways of DE RNAs in the axon with PGE_2	Embryo Z-score	Adult Z-score
Synaptogenesis Signalling Pathway	-0.816	3.162
Erythropoietin Signalling Pathway	-2.236	1
Tumour Microenvironment Pathway	2.236	0.905
cAMP-mediated signalling	1.633	1.414
IL-17 Signalling	2.333	0.447
Senescence Pathway	-0.333	2
Dopamine-DARPP32 Feedback in cAMP Signalling	N/A	2
Amyotrophic Lateral Sclerosis Signalling	N/A	2
Protein Kinase A Signalling	0.816	1.155
Systemic Lupus Erythematosus In B Cell Signalling Pathway	1.633	0.277
Cardiac Hypertrophy Signalling (Enhanced)	0.333	1.528
Ferroptosis Signalling Pathway	-1.414	0.447
IL-6 Signalling	1	0.816
CREB Signalling in Neurons	-0.728	0.943
STAT3 Pathway	N/A	1.633
Corticotropin Releasing Hormone Signalling	0.816	0.707
LPS/IL-1 Mediated Inhibition of RXR Function	1	-0.378
TREM1 Signalling	N/A	1.342
Fc Epsilon RI Signalling	N/A	-1.342
White Adipose Tissue Browning Pathway	0.447	0.816

Table 5.11: *Top 20 canonical pathways of RNAs increased with PGE_2 in the axon for both E16.5 and 8WO mice. Colour-coding indicates negative (blue) and positive (red) activation Z-score. Activation Z-score is a numerical indicator of whether a given pathway is activated or inhibited based on*

expression of mediators of the pathway in the dataset. N/A defines a pathway with no clear directionality

The top 20 canonical pathways varied greatly between embryonic and adult mice, however, some pathways of interest were found to overlap including cAMP-mediated signalling and signalling of pro-inflammatory cytokines IL-17 and IL-6 (Table 5.11).

In contrast to the canonical pathways, a large overlap was observed when considering the top 20 predicted upstream regulators (Table 5.12).

Upstream Regulators of DE RNAs in the axon with PGE_2	Embryo Z-score	Adult Z-score
CREB1	4.144	4.679
forskolin	3.583	3.227
PDGF BB	3.751	2.875
LY294002	-4.031	-2.312
SB203580	-4.389	-1.871
H89	-2.421	-3.819
IL1B	3.459	2.764
F2	3.65	2.566
EGF	3.297	2.906
bucladesine	2.754	3.339
TGFB1	3.929	2.152
lipopolysaccharide	4.979	0.885
cyclic AMP	1.834	3.761
adenosine triphosphate	2.731	2.794
FGF2	3.641	1.741
GNAS	2.63	2.63
Salmonella enterica serotype abortus equi lipopolysaccharide	3.148	2.098
prostaglandin E2	2.461	2.682
HGF	2.099	2.96
P38 MAPK	3.314	1.681

Table 5.12: *Top 20 predicted upstream regulators of RNAs increased with PGE_2 in the axon for both E16.5 and 8WO mice. Colour-coding indicates negative (blue) and positive (red) activation Z-score*

Reassuringly, PGE_2 is a predicted upstream regulator for both embryonic and adult datasets, demonstrating that these data indeed represent the effects of PGE_2-induced sensitisation in the axonal compartment. Interestingly, CREB1 is a predicted upstream regulator in the axon following PGE_2-sensitisation for both E16.5 and 8WO, despite CREB signalling in neurons appearing repressed in axons when comparing to soma for both embryonic and adult mice (Table 5.10). The canonical pathway analysis shows CREB signalling in neurons to be activated for adult mice and inhibited in embryonic mice in the axon following the PGE_2-protocol (Table 5.11). A closer look at the CREB1 pathway map shows differentiation in the increased and decreased RNAs of the pathway between E16.5 and 8WO DRG-cells following PGE_2-sensitisation (Figure 5.7). The CREB1 pathway shows how upstream regulators can induce pathways differently in different environments.

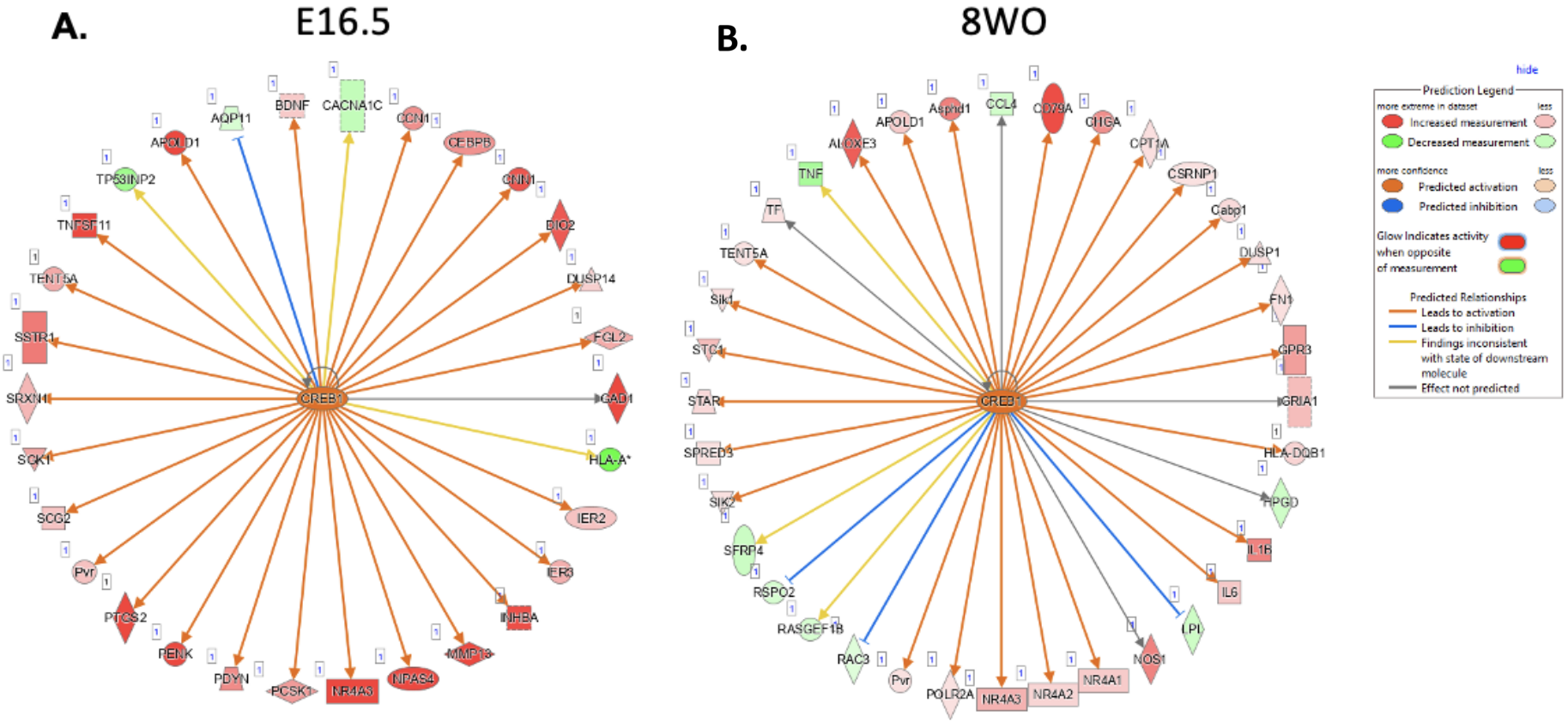

Figure 5.7: *Predicted upstream regulator CREB1 and the downstream effects following PGE_2-treatment on RNAs in the axon of* ***A.*** *E16.5 or* ***B.*** *8WO DRG-cells compared to control*

Consequently, IPA was used to explore patterns characterising the axon of E16.5 and 8WO DRG-cells. The age of the mouse did not appear to affect the pathways defining the RNAs of the axonal compartment. The canonical pathways defining the axonal compartment were very similar, including eIF2 and oxidative phosphorylation signalling significantly activated, while CREB signalling in neurons was repressed. In contrast, when considering the changes to the axon induced by PGE_2-sensitisation, significant differences were found between embryonic and adult mice. Different canonical pathways characterised the transcriptome of the sensitised axon, however, predicted upstream regulators, including PGE_2 and CREB1 were shown for both embryonic and adult mice. This suggests that although PGE_2-induced transcriptome changes in the axon are different between DRG-cells from embryonic and adult mice, the underlying regulatory pathways are the same.

5.4 Discussion

In this chapter the local transcriptome of the axon of sensory neuronal cells was explored. A distinct axonal transcriptome was shown, with high correlation between data from embryonic and adult mice. Transcriptome changes to the axon induced by the PGE_2-sensitisation protocol were characterised by different RNA expression profiles for embryonic and adult mice, however, with overlapping regulatory pathways.

5.4.1 The axonal transcriptome was distinct compared to the soma

Clustering of RNA samples was shown according to compartment of the DRG-cell. The axonal and somal samples from embryonic and adult mice exhibited clear clustering according to the cell-compartment, predicting large distinct differences to the transcriptome. In contrast, treatment with PGE_2 did not induce changes capable of driving separate clustering in the axon, which was to be expected (data not shown). A closer look at the RNA expression profile of the axon showed almost 50% overlap of RNAs enriched in the axon for embryonic mice with RNAs enriched in the axon for adult mice, showing a striking overlap between mice of different maturity. Previously an assessment of RNAs between two spinal levels showed about 10% of the differentially expressed RNAs in embryonic cells were also

differentially expressed in the adult dataset, where they accounted for about 25% (Smith-Anttila et al., 2020). These data indicated progressive development of distinct spinal levels between embryonic to adult cells, reflected in changes to the transcriptome. In contrast, our data show a distinct axonal transcriptome likely develops early and is retained through development from embryo to adulthood.

There is large diversity of cell-types found in dissociated DRG-cultures with some data showing as little as 10% of the cells to be of a neuronal subtype (Thakur et al., 2014). Indeed, when evaluating the expression of neuronal and non-neuronal markers a clear pattern of a distinct neuronal population was not evident in the somal or axonal compartment, rather broadly heterogenous expression was observed. A comparative assessment of RNAs which had previously been established as enriched in a broader neurite transcriptome, showed striking increased expression in our axonal samples (von Kügelgen & Chekulaeva, 2020). The marker-genes for the core neurite transcriptome included several RNAs encoding ribosomal-proteins (*Rps18, Fau, Rps12, Rps2, Rplp1*), as well as RNAs with a variety of signalling and localised roles; *Cox6a1* (mitochondrial function), *Usf2* (Ca2+ responsive transcription), *S100a13* (Ca2+ responsive protein secretion), *Nes* (outgrowth formation), *Anp32b* (nuclear protein), *Rhoc* (plasma membrane), *Ybx1* (RNA binding), *Eif3f* (translation machinery).

Previously, immunocytochemistry indicated the exclusive penetration of axonal growths through the porous membrane of the compartmentalised chamber used for cell culturing (see Chapter 3). The RNAseq data confirm a distinct biologically homogenous fraction is obtained, exhibiting a unique transcriptome profile defining the axonal compartment of the porous membrane chamber, with a large quantity of retained information between embryonic and adult mice. However, variability was observed in PCA plots indicating variation between axonal samples, in addition to a comparative analysis of cell-subtype distribution through expression of marker genes for non-neuronal cells. Non-neuronal contamination may be a source of variation within all axonal preparations as indicated by the marker genes characterising the neurite transcriptome. This should be addressed through cell

sorting to obtain a purely neuronal culture from which axonal RNA could be extracted.

5.4.2 The axonal transcriptome was characterised in part by eIF2 signalling

Pathway analysis showed a high overlap of canonical pathways characterising the axonal transcriptome for E16.5 and 8WO (Table 5.11). Of particular interest were the pathways predicted to be activated through a positive Z-score, which included eIF2 signalling, oxidative phosphorylation and assembly of RNA polymerase II complex. Previous research has already shown a role for eIF2 signalling in local translation within the axon through an mTOR/PERK and calreticulin pathway (Cagnetta et al., 2019; Pacheco et al., 2020). *Rpl7a* mRNA, which was found significantly increased in the axon for both embryonic and adult mice, has been shown to play a key role in eIF2 signalling of local translation driving axon guidance and branching, measured through immunofluorescent imaging following stimulation of eIF2-phosphorylation (Cagnetta et al., 2019). Oxidative phosphorylation has additionally been previously shown as an activated pathway within axons during eIF2 signalling (Cagnetta et al., 2019). Oxidative phosphorylation is commonly associated with mitochondrial activity and has previously been shown as an activated pathway in mature myelinated axons obtained from rats *in vivo* (Farias et al., 2020). These findings have not previously been established in mice, thus this data provides novel additional support for these signalling pathways being retained in mice**.**

The prediction of the activation of the pathway for assembly of RNA polymerase II complex is not immediately apprehensible, as RNAs are well-known to only be transcribed within the nucleus of cells. However, the presence of mRNAs encoding transcription factors, as well as nuclear transport machinery in the axon has been shown previously (S.-J. Ji & Jaffrey, 2014; Minis et al., 2014). It is suggested that retrograde transport of axonally translated and synthesised transcription factors, such as CREB1, may follow axonal injury to drive expression profile changes (Korsak et al., 2016; Melemedjian et al., 2014). Interestingly, a closer look at the axonal datasets from E16.5 and 8WO show high expression of mRNAs encoding transcription factors *Atf4* and *Creb1*, which have been associated with local

translation and in research of pain pathways (Cagnetta et al., 2019; Cox et al., 2008; L. Dong et al., 2011). Additionally, *Atf4* expression is known to be subject to regulation by the eIF2 pathway in pathological conditions in neurons of the CNS, with elevated *Atf4* associated with misregulation of protein synthesis (Krukowski et al., 2020; Pitale et al., 2017). Furthermore, elevated expression of *Atf4* RNA was associated with increased expression of inflammatory and nociceptive mediators IL-1β, IL-6 and TNF-α, in retinal cells undergoing degeneration, in addition to several chemokines, at both RNA and protein level in a pathway mediated by eIF2-α (Rana et al., 2014).

Mediators of the CREB signalling pathway, which exhibited lowered expression in the axon compared to the soma, included *Ptgir* and *Cacna1h* which encode a prostaglandin receptor and a subunit of a Ca^{2+} channel. This is puzzling, however, correlates with previous data that has shown comparatively repressed expression of RNAs encoding membrane-associated and transmembrane proteins in the axon, despite elevated expression at the protein level (Minis et al., 2014).

In summary, a distinct axonal transcriptome is apparent, characterised by expression of RNAs encoding ribosome-proteins and transcription factors, as well as mediators of local translation.

5.4.3 PGE_2-sensitisation induced changes to the axonal transcriptome associated with PKA- and cAMP-signalling

To assess the differences in cells from embryonic and adult mice, the PGE_2-experimental design was repeated with DRG-cells from 8WO adult mice. However, the treatment with PGE_2 was reduced to 12H due to practical constraints within the laboratory. Nevertheless, *Ngf* was found significantly increased in the transcriptomic analysis following PGE_2-treatment in cells from adult mice, confirming a validation measure from the embryonic model. Additionally, pathway analysis using IPA shows PGE_2 as a predicted upstream regulator for both embryonic and adult axonal RNA following PGE_2 pre-treatment, further confirming comparability of the results, despite the differing treatment times.

23 RNAs were significantly increased in the axon following PGE_2-sensitisation for both embryonic and adult mice. Interestingly, *Ngf*, was the only mRNA which exhibited enrichment in the axon for both embryonic and adult mice, and additionally exhibited significantly increased expression in the axon for both embryonic and adult mice. The role of *Ngf* as a mediator of nociceptive plasticity has previously been attributed to stimulation of neuronal cells by the NGF protein produced by primarily immune cells in the periphery, however, these results suggest a possible autocrine mechanism, where *Ngf* mRNA translocation to the axon plays a role in sensitisation (Denk et al., 2017; Schmelz et al., 2019).

Due to the large variations in significantly increased RNAs following PGE_2-sensitisation, pathway analysis showed variations in the canonical pathways characterising the PGE_2-sensitised axonal transcriptome, however, interesting overlaps were nevertheless observed. IL-6, protein kinase A (PKA), and cyclic AMP (cAMP)-mediated signalling exhibited positive activation Z-scores (Table 5.11). These signalling pathways have all in previous research been linked to PGE_2-mediated sensitisation of DRG nociceptors (L.-Y. M. Huang & Gu, 2017; St-Jacques & Ma, 2014). IL-6 is a known key mediator of inflammatory and neuropathic pain, inducing hyperexcitability in nociceptors through ERK/MAPK and MNK1/2-eIF4E signalling inducing increased activation of voltage-gated Ca^{2+} channels, as well as increased PGE_2-induced signalling and expression of TRPV1-receptors (Kummer et al., 2021; Moy et al., 2017). cAMP/PKA signalling has been shown to induce significantly increased amplitude of ATP-currents, mediated by homomeric P2X3-receptors in DRG-cells through PGE_2 binding to the EP3 receptor (C. Wang et al., 2007). The role of PKA was shown through the PKA-inhibitor H89, which is additionally found to exhibit a confident negative activation score in the axonal transcriptome following PGE_2-sensitisation, corresponding to an activated PGE_2/PKA-mediated pathway of sensitisation (Table 5.12). Consequently, the PGE_2 protocol is shown to induce relevant pathways of sensitisation.

Predicted upstream regulators of the axonal transcriptome following PGE_2-treatments were, in contrast to canonical pathways, found to largely overlap for samples from E16.5 and 8WO (Table 5.10). Discrepancies emerged, as CREB1 was

predicted as an upstream regulator, while CREB signalling in neurons have opposite activation scores in the canonical pathway analysis. The differences are explored through a detailed look at the expression of downstream targets of CREB1 in our datasets (Figure 5.7). While similarities are observed, different downstream targets are shown for E16.5 and 8WO. The discrepancies are predicted to be attributed to either the maturity of the cell or the variation in the length of PGE_2-exposure. The differences within the PGE_2-protocol could result in the *in vitro* model exhibiting different stages of the development of hyperalgesia. Similarly, the differences in RNA expression attributed to maturity may lead to diverse representation of CREB1 signalling.

5.4.4 Conclusions

In this chapter the local axonal transcriptome of DRG-cells was explored and characterised through RNAseq and pathway analysis. A distinct axonal transcriptome emerged, indicating a large overlap between embryonic and adult mice. Pathway analysis showed significant overlap in the pathways defining the local transcriptome including eIF2 signalling, and mediators of pathways of local translation.

The changes to the axonal transcriptome driving hyperalgesic priming following PGE_2-sensitisation protocol, showed differences to the RNA expression profiles between embryonic and adult mice, however broad overlap in the predicted regulatory mechanisms. This was suggested to be due to different stages of hyperalgesic priming.

This is believed to be the first research to comprehensively assess the differences to the axonal transcriptome in a model of sensitisation in mice, facilitating the search for novel localised targets. Local targets, specifically RNAs playing key roles in the manifestation of a sensitised state, are of particular interest as they can be further explored as possible targets for novel therapeutics. Consequently, it was of interest to further explore select RNAs emerging as significantly increased in the axon following PGE_2-sensitisation to assess potential targets of clinical relevance.

Chapter 6: Novel mRNAs localised to the axon facilitate the development of sensitisation

6.1 Introduction

Extensive research has gone into exploring the development of pain pathways, however, despite this, few broadly effective treatments for chronic pain are available. This may be due to limited understanding of the specific changes within nociceptors driving the manifestation of chronic pain. Specifically, local protein translation has been shown to drive development of hyperalgesia, therefore changes to the transcriptome of the axon are predicted to be of key relevance (Ferrari et al., 2013; Jiménez-Díaz et al., 2008; Zappulo et al., 2017).

6.1.1 Specific RNAs drive the development of sensitisation in the axon of nociceptors

The search for novel targets for therapeutics is of particular interest in the field of chronic pain. Next generation sequencing (NGS) has been utilised to identify specific markers and targets in other fields of research such as *SELENBP1* and *SLC4A1* RNA as biomarkers and possible therapeutic targets for hepatocellular cancer (Han et al., 2021; Zhao et al., 2019). The surge in NGS studies presents a novel opportunity to similarly apply the technique in the pursuit of novel targets for therapeutics for chronic pain. As previously discussed, RNAseq has been used to characterise sensory neuronal cells, as well as nociceptors specifically (see Chapter 1). Additionally, in the last decade a number of studies have been published exploring the changes to the transcriptome of nociceptors in chronic pain states (J. Ma et al., 2015; Uttam et al., 2018; Wu et al., 2016; Yin et al., 2016). Transcriptional changes to pathways of inflammation were predicted and confirmed through sequencing of DRG-cells following the induction of *in vivo* models of chronic pain (J. Ma et al., 2015; Uttam et al., 2018). Neuroplastic changes inducing sensitisation in nociceptors were additionally found to include increased expression of mediators of axonal guidance in an *in vivo* model of burn pain (Yin et al., 2016). Furthermore, axonal guidance and growth is mediated through localised translation, showing the need for further research of the changes to the local transcriptome and regulation thereof in the axon in states of chronic pain (Verma et al., 2005; Vogelaar et al., 2009; J.-Q. Zheng et al., 2001).

Through the use of translation inhibitors, including rapamycin, cordycepin, and anisomycin, injected into the paw of rats, localised protein translation has been shown to play a key role in the development of hyperalgesia *in vivo* (Bogen et al., 2012; Ferrari et al., 2013; Jiménez-Díaz et al., 2008) (see also Chapter 5). Additionally, the expression patterns of RNAs localised to the axon has been shown to correlate with the probability of local translation (Shigeoka et al., 2016; Zappulo et al., 2017). The existence of a distinct axonal transcriptome, subject to changes during the development of sensitisation, introduces the possibility of interventions delivered specifically to the periphery, targeting specific local mechanisms to prevent or reverse the development of sensitisation. The characterisation of the axonal transcriptome following PGE_2-sensitisation facilitates the search for novel RNA targets, mediating the localised neuroplastic changes driving hyperalgesic priming of sensory neuronal cells.

In this chapter, 3 RNAs (*Cebpb*, *Arid5a* and *Tnfrsf12a*) shown to be significantly increased in the axon following PGE_2-sensitisation protocol, were depleted prior to initiating the PGE_2-protocol, to assess the effect of specific RNAs playing key roles in the axon on the development of sensitisation. *Cebpb* encodes the transcription factor C/EBPβ and was identified as significantly increased in the axon with PGE_2 for embryonic mice. *Arid5a* encodes the RNA-binding protein (RBP) Arid5a and was found to be significantly increased with PGE_2 in the axon for both embryonic and adult mice. *Tnfrsf12a* mRNA encodes the TWEAK receptor, Fn14, and was significantly increased with PGE_2 in the axon for embryonic mice, as well as enriched in the axon for both embryonic and adult mice.

6.2 Hypothesis and objectives

The hypothesis of this chapter is that inhibition of select RNAs, involved in the development of sensitisation in the axon of DRG-cells, inhibits the development of PGE_2-induced sensitisation.

The objectives of this chapter were to:

- assess the effect of inhibition of *Cebpb*, *Arid* and *Tnfrsf12a* mRNA from DRG-cells prior to initiating PGE_2-sensitisation protocol, on nociceptor excitability

6.3 Methods

The PGE_2-model was optimised by using a stabilised version of PGE_2, 16,16-dimethyl PGE_2 (16,16-PGE_2), which only had to be supplemented every 12H to maintain a stable concentration (see detailed methods in Chapter 2.3)

A list of possible RNAs of interest was selected based on initial unbiased bioinformatic analysis identifying RNAs which were enriched in the axon, and significantly increased in the axon following PGE_2-sensitisation protocol (see detailed methods in Chapter 2.11). 3 RNAs were selected:

- *Cebpb* is significantly increased in the axon with PGE_2 for embryonic mice
- *Arid5a* is significantly increased with PGE_2 in the axon for both embryonic and adult mice. Expression was confirmed in the control axon, however, in control samples expression is significantly lower in the axon compared to the soma by about 50%
- *Tnfrsf12a* is significantly increased with PGE_2 in the axon for embryonic mice, as well as enriched in the axon for both embryonic and adult mice

To validate the RNAseq results, *Cebpb*, *Arid5a*, and *Tnfrsf12a* mRNA was measured using qPCR of somal and axonal RNA from E16.5 DRG-cells exposed to the PGE_2- or the control-protocol (see detailed methods in Chapter 2.8)

siRNAs specific for the RNAs of interest were introduced to the 16,16-PGE_2-model of hyperalgesia. E16.5 DRG-cells were exposed to 1µM siRNA targeting one of the 3 RNAs of interest, or a non-targeting control siRNA, for 48H. After 24H of siRNA treatment, the 16,16-PGE_2-sensitisation- or control- protocol was commenced. Subsequently, the excitability of the nociceptors was measured in response to capsaicin activation through Ca^{2+} imaging according to previously described method (see detailed methods in Chapter 2.4 and 2.9).

6.4 Results

6.4.1 Stabilised 16,16-PGE_2 induces sensitisation of nociceptors

The efficacy of stabilised 16,16-PGE_2 as an inducer of sensitisation was assessed through measurements of the excitability of nociceptors using Ca^{2+} imaging following activation with capsaicin (Figure 6.1).

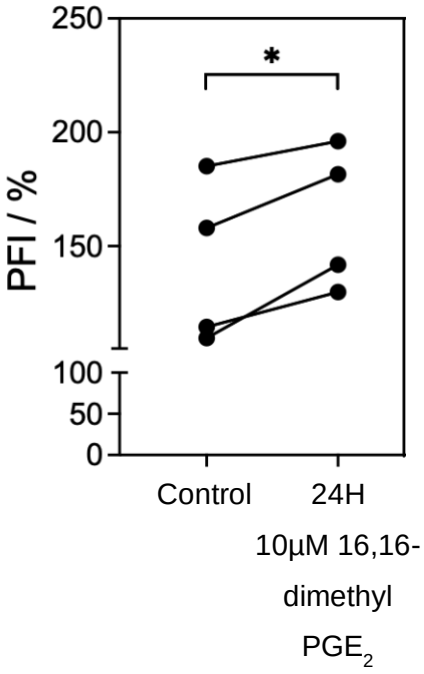

Figure 6.1: *PFI of DRG-cells exposed to 24H 10µM 16,16-PGE_2 is significantly increased compared to control-protocol following stimulation with capsaicin. A significant increase (20.5±4.7%) in excitability is observed following 200nM capsaicin stimulation in DRG-cells exposed to 16,16-PGE_2 compared to control cells (* = p-value = 0.0221, paired t-test, n=4)*

16,16-PGE_2 was found to induce a significant increase in Ca^{2+} transients, measured as peak fluorescent intensity (PFI), of the nociceptors following capsaicin activation, mimicking the functional model of hyperalgesia induced by PGE_2.

6.4.2 Inhibition of target RNAs affect the establishment of sensitisation

3 RNAs were selected as possible key mediators of the manifestation of PGE_2-induced sensitisation, and qPCR was used to validate the RNAseq results.

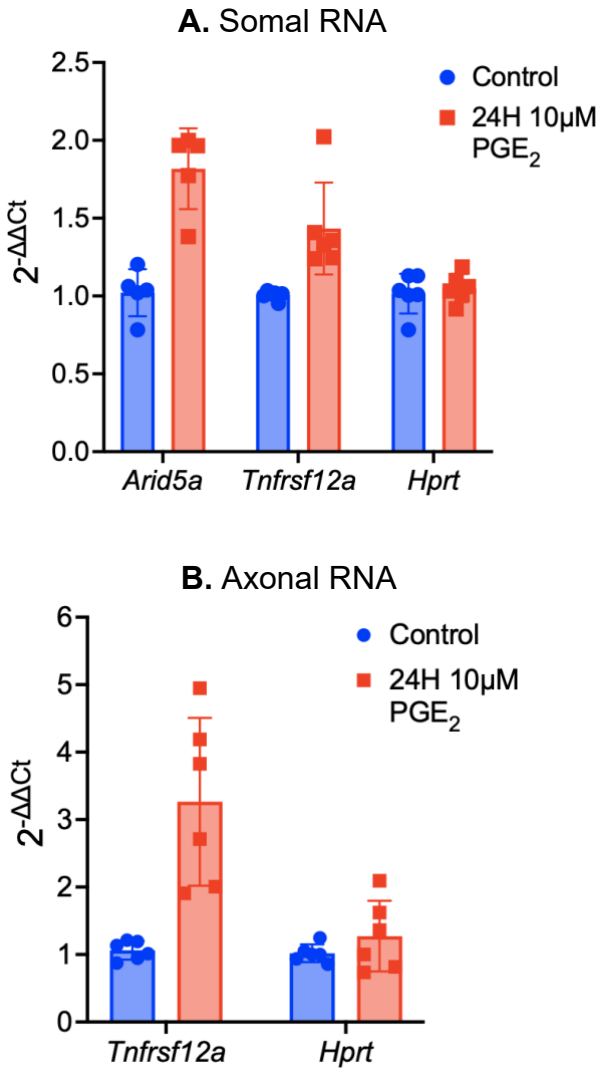

Figure 6.2: *RT-qPCRs of target RNAs Arid5a and Tnfrsf12a, and housekeeping RNA Hprt in* ***A.*** *somal samples and* ***B.*** *axonal samples. In the soma Tnfrsf12a and Arid5a are increased following 24H 10μM PGE_2, while Hprt expression remains stable. In the axon Tnfrsf12a is increased while Hprt shows slight variation in expression following 24H 10μM PGE_2. qPCRs are carried out with Gapdh as the reference gene and n=2 biological replicates*

Measurements of expression of target RNAs in the somal fraction of RNA from E16.5 DRG-cells confirmed the increase in expression of *Arid5a* and *Tnfrsf12a* following PGE_2-sensitisation protocol, while the reference gene *Hprt* remained stable (Figure 6.2A). Measurements of expression of target RNAs in the axonal fraction of RNA from E16.5 DRG-cells confirmed the increase in *Tnfrsf12a* expression following PGE_2-sensitisation protocol (Figure 6.2B). Variation in housekeeping gene *Hprt* expression was observed in the axonal sample, however, this was minor in comparison to the increase in *Tnfrsf12a*. *Cebpb and Arid5a* could not be measured in the axonal samples (data not shown). Only 2 biological

replicates were assessed to show proof of principle, therefore, statistical significance was not calculated due to low n-numbers.

Cebpb, *Arid5a*, and *Tnfrsf12a* RNA was separately depleted from E16.5 DRG-cells prior to initiating the 16,16-PGE_2-senstisation protocol. The activity level was compared to untreated control cells, which were neither exposed to siRNAs nor 16,16-PGE_2. The activity level of DRG-cells exposed to target siRNAs was additionally compared to the PFI of DRG-cells exposed to a non-targeting siRNA control as well as 16,16-PGE_2.

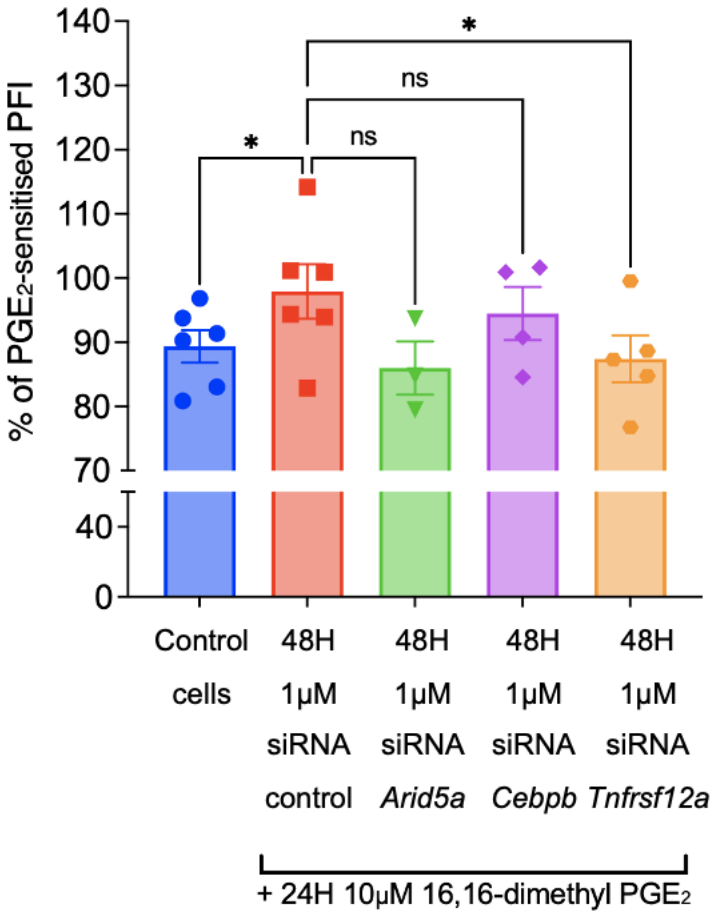

Figure 6.3: *% of PGE_2-sensitised PFI of E16.5 DRG-cells activated with 200nM capsaicin after incubation with 48H 1µM target siRNA and 24H 10µM 16,16-dimethyl PGE_2, compared to untreated control cells, shows the effect of inhibition of select target RNAs on manifestation of sensitisation. A significant increase was measured in cells pre-treated with siRNA control and 16,16-dimethyl PGE_2 compared to control (n=6, * = p-value=0.0386, mixed effects ANOVA). A significant decrease (-10.5±1.8%) was measured in cells pre-treated with Tnfrsf12a siRNA and 16,16-dimethyl PGE_2 compared to the siRNA control with 16,16-dimethyl PGE_2 (n=5, * = p-value=0.0134, mixed effects ANOVA). A non-significant decrease (n=3, -11.9±3.5%) was measured in cells pre-treated with Arid5a siRNA prior to pre-treatment with 16,16-PGE_2 compared to siRNA control and 16,16-dimethyl PGE_2.*

Pre-treatment with Cebpb siRNA prior to pre-treatment with 16,16-PGE_2 did not appear to affect the sensitisation with 16,16-PGE_2

A significant increase in the excitability of DRG-cells exposed to 16,16-PGE_2+siRNA control compared to the untreated control cells was observed, demonstrating a model of sensitisation was indeed induced with 16,16-PGE_2 treatment, which was unaffected by control siRNA (Figure 6.3). Inhibition of *Arid5a* RNA prior to 16,16-PGE_2-sensitisation was found to reduce the activity of cells, however this was not significant. Inhibition of *Cebpb* RNA prior to 16,16-PGE_2 sensitisation did not appear to affect the activity of cells. *Tnfrsf12a* RNA inhibition induced a statistically signification decrease in excitability of nociceptors compared to DRG-cells treated with control siRNA of ~–15%, with the excitability level equivalent to that of untreated control cells. These results show that knockdown of axonally localised *Tnfrsf12a* RNA plays a key role in 16,16-PGE_2-induced sensitisation in DRG-cells.

6.5 Discussion

Previous studies have reported a key role for local translation in the axon in mediating the development of hyperalgesia (Bogen et al., 2012; Ferrari et al., 2013; Jiménez-Díaz et al., 2008; Melemedjian et al., 2014). Additionally, local RNA expression has been shown to correlate with local translation, predicting the significant effect of changes to the axonal transcriptome on the development of sensitisation (von Kügelgen & Chekulaeva, 2020; Zappulo et al., 2017).

In this chapter, novel RNA targets from the sensitised axonal transcriptome were shown to affect hyperalgesic priming.

6.5.1 Inhibition of *Cebpb* RNA did not affect PGE_2-induced sensitisation

Bioinformatic analysis showed *Cebpb* mRNA was significantly increased in the axon of E16.5 DRG-cells following prolonged PGE_2-incubation. In this chapter, increased expression of *Cebpb* in the axon following incubation with PGE_2 could not be confirmed through qPCR experiments. However, this could be attributed to very low quantities of RNA in the axon, or even flawed primers as the RNA expression could not be confirmed in control or somal samples either. Subsequent inhibition of

Cebpb mRNA using siRNA did not appear to affect the activity-level of nociceptors, measured as Ca^{2+} transients following capsaicin activation.

Cebpb mRNA encodes the transcription factor C/EBPβ, which is highly conserved in mammals (Pulido-Salgado et al., 2015). C/EBPβ has in rats been shown to play a role in upregulated expression of P2X3R and TRPV1, both key receptors of nociceptive signalling in DRGs, by forming a complex containing the transcription factor Runx1 (Ugarte et al., 2012, 2013). In DRG-cells from mice an increase in C/EBPβ has additionally been associated with a decrease in abundance of $K_V1.2$ and μ-opioid receptor MOR, similarly leading to an increased excitability of sensory neuronal cells (Z. Li et al., 2017). Data from rat and human cells show a functional regulatory role of C/EBPβ in induction of *mPGES-1* mRNA, a specific PGE_2 terminal synthase, further demonstrating the involvement in known pain pathways (Walters et al., 2012). Extensive research on the role of C/EBPβ in the CNS shows an increase in expression of the transcription factor following cAMP or dopamine increase, or depolarisation of the cell, however, also more broadly in inflammation states in glial cells and memory formation in neuronal cells (Pulido-Salgado et al., 2015). Remarkable similarities have previously been shown between memory formation and the plasticity of sensory neuronal cells driving a state of sensitisation (Price & Inyang, 2015). In several other non-neuronal cell-types, including osteoblasts and chondrocytes, C/EBPβ has been linked to the development of arthritis through NF-κB-driven regulation of IL-6 expression and the expression of other inflammatory mediators (Nishimura et al., 2020; Yan et al., 2010). *Cebpb* mRNA is a highly likely mediator of pathways of sensitisation in the DRG, however, a localised effect of the transcription factor has not yet been explored.

Due to previous assessments of the diversity of cell-types within DRG-cultures, the expression pattern of *Cebpb* RNA in MACS-identified nociceptor cultures was evaluated using the Neuro-Immune Interactions in the Periphery (NIPPY) database, published by the Denk laboratory (Liang et al., 2020). *Cebpb* could not be confirmed as expressed in MACS-sensory neurons in any condition above the margin of error-threshold, demonstrating the mRNA is possibly primarily non-neuronal.

Consequently, while *Cebpb* was indicated as a promising local target in bioinformatic analysis of RNAseq data, as well as in previous research, our results show that the inhibition of *Cebpb* RNA does not inhibit the development of a sensitised state in DRG-cells. However, the indiscriminate inhibition of *Cebpb* RNA expression could be hypothesised to induce a pathway to counteract the loss of the transcription factor. An interesting future experiment would be to selectively deplete the transcription factor in the axon of sensory neuronal cells as well as in macrophages, where the transcription factor has been confirmed to play a role, using microfluidic chambers with fluidic isolation and cell-specific RNAi such as targeted AAV-vector based shRNA depletion, prior to the PGE_2-sensitisation protocol (S.-C. Kim et al., 2022). This would facilitate the study of the localised role of *Cebpb* mRNA in the axon in during the development of sensation.

6.5.2 Inhibition of *Arid5a* RNA affected PGE_2-induced sensitisation

Bioinformatic analysis of RNAseq data established *Arid5a* as significantly increased in the axon following PGE_2-sensitisation protocol in both E16.5 and 8WO DRG-cells. In this chapter, increased expression of *Arid5a* in the cell body was established using qPCR following prolonged incubation with PGE_2, however, the expression could not be validated in the axon. The mRNA had exhibited measurable expression in the control axon through RNAseq, however, the RNA could not be measured in either control or PGE_2 axonal samples using qPCR. The lack of measurable expression using qPCR may therefore be due to low general expression in the axon. Knockdown of *Arid5a* RNA through siRNA incubation was found to prevent the development of a sensitised state, however, these results were not statistically significant. This lack of statistical significance could be hypothesised to be due to low n-numbers. Future experiments should be carried out to increase the n-numbers, however, this could not be accomplished for this thesis due to time-constraints.

Arid5a mRNA encodes the RNA-binding protein (RBP) Arid5a, which is known to have both transcriptional and post-transcriptional roles (Nyati & Kishimoto, 2022). Arid5a has been comprehensively associated with inflammation in both *in vitro* and *in vivo* studies, associated with diseases including cancer, cardiac inflammation and

autoimmune diseases (Nyati & Kishimoto, 2022; Tanaka et al., 2020). The RBP is localised to the nucleus in stable cells but translocated to the cytoplasm in inflammatory states where it is involved in specific mRNA stabilisation. Specifically, Arid5a appears to be closely linked to regulation of the *Il6* mRNA (which encodes IL-6) by binding to the 3'UTR of the mRNA and preventing degradation (Masuda et al., 2013; Nyati & Kishimoto, 2022). Arid5a has been linked to two different pathways of activation. Comprehensive research in murine macrophages shows the involvement of a Toll-like receptor 4 (TLR4) and NF-κB/MAPK pathway to regulate Arid5a which stabilises *Il6* mRNA inducing increased IL-6 expression which in turn induces *Arid5a* expression in a circular pathway (Masuda et al., 2013; Nyati et al., 2017). Toll-like receptor stimulation of DRG-neurons has been shown to induce pain behaviours, with confirmation of TLR4 expression in sensory neuronal cells sensitive to capsaicin-activation (Qi et al., 2011). Additional research indicates a cAMP/PKA/CREB pathway of *Arid5a* induction causing an upregulation of *Il6* expression in cardiac fibroblasts (Tanaka et al., 2020). These posttranscriptional mechanisms are of particular interest as IL-6 is a well-known and validated mediator of chronic pain (Melemedjian et al., 2010; Segond von Banchet et al., 2005). IL-6, NF-κB, MAPK, cAMP, CREB and PKA pathways have been associated with PGE_2-induced sensitisation of DRGs (St-Jacques & Ma, 2011). *Arid5a* mRNA could therefore be predicted to play a role in nociceptive plasticity within these pathways. Further supporting a local role, is research implicating axonal translation of CREB following IL-6 stimulation to induce sensitisation (Melemedjian et al., 2014). Consequently, *Arid5a* is suggested to play a role in the manifestation of chronic pain by stabilising *Il6* mRNA in the axon, in a feedback loop where CREB upregulation following IL-6 stimulation induces further *Arid5a* expression.

The expression of *Arid5a* was confirmed in MACS-identified nociceptor cells in both sham operated mice, as well as sensory neurons of the ipsilateral and contralateral side 8 days following PSNL (Liang et al., 2020). The expression of *Arid5a* mRNA appeared to be increased in the ipsilateral joint, further supporting a role in pathways of functional hyperalgesia.

Consequently, *Arid5a* is predicted to play a role in the manifestation of a sensitised state localised to the axon of sensory neuronal cells, possibly through CREB- and IL-6-pathways.

6.5.3 Inhibition of *Tnfrsf12a* prevented PGE_2-induced sensitisation

Tnfrsf12a was established as significantly increased in the axon following prolonged incubation with PGE_2 in E16.5 DRG-cells, and additionally shown to be enriched in the axon for both E16.5 and 8WO DRG-cells. *Tnfrsf12a* was confirmed to be increased following PGE_2-sensitisation protocol in both the soma and the axon of embryonic DRG-cells through qPCR. Inhibiting *Tnfrsf12a* RNA through siRNA incubation was found to effectively prevent a sensitised state from developing, as the excitability of nociceptors remained equivalent to that of control cells.

Tnfrsf12a mRNA encodes the TWEAK receptor, also known as Fn14. TWEAK/Fn14 activity has been implicated in a plethora of pathologies including cancer (Hu et al., 2017), respiratory diseases (M. Wang et al., 2020), autoimmune diseases (W.-D. Xu et al., 2016), heart failure (Ren & Sui, 2012), and bone loss (Du et al., 2015). TWEAK/Fn14 effects are executed through interactions with the TRAF family of adaptor molecules which bind to specific binding sites in the cytoplasmic domain of Fn14 and subsequently induce downstream signalling pathways (Hu et al., 2017). The TWEAK/Fn14 axis is found to initiate inflammatory pathways, including NF-κB/STAT3, MAPK, and PI3K/AKT which induce increased expression of pro-inflammatory cytokines and inflammatory mediators including TNF-α, IL-6, IL-1β and IL-8 (Du et al., 2015; Hu et al., 2017; Ren & Sui, 2012; M. Wang et al., 2020; W.-D. Xu et al., 2016). TWEAK/Fn14 activity has been shown in both the healthy CNS and in disease states such as multiple sclerosis and cerebral oedema (Yepes, 2007). Once again, an inflammation pathway is suggested, as treatments with TWEAK induces increases in IL-6 and IL-8. A limited body of work has been found to explore Fn14 activity in sensory neuronal cells of the DRG (L.-N. Huang et al., 2019; Tanabe et al., 2003). An increase in Fn14 was initially reported following peripheral nerve injury, and subsequently related to axonal regeneration, however, interestingly, independent of TWEAK expression (Tanabe et al., 2003). The effect of increased Fn14 expression was attributed to ligand-independent TRAF-driven activation of the

NF-κB pathway. Furthermore, increased expression of *Tnfrsf12a* mRNA, as well as Fn14 protein, in DRG-cells, independent of TWEAK expression changes, has been shown to drive pain behaviours in SNL-induced model of neuropathic pain in mice (L.-N. Huang et al., 2019). Increased Fn14 expression was suggested to be mediated through the NF-κB pathway, through nuclear translocation of p65 protein, with microinjection of *Tnfrsf12a* shRNA into the ipsilateral L4 DRG attenuating neuropathic pain behaviours (L.-N. Huang et al., 2019). A localised role for Fn14 in the axon of nociceptors would provide a novel supporting angle to an emerging story of *Tnfrsf12a* RNA driving sensitisation.

Interestingly, when assessing the expression level in MACS-identified nociceptors, *Tnfrsf12a* was found expressed only in the ipsilateral joint following PSNL. The lack of expression in control conditions indicates a unique role in hyperalgesic priming, unlike the CNS where TWEAK/Fn14 activity has been established outside disease states (Yepes, 2007). Consequently, *Tnfrsf12a* RNA is suggested to play a key role, localised to the axon of sensory neuronal cells, in the manifestation of a sensitised state.

6.5.4 Conclusions

In summary, these experiments investigated the effect of inhibition of specific RNAs on the development of a sensitised state in DRG-cells *in vitro*. Knockdown of *Tnfrsf12a* mRNA induced a significant effect on PGE_2-induced sensitisation, preventing the development of hyperexcitability of nociceptors. Knockdown of *Arid5a*, while underpowered, additionally indicates an effect on the development of PGE_2-induced sensitisation. These data suggest *Tnfrsf12a,* and possibly *Arid5a*, mediate neuroplastic pain pathways likely within the axon of nociceptors.

Chapter 7: General Discussion and Conclusions

7.1 Summary of key findings

The work in this thesis characterises the axonal transcriptome of DRG-cells from embryonic and adult mice, as well as the changes thereof in an *in vitro* model of sensitisation. Through the use of porous membrane chambers and prolonged PGE_2-exposure, established as a key mediator of neuroplastic pathways of chronic pain, an *in vitro* model of sensitisation was developed, and the changes to the axonal transcriptome assessed (Chapter 3 and 4). Widespread conservation of the axonal transcriptome was established between control embryonic and adult neuronal DRG-cells. Pathways associated with local translation, including eIF2-signalling, were observed in the axonal transcriptome (Chapter 5). Pathways of inflammation and neuroplasticity including IL-6-, IL-17-, and cAMP-signalling, were indicated to characterise the changes to the transcriptome following PGE_2-sensitisation (Chapter 5). 3 target RNAs (*Arid5a*, *Cebpb*, and *Tnfrsf12a*) were significantly increased in the axon of DRGs and selected as possible key mediators of sensitisation in the local transcriptome. Knockdown of *Tnfrsf12a* significantly inhibited PGE_2-induced sensitisation *in vitro* (Chapter 6). *Tnfrsf12a* encodes the TWEAK receptor Fn14 and both the mRNA and protein have been found increased in the DRG in a neuropathic pain state, as well as associated with neurite outgrowth of neuronal cells, indicating a role in pathways of synaptic plasticity (L.-N. Huang et al., 2019; Tanabe et al., 2003). Additionally, while underpowered, knockdown of *Arid5a* mRNA reduced hyperexcitability of nociceptors of embryonic DRGs (Chapter 6). *Arid5a* encodes the RNA-binding protein Arid5a which has been associated with IL-6-, NF-κB-, cAMP- and CREB-signalling pathways in inflammatory pathways, however, it has not previously been studied in neuronal cells (Nyati et al., 2020; Tanaka et al., 2020). These RNAs are consequently suggested as possible mediators of the development of sensitisation in the axon of nociceptors.

7.1 The axonal transcriptome

The axonal transcriptome from DRG-cells of embryonic and adult mice was characterised in Chapter 5. The axonal transcriptome was confirmed to reflect the established neurite transcriptome, which identifies 61 RNAs including RNAs encoding ribosomal proteins, but also translation mediators and Ca^{2+} response

proteins (von Kügelgen & Chekulaeva, 2020). While a conserved core transcriptome is established for neurites, and now axons, differences to expression patterns of other RNAs in the localised transcriptome have previously been attributed to maturity or age of the animal (N. Sharma et al., 2020; Smith-Anttila et al., 2020), gender of the animal (Mecklenburg et al., 2020; Smith-Anttila et al., 2020), or even the spinal level of the DRG (Smith-Anttila et al., 2020). The axon of sensory neuronal cells relies on regulatory mechanisms of local translation to facilitate adaptation to external stimuli and changes in the physiological environment (Costa et al., 2021; Melemedjian et al., 2010; Obara et al., 2012; Price & Géranton, 2009; J.-Q. Zheng et al., 2001). Local translation drives synaptic plasticity and has been shown to affect the protein expression of translational mediators, scaffolding proteins, and neurotransmitter receptors in neuronal cells (Kindler & Kreienkamp, 2012; Shigeoka et al., 2016). The specific changes to the proteome induced through local translation is shown to depend on the compartmentalised localisation of mRNAs and local regulatory mechanisms thereof (Zappulo et al., 2017). Therefore, in this thesis, I used porous membrane chambers to assess the subcellular transcriptomes (axons vs cell bodies) of DRG-cells from embryonic and adult mice.

Almost 50% of the RNAs enriched in the axon of embryonic DRG-cells were also enriched in the axon of DRG-cells from adult mice (Chapter 5). Similarly to previous studies, I found higher quantities of total RNAs in the axon of DRG-cells from adult mice compared to embryonic mice (Gumy et al., 2011). Comparative pathway analysis identified mediators of eIF2- and oxidative phosphorylation signalling as enriched in the axon in DRG-cells from both embryonic and adult mice.

EIF2 signalling has in previous research been identified as a key pathway involved in proinflammatory cytokine expression, axon regeneration, and synaptic plasticity through regulation of translation initiation (Pacheco et al., 2020; V. Sharma et al., 2020; Shrestha et al., 2012). Oxidative phosphorylation is associated with mitochondrial activity, the local presence of which in the axon has similarly been indicated to play a key role in localised translation (Hollenbeck & Saxton, 2005; Kar et al., 2014). Interestingly, not only was oxidative phosphorylation signalling found to characterise the axonal transcriptome of both embryonic and adult rats, but

mediators of eIF2-signalling were also enriched in the axonal transcriptome of DRG-cells from embryonic and adult rats (Gumy et al., 2011). Consequently, the axonal transcriptome is shown to contain highly conserved RNA expression patterns, constituting a core transcriptome which likely facilitates local translation. The variable elements of the axonal transcriptome are predicted to mediate the rapid adaptation of the axon to changing physiological environment and cellular mechanisms.

7.2 Changes to the axonal transcriptome during sensitisation

Hyperalgesia is associated with increased excitability of nociceptors established through lowered threshold for action potentials and shorter refractory period facilitating increased frequency of action potentials (J. Huang et al., 2006; Khomula et al., 2019; Weng et al., 2012). The manifestation of hyperalgesia is predicted to rely on neuroplasticity mediated through regulatory mechanisms of local translation (Ferrari et al., 2013; Kandasamy & Price, 2015; Khomula et al., 2019). *In vivo* studies have demonstrated that local translation induces neuroplastic changes: Injections of translation inhibitors, including cordycepin, anisomycin and rapamycin, into the paw of rats was found sufficient to prevent or even reverse *in vivo* models of hyperalgesia (Bogen et al., 2012; Ferrari et al., 2013; Jiménez-Díaz et al., 2008). Therefore, I wished to assess the changes to the axonal transcriptome during sensitisation, and subsequently specific localised transcripts, predicting the effect thereof on local translation regulation and protein synthesis. The specific changes to the axonal transcriptome were explored in our *in vitro* model of PGE_2-induced sensitisation of DRG-cells in embryonic and adult mice (Chapter 3 and 4). The PGE_2-protocol was found to induce varying effects on the expression patterns of RNAs in the axon between DRG-cells from embryonic and adult mice.

PGE_2-triggered increased expression of mediators of synaptogenesis and CREB signalling in the axon of DRG-cells from adult mice, pathways which were indicated to be repressed in the axons of embryonic DRG-cells. Mediators of IL-7, IL-6, and cAMP signalling pathways were increased in the PGE_2-sensitised DRG-cells from both embryonic and adult mice, however, the specific enrichment patterns varied.

Of the IL-7 signalling pathway *Clcf1*, *Il36g*, *Map2k6*, *Mmp13*, *Cebpb*, *Tnfsf11*, *Il11*, *Ccl20*, and *Ptgs2* (COX2) mRNAs were increased in embryonic transcriptome, while *Il1b*, *Il1F10*, *Il6*, *Rasd2* and *Tnf* were increased in the adult transcriptome. The variation in individual mRNA expression patterns of the same pathway is similarly observed for CREB signalling. While CREB signalling was shown to be increased in the axon of DRG-cells from adult mice and repressed in axons from embryonic mice, CREB1 was strongly predicted as an upstream regulator of PGE_2-sensitisation in the axon for both embryonic and adult mice. Interestingly, previous studies have shown a time-dependent increase in phosphorylation of CREB following increased cAMP-signalling in the spinal cord, specifically in the early development of hyperalgesia *in vivo* (Hoeger-Bement & Sluka, 2003; Liou et al., 2007). 24H, but not 1week, after induction of a surgical and a chemical model of *in vivo* chronic pain, increased phosphorylation of CREB was associated with mechanical hyperalgesia, the development of which was inhibited through early treatment with PKA inhibitors (Hoeger-Bement & Sluka, 2003; Liou et al., 2007). Discrepancies regarding the effect of cAMP-signalling in hyperalgesic priming remain evident, as both targeted inhibition and activation of the pathway is associated with decreased neuropathic pain behaviours (Skyba et al., 2004; F. Zhang et al., 2022). These inherent differences may contribute to the variation in cAMP and CREB signalling pathways shown in the axon of embryonic and adult DRG-cells following PGE_2-induced sensitisation.

Consequently, the results from 8WO DRG-cells contained similarities compared to E16.5 DRGs, as well as distinct differences in the changes to the axonal transcriptome following PGE_2-sensitisation.

7.3 Addressing limitations of the experimental design

While the differences in the axonal transcriptome following sensitisation could be attributed to the difference in the age of the mice or the change to the PGE_2-protocol, additional variations in the experimental design should be addressed. Variation in the PGE_2-protocol were imposed due to laboratory restrictions, such that adult DRG-cells were exposed to 12H PGE_2 rather than the 24H-protocol

imposed for embryonic DRG-cells. 12H PGE_2-exposure of adult DRG-cells was sufficient to induce increased *Ngf* mRNA expression, as well as to predict PGE_2 as an upstream regulator, thus it was accepted as an equivalent model of sensitisation (Chapter 5). However, it cannot be refuted that the variation in PGE_2-exposure may cause the *in vitro* models to represent 2 different stages of sensitisation.

Differences to the library preparation (rRNA depletion for embryonic samples and poly(A)-selection for adult samples) during RNAseq preparations were directly addressed by imposing restrictions such that only protein-coding RNAs were included in the comparative analysis. Additionally, while reads of non-neuronal RNAs could have prevented reads for lowly expressed RNAs in the embryonic samples due to rRNA depletion, increased sequencing depth of embryonic samples is expected to compensate for this variation.

Finally, variation in the experimental design included gender-differences. While the DRG-cells from adult mice were extracted from exclusively female mice, the embryos were not gender-identified prior to DRG-extraction. Male embryos are consequently expected, which is confirmed through the presence of Y-chromosome associated genes in the transcriptome from embryonic DRGs. Several research groups have presented significant sex-associated differences in pain pathways and the development of hyperalgesia (Smith-Anttila et al., 2020; Tavares-Ferreira, Ray, et al., 2022). Additionally, female mice have been shown to exhibit increased pain behaviours to intraplantar PGE_2-injections (Tavares-Ferreira, Ray, et al., 2022). The differences in our results of the transcriptome following PGE_2-sensitisation may therefore similarly be partially due to the adult DRGs exclusively containing sensory neuronal cells of female mice, while the embryonic DRGs assessed sensory neuronal cells of both male and female mice.

Consequently, the variations in the compartmentalised transcriptome of the embryonic and adult DRGs observed in our *in vitro* models, may be at least partially influenced by the above-described experimental differences. However, despite the variations, prolonged exposure to PGE_2 was shown to induce pathways associated with sensitisation in DRG-cells from both embryonic and adult mice, through

increased expression of inflammatory mediators, including *Ngf*, *Il1β, Il6, Ill11, Tnf* and predicted activation of neuroplastic pathways including cAMP- and PKA-signalling, confirming the use of the PGE_2-protocol for inducing sensitisation in DRG-cells (Chapter 5).

7.4 The role of polyadenylation in nociceptor priming

Through the development of our *in vitro* model of sensitisation, I aimed to assess whether specific RNAs or pathways could be targeted to inhibit or reverse the hyperexcitability of nociceptors. The polyadenylation inhibitor cordycepin (3'-deoxyadenosine) is an adenosine analogue with specific effects on inflammatory pathways of chronic pain. Cordycepin prevents the addition of a poly-A tail of select RNAs in inflammatory states, hypothesised to be mediated through targeted arrest of polyadenylation factors Wdr33 and CPSF4 on the mRNA (Ashraf et al., 2019). Cordycepin treatment is associated with activation of AMPK and repression of PI3K/mTOR/Akt and NF-κB pathways, pathways which are linked to regulating protein synthesis (Engelmann & Haenold, 2016; Klann et al., 2004; Radhi et al., 2021). The polyadenylation inhibitor has been shown to prevent and reverse hyperalgesic behaviours in several *in vivo* models of chronic pain, including carrageenan and PGE_2-exposure (Ferrari et al., 2013), bee-venom exposure (Yang et al., 2017), opioid-induced hyperalgesia (Khomula et al., 2019), and surgical models in rodents (Ashraf et al., 2019). It was therefore of interest to assess the effects of cordycepin on our *in vitro* model of PGE_2-induced sensitisation. Initial experiments revealed that concentrations higher than 20nM caused the DRG-cell-cultures to detach from their plates prior to imaging. 20nM is considered strikingly low compared to previous experiments with cordycepin, and it is hypothesised that the toxic effects of the compound may be due to metabolite contamination (Radhi et al., 2021). Cordycepin from 2 sources (cs-cordycepin and sa-cordycepin) was used in the PGE_2-protocol. Cordycepin (20nM) was given 12H after the PGE_2-protocol was initiated, for 12H of treatment (see Appendix A.3). Cs-cordycepin appeared to alter the hyperexcitability induced by PGE_2, however, limited n-numbers prevented reliable statistical analysis. Sa-cordycepin did not appear to affect the hyperexcitability induced by PGE_2 at the concentration used. In a previous *in vivo*

model of osteoarthritis, cordycepin was found to target macrophages and prevent tissue degradation which was associated with reduced pain behaviours (Ashraf et al., 2019). The effect of cordycepin could consequently be mediated by non-neuronal cells, the growth of which is minimised in *in vitro* cultures through additions of growth factors (see Chapter 2 and 3). Furthermore, the different results from 2 sources of cordycepin indicated variation in the composition of the compound, consequently introducing the possibility that the effects of cs-cordycepin could be due to metabolite contamination. Therefore, the effects of cordycepin could not be confirmed in our experimental model, however, it is suggested that the experiment should be replicated with validated preparations of cordycepin at higher concentrations to obtain confident results.

7.5 Translatability of findings

The success-rate of translating preclinical findings to successful therapeutic outcomes is a key concern. Translatability of results is particularly challenging from animal models to successful clinical trials in humans, with notable examples of failures such as compounds targeting NaV1.7 channels and NMDA receptors (Burma et al., 2017; Fisher et al., 2021). Discrepancies are attributed to multiple factors including variation in drug pharmacology in different species, heterogeneity of human chronic pain conditions, and measured behavioural end-points, which should be considered for the development of future *in vivo* assessments (Burma et al., 2017). Similarly, considerations can be made which improves the initial selection of targets taken forward at the preclinical stage from *in vitro* studies to *in vivo* studies, by assessing the conservation of targets between species. It is therefore imperative to explore how comparable the transcriptome profile of human sensory neuronal cells is to the transcriptome of sensory neuronal cells to mice. Research to explore the differences and similarities between human DRGs (hDRGs) and mouse DRGs (mDRGs) have been initiated by several research groups (Chapter 1 Table 1.2) (Nguyen et al., 2021; Ray et al., 2018; Sapio et al., 2016; Tavares-Ferreira, Shiers, et al., 2022; Wangzhou et al., 2020). Expression patterns of stimuli-specific receptors such as TRPM8 (cold-sensing) and PIEZO2 (gentle touch), as well as broader expression of TRPV1 in most hDRG cell subtypes was observed,

indicating different neuronal subtypes within hDRGs compared to mDRGs (Nguyen et al., 2021; Shiers et al., 2020). Despite the inherent heterogeneity, similarities between the transcriptome profiles of mDRGs and hDRGs were established (Ray et al., 2018; Wangzhou et al., 2020). High conservation of pharmacological targets including transcription factors, receptors and ion channels was established between mDRGs and hDRGs (Ray et al., 2018). However, interestingly, the process of culturing DRG-cells from both humans and mice were found to induce differences in gene expression profiles compared to cells that were sequenced immediately following extraction (Wangzhou et al., 2020). While many neuronal targets, as well as RNAs encoding ion channels and GPCR, showed lowered expression following culturing, they were confirmed to remain expressed, which supported the use of cultured cells. However, an increase in inflammatory markers was observed in cultured cells, which was associated with transcriptome changes of axonal injury or neuropathic pain. The differences attributed to culturing of cells indicated possible inherent sensitisation in *in vitro* models. These findings demonstrate the importance of verifying the *in vitro* model of hyperexcitability prior to sequencing, to confirm the difference of the control-condition to the sensitisation-model.

Consequently, differences between mDRGs and hDRGs are clearly evident, however, similarities are established which indicate translatability of results from mDRGs in *in vitro* models once appropriate consideration and assessments are made. *Tnfrsf12a* and *Arid5a* mRNAs were confirmed as expressed in hDRG-cells through comparisons with published datasets (North et al., 2019), showing conservation of the RNAs and implying promising translatability of the *in vitro* results. Following results which demonstrate the knockdown of *Tnfrsf12a* successfully prevents the development of PGE_2-induced sensitisation in embryonic DRG-cells, *Tnfrsf12a* is presented as a promising novel target for future analgesic therapeutics. Additional replicates are required to confidently assess the role of *Arid5a* in the development of PGE_2-induced sensitisation, however, underpowered results imply *Arid5a* also mediate the development of sensitisation.

7.5 Concluding remarks and future directions

Future studies should attempt to further explore the regulatory mechanisms of local translation of key RNAs in the axon in sensitisation development. Experiments have demonstrated the role of alternative splicing in targeting RNAs for axonal localisation and translation, specifically showing preferential expression of short sequence motifs in the axon (Minis et al., 2014; Shigeoka et al., 2016). Additionally, alternative splicing of key RNAs has been associated with the development of neuropathic pain (Donaldson & Beazley-Long, 2016). It is predicted that bioinformatic analysis of accessible RNAseq results from the axonal compartment of sensory neuronal cells, could be used to identify specific local RNAs driving sensitisation (Ha et al., 2018; X. Wang & Cairns, 2013). Furthermore, findings regarding changes to the transcriptome should be supported by assessments of the translatome of axons from sensory neuronal cells. This could be carried out using established methods for sequencing of mRNA-ribosome complexes isolated from the axon, such as axon-TRAP-RiboTag (Shigeoka et al., 2016). Finally, it is suggested that future work should be carried out using hDRG-cells to assess the role of key RNAs, such as *Tnfrsf12a* and *Arid5a*, in human neuronal cells thereby aiming to increase the translatability and clinical relevance of results. A key experiment of interest with hDRG-cells is proposed, where the effect of exclusively axonal knockdown of key RNAs on the development of sensitisation is assessed through the use of compartmentalised microfluidic chambers and functional measurements such as cell excitability in an *in vitro* model of sensitisation.

This is believed to be the first study to use sequencing to attempt profiling of the axonal transcriptome in a sensitised state in mice. An age-independent axonal transcriptome in DRG-neurons is demonstrated, which is suggested to play a large role in axon growth, functional maintenance, and nociceptive signalling. Importantly, the axonal transcriptome is shown to be modulated by PGE_2, inducing sensitisation. Knockdown demonstrated that at least one axonal mRNA (*Tnfrsf12a*) mediates the development of sensitisation of nociceptors in our system. These data are likely to ultimately contribute to the development of novel analgesic therapeutics.

Appendix

A.1 FastQC files show quality of base-calls for RNAseq files

To evaluate the quality of the RNAseq files, FastQC files were obtained in a local instance of Galaxy. FastQC files shows the estimated quality of the predicted base-call for each position in a given read. A high score indicates high quality (Q) corresponding to the background colour with green (Q=28-40) indicating a high quality, yellow (Q=20-28) indicating acceptable quality and red (Q=0-20) indicating poor quality. Q is defined by the equation:

$Q = -\log_{10}(e)$

Thus Q=20 equals an error rate of 1 in 100.

A.1.1 FastQC files for RNA samples from embryonic mice (E16.5)

TA1 R1

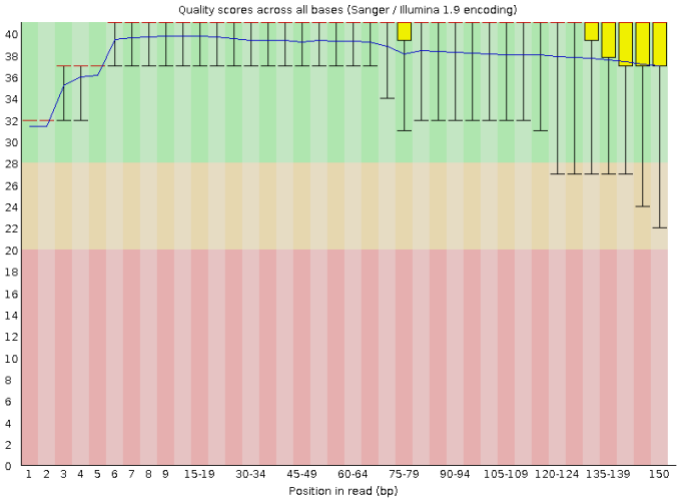

TA1 R2

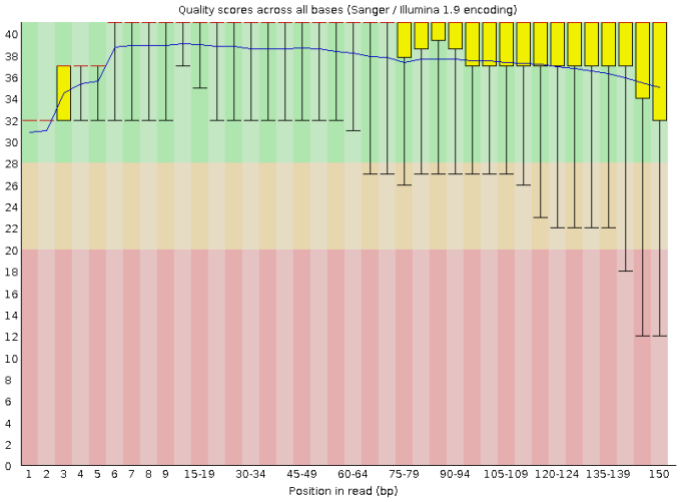

TA2 R1

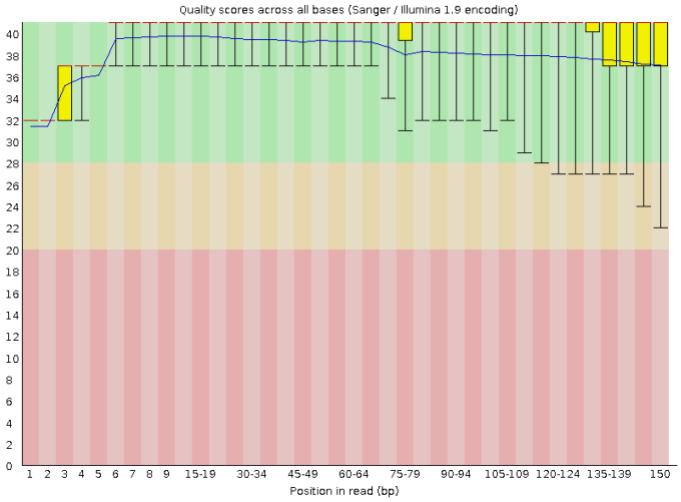

TA2 R2

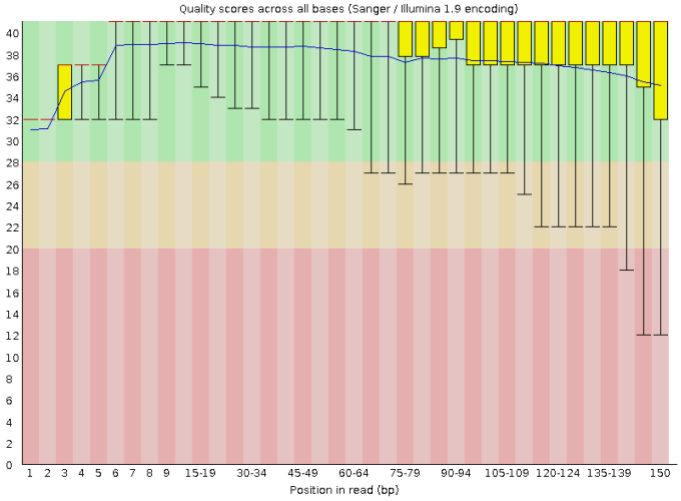

TAD R1

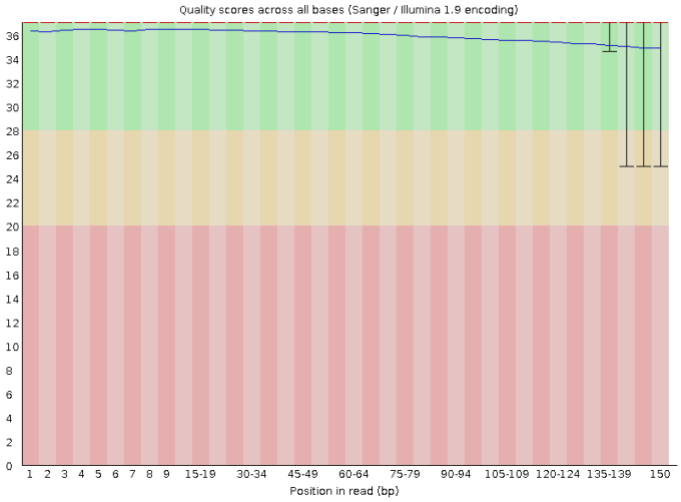

TAD R2

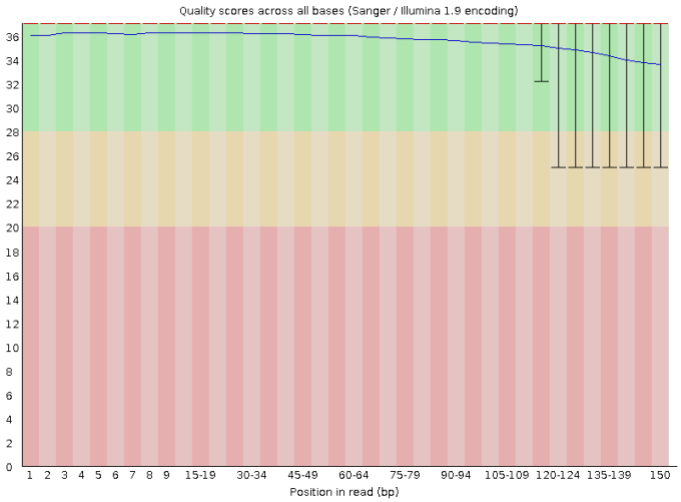

VA1 R1

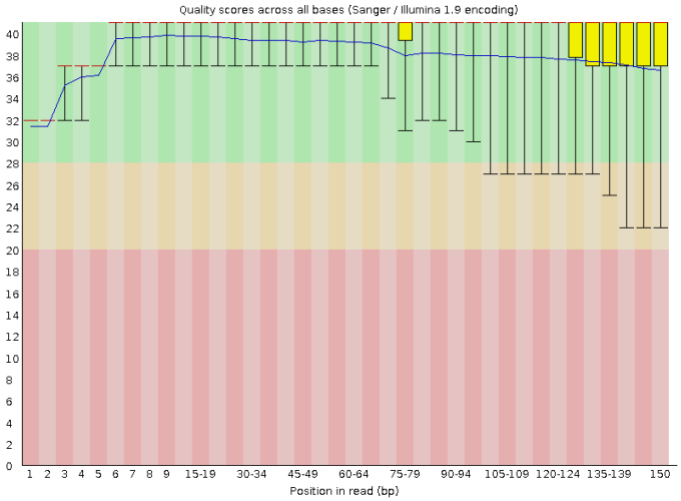

VA1 R2

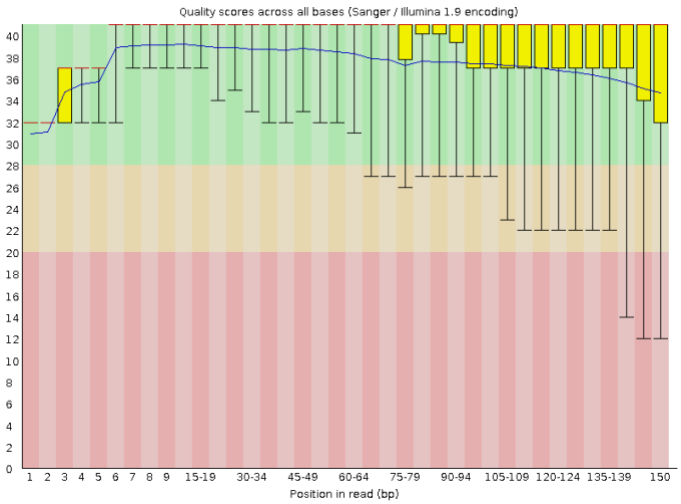

VA2 R1

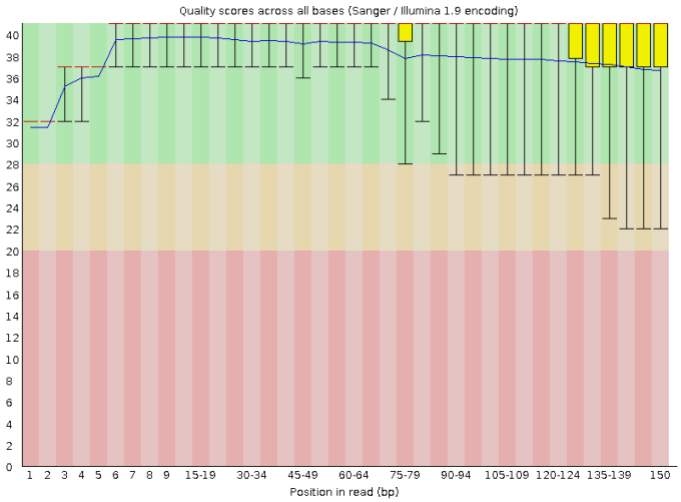

VA2 R2

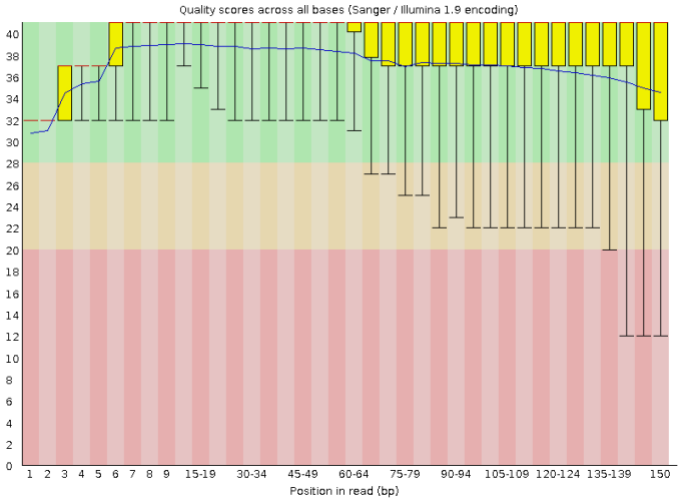

VAD R1

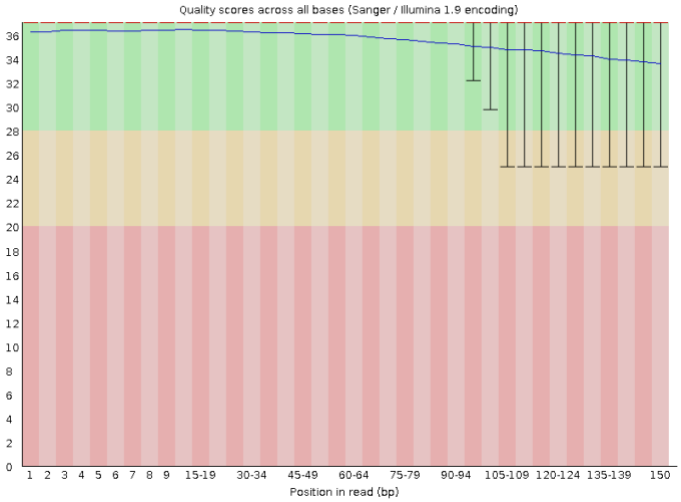

VAD R2

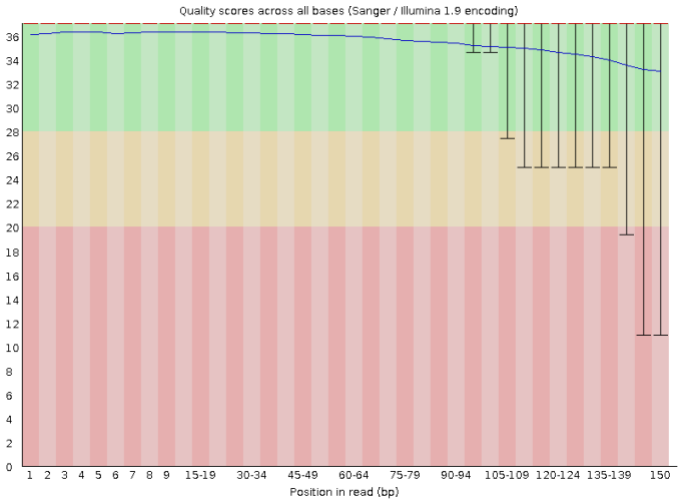

TS1 R1

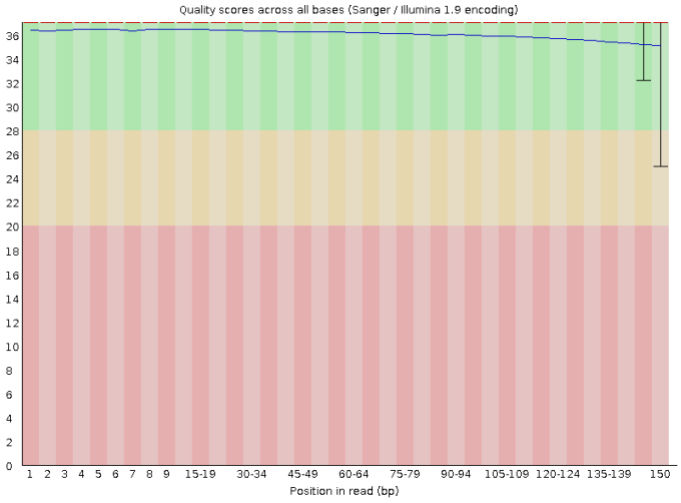

TS1 R2

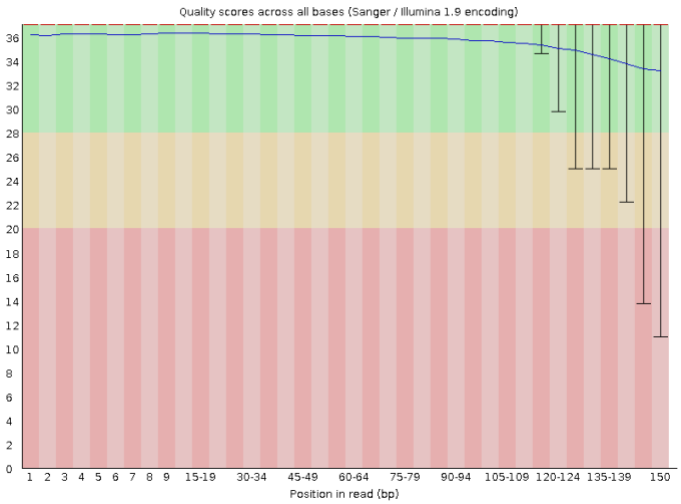

TSB R1

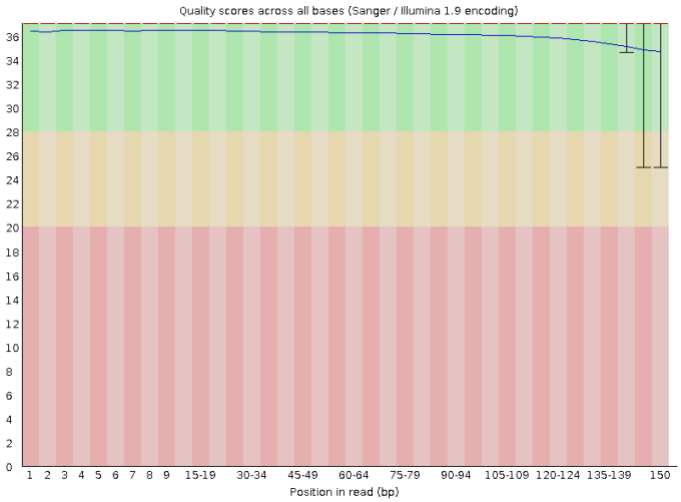

TSB R2

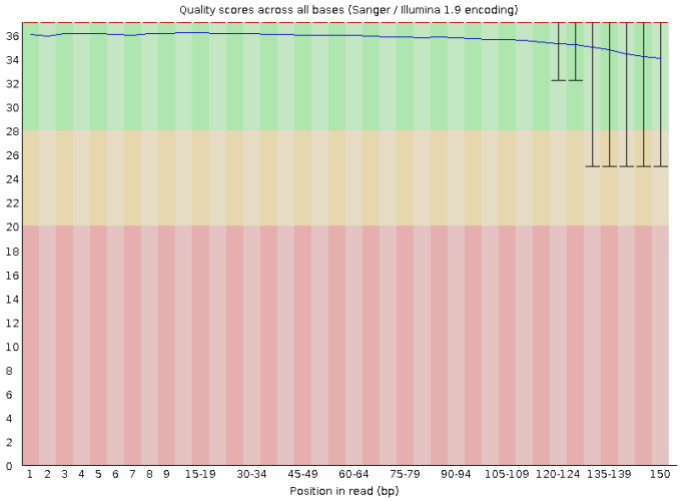

TSD R1

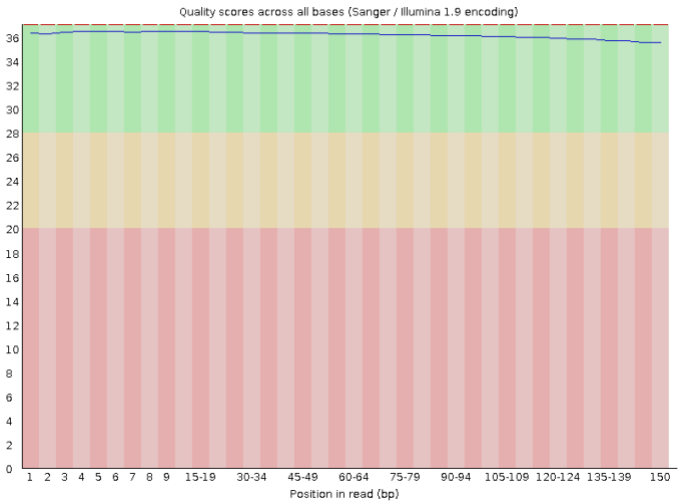

TSD R2

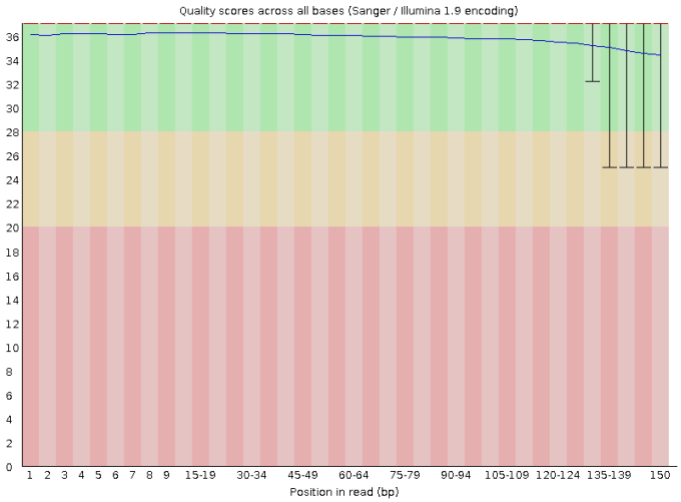

VS1 R1

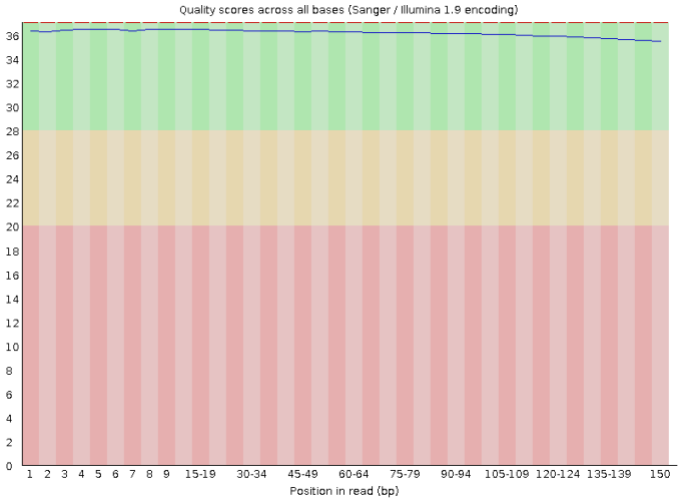

VS1 R2

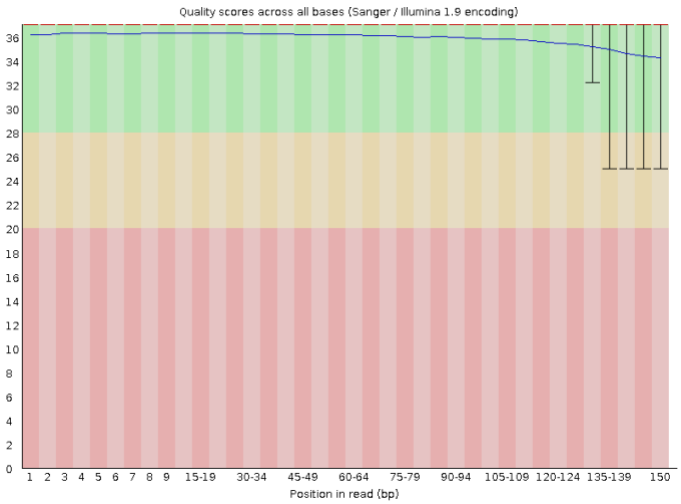

VSB R1

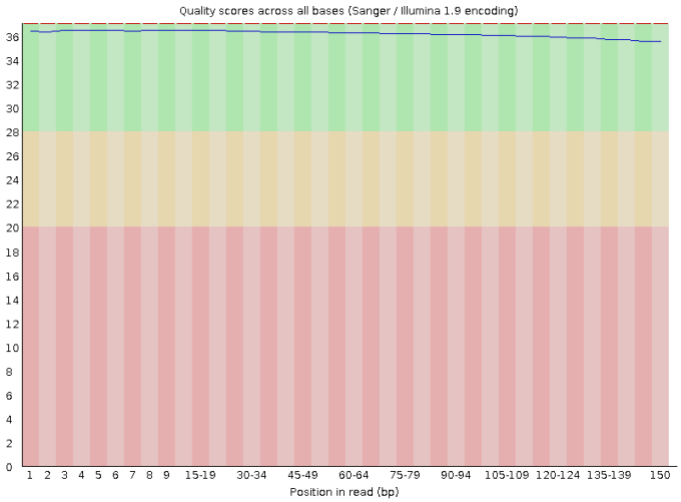

VSB R2

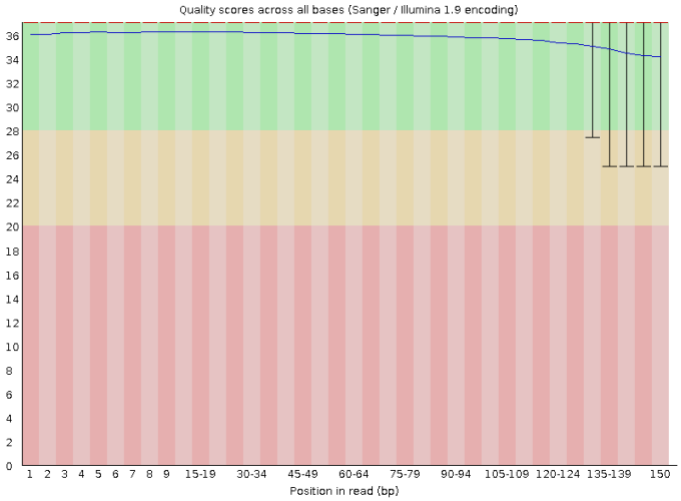

VSD R1

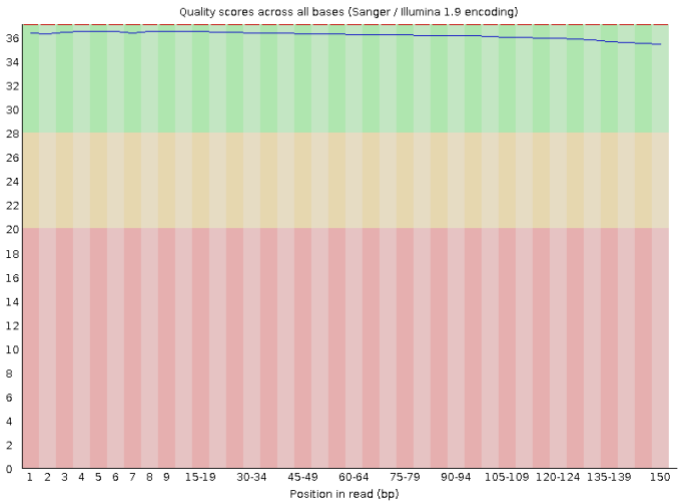

VSD R2

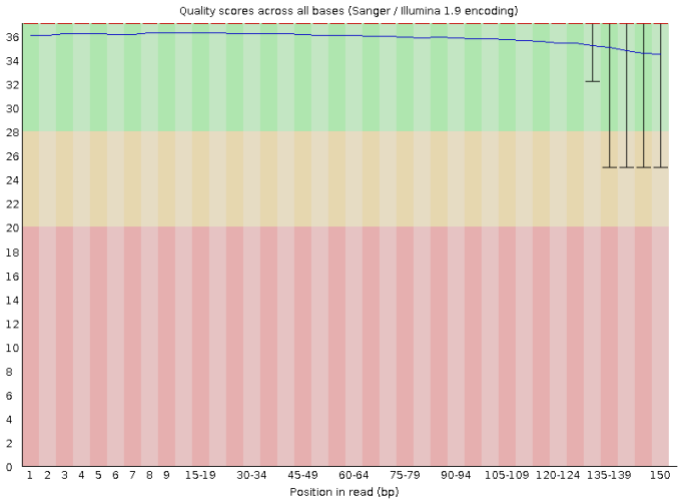

A.1.2 FastQC files for RNA samples from adult mice (8WO)

TA1

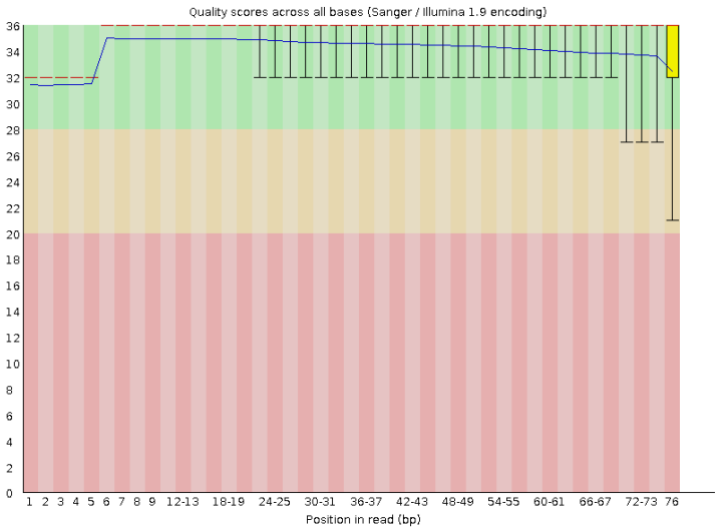

TA2

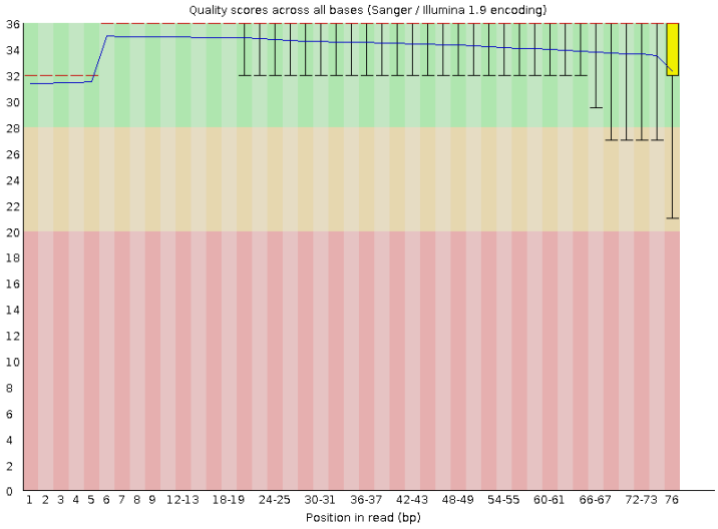
Quality scores across all bases (Sanger / Illumina 1.9 encoding)
Position in read (bp)

TA3

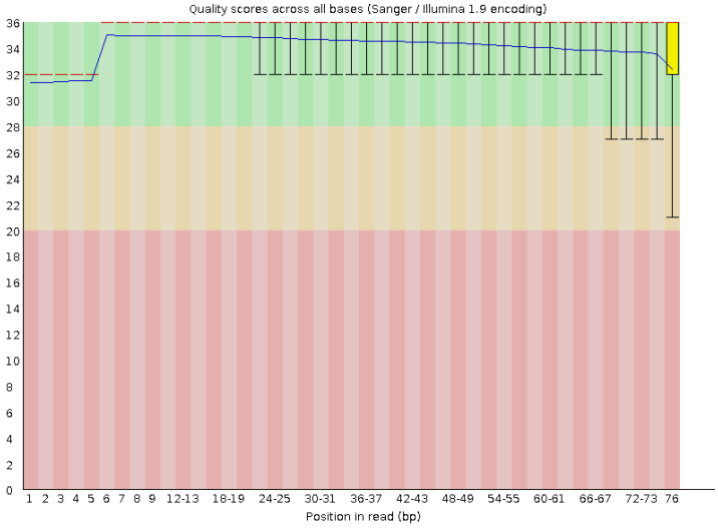
Quality scores across all bases (Sanger / Illumina 1.9 encoding)
Position in read (bp)

VA1

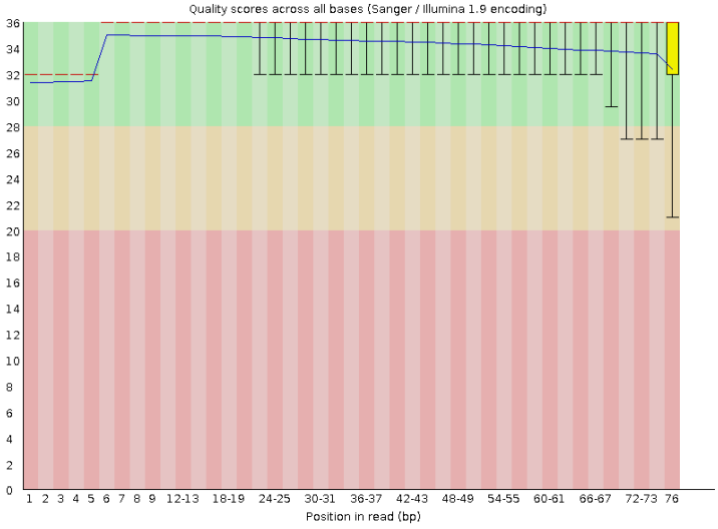
Quality scores across all bases (Sanger / Illumina 1.9 encoding)
Position in read (bp)

VA2

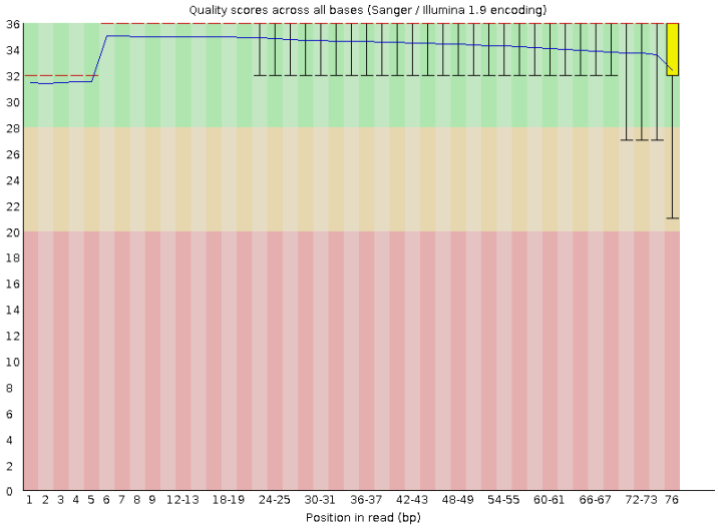
Quality scores across all bases (Sanger / Illumina 1.9 encoding)
36
34
32
30
28
26
24
22
20
18
16
14
12
10
8
6
4
2
0
1 2 3 4 5 6 7 8 9 12-13 18-19 24-25 30-31 36-37 42-43 48-49 54-55 60-61 66-67 72-73 76
Position in read (bp)

VA3

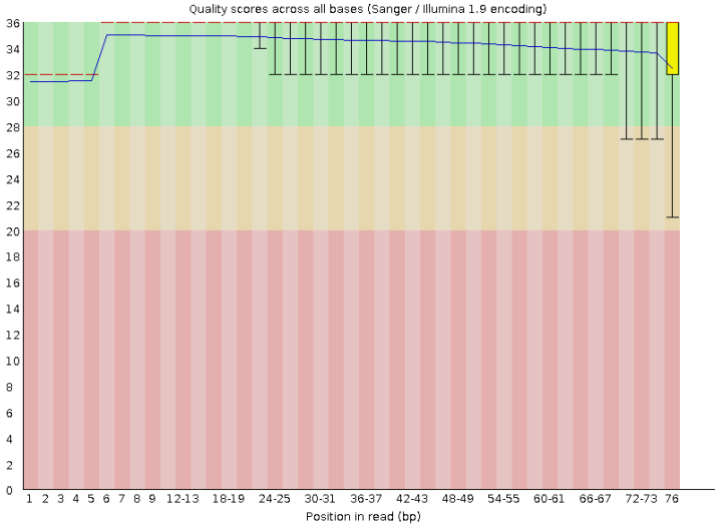
Quality scores across all bases (Sanger / Illumina 1.9 encoding)
36
34
32
30
28
26
24
22
20
18
16
14
12
10
8
6
4
2
0
1 2 3 4 5 6 7 8 9 12-13 18-19 24-25 30-31 36-37 42-43 48-49 54-55 60-61 66-67 72-73 76
Position in read (bp)

TS1

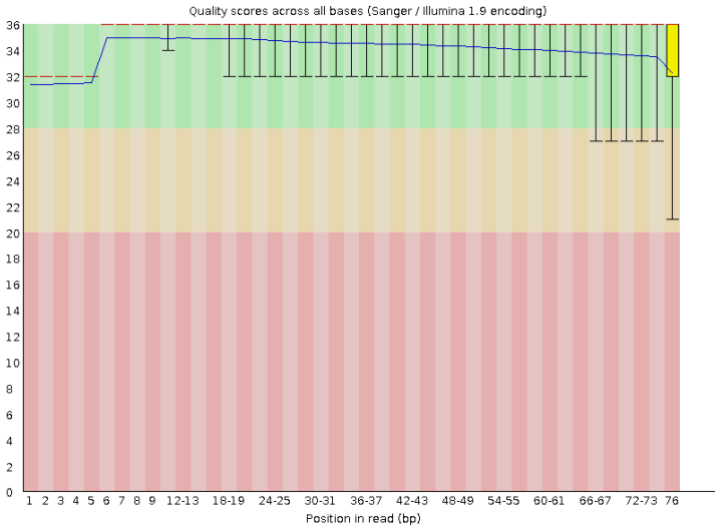
Quality scores across all bases (Sanger / Illumina 1.9 encoding)
36
34
32
30
28
26
24
22
20
18
16
14
12
10
8
6
4
2
0
1 2 3 4 5 6 7 8 9 12-13 18-19 24-25 30-31 36-37 42-43 48-49 54-55 60-61 66-67 72-73 76
Position in read (bp)

TS2

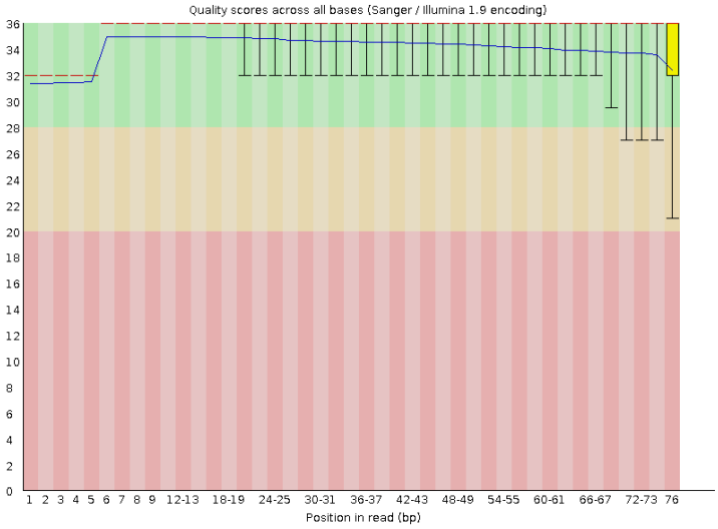
Quality scores across all bases (Sanger / Illumina 1.9 encoding)
Position in read (bp)

TS3

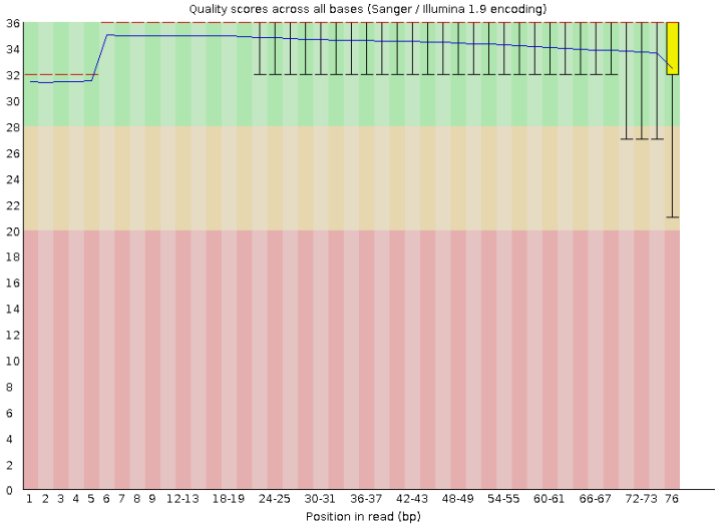
Quality scores across all bases (Sanger / Illumina 1.9 encoding)
Position in read (bp)

VS1

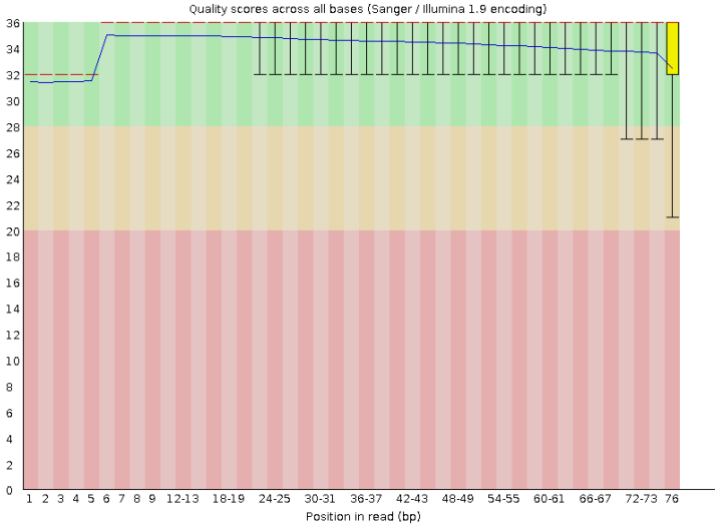
Quality scores across all bases (Sanger / Illumina 1.9 encoding)
Position in read (bp)

VS2

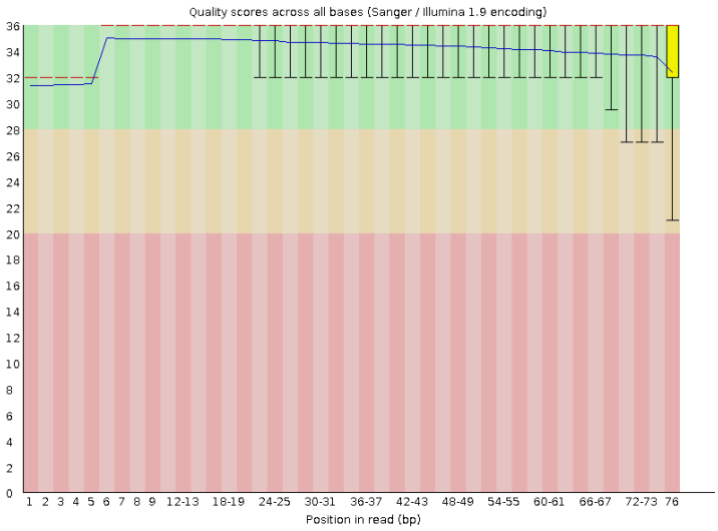

VS3

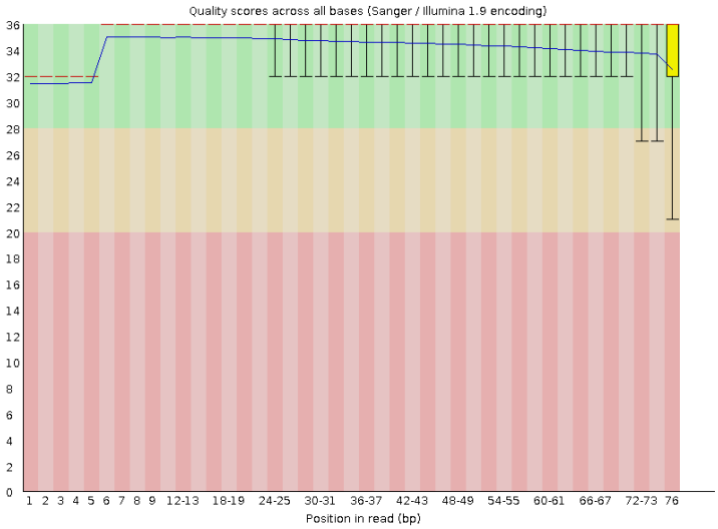

A.2 Coding scripts

A.2.1 Coding masterscript for data-files from E16.5 mice

#STAR generates genome files:

STAR --runMode genomeGenerate --genomeFastaFiles

~/RNAseq/Resources/GRCm38.primary_assembly.genome.fa --genomeDir

~/RNAseq/Resources/STAR_idx/ --runThreadN 6 --sjdbGTFfile

~/RNAseq/Resources/gencode.vM25.annotation.gtf --sjdbOverhang 50

```
for x in `ls ~/RNAseq/DRG_totalembryo/*.fastq.gz | sed "s/.*\///g" | sed "s/[.]fastq[.]gz//g" |
sed "s/_001//g" | sed "s/_R[12]//g" | uniq `

do

    echo ===== file $x ======= ;

    rm -f ~/RNAseq/temp/BAMsort/0/*
    rm -f ~/RNAseq/temp/BAMsort/1/*
    rm -f ~/RNAseq/temp/BAMsort/2/*
    rm -f ~/RNAseq/temp/BAMsort/3/*
    rm -f ~/RNAseq/temp/BAMsort/4/*
    rm -f ~/RNAseq/temp/BAMsort/5/*
    rmdir ~/RNAseq/temp/BAMsort/*
    rmdir ~/RNAseq/temp/BAMsort
    rm -f ~/RNAseq/temp/*
    rmdir ~/RNAseq/temp

#Mapping with STAR

echo run STAR
    STAR --genomeDir  ~/RNAseq/Resources/STAR_idx/ \
        --runThreadN 6 \
        --readFilesCommand zcat \
        --readFilesIn ~/RNAseq/DRG_totalembryo/${x}_R1_001.fastq.gz
~/RNAseq/DRG_totalembryo/${x}_R2_001.fastq.gz \
        --outFileNamePrefix ~/RNAseq/DRG_totalembryo/STAR_output/${x} \
        --outTmpDir ~/RNAseq/temp \
        --outSAMtype BAM SortedByCoordinate \
        --quantMode GeneCounts \
        --clip5pNbases 5 \
```

```
        --clip3pNbases 94

done

#echo finished STAR

#Sorting with samtools

for x in `ls ~/RNAseq/DRG_totalembryo/STAR_output/*.sortedByCoord.out.bam | sed
"s/.*\///g" | sed "s/[.]sortedByCoord[.]out[.]bam//g" | sed "s/Aligned//g" | uniq `

do

   echo ===== file $x ======= ;

 samtools index
~/RNAseq/DRG_totalembryo/STAR_output/${x}Aligned.sortedByCoord.out.bam
 samtools sort -n -o ~/RNAseq/DRG_totalembryo/samtools_output/${x}.sort_readid.bam
~/RNAseq/DRG_totalembryo/STAR_output/${x}Aligned.sortedByCoord.out.bam

done

echo finished samtools

#Counting with htseq

for x in `ls ~/RNAseq/DRG_totalembryo/samtools_output/*sort_readid.bam | sed "s/.*\///g" |
sed "s/[.]sort_readid[.]bam//g" | uniq `

do
        echo ====== file ${x} ==========
```

```
    htseq-count --format=bam --order=name --stranded=no --idattr=gene_id
~/RNAseq/DRG_totalembryo/samtools_output/${x}.sort_readid.bam
~/RNAseq/Resources/gencode.vM25.annotation.gtf >
~/RNAseq/DRG_totalembryo/htseq_counts/${x}_counts.txt;

done

echo finito
```

A.2.2 Coding masterscript for data-files from 8WO mice

```
for x in `ls ~/RNAseq/DRG_adult/*.fastq.gz | sed "s/.*\///g" | sed "s/[.]fastq[.]gz//g" | sed
"s/152-//g" | uniq `
do

  echo ===== file $x ======= ;


  rm -f ~/RNAseq/temp/BAMsort/0/*
  rm -f ~/RNAseq/temp/BAMsort/1/*
  rm -f ~/RNAseq/temp/BAMsort/2/*
  rm -f ~/RNAseq/temp/BAMsort/3/*
  rm -f ~/RNAseq/temp/BAMsort/4/*
  rm -f ~/RNAseq/temp/BAMsort/5/*
  rmdir ~/RNAseq/temp/BAMsort/*
  rmdir ~/RNAseq/temp/BAMsort
  rm -f ~/RNAseq/temp/*
  rmdir ~/RNAseq/temp
```

```
#STAR is run with previous genome files, without cutting and only with one file per sample
(not paired sequencing)

   echo run STAR
   STAR --genomeDir  ~/RNAseq/Resources/STAR_idx/ \
        --runThreadN 6 \
        --readFilesCommand zcat \
        --readFilesIn ~/RNAseq/DRG_adult/152-${x}.fastq.gz \
        --outFileNamePrefix ~/RNAseq/DRG_adult/STAR_output/${x} \
        --outTmpDir ~/RNAseq/temp \
        --outSAMtype BAM SortedByCoordinate \
        --quantMode GeneCounts \

done

echo finished STAR

 for x in `ls ~/RNAseq/DRG_adult/STAR_output/*.sortedByCoord.out.bam | sed "s/.*\///g" |
sed "s/[.]sortedByCoord[.]out[.]bam//g" | sed "s/STAR_bam_//g"  | sed "s/Aligned//g" | uniq `
do

   echo ===== file $x ======= ;

samtools index ~/RNAseq/DRG_adult/STAR_output/${x}Aligned.sortedByCoord.out.bam
samtools sort -n -o ~/RNAseq/DRG_adult/samtools_output/${x}.sort_readid.bam
~/RNAseq/DRG_adult/STAR_output/${x}Aligned.sortedByCoord.out.bam

done

echo finished samtools
```

```
for x in `ls ~/RNAseq/DRG_adult/samtools_output/*sort_readid.bam | sed "s/.*\///g" | sed
"s/[.]sort_readid[.]bam//g" | uniq `

do
        echo ====== ${x} ==========


htseq-count --format=bam --order=name --stranded=no --idattr=gene_id
~/RNAseq/DRG_adult/samtools_output/${x}.sort_readid.bam
~/RNAseq/Resources/gencode.vM25.annotation.gtf >
~/RNAseq/DRG_adult/htseq_counts/${x}_counts.txt;

done

echo finite
```

A.2.3 DESeq2 in R

```
directory <- "/users/paxaat/RNAseq/DRG_adult/htseq_counts/"
sampleFiles <- grep("counts",list.files(directory),value=TRUE)
sampleFiles

#Sample files are printed

sampleCondition<- c("T","T","T","T","T","T","V","V","V","V","V","V")
sampleGroup<- c("TA","TA","TA","TS","TS","TS","VA","VA","VA","VS","VS","VS")
sampleTable<-data.frame(sampleName=sampleFiles, fileName=sampleFiles,
condition=sampleCondition, group=sampleGroup)
sampleTable

#Sampletable is printed
```

```
library("DESeq2")
dds<- DESeqDataSetFromHTSeqCount(sampleTable = sampleTable, directory=directory,
design=~group)
colData(dds)

#DataFrame is printed w 12 rows and 2 columns

dds$condition

#Levels of conditions are printed

dds$group

#Levels of groups are printed

dds<- DESeq(dds)

#Runs DESeq on defined pairs w listed conditions and groups

res_TVA<- results(dds, contrast=c("group","TA","VA"))
res_TVS<- results(dds, contrast=c("group","TS","VS"))
res_VAS<- results(dds, contrast=c("group","VA","VS"))
res_TAS<- results(dds, contrast=c("group","TA","TS"))

#Results tables w according contrasts are saved

plotCounts(dds, gene=which.min(res_TVA$padj), intgroup="group")

resOrdered_TVA <- res_TVA[order(res_TVA$pvalue),]
resOrdered_TVS <- res_TVS[order(res_TVS$pvalue),]
```

```
resOrdered_VAS <- res_VAS[order(res_VAS$pvalue),]
resOrdered_TAS <- res_TAS[order(res_TAS$pvalue),]

message("TVA")
head(resOrdered_TVA,20)
message("TVS")
head(resOrdered_TVS,20)
message("VAS")
head(resOrdered_VAS,20)
message("TAS")
head(resOrdered_TAS,20)

out1<- capture.output(summary(res_TVA))
cat("Summary Treated vs Vehicle axonal fraction", out1, file="summary_T_vs_V_axon.txt",
sep="\n")
out2<- capture.output(summary(res_TVS))
cat("Summary Treated vs Vehicle somal fraction", out2, file="summary_T_vs_V_soma.txt",
sep="\n")
out3<- capture.output(summary(res_VAS))
cat("Summary Vehicle axon vs soma", out3, file="summary_V_axon_vs_soma.txt", sep="\n")
out4<- capture.output(summary(res_TAS))
cat("Summary Treated axon vs soma", out4, file="summary_T_axon_vs_soma.txt", sep="\n")

#Summary of results are saved

write.csv(as.data.frame(res_TVA), file="T_vs_V_axon")
write.csv(as.data.frame(res_TVS), file="T_vs_V_soma")
write.csv(as.data.frame(res_VAS), file="V_axon_vs_soma")
write.csv(as.data.frame(res_TAS), file="T_axon_vs_soma")
```

A.3 The effect of cordycepin on PGE_2-induced sensitisation

The polyadenylation inhibitor cordycepin was introduced to the 16,16-PGE_2-protocol of sensitisation to assess whether select polyadenylation inhibition would prevent the development of a model of sensitisation. Cordycepin from two sources, sa-cordycepin (sigma-aldrich, reference, PHL82505) and cs-cordycepin (carbosynth, ND02930), were introduced to the 16,16-PGE_2-model. Cordycepin from two sources were tested and separately analysed due to, as of yet, unpublished results from the present laboratory indicating a striking difference in the verifiable concentration of cordycepin from different sources. The discrepancies were shown in LC-MS experiments and hypothesised to be due to metabolite contamination in the obtained compounds.

Dissociated E16.5 DRG-cells were exposed to 20nM sa-cordycepin or cs-cordycepin after 12-hours of 16,16-PGE_2 for 12-hours of treatment. The effect of cordycepin on the development of 16,16-PGE_2-induced hyperexcitability was evaluated through measurements of Ca^{2+} transients using Ca^{2+} imaging according to previously described methodology (See Chapter 2.9). The PFI following capsaicin activation was normalised to the PFI of 16,16-PGE_2-sensitised cells and subsequently cordycepin-treated cells were compared to untreated control cells (Figure A.1).

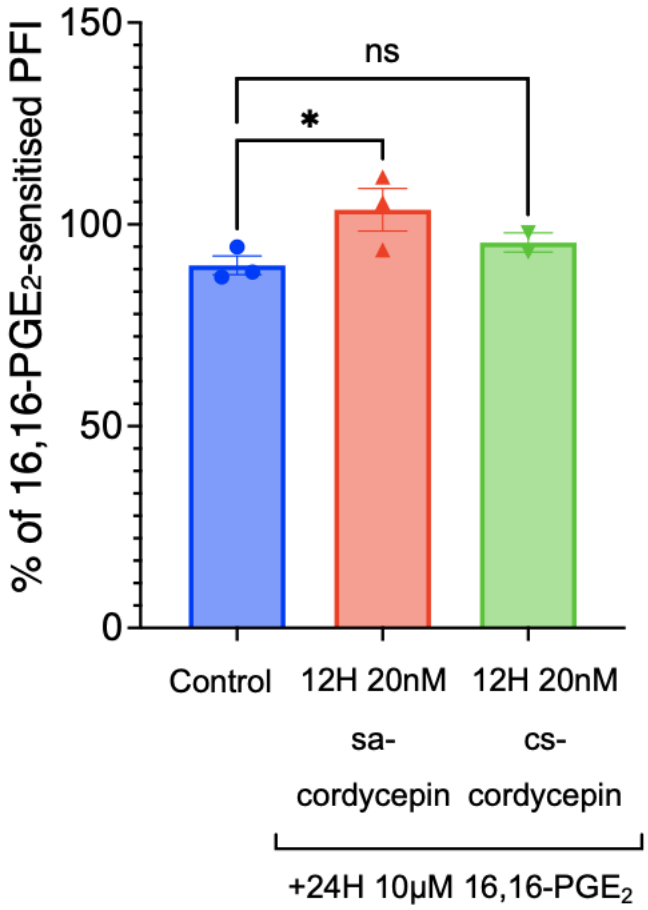

Figure A.1: Activity of E16.5 DRG-cells measured as % of PFI of DRG-cells sensitised by prolonged treatment with 16,16-PGE_2. DRG-cells were sensitised through 24H treatment with 10µM, however, following 12H of treatment cells 20nM sa-cordycepin (n=3) or cs-cordycepin (n=2) was introduced for the remaining 12H. sa-cordycepin did not appear to affect the significant increase in activity induced by 16,16-PGE_2 (* = p-value = 0.0444, n=3, 2way ANOVA), however no significant increase was observed when comparing control to cs-cordycepin treated cells (n=2).

Introducing sa-cordycepin did not decrease the PFI, indicating that sa-cordycepin did not prevent the development of 16,16-induced hyperalgesic priming. However, a decrease in the activity of DRG-cells was observed following cs-cordycepin treatment, bringing the PFI closer to the level of control cells. While this initially appears to indicate that cs-cordycepin has inhibited the development of sensitisation, it is important to note that only n=2 biological replicates were obtained and presented, which hinders reliable statistical analysis

References

Abbas-Aghababazadeh, F., Li, Q., & Fridley, B. L. (2018). Comparison of normalization approaches for gene expression studies completed with high-throughput sequencing. *PLOS ONE*, *13*(10), e0206312. https://doi.org/10.1371/journal.pone.0206312

Abraira, V. E., & Ginty, D. D. (2013). The Sensory Neurons of Touch. *Neuron*, *79*(4), 10.1016/j.neuron.2013.07.051. https://doi.org/10.1016/j.neuron.2013.07.051

Anders, S., & Huber, W. (2010). Differential expression analysis for sequence count data. *Genome Biology*, *11*(10), R106. https://doi.org/10.1186/gb-2010-11-10-r106

Anders, S., Pyl, P. T., & Huber, W. (2015). HTSeq—A Python framework to work with high-throughput sequencing data. *Bioinformatics*, *31*(2), 166–169. https://doi.org/10.1093/bioinformatics/btu638

Andersen, H. H., Duroux, M., & Gazerani, P. (2014). MicroRNAs as modulators and biomarkers of inflammatory and neuropathic pain conditions. *Neurobiology of Disease*, *71*, 159–168. https://doi.org/10.1016/j.nbd.2014.08.003

Arora, M. K., & Singh, U. K. (2013). Molecular mechanisms in the pathogenesis of diabetic nephropathy: An update. *Vascular Pharmacology*, *58*(4), 259–271. https://doi.org/10.1016/j.vph.2013.01.001

Ashraf, S., Radhi, M., Gowler, P., Burston, J. J., Gandhi, R. D., Thorn, G. J., Piccinini, A. M., Walsh, D. A., Chapman, V., & de Moor, C. H. (2019). The polyadenylation inhibitor cordycepin reduces pain, inflammation and joint pathology in rodent models of osteoarthritis. *Scientific Reports*, *9*(1), Article 1. https://doi.org/10.1038/s41598-019-41140-1

Atmaramani, R. R., Black, B. J., de la Peña, J. B., Campbell, Z. T., & Pancrazio, J. J. (2020). Conserved Expression of Nav1.7 and Nav1.8 Contribute to the Spontaneous and Thermally Evoked Excitability in IL-6 and NGF-Sensitized Adult Dorsal Root Ganglion Neurons In Vitro. *Bioengineering*, *7*(2). https://doi.org/10.3390/bioengineering7020044

Autilio, L. A., Appel, S. H., Pettis, Penelope., & Gambetti, P. Luigi. (1968). Biochemical studies of synapses in vitro. I. Protein synthesis. *Biochemistry*, *7*(7), 2615–2622. https://doi.org/10.1021/bi00847a025

Bahar, E., Kim, H., & Yoon, H. (2016). ER Stress-Mediated Signaling: Action Potential and Ca2+ as Key Players. *International Journal of Molecular Sciences*, *17*(9), 1558. https://doi.org/10.3390/ijms17091558

Bandell, M., Story, G. M., Hwang, S. W., Viswanath, V., Eid, S. R., Petrus, M. J., Earley, T. J., & Patapoutian, A. (2004). Noxious Cold Ion Channel TRPA1 Is Activated by Pungent Compounds and Bradykinin. *Neuron*, *41*(6), 849–857. https://doi.org/10.1016/S0896-6273(04)00150-3

Barnett, M. W., & Larkman, P. M. (2007). The action potential. *Practical Neurology*, *7*(3), 192–197.

Basbaum, A. I., Bautista, D. M., Scherrer, G., & Julius, D. (2009). Cellular and Molecular Mechanisms of Pain. *Cell*, *139*(2), 267–284. https://doi.org/10.1016/j.cell.2009.09.028

Bean, B. P. (2007). The action potential in mammalian central neurons. *Nature Reviews Neuroscience*, *8*(6), Article 6. https://doi.org/10.1038/nrn2148

Becker, C., Hammerle-Fickinger, A., Riedmaier, I., & Pfaffl, M. W. (2010). MRNA and microRNA quality control for RT-qPCR analysis. *Methods*, *50*(4), 237–243. https://doi.org/10.1016/j.ymeth.2010.01.010

Berman, A. J., Thoreen, C. C., Dedeic, Z., Chettle, J., Roux, P. P., & Blagden, S. P. (2021). Controversies around the function of LARP1. *RNA Biology*, *18*(2), 207–217. https://doi.org/10.1080/15476286.2020.1733787

Berridge, M. J., Bootman, M. D., & Roderick, H. L. (2003). Calcium signalling: Dynamics, homeostasis and remodelling. *Nature Reviews Molecular Cell Biology*, *4*(7), Article 7. https://doi.org/10.1038/nrm1155

Berta, T., Qadri, Y., Tan, P.-H., & Ji, R.-R. (2017). Targeting dorsal root ganglia and primary sensory neurons for the treatment of chronic pain. *Expert Opinion on Therapeutic Targets*, *21*(7), 695–703. https://doi.org/10.1080/14728222.2017.1328057

Bestall, S. M., Hulse, R. P., Blackley, Z., Swift, M., Ved, N., Paton, K., Beazley-Long, N., Bates, D. O., & Donaldson, L. F. (2018). Sensory neuronal sensitisation occurs through HMGB-1/ RAGE and TRPV1 in high glucose conditions. *Journal of Cell Science*. https://doi.org/10.1242/jcs.215939

Bhat, M., Robichaud, N., Hulea, L., Sonenberg, N., Pelletier, J., & Topisirovic, I. (2015). Targeting the translation machinery in cancer. *Nature Reviews Drug Discovery*, *14*(4), Article 4. https://doi.org/10.1038/nrd4505

Bhatheja, K., & Field, J. (2006). Schwann cells: Origins and role in axonal maintenance and regeneration. *The International Journal of Biochemistry & Cell Biology*, *38*(12), 1995–1999. https://doi.org/10.1016/j.biocel.2006.05.007

Bigler, R. L., Kamande, J. W., Dumitru, R., Niedringhaus, M., & Taylor, A. M. (2017). Messenger RNAs localized to distal projections of human stem cell derived neurons. *Scientific Reports*, *7*, 611. https://doi.org/10.1038/s41598-017-00676-w

Bogen, O., Alessandri-Haber, N., Chu, C., Gear, R. W., & Levine, J. D. (2012). Generation of a Pain Memory in the Primary Afferent Nociceptor Triggered by PKCε Activation of CPEB. *Journal of Neuroscience*, *32*(6), 2018–2026. https://doi.org/10.1523/JNEUROSCI.5138-11.2012

Bourne, S., Machado, A. G., & Nagel, S. J. (2014). Basic Anatomy and Physiology of Pain Pathways. *Neurosurgery Clinics of North America*, *25*(4), 629–638. https://doi.org/10.1016/j.nec.2014.06.001

Bracci-Laudiero, L., & De Stefano, M. E. (2016). NGF in Early Embryogenesis, Differentiation, and Pathology in the Nervous and Immune Systems. In R. M. Kostrzewa & T. Archer (Eds.), *Neurotoxin Modeling of Brain Disorders—Life-long Outcomes in Behavioral Teratology* (pp. 125–152). Springer International Publishing. https://doi.org/10.1007/7854_2015_420

Briese, M., Saal, L., Appenzeller, S., Moradi, M., Baluapuri, A., & Sendtner, M. (2016). Whole transcriptome profiling reveals the RNA content of motor axons. *Nucleic Acids Research*, *44*(4), e33. https://doi.org/10.1093/nar/gkv1027

Burma, N. E., Leduc-Pessah, H., Fan, C. Y., & Trang, T. (2017). Animal models of chronic pain: Advances and challenges for clinical translation. *Journal of Neuroscience Research*, *95*(6), 1242–1256. https://doi.org/10.1002/jnr.23768

Bush, S. J., McCulloch, M. E. B., Summers, K. M., Hume, D. A., & Clark, E. L. (2017). Integration of quantitated expression estimates from polyA-selected and rRNA-depleted RNA-seq libraries. *BMC Bioinformatics*, *18*(1), 301. https://doi.org/10.1186/s12859-017-1714-9

Cagnetta, R., Wong, H. H.-W., Frese, C. K., Mallucci, G. R., Krijgsveld, J., & Holt, C. E. (2019). Noncanonical Modulation of the eIF2 Pathway Controls an Increase in Local Translation during Neural Wiring. *Molecular Cell*, *73*(3), 474-489.e5. https://doi.org/10.1016/j.molcel.2018.11.013

Cajigas, I. J., Tushev, G., Will, T. J., tom Dieck, S., Fuerst, N., & Schuman, E. M. (2012). The Local Transcriptome in the Synaptic Neuropil Revealed by Deep Sequencing and High-Resolution Imaging. *Neuron*, *74*(3), 453–466. https://doi.org/10.1016/j.neuron.2012.02.036

Callaghan, B. C., Cheng, H. T., Stables, C. L., Smith, A. L., & Feldman, E. L. (2012). Diabetic neuropathy: Clinical manifestations and current treatments. *The Lancet Neurology*, *11*(6), 521–534. https://doi.org/10.1016/S1474-4422(12)70065-0

Catala, M., & Kubis, N. (2013). Chapter 3—Gross anatomy and development of the peripheral nervous system. In G. Said & C. Krarup (Eds.), *Handbook of Clinical Neurology* (Vol. 115, pp. 29–41). Elsevier. https://doi.org/10.1016/B978-0-444-52902-2.00003-5

Caterina, M. J., Schumacher, M. A., Tominaga, M., Rosen, T. A., Levine, J. D., & Julius, D. (1997). The capsaicin receptor: A heat-activated ion channel in the pain pathway. *Nature*, *389*(6653), Article 6653. https://doi.org/10.1038/39807

Cavanaugh, D. J., Lee, H., Lo, L., Shields, S. D., Zylka, M. J., Basbaum, A. I., & Anderson, D. J. (2009). Distinct subsets of unmyelinated primary sensory fibers mediate behavioral responses to noxious thermal and mechanical stimuli. *Proceedings of the National Academy of Sciences of the United*

States of America, *106*(22), 9075–9080. https://doi.org/10.1073/pnas.0901507106

Chakrabarti, S., Jadon, D. R., Bulmer, D. C., & Smith, E. St. J. (2020). Human osteoarthritic synovial fluid increases excitability of mouse dorsal root ganglion sensory neurons: An in-vitro translational model to study arthritic pain. *Rheumatology*, *59*(3), 662–667. https://doi.org/10.1093/rheumatology/kez331

Chambers, D. C., Carew, A. M., Lukowski, S. W., & Powell, J. E. (2019). Transcriptomics and single-cell RNA-sequencing. *Respirology*, *24*(1), 29–36. https://doi.org/10.1111/resp.13412

Charlesworth, A., Meijer, H. A., & de Moor, C. H. (2013). Specificity factors in cytoplasmic polyadenylation. *Wiley Interdisciplinary Reviews. RNA*, *4*(4), 437–461. https://doi.org/10.1002/wrna.1171

Chen, L., Yang, G., & Grosser, T. (2013). Prostanoids and inflammatory pain. *Prostaglandins & Other Lipid Mediators*, *104–105*, 58–66. https://doi.org/10.1016/j.prostaglandins.2012.08.006

Chen, O., Donnelly, C. R., & Ji, R.-R. (2020). Regulation of pain by neuro-immune interactions between macrophages and nociceptor sensory neurons. *Current Opinion in Neurobiology*, *62*, 17–25. https://doi.org/10.1016/j.conb.2019.11.006

Cheng, X., Ji, Z., Tsalkova, T., & Mei, F. (2008). Epac and PKA: A tale of two intracellular cAMP receptors. *Acta Biochimica et Biophysica Sinica*, *40*(7), 651–662.

Chierzi, S., Ratto, G. M., Verma, P., & Fawcett, J. W. (2005). The ability of axons to regenerate their growth cones depends on axonal type and age, and is regulated by calcium, cAMP and ERK. *European Journal of Neuroscience*, *21*(8), 2051–2062. https://doi.org/10.1111/j.1460-9568.2005.04066.x

Ciolli Mattioli, C., Rom, A., Franke, V., Imami, K., Arrey, G., Terne, M., Woehler, A., Akalin, A., Ulitsky, I., & Chekulaeva, M. (2019). Alternative 3′ UTRs direct localization of functionally diverse protein isoforms in neuronal compartments. *Nucleic Acids Research*, *47*(5), 2560–2573. https://doi.org/10.1093/nar/gky1270

Clark, P., Rowland, S. E., Denis, D., Mathieu, M.-C., Stocco, R., Poirier, H., Burch, J., Han, Y., Audoly, L., Therien, A. G., & Xu, D. (2008). MF498 [N-{[4-(5,9-Diethoxy-6-oxo-6,8-dihydro-7H-pyrrolo[3,4-g]quinolin-7-yl)-3-methylbenzyl]sulfonyl}-2-(2-methoxyphenyl)acetamide], a Selective E Prostanoid Receptor 4 Antagonist, Relieves Joint Inflammation and Pain in Rodent Models of Rheumatoid and Osteoarthritis. *Journal of Pharmacology and Experimental Therapeutics*, *325*(2), 425–434. https://doi.org/10.1124/jpet.107.134510

Classification of Chronic Pain, Second Edition (Revised). (2011). *International Association for the Study of Pain (IASP)*. https://www.iasp-pain.org/publications/free-ebooks/classification-of-chronic-pain-second-edition-revised/

Colloca, L., Ludman, T., Bouhassira, D., Baron, R., Dickenson, A. H., Yarnitsky, D., Freeman, R., Truini, A., Attal, N., Finnerup, N. B., Eccleston, C., Kalso, E., Bennett, D. L., Dworkin, R. H., & Raja, S. N. (2017). Neuropathic pain. *Nature Reviews. Disease Primers*, *3*, 17002. https://doi.org/10.1038/nrdp.2017.2

Conesa, A., Madrigal, P., Tarazona, S., Gomez-Cabrero, D., Cervera, A., McPherson, A., Szcześniak, M. W., Gaffney, D. J., Elo, L. L., Zhang, X., & Mortazavi, A. (2016). A survey of best practices for RNA-seq data analysis. *Genome Biology*, *17*(1), 13. https://doi.org/10.1186/s13059-016-0881-8

Costa, I. D., Buchanan, C. N., Zdradzinski, M. D., Sahoo, P. K., Smith, T. P., Thames, E., Kar, A. N., & Twiss, J. L. (2021). The functional organization of axonal mRNA transport and translation. *Nature Reviews. Neuroscience*, *22*(2), 77–91. https://doi.org/10.1038/s41583-020-00407-7

Costa-Mattioli, M., Gobert, D., Stern, E., Gamache, K., Colina, R., Cuello, C., Sossin, W., Kaufman, R., Pelletier, J., Rosenblum, K., Krnjević, K., Lacaille, J.-C., Nader, K., & Sonenberg, N. (2007). EIF2α phosphorylation bidirectionally regulates the switch from short to long-term synaptic plasticity and memory. *Cell*, *129*(1), 195–206. https://doi.org/10.1016/j.cell.2007.01.050

Costa-Silva, J., Domingues, D., & Lopes, F. M. (2017). RNA-Seq differential expression analysis: An extended review and a software tool. *PLoS ONE*, *12*(12), e0190152. https://doi.org/10.1371/journal.pone.0190152

Court, F. A., Hendriks, W. T. J., MacGillavry, H. D., Alvarez, J., & van Minnen, J. (2008). Schwann Cell to Axon Transfer of Ribosomes: Toward a Novel Understanding of the Role of Glia in the Nervous System. *The Journal of Neuroscience*, *28*(43), 11024–11029. https://doi.org/10.1523/JNEUROSCI.2429-08.2008

Cox, L. J., Hengst, U., Gurskaya, Nadya., Lukyanov, K. A., & Jaffrey, S. R. (2008). Intra-axonal translation and retrograde trafficking of CREB promotes neuronal survival. *Nature Cell Biology*, *10*(2), 149–159. https://doi.org/10.1038/ncb1677

Cranfill, S. L., & Luo, W. (2021). Chapter Eleven - The development of somatosensory neurons: Insights into pain and itch. In G. J. Bashaw (Ed.), *Current Topics in Developmental Biology* (Vol. 142, pp. 443–475). Academic Press. https://doi.org/10.1016/bs.ctdb.2020.10.005

Crawford, L. K., & Caterina, M. J. (2020). Functional Anatomy of the Sensory Nervous System: Updates From the Neuroscience Bench. *Toxicologic Pathology*, *48*(1), 174–189. https://doi.org/10.1177/0192623319869011

Dawes, J. M., Andersson, D. A., Bennett, D. L. H., Bevan, S., & McMahon, S. B. (2013). Chapter 3—Inflammatory Mediators and Modulators of Pain. In *Textbook of Pain* (Sixth, pp. 48–67). Elsevier.

DeFelipe, J. (2013). Cajal and the discovery of a new artistic world. In *Progress in Brain Research* (Vol. 203, pp. 201–220). Elsevier. https://doi.org/10.1016/B978-0-444-62730-8.00008-6

Denk, F., Bennett, D. L., & McMahon, S. B. (2017). Nerve Growth Factor and Pain Mechanisms. *Annual Review of Neuroscience*, *40*(1), 307–325. https://doi.org/10.1146/annurev-neuro-072116-031121

Deval, E., & Lingueglia, E. (2015). Acid-Sensing Ion Channels and nociception in the peripheral and central nervous systems. *Neuropharmacology*, *94*, 49–57. https://doi.org/10.1016/j.neuropharm.2015.02.009

Dewanjee, S., Das, S., Das, A. K., Bhattacharjee, N., Dihingia, A., Dua, T. K., Kalita, J., & Manna, P. (2018). Molecular mechanism of diabetic neuropathy and its pharmacotherapeutic targets. *European Journal of Pharmacology*, *833*, 472–523. https://doi.org/10.1016/j.ejphar.2018.06.034

Di Liegro, C. M., SCHIERA, G., & DI LIEGRO, I. (2014). Regulation of mRNA transport, localization and translation in the nervous system of mammals (Review). *International Journal of Molecular Medicine*, *33*(4), 747–762. https://doi.org/10.3892/ijmm.2014.1629

Dib-Hajj, S. D., Black, J. A., & Waxman, S. G. (2009). Voltage-Gated Sodium Channels: Therapeutic Targets for Pain. *Pain Medicine*, *10*(7), 1260–1269. https://doi.org/10.1111/j.1526-4637.2009.00719.x

Dillies, M.-A., Rau, A., Aubert, J., Hennequet-Antier, C., Jeanmougin, M., Servant, N., Keime, C., Marot, G., Castel, D., Estelle, J., Guernec, G., Jagla, B., Jouneau, L., Laloë, D., Le Gall, C., Schaëffer, B., Le Crom, S., Guedj, M., & Jaffrézic, F. (2013). A comprehensive evaluation of normalization methods for Illumina high-throughput RNA sequencing data analysis. *Briefings in Bioinformatics*, *14*(6), 671–683. https://doi.org/10.1093/bib/bbs046

Djouhri, L., & Lawson, S. N. (2004). Aβ-fiber nociceptive primary afferent neurons: A review of incidence and properties in relation to other afferent A-fiber neurons in mammals. *Brain Research Reviews*, *46*(2), 131–145. https://doi.org/10.1016/j.brainresrev.2004.07.015

Dobin, A., & Gingeras, T. R. (2015). Mapping RNA-seq Reads with STAR. *Current Protocols in Bioinformatics / Editoral Board, Andreas D. Baxevanis ... [et Al.]*, *51*, 11.14.1-11.14.19. https://doi.org/10.1002/0471250953.bi1114s51

Dolga, A. M., Granic, I., Blank, T., Knaus, H.-G., Spiess, J., Luiten, P. G. M., Eisel, U. L. M., & Nijholt, I. M. (2008). TNF-α-mediates neuroprotection against glutamate-induced excitotoxicity via NF-κB-dependent up-regulation of KCa2.2 channels. *Journal of Neurochemistry*, *107*(4), 1158–1167. https://doi.org/10.1111/j.1471-4159.2008.05701.x

Donaldson, L. F., & Beazley-Long, N. (2016). Alternative RNA splicing: Contribution to pain and potential therapeutic strategy. *Drug Discovery Today*, *21*(11), 1787–1798. https://doi.org/10.1016/j.drudis.2016.06.017

Dong, L., Guarino, B. B., Jordan-Sciutto, K. L., & Winkelstein, B. A. (2011). Activating transcription factor 4, a mediator of the integrated stress response, is increased in the dorsal root ganglia following painful facet joint distraction. *Neuroscience*, *193*, 377–386. https://doi.org/10.1016/j.neuroscience.2011.07.059

Dong, Y., Siegwart, D. J., & Anderson, D. G. (2019). Strategies, Design, and Chemistry in siRNA Delivery Systems. *Advanced Drug Delivery Reviews*, *144*, 133–147. https://doi.org/10.1016/j.addr.2019.05.004

Donnelly, C. J., Park, M., Spillane, M., Yoo, S., Pacheco, A., Gomes, C., Vuppalanchi, D., McDonald, M., Kim, H. H., Merianda, T. T., Gallo, G., & Twiss, J. L. (2013). Axonally Synthesized β-Actin and GAP-43 Proteins Support Distinct Modes of Axonal Growth. *Journal of Neuroscience*, *33*(8), 3311–3322. https://doi.org/10.1523/JNEUROSCI.1722-12.2013

Du, Y.-Y., Zhao, Y.-X., Liu, Y.-P., Liu, W., Wang, M.-M., & Yuan, C.-M. (2015). Regulatory Tweak/Fn14 signaling pathway as a potent target for controlling bone loss. *Biomedicine & Pharmacotherapy*, *70*, 170–173. https://doi.org/10.1016/j.biopha.2015.01.005

Dubin, A. E., & Patapoutian, A. (2010). Nociceptors: The sensors of the pain pathway. *The Journal of Clinical Investigation*, *120*(11), 3760–3772. https://doi.org/10.1172/JCI42843

Ebbinghaus, M., Segond von Banchet, G., Massier, J., Gajda, M., Bräuer, R., Kress, M., & Schaible, H.-G. (2015). Interleukin-6-dependent influence of nociceptive sensory neurons on antigen-induced arthritis. *Arthritis Research & Therapy*, *17*(1), 334. https://doi.org/10.1186/s13075-015-0858-0

Edelstein, A., Amodaj, N., Hoover, K., Vale, R., & Stuurman, N. (2010). Computer Control of Microscopes Using μManager. *Current Protocols in Molecular Biology*, *92*(1), 14.20.1-14.20.17. https://doi.org/10.1002/0471142727.mb1420s92

Ellenbroek, B., & Youn, J. (2016). Rodent models in neuroscience research: Is it a rat race? *Disease Models & Mechanisms*, *9*(10), 1079–1087. https://doi.org/10.1242/dmm.026120

Eng, H., Lund, K., & Campenot, R. B. (1999). Synthesis of β-Tubulin, Actin, and Other Proteins in Axons of Sympathetic Neurons in Compartmented Cultures. *The Journal of Neuroscience*, *19*(1), 1–9. https://doi.org/10.1523/JNEUROSCI.19-01-00001.1999

Engelmann, C., & Haenold, R. (2016). Transcriptional Control of Synaptic Plasticity by Transcription Factor NF-κB. *Neural Plasticity*, *2016*, 7027949. https://doi.org/10.1155/2016/7027949

Esposito, M. F., Malayil, R., Hanes, M., & Deer, T. (2019). Unique Characteristics of the Dorsal Root Ganglion as a Target for Neuromodulation. *Pain Medicine: The Official Journal of the American Academy of Pain Medicine*, *20*(Suppl 1), S23–S30. https://doi.org/10.1093/pm/pnz012

Farias, J., Holt, C. E., Sotelo, J. R., & Sotelo-Silveira, J. R. (2020). Axon microdissection and transcriptome profiling reveals the in vivo RNA content of fully differentiated myelinated motor axons. *RNA*, *26*(5), 595–612. https://doi.org/10.1261/rna.073700.119

Farris, S., Ward, J. M., Carstens, K. E., Samadi, M., Wang, Y., & Dudek, S. M. (2019). Hippocampal subregions express distinct dendritic transcriptomes that reveal unexpected differences in mitochondrial function in CA2. *Cell Reports*, *29*(2), 522-539.e6. https://doi.org/10.1016/j.celrep.2019.08.093

Fattori, V., Hohmann, M. S. N., Rossaneis, A. C., Pinho-Ribeiro, F. A., & Verri, W. A. (2016). Capsaicin: Current Understanding of Its Mechanisms and Therapy of Pain and Other Pre-Clinical and Clinical Uses. *Molecules*, *21*(7), 844. https://doi.org/10.3390/molecules21070844

Feldman, E. L., Callaghan, B. C., Pop-Busui, R., Zochodne, D. W., Wright, D. E., Bennett, D. L., Bril, V., Russell, J. W., & Viswanathan, V. (2019). Diabetic neuropathy. *Nature Reviews. Disease Primers*, *5*(1), 42. https://doi.org/10.1038/s41572-019-0097-9

Ferrari, L. F., Bogen, O., Chu, C., & Levine, J. D. (2013). Peripheral Administration of Translation Inhibitors Reverses Increased Hyperalgesia in a Model of Chronic Pain in the Rat. *The Journal of Pain : Official Journal of the American Pain Society*, *14*(7), 731–738. https://doi.org/10.1016/j.jpain.2013.01.779

Ferrari, L. F., Bogen, O., & Levine, J. D. (2010). Nociceptor subpopulations involved in hyperalgesic priming. *Neuroscience*, *165*(3), 896–901. https://doi.org/10.1016/j.neuroscience.2009.11.029

Finnerup, N. B., Kuner, R., & Jensen, T. S. (2021). Neuropathic Pain: From Mechanisms to Treatment. *Physiological Reviews*, *101*(1), 259–301. https://doi.org/10.1152/physrev.00045.2019

Fisher, A. S., Lanigan, M. T., Upton, N., & Lione, L. A. (2021). Preclinical Neuropathic Pain Assessment; the Importance of Translatability and Bidirectional Research. *Frontiers in Pharmacology*, *11*, 614990. https://doi.org/10.3389/fphar.2020.614990

Fornaro, M., Sharthiya, H., & Tiwari, V. (2018). Adult Mouse DRG Explant and Dissociated Cell Models to Investigate Neuroplasticity and Responses to Environmental Insults Including Viral Infection. *Journal of Visualized Experiments : JoVE*, *133*, 56757. https://doi.org/10.3791/56757

Frankish, A., Diekhans, M., Ferreira, A.-M., Johnson, R., Jungreis, I., Loveland, J., Mudge, J. M., Sisu, C., Wright, J., Armstrong, J., Barnes, I., Berry, A., Bignell, A., Carbonell Sala, S., Chrast, J., Cunningham, F., Di Domenico, T.,

Donaldson, S., Fiddes, I. T., … Flicek, P. (2019). GENCODE reference annotation for the human and mouse genomes. *Nucleic Acids Research*, *47*(D1), D766–D773. https://doi.org/10.1093/nar/gky955

Frankish, A., Uszczynska, B., Ritchie, G. R., Gonzalez, J. M., Pervouchine, D., Petryszak, R., Mudge, J. M., Fonseca, N., Brazma, A., Guigo, R., & Harrow, J. (2015). Comparison of GENCODE and RefSeq gene annotation and the impact of reference geneset on variant effect prediction. *BMC Genomics*, *16*(8), S2. https://doi.org/10.1186/1471-2164-16-S8-S2

Freedman, A. H., Gaspar, J. M., & Sackton, T. B. (2020). Short paired-end reads trump long single-end reads for expression analysis. *BMC Bioinformatics*, *21*, 149. https://doi.org/10.1186/s12859-020-3484-z

Garcez, P. P., Guillemot, F., & Dajas-Bailador, F. (2017). Study of miRNA Function in the Developing Axons of Mouse Cortical Neurons: Use of Compartmentalized Microfluidic Chambers and In Utero Electroporation. In M. J. Kye (Ed.), *MicroRNA Technologies* (pp. 59–71). Springer. https://doi.org/10.1007/7657_2016_12

García-Añoveros, J., & Nagata, K. (2007). TRPA1. In V. Flockerzi & B. Nilius (Eds.), *Transient Receptor Potential (TRP) Channels* (pp. 347–362). Springer. https://doi.org/10.1007/978-3-540-34891-7_21

Gardiner, N. J., & Freeman, O. J. (2016). Chapter Five—Can Diabetic Neuropathy Be Modeled In Vitro? In N. A. Calcutt & P. Fernyhough (Eds.), *International Review of Neurobiology* (Vol. 127, pp. 53–87). Academic Press. https://doi.org/10.1016/bs.irn.2016.02.004

Gibbs, K. L., Greensmith, L., & Schiavo, G. (2015). Regulation of Axonal Transport by Protein Kinases. *Trends in Biochemical Sciences*, *40*(10), 597–610. https://doi.org/10.1016/j.tibs.2015.08.003

Giuditta, A., Dettbarn, W. D., & Brzin, M. (1968). Protein synthesis in the isolated giant axon of the squid. *Proceedings of the National Academy of Sciences of the United States of America*, *59*(4), 1284–1287.

Giuditta, A., Menichini, E., Perrone Capano, C., Langella, M., Martin, R., Castigli, E., & Kaplan, B. B. (1991). Active polysomes in the axoplasm of the squid giant axon. *Journal of Neuroscience Research*, *28*(1), 18–28. https://doi.org/10.1002/jnr.490280103

Gkogkas, C., Sonenberg, N., & Costa-Mattioli, M. (2010). Translational Control Mechanisms in Long-lasting Synaptic Plasticity and Memory. *The Journal of Biological Chemistry*, *285*(42), 31913–31917. https://doi.org/10.1074/jbc.R110.154476

Glock, C., Heumüller, M., & Schuman, E. M. (2017). MRNA transport & local translation in neurons. *Current Opinion in Neurobiology*, *45*, 169–177. https://doi.org/10.1016/j.conb.2017.05.005

Glusman, G., Caballero, J., Robinson, M., Kutlu, B., & Hood, L. (2013). Optimal Scaling of Digital Transcriptomes. *PLoS ONE*, *8*(11). https://doi.org/10.1371/journal.pone.0077885

Gobert, D., Topolnik, L., Azzi, M., Huang, L., Badeaux, F., DesGroseillers, L., Sossin, W. S., & Lacaille, J.-C. (2008). Forskolin induction of late-LTP and up-regulation of 5′ TOP mRNAs translation via mTOR, ERK, and PI3K in hippocampal pyramidal cells. *Journal of Neurochemistry*, *106*(3), 1160–1174. https://doi.org/10.1111/j.1471-4159.2008.05470.x

Gold, M. S., Weinreich, D., Kim, C.-S., Wang, R., Treanor, J., Porreca, F., & Lai, J. (2003). Redistribution of NaV1.8 in Uninjured Axons Enables Neuropathic Pain. *The Journal of Neuroscience*, *23*(1), 158–166. https://doi.org/10.1523/JNEUROSCI.23-01-00158.2003

Goldstein, B. (2001). Anatomy of the Peripheral Nervous System. *Physical Medicine and Rehabilitation Clinics of North America*, *12*(2), 207–236. https://doi.org/10.1016/S1047-9651(18)30066-4

González, C., & Couve, A. (2014). The axonal endoplasmic reticulum and protein trafficking: Cellular bootlegging south of the soma. *Seminars in Cell & Developmental Biology*, *27*, 23–31. https://doi.org/10.1016/j.semcdb.2013.12.004

González, E., & Joly, S. (2013). Impact of RNA-seq attributes on false positive rates in differential expression analysis of de novo assembled transcriptomes. *BMC Research Notes*, *6*, 503. https://doi.org/10.1186/1756-0500-6-503

Goswami, S. C., Mishra, S. K., Maric, D., Kaszas, K., Gonnella, G. L., Clokie, S. J., Kominsky, H. D., Gross, J. R., Keller, J. M., Mannes, A. J., Hoon, M. A., & Iadarola, M. J. (2014). Molecular signatures of mouse TRPV1-lineage neurons revealed by RNA-Seq transcriptome analysis. *The Journal of Pain : Official Journal of the American Pain Society*, *15*(12), 1338–1359. https://doi.org/10.1016/j.jpain.2014.09.010

Grabherr, M. G., Haas, B. J., Yassour, M., Levin, J. Z., Thompson, D. A., Amit, I., Adiconis, X., Fan, L., Raychowdhury, R., Zeng, Q., Chen, Z., Mauceli, E., Hacohen, N., Gnirke, A., Rhind, N., di Palma, F., Birren, B. W., Nusbaum, C., Lindblad-Toh, K., … Regev, A. (2011). Full-length transcriptome assembly from RNA-Seq data without a reference genome. *Nature Biotechnology*, *29*(7), Article 7. https://doi.org/10.1038/nbt.1883

Gumy, L. F., Bampton, E. T. W., & Tolkovsky, A. M. (2008). Hyperglycaemia inhibits Schwann cell proliferation and migration and restricts regeneration of axons and Schwann cells from adult murine DRG. *Molecular and Cellular Neuroscience*, *37*(2), 298–311. https://doi.org/10.1016/j.mcn.2007.10.004

Gumy, L. F., Yeo, G. S. H., Tung, Y.-C. L., Zivraj, K. H., Willis, D., Coppola, G., Lam, B. Y. H., Twiss, J. L., Holt, C. E., & Fawcett, J. W. (2011). Transcriptome analysis

of embryonic and adult sensory axons reveals changes in mRNA repertoire localization. *RNA*, *17*(1), 85–98. https://doi.org/10.1261/rna.2386111

Ha, K. C. H., Blencowe, B. J., & Morris, Q. (2018). QAPA: A new method for the systematic analysis of alternative polyadenylation from RNA-seq data. *Genome Biology*, *19*(1), 45. https://doi.org/10.1186/s13059-018-1414-4

Haberberger, R. V., Barry, C., Dominguez, N., & Matusica, D. (2019). Human Dorsal Root Ganglia. *Frontiers in Cellular Neuroscience*, *13*. https://www.frontiersin.org/article/10.3389/fncel.2019.00271

Hafner, A.-S., Donlin-Asp, P. G., Leitch, B., Herzog, E., & Schuman, E. M. (2018). *Local protein synthesis in axon terminals and dendritic spines differentiates plasticity contexts* (p. 363184). bioRxiv. https://doi.org/10.1101/363184

Hamilton, S. G., & McMahon, S. B. (2000). ATP as a peripheral mediator of pain. *Journal of the Autonomic Nervous System*, *81*(1), 187–194. https://doi.org/10.1016/S0165-1838(00)00137-5

Han, Z., Feng, W., Hu, R., Ge, Q., Ma, W., Zhang, W., Xu, S., Zhan, B., Zhang, L., Sun, X., & Zhou, X. (2021). RNA-seq profiling reveals PBMC RNA as a potential biomarker for hepatocellular carcinoma. *Scientific Reports*, *11*, 17797. https://doi.org/10.1038/s41598-021-96952-x

Hayes, A. G., & Tyers, M. B. (1980). Effects of capsaicin on nociceptive heat, pressure and chemical thresholds and on substance P levels in the rat. *Brain Research*, *189*(2), 561–564. https://doi.org/10.1016/0006-8993(80)90369-8

Heinricher and Fields. (2013). Chapter 8—Central Nervous System Mechanisms of Pain Modulation. In *Textbook of Pain* (Sixth, pp. 129–142). Elsevier.

Hellen, C. U. T. (2018). Translation Termination and Ribosome Recycling in Eukaryotes. *Cold Spring Harbor Perspectives in Biology*, *10*(10), a032656. https://doi.org/10.1101/cshperspect.a032656

Hjerling-Leffler, J., AlQatari, M., Ernfors, P., & Koltzenburg, M. (2007). Emergence of Functional Sensory Subtypes as Defined by Transient Receptor Potential Channel Expression. *The Journal of Neuroscience*, *27*(10), 2435–2443. https://doi.org/10.1523/JNEUROSCI.5614-06.2007

Hockley, J. R. F., Taylor, T. S., Callejo, G., Wilbrey, A. L., Gutteridge, A., Bach, K., Winchester, W. J., Bulmer, D. C., McMurray, G., & Smith, E. S. J. (2019). Single-cell RNAseq reveals seven classes of colonic sensory neuron. *Gut*, *68*(4), 633–644. https://doi.org/10.1136/gutjnl-2017-315631

Hoeger-Bement, M. K., & Sluka, K. A. (2003). Phosphorylation of CREB and Mechanical Hyperalgesia Is Reversed by Blockade of the cAMP Pathway in a Time-Dependent Manner after Repeated Intramuscular Acid Injections. *The Journal of Neuroscience*, *23*(13), 5437–5445. https://doi.org/10.1523/JNEUROSCI.23-13-05437.2003

Hollenbeck, P. J., & Saxton, W. M. (2005). The axonal transport of mitochondria. *Journal of Cell Science*, *118*(Pt 23), 5411–5419. https://doi.org/10.1242/jcs.02745

Holt, C. E., Martin, K. C., & Schuman, E. M. (2019). Local translation in neurons: Visualization and function. *Nature Structural & Molecular Biology*, *26*(7), Article 7. https://doi.org/10.1038/s41594-019-0263-5

Hu, G., Zeng, W., & Xia, Y. (2017). TWEAK/Fn14 signaling in tumors. *Tumor Biology*, *39*(6), 1010428317714624. https://doi.org/10.1177/1010428317714624

Huang, E. J., & Reichardt, L. F. (2001). Neurotrophins: Roles in Neuronal Development and Function. *Annual Review of Neuroscience*, *24*, 677–736. https://doi.org/10.1146/annurev.neuro.24.1.677

Huang, J., Zhang, X., & McNaughton, P. A. (2006). Inflammatory Pain: The Cellular Basis of Heat Hyperalgesia. *Current Neuropharmacology*, *4*(3), 197–206.

Huang, L.-N., Zou, Y., Wu, S.-G., Zhang, H.-H., Mao, Q.-X., Li, J.-B., & Tao, Y.-X. (2019). Fn14 Participates in Neuropathic Pain Through NF-κB Pathway in Primary Sensory Neurons. *Molecular Neurobiology*, *56*(10), 7085–7096. https://doi.org/10.1007/s12035-019-1545-y

Huang, L.-Y. M., & Gu, Y. (2017). Epac and nociceptor sensitization. *Molecular Pain*, *13*, 1744806917716234. https://doi.org/10.1177/1744806917716234

Huang, S., Ziegler, C. G. K., Austin, J., Mannoun, N., Vukovic, M., Ordovas-Montanes, J., Shalek, A. K., & Andrian, U. H. von. (2021). Lymph nodes are innervated by a unique population of sensory neurons with immunomodulatory potential. *Cell*, *184*(2), 441-459.e25. https://doi.org/10.1016/j.cell.2020.11.028

Huang, Y.-S., & Richter, J. D. (2004). Regulation of local mRNA translation. *Current Opinion in Cell Biology*, *16*(3), 308–313. https://doi.org/10.1016/j.ceb.2004.03.002

Hucho, T., & Levine, J. D. (2007). Signaling Pathways in Sensitization: Toward a Nociceptor Cell Biology. *Neuron*, *55*(3), 365–376. https://doi.org/10.1016/j.neuron.2007.07.008

Hulsen, T., de Vlieg, J., & Alkema, W. (2008). BioVenn – a web application for the comparison and visualization of biological lists using area-proportional Venn diagrams. *BMC Genomics*, *9*(1), 488. https://doi.org/10.1186/1471-2164-9-488

Iannone, F., De Bari, C., Dell'Accio, F., Covelli, M., Patella, V., Lo Bianco, G., & Lapadula, G. (2002). Increased expression of nerve growth factor (NGF) and high affinity NGF receptor (p140 TrkA) in human osteoarthritic chondrocytes. *Rheumatology*, *41*(12), 1413–1418. https://doi.org/10.1093/rheumatology/41.12.1413

Imbeaud, S., Graudens, E., Boulanger, V., Barlet, X., Zaborski, P., Eveno, E., Mueller, O., Schroeder, A., & Auffray, C. (2005). Towards standardization of RNA

quality assessment using user-independent classifiers of microcapillary electrophoresis traces. *Nucleic Acids Research*, *33*(6), e56. https://doi.org/10.1093/nar/gni054

Jager, S. E., Pallesen, L. T., Richner, M., Harley, P., Hore, Z., McMahon, S., Denk, F., & Vægter, C. B. (2020). Changes in the transcriptional fingerprint of satellite glial cells following peripheral nerve injury. *Glia*, *68*(7), 1375–1395. https://doi.org/10.1002/glia.23785

Jansen, L.-A. R., Forster, L. A., Smith, X. L., Rubaharan, M., Murphy, A. Z., & Baro, D. J. (2020). Changes in peripheral HCN2 channels during persistent inflammation. *Channels*, *15*(1), 165–179. https://doi.org/10.1080/19336950.2020.1870086

Jeanjean, A. P., Moussaoui, S. M., Maloteaux, J.-M., & Laduron, P. M. (1995). Interleukin-1β induces long-term increase of axonally transported opiate receptors and substance P. *Neuroscience*, *68*(1), 151–157. https://doi.org/10.1016/0306-4522(95)00106-S

Ji, R.-R., Berta, T., & Nedergaard, M. (2013). Glia and pain: Is chronic pain a gliopathy? *Pain*, *154*(0 1), S10–S28. https://doi.org/10.1016/j.pain.2013.06.022

Ji, R.-R., Chamessian, A., & Zhang, Y.-Q. (2016). Pain Regulation by Non-neuronal Cells and Inflammation. *Science (New York, N.Y.)*, *354*(6312), 572–577. https://doi.org/10.1126/science.aaf8924

Ji, R.-R., Samad, T. A., Jin, S.-X., Schmoll, R., & Woolf, C. J. (2002). P38 MAPK Activation by NGF in Primary Sensory Neurons after Inflammation Increases TRPV1 Levels and Maintains Heat Hyperalgesia. *Neuron*, *36*(1), 57–68. https://doi.org/10.1016/S0896-6273(02)00908-X

Ji, R.-R., Xu, Z.-Z., & Gao, Y.-J. (2014). Emerging targets in neuroinflammation-driven chronic pain. *Nature Reviews. Drug Discovery*, *13*(7), 533–548. https://doi.org/10.1038/nrd4334

Ji, S.-J., & Jaffrey, S. R. (2014). Axonal transcription factors: Novel regulators of growth cone-to-nucleus signaling. *Developmental Neurobiology*, *74*(3), 245–258. https://doi.org/10.1002/dneu.22112

Jiménez-Díaz, L., Géranton, S. M., Passmore, G. M., Leith, J. L., Fisher, A. S., Berliocchi, L., Sivasubramaniam, A. K., Sheasby, A., Lumb, B. M., & Hunt, S. P. (2008). Local Translation in Primary Afferent Fibers Regulates Nociception. *PLoS ONE*, *3*(4). https://doi.org/10.1371/journal.pone.0001961

Johnson, C. I., Argyle, D. J., & Clements, D. N. (2016). In vitro models for the study of osteoarthritis. *The Veterinary Journal*, *209*, 40–49. https://doi.org/10.1016/j.tvjl.2015.07.011

Jung, H., Gkogkas, C. G., Sonenberg, N., & Holt, C. E. (2014). Remote Control of Gene Function by Local Translation. *Cell*, *157*(1), 26–40. https://doi.org/10.1016/j.cell.2014.03.005

Kaliyaperumal, S., Wilson, K., Aeffner, F., & Dean, C. (2020). Animal Models of Peripheral Pain: Biology Review and Application for Drug Discovery. *Toxicologic Pathology*, *48*(1), 202–219. https://doi.org/10.1177/0192623319857051

Kanai, Y., Dohmae, N., & Hirokawa, N. (2004). Kinesin Transports RNA: Isolation and Characterization of an RNA-Transporting Granule. *Neuron*, *43*(4), 513–525. https://doi.org/10.1016/j.neuron.2004.07.022

Kandasamy, R., & Price, T. J. (2015). The Pharmacology of Nociceptor Priming. *Handbook of Experimental Pharmacology*, *227*, 15–37. https://doi.org/10.1007/978-3-662-46450-2_2

Kar, A. N., Lee, S. J., & Twiss, J. L. (2018). Expanding axonal transcriptome brings new functions for axonally-synthesized proteins in health and disease. *The Neuroscientist : A Review Journal Bringing Neurobiology, Neurology and Psychiatry*, *24*(2), 111–129. https://doi.org/10.1177/1073858417712668

Kar, A. N., Sun, C.-Y., Reichard, K., Gervasi, N. M., Pickel, J., Nakazawa, K., Gioio, A. E., & Kaplan, B. B. (2014). Dysregulation of the Axonal Trafficking of Nuclear-encoded Mitochondrial mRNA alters Neuronal Mitochondrial Activity and Mouse Behavior. *Developmental Neurobiology*, *74*(3), 333–350. https://doi.org/10.1002/dneu.22141

Kasai, M., & Mizumura, K. (2001). Effects of PGE2 on neurons from rat dorsal root ganglia in intact and adjuvant-inflamed rats: Role of NGF on PGE2-induced depolarization. *Neuroscience Research*, *41*(4), 345–353. https://doi.org/10.1016/S0168-0102(01)00291-7

Kawabata, A. (2011). Prostaglandin E2 and Pain-An Update. *Biological and Pharmaceutical Bulletin*, *34*(8), 1170–1173. https://doi.org/10.1248/bpb.34.1170

Kelleher, R. J., Govindarajan, A., & Tonegawa, S. (2004). Translational Regulatory Mechanisms in Persistent Forms of Synaptic Plasticity. *Neuron*, *44*(1), 59–73. https://doi.org/10.1016/j.neuron.2004.09.013

Khomula, E. V., Araldi, D., & Levine, J. D. (2019). In Vitro Nociceptor Neuroplasticity Associated with In Vivo Opioid-Induced Hyperalgesia. *The Journal of Neuroscience*, *39*(36), 7061–7073. https://doi.org/10.1523/JNEUROSCI.1191-19.2019

Khoutorsky, A., Bonin, R. P., Sorge, R. E., Gkogkas, C. G., Pawlowski, S. A., Jafarnejad, S. M., Pitcher, M. H., Alain, T., Perez-Sanchez, J., Salter, E. W., Martin, L., Ribeiro-da-Silva, A., De Koninck, Y., Cervero, F., Mogil, J. S., & Sonenberg, N. (2015). Translational control of nociception via 4E-binding protein 1. *ELife*, *4*, e12002. https://doi.org/10.7554/eLife.12002

Khoutorsky, A., & Price, T. J. (2018). Translational Control Mechanisms in Persistent Pain. *Trends in Neurosciences*, *41*(2), 100–114. https://doi.org/10.1016/j.tins.2017.11.006

Kilkenny, C., Browne, W. J., Cuthill, I. C., Emerson, M., & Altman, D. G. (2010). Improving Bioscience Research Reporting: The ARRIVE Guidelines for Reporting Animal Research. *PLOS Biology*, *8*(6), e1000412. https://doi.org/10.1371/journal.pbio.1000412

Kim, E., & Jung, H. (2020). Local mRNA translation in long-term maintenance of axon health and function. *Current Opinion in Neurobiology*, *63*, 15–22. https://doi.org/10.1016/j.conb.2020.01.006

Kim, S.-C., Kim, A., Park, J.-Y., & Hwang, E. M. (2022). Improved AAV vector system for cell-type-specific RNA interference. *Journal of Neuroscience Methods*, *368*, 109452. https://doi.org/10.1016/j.jneumeth.2021.109452

Kindler, S., & Kreienkamp, H.-J. (2012). Dendritic mRNA Targeting and Translation. In M. R. Kreutz & C. Sala (Eds.), *Synaptic Plasticity* (Vol. 970, pp. 285–305). Springer Vienna. https://doi.org/10.1007/978-3-7091-0932-8_13

Klann, E., Antion, M. D., Banko, J. L., & Hou, L. (2004). Synaptic Plasticity and Translation Initiation. *Learning & Memory*, *11*(4), 365–372. https://doi.org/10.1101/lm.79004

Knight, J. R. P., Garland, G., Pöyry, T., Mead, E., Vlahov, N., Sfakianos, A., Grosso, S., De-Lima-Hedayioglu, F., Mallucci, G. R., von der Haar, T., Smales, C. M., Sansom, O. J., & Willis, A. E. (2020). Control of translation elongation in health and disease. *Disease Models & Mechanisms*, *13*(3), dmm043208. https://doi.org/10.1242/dmm.043208

Koch, C. M., Chiu, S. F., Akbarpour, M., Bharat, A., Ridge, K. M., Bartom, E. T., & Winter, D. R. (2018). A Beginner's Guide to Analysis of RNA Sequencing Data. *American Journal of Respiratory Cell and Molecular Biology*, *59*(2), 145–157. https://doi.org/10.1165/rcmb.2017-0430TR

Koltzenburg, M. (1999). The changing sensitivity in the life of the nociceptor. *PAIN*, *82*, S93. https://doi.org/10.1016/S0304-3959(99)00142-6

Korsak, L. I. T., Mitchell, M. E., Shepard, K. A., & Akins, M. R. (2016). Regulation of neuronal gene expression by local axonal translation. *Current Genetic Medicine Reports*, *4*(1), 16–25. https://doi.org/10.1007/s40142-016-0085-2

Krämer, A., Green, J., Pollard, J., Jr, & Tugendreich, S. (2014). Causal analysis approaches in Ingenuity Pathway Analysis. *Bioinformatics*, *30*(4), 523–530. https://doi.org/10.1093/bioinformatics/btt703

Kraus, A. J., Brink, B. G., & Siegel, T. N. (2019). Efficient and specific oligo-based depletion of rRNA. *Scientific Reports*, *9*(1), 12281. https://doi.org/10.1038/s41598-019-48692-2

Kress, M., Hüttenhofer, A., Landry, M., Kuner, R., Favereaux, A., Greenberg, D., Bednarik, J., Heppenstall, P., Kronenberg, F., Malcangio, M., Rittner, H., Üçeyler, N., Trajanoski, Z., Mouritzen, P., Birklein, F., Sommer, C., & Soreq, H. (2013). MicroRNAs in nociceptive circuits as predictors of future clinical

applications. *Frontiers in Molecular Neuroscience*, *6*. https://www.frontiersin.org/article/10.3389/fnmol.2013.00033

Krukowski, K., Nolan, A., Frias, E. S., Boone, M., Ureta, G., Grue, K., Paladini, M.-S., Elizarraras, E., Delgado, L., Bernales, S., Walter, P., & Rosi, S. (2020). Small molecule cognitive enhancer reverses age-related memory decline in mice. *ELife*, *9*, e62048. https://doi.org/10.7554/eLife.62048

Kukurba, K. R., & Montgomery, S. B. (2015). RNA Sequencing and Analysis. *Cold Spring Harbor Protocols*, *2015*(11), 951–969. https://doi.org/10.1101/pdb.top084970

Kummer, K. K., Zeidler, M., Kalpachidou, T., & Kress, M. (2021). Role of IL-6 in the regulation of neuronal development, survival and function. *Cytokine*, *144*, 155582. https://doi.org/10.1016/j.cyto.2021.155582

Kuner, R., & Kuner, T. (2021). Cellular Circuits in the Brain and Their Modulation in Acute and Chronic Pain. *Physiological Reviews*, *101*(1), 213–258. https://doi.org/10.1152/physrev.00040.2019

Lamarre, S., Frasse, P., Zouine, M., Labourdette, D., Sainderichin, E., Hu, G., Le Berre-Anton, V., Bouzayen, M., & Maza, E. (2018). Optimization of an RNA-Seq Differential Gene Expression Analysis Depending on Biological Replicate Number and Library Size. *Frontiers in Plant Science*, *9*, 108. https://doi.org/10.3389/fpls.2018.00108

Landy, M. A., Goyal, M., Casey, K. M., Liu, C., & Lai, H. C. (2021). Loss of Prdm12 during development, but not in mature nociceptors, causes defects in pain sensation. *Cell Reports*, *34*(13), 108913. https://doi.org/10.1016/j.celrep.2021.108913

Lasek, R. J., Dabrowski, C., & Nordlander, R. (1973). Analysis of Axoplasmic RNA from Invertebrate Giant Axons. *Nature New Biology*, *244*(136), Article 136. https://doi.org/10.1038/newbio244162a0

Lee, A. S., Ellman, M. B., Yan, D., Kroin, J. S., Cole, B. J., van Wijnen, A. J., & Im, H.-J. (2013). A current review of molecular mechanisms regarding osteoarthritis and pain. *Gene*, *527*(2), 440–447. https://doi.org/10.1016/j.gene.2013.05.069

Lee, G. I., & Neumeister, M. W. (2020). Pain: Pathways and Physiology. *Clinics in Plastic Surgery*, *47*(2), 173–180. https://doi.org/10.1016/j.cps.2019.11.001

Lehmann, S. M., Krüger, C., Park, B., Derkow, K., Rosenberger, K., Baumgart, J., Trimbuch, T., Eom, G., Hinz, M., Kaul, D., Habbel, P., Kälin, R., Franzoni, E., Rybak, A., Nguyen, D., Veh, R., Ninnemann, O., Peters, O., Nitsch, R., … Lehnardt, S. (2012). An unconventional role for miRNA: Let-7 activates Toll-like receptor 7 and causes neurodegeneration. *Nature Neuroscience*, *15*(6), Article 6. https://doi.org/10.1038/nn.3113

Lever, J., Krzywinski, M., & Altman, N. (2017). Principal component analysis. *Nature Methods*, *14*(7), Article 7. https://doi.org/10.1038/nmeth.4346

Li, C.-L., Li, K.-C., Wu, D., Chen, Y., Luo, H., Zhao, J.-R., Wang, S.-S., Sun, M.-M., Lu, Y.-J., Zhong, Y.-Q., Hu, X.-Y., Hou, R., Zhou, B.-B., Bao, L., Xiao, H.-S., & Zhang, X. (2016). Somatosensory neuron types identified by high-coverage single-cell RNA-sequencing and functional heterogeneity. *Cell Research*, *26*(1), 83–102. https://doi.org/10.1038/cr.2015.149

Li, H., Handsaker, B., Wysoker, A., Fennell, T., Ruan, J., Homer, N., Marth, G., Abecasis, G., & Durbin, R. (2009). The Sequence Alignment/Map format and SAMtools. *Bioinformatics*, *25*(16), 2078–2079. https://doi.org/10.1093/bioinformatics/btp352

Li, L., Rutlin, M., Abraira, V. E., Cassidy, C., Kus, L., Gong, S., Jankowski, M. P., Luo, W., Heintz, N., Koerber, H. R., Woodbury, C. J., & Ginty, D. D. (2011). The functional organization of cutaneous low-threshold mechanosensory neurons. *Cell*, *147*(7), 1615–1627. https://doi.org/10.1016/j.cell.2011.11.027

Li, X., Gibson, G., Kim, J.-S., Kroin, J., Xu, S., van Wijnen, A. J., & Im, H.-J. (2011). MicroRNA-146a is linked to pain-related pathophysiology of osteoarthritis. *Gene*, *480*(1), 34–41. https://doi.org/10.1016/j.gene.2011.03.003

Li, Z., Mao, Y., Liang, L., Wu, S., Yuan, J., Mo, K., Cai, W., Mao, Q., Cao, J., Bekker, A., Zhang, W., & Tao, Y.-X. (2017). The transcription factor C/EBPβ in the dorsal root ganglion contributes to peripheral nerve trauma–induced nociceptive hypersensitivity. *Science Signaling*, *10*(487), eaam5345. https://doi.org/10.1126/scisignal.aam5345

Liang, Z., Hore, Z., Harley, P., Uchenna Stanley, F., Michrowska, A., Dahiya, M., La Russa, F., Jager, S. E., Villa-Hernandez, S., & Denk, F. (2020). A transcriptional toolbox for exploring peripheral neuroimmune interactions. *PAIN*, *161*(9), 2089–2106. https://doi.org/10.1097/j.pain.0000000000001914

Lin, Y.-T., & Chen, J.-C. (2018). Dorsal Root Ganglia Isolation and Primary Culture to Study Neurotransmitter Release. *Journal of Visualized Experiments : JoVE*, *140*, 57569. https://doi.org/10.3791/57569

Liou, J.-T., Liu, F.-C., Hsin, S.-T., Yang, C.-Y., & Lui, P.-W. (2007). Inhibition of the Cyclic Adenosine Monophosphate Pathway Attenuates Neuropathic Pain and Reduces Phosphorylation of Cyclic Adenosine Monophosphate Response Element-Binding in the Spinal Cord After Partial Sciatic Nerve Ligation in Rats. *Anesthesia & Analgesia*, *105*(6), 1830–1837. https://doi.org/10.1213/01.ane.0000287652.42309.5c

Lippoldt, E. K., Elmes, R. R., McCoy, D. D., Knowlton, W. M., & McKemy, D. D. (2013). Artemin, a Glial Cell Line-Derived Neurotrophic Factor Family Member, Induces TRPM8-Dependent Cold Pain. *The Journal of Neuroscience*, *33*(30), 12543–12552. https://doi.org/10.1523/JNEUROSCI.5765-12.2013

Liu, Y., Mikrani, R., He, Y., Faran Ashraf Baig, M. M., Abbas, M., Naveed, M., Tang, M., Zhang, Q., Li, C., & Zhou, X. (2020). TRPM8 channels: A review of distribution and clinical role. *European Journal of Pharmacology*, *882*, 173312. https://doi.org/10.1016/j.ejphar.2020.173312

Liu-Yesucevitz, L., Bassell, G. J., Gitler, A. D., Hart, A. C., Klann, E., Richter, J. D., Warren, S. T., & Wolozin, B. (2011). Local RNA Translation at the Synapse and in Disease. *The Journal of Neuroscience*, *31*(45), 16086–16093. https://doi.org/10.1523/JNEUROSCI.4105-11.2011

Livak, K. J., & Schmittgen, T. D. (2001). Analysis of Relative Gene Expression Data Using Real-Time Quantitative PCR and the 2−ΔΔCT Method. *Methods*, *25*(4), 402–408. https://doi.org/10.1006/meth.2001.1262

Lock, J. T., Parker, I., & Smith, I. F. (2015). A comparison of fluorescent Ca2+ indicators for imaging local Ca2+ signals in cultured cells. *Cell Calcium*, *58*(6), 638–648. https://doi.org/10.1016/j.ceca.2015.10.003

Lopes, D. M., Denk, F., & McMahon, S. B. (2017). The Molecular Fingerprint of Dorsal Root and Trigeminal Ganglion Neurons. *Frontiers in Molecular Neuroscience*, *10*, 304. https://doi.org/10.3389/fnmol.2017.00304

LoPresti, P., Poluha, W., Poluha, D. K., Drinkwater, E., & Ross, A. H. (1992). Neuronal differentiation triggered by blocking cell proliferation. *Cell Growth & Differentiation: The Molecular Biology Journal of the American Association for Cancer Research*, *3*(9), 627–635.

Love, M. I., Huber, W., & Anders, S. (2014). Moderated estimation of fold change and dispersion for RNA-seq data with DESeq2. *Genome Biology*, *15*(12), 550. https://doi.org/10.1186/s13059-014-0550-8

Lu, S.-G., & Gold, M. S. (2008). Inflammation-Induced Increase in Evoked Calcium Transients in Subpopulations of Rat DRG Neurons. *Neuroscience*, *153*(1), 279–288. https://doi.org/10.1016/j.neuroscience.2008.02.006

Lucci, C., Mesquita-Ribeiro, R., Rathbone, A., & Dajas-Bailador, F. (2020). Spatiotemporal regulation of GSK3β levels by miRNA-26a controls axon development in cortical neurons. *Development (Cambridge, England)*, *147*(3), dev180232. https://doi.org/10.1242/dev.180232

Ma, J., Pan, P., Anyika, M., Blagg, B. S. J., & Dobrowsky, R. T. (2015). Modulating Molecular Chaperones Improves Mitochondrial Bioenergetics and Decreases the Inflammatory Transcriptome in Diabetic Sensory Neurons. *ACS Chemical Neuroscience*, *6*(9), 1637–1648. https://doi.org/10.1021/acschemneuro.5b00165

Ma, J., Patil, V., Pandit, A., Quinlan, L. R., Finn, D. P., Grad, S., Alini, M., & Peroglio, M. (2021). In Vitro Model to Investigate Communication between Dorsal Root Ganglion and Spinal Cord Glia. *International Journal of Molecular Sciences*, *22*(18), 9725. https://doi.org/10.3390/ijms22189725

Ma, R. S. Y., Kayani, K., Whyte-Oshodi, D., Whyte-Oshodi, A., Nachiappan, N., Gnanarajah, S., & Mohammed, R. (2019). Voltage gated sodium channels as therapeutic targets for chronic pain. *Journal of Pain Research*, *12*, 2709–2722. https://doi.org/10.2147/JPR.S207610

Ma, W. (2010). Chronic prostaglandin E2 treatment induces the synthesis of the pain-related peptide substance P and calcitonin gene-related peptide in cultured sensory ganglion explants. *Journal of Neurochemistry*, *115*(2), 363–372. https://doi.org/10.1111/j.1471-4159.2010.06927.x

Ma, W., & Eisenach, J. C. (2003). Cyclooxygenase 2 in infiltrating inflammatory cells in injured nerve is universally up-regulated following various types of peripheral nerve injury. *Neuroscience*, *121*(3), 691–704. https://doi.org/10.1016/S0306-4522(03)00495-0

Ma, W., & St-Jacques, B. (2018). Signalling transduction events involved in agonist-induced PGE2/EP4 receptor externalization in cultured rat dorsal root ganglion neurons. *European Journal of Pain*, *22*(5), 845–861. https://doi.org/10.1002/ejp.1172

Maciel, R., Bis, D. M., Rebelo, A. P., Saghira, C., Züchner, S., & Saporta, M. A. (2018). The human motor neuron axonal transcriptome is enriched for transcripts related to mitochondrial function and microtubule-based axonal transport. *Experimental Neurology*, *307*, 155–163. https://doi.org/10.1016/j.expneurol.2018.06.008

Maday, S., Twelvetrees, A. E., Moughamian, A. J., & Holzbaur, E. L. F. (2014). AXONAL TRANSPORT: CARGO-SPECIFIC MECHANISMS OF MOTILITY AND REGULATION. *Neuron*, *84*(2), 292–309. https://doi.org/10.1016/j.neuron.2014.10.019

Malone, T. J., & Kaczmarek, L. K. (2022). The role of altered translation in intellectual disability and epilepsy. *Progress in Neurobiology*, *213*, 102267. https://doi.org/10.1016/j.pneurobio.2022.102267

Manteniotis, S., Lehmann, R., Flegel, C., Vogel, F., Hofreuter, A., Schreiner, B. S. P., Altmüller, J., Becker, C., Schöbel, N., Hatt, H., & Gisselmann, G. (2013). Comprehensive RNA-Seq Expression Analysis of Sensory Ganglia with a Focus on Ion Channels and GPCRs in Trigeminal Ganglia. *PLoS ONE*, *8*(11), e79523. https://doi.org/10.1371/journal.pone.0079523

Markus, A., Patel, T. D., & Snider, W. D. (2002). Neurotrophic factors and axonal growth. *Current Opinion in Neurobiology*, *12*(5), 523–531. https://doi.org/10.1016/S0959-4388(02)00372-0

Marshall, J. S., Gomi, K., Blennerhassett, M. G., & Bienenstock, J. (1999). Nerve Growth Factor Modifies the Expression of Inflammatory Cytokines by Mast Cells Via a Prostanoid-Dependent Mechanism. *The Journal of Immunology*, *162*(7), 4271–4276.

Martin, K. C., & Ephrussi, A. (2009). mRNA Localization: Gene Expression in the Spatial Dimension. *Cell*, *136*(4), 719. https://doi.org/10.1016/j.cell.2009.01.044

Masuda, K., Ripley, B., Nishimura, R., Mino, T., Takeuchi, O., Shioi, G., Kiyonari, H., & Kishimoto, T. (2013). Arid5a controls IL-6 mRNA stability, which contributes to elevation of IL-6 level in vivo. *Proceedings of the National Academy of Sciences of the United States of America*, *110*(23), 9409–9414. https://doi.org/10.1073/pnas.1307419110

Mayr, C. (2016). Evolution and Biological Roles of Alternative 3'UTRs. *Trends in Cell Biology*, *26*(3), 227–237. https://doi.org/10.1016/j.tcb.2015.10.012

Mecklenburg, J., Zou, Y., Wangzhou, A., Garcia, D., Lai, Z., Tumanov, A. V., Dussor, G., Price, T. J., & Akopian, A. N. (2020). Transcriptomic sex differences in sensory neuronal populations of mice. *Scientific Reports*, *10*(1), Article 1. https://doi.org/10.1038/s41598-020-72285-z

Melemedjian, O. K., Asiedu, M. N., Tillu, D. V., Peebles, K. A., Yan, J., Ertz, N., Dussor, G. O., & Price, T. J. (2010). IL-6- and NGF-induced rapid control of protein synthesis and nociceptive plasticity via convergent signaling to the eIF4F complex. *The Journal of Neuroscience: The Official Journal of the Society for Neuroscience*, *30*(45), 15113–15123. https://doi.org/10.1523/JNEUROSCI.3947-10.2010

Melemedjian, O. K., Tillu, D. V., Moy, J. K., Asiedu, M. N., Mandell, E. K., Ghosh, S., Dussor, G., & Price, T. J. (2014). Local translation and retrograde axonal transport of CREB regulates IL-6-induced nociceptive plasticity. *Molecular Pain*, *10*, 45. https://doi.org/10.1186/1744-8069-10-45

Meltzer, S., Santiago, C., Sharma, N., & Ginty, D. D. (2021). The cellular and molecular basis of somatosensory neuron development. *Neuron*, *109*(23), 3736–3757. https://doi.org/10.1016/j.neuron.2021.09.004

Middleton, S. A., Eberwine, J., & Kim, J. (2019). Comprehensive catalog of dendritically localized mRNA isoforms from sub-cellular sequencing of single mouse neurons. *BMC Biology*, *17*, 5. https://doi.org/10.1186/s12915-019-0630-z

Miller, R. E., & Malfait, A.-M. (2017). Osteoarthritis pain: What are we learning from animal models? *Best Practice & Research Clinical Rheumatology*, *31*(5), 676–687. https://doi.org/10.1016/j.berh.2018.03.003

Minett, M. S., Pereira, V., Sikandar, S., Matsuyama, A., Lolignier, S., Kanellopoulos, A. H., Mancini, F., Iannetti, G. D., Bogdanov, Y. D., Santana-Varela, S., Millet, Q., Baskozos, G., MacAllister, R., Cox, J. J., Zhao, J., & Wood, J. N. (2015). Endogenous opioids contribute to insensitivity to pain in humans and mice lacking sodium channel Nav1.7. *Nature Communications*, *6*, 8967. https://doi.org/10.1038/ncomms9967

Minis, A., Dahary, D., Manor, O., Leshkowitz, D., Pilpel, Y., & Yaron, A. (2014). Subcellular transcriptomics—Dissection of the mRNA composition in the axonal compartment of sensory neurons. *Developmental Neurobiology*, *74*(3), 365–381. https://doi.org/10.1002/dneu.22140

Moine, H., & Vitale, N. (2019). Of local translation control and lipid signaling in neurons. *Advances in Biological Regulation*, *71*, 194–205. https://doi.org/10.1016/j.jbior.2018.09.005

Molliver, D. C., Cook, S. P., Carlsten, J. A., Wright, D. E., & McCleskey, E. W. (2002). ATP and UTP excite sensory neurons and induce CREB phosphorylation through the metabotropic receptor, P2Y2. *European Journal of Neuroscience*, *16*(10), 1850–1860. https://doi.org/10.1046/j.1460-9568.2002.02253.x

Momin, A., Cadiou, H., Mason, A., & McNaughton, P. A. (2008). Role of the hyperpolarization-activated current Ih in somatosensory neurons. *The Journal of Physiology*, *586*(Pt 24), 5911–5929. https://doi.org/10.1113/jphysiol.2008.163154

Momin, A., & McNaughton, P. A. (2009). Regulation of firing frequency in nociceptive neurons by pro-inflammatory mediators. *Experimental Brain Research*, *196*(1), 45–52. https://doi.org/10.1007/s00221-009-1744-2

Moy, J. K., Khoutorsky, A., Asiedu, M. N., Black, B. J., Kuhn, J. L., Barragán-Iglesias, P., Megat, S., Burton, M. D., Burgos-Vega, C. C., Melemedjian, O. K., Boitano, S., Vagner, J., Gkogkas, C. G., Pancrazio, J. J., Mogil, J. S., Dussor, G., Sonenberg, N., & Price, T. J. (2017). The MNK–eIF4E Signaling Axis Contributes to Injury-Induced Nociceptive Plasticity and the Development of Chronic Pain. *The Journal of Neuroscience*, *37*(31), 7481–7499. https://doi.org/10.1523/JNEUROSCI.0220-17.2017

Muley, M. M., Krustev, E., & McDougall, J. J. (2015). Preclinical Assessment of Inflammatory Pain. *CNS Neuroscience & Therapeutics*, *22*(2), 88–101. https://doi.org/10.1111/cns.12486

Mundy, W. R., Radio, N. M., & Freudenrich, T. M. (2010). Neuronal models for evaluation of proliferation in vitro using high content screening. *Toxicology*, *270*(2), 121–130. https://doi.org/10.1016/j.tox.2010.02.004

Nandagopal, N., & Roux, P. P. (2015). Regulation of global and specific mRNA translation by the mTOR signaling pathway. *Translation*, *3*(1), e983402. https://doi.org/10.4161/21690731.2014.983402

Nguyen, M. Q., von Buchholtz, L. J., Reker, A. N., Ryba, N. J., & Davidson, S. (2021). Single-nucleus transcriptomic analysis of human dorsal root ganglion neurons. *ELife*, *10*, e71752. https://doi.org/10.7554/eLife.71752

Nijssen, J., Aguila, J., Hoogstraaten, R., Kee, N., & Hedlund, E. (2018). Axon-Seq Decodes the Motor Axon Transcriptome and Its Modulation in Response to

ALS. *Stem Cell Reports*, *11*(6), 1565–1578. https://doi.org/10.1016/j.stemcr.2018.11.005

Nishimura, R., Hata, K., Takahata, Y., Murakami, T., Nakamura, E., Ohkawa, M., & Ruengsinpinya, L. (2020). Role of Signal Transduction Pathways and Transcription Factors in Cartilage and Joint Diseases. *International Journal of Molecular Sciences*, *21*(4), 1340. https://doi.org/10.3390/ijms21041340

North, R. Y., Li, Y., Ray, P., Rhines, L. D., Tatsui, C. E., Rao, G., Johansson, C. A., Zhang, H., Kim, Y. H., Zhang, B., Dussor, G., Kim, T. H., Price, T. J., & Dougherty, P. M. (2019). Electrophysiological and transcriptomic correlates of neuropathic pain in human dorsal root ganglion neurons. *Brain*, *142*(5), 1215–1226. https://doi.org/10.1093/brain/awz063

Nyati, K. K., & Kishimoto, T. (2022). Recent Advances in the Role of Arid5a in Immune Diseases and Cancer. *Frontiers in Immunology*, *12*, 827611. https://doi.org/10.3389/fimmu.2021.827611

Nyati, K. K., Masuda, K., Zaman, M. M.-U., Dubey, P. K., Millrine, D., Chalise, J. P., Higa, M., Li, S., Standley, D. M., Saito, K., Hanieh, H., & Kishimoto, T. (2017). TLR4-induced NF-κB and MAPK signaling regulate the IL-6 mRNA stabilizing protein Arid5a. *Nucleic Acids Research*, *45*(5), 2687–2703. https://doi.org/10.1093/nar/gkx064

Nyati, K. K., Zaman, M. M.-U., Sharma, P., & Kishimoto, T. (2020). Arid5a, an RNA-Binding Protein in Immune Regulation: RNA Stability, Inflammation, and Autoimmunity. *Trends in Immunology*, *41*(3), 255–268. https://doi.org/10.1016/j.it.2020.01.004

Obara, I., Géranton, S. M., & Hunt, S. P. (2012). Axonal protein synthesis: A potential target for pain relief? *Current Opinion in Pharmacology*, *12*(1), 42–48. https://doi.org/10.1016/j.coph.2011.10.005

O'Brien, P. D., Sakowski, S. A., & Feldman, E. L. (2014). Mouse Models of Diabetic Neuropathy. *ILAR Journal*, *54*(3), 259–272. https://doi.org/10.1093/ilar/ilt052

Oshlack, A., & Wakefield, M. J. (2009). Transcript length bias in RNA-seq data confounds systems biology. *Biology Direct*, *4*(1), 14. https://doi.org/10.1186/1745-6150-4-14

Pacheco, A., Merianda, T., Twiss, J. L., & Gallo, G. (2020). Mechanism and role of the intra-axonal Calreticulin translation in response to axonal injury. *Experimental Neurology*, *323*, 113072. https://doi.org/10.1016/j.expneurol.2019.113072

Paredes, R. M., Etzler, J. C., Watts, L. T., & Lechleiter, J. D. (2008). Chemical Calcium Indicators. *Methods (San Diego, Calif.)*, *46*(3), 143–151. https://doi.org/10.1016/j.ymeth.2008.09.025

Parpaite, T., Brosse, L., Séjourné, N., Laur, A., Mechioukhi, Y., Delmas, P., & Coste, B. (2021). Patch-seq of mouse DRG neurons reveals candidate genes for

specific mechanosensory functions. *Cell Reports*, *37*(5), 109914. https://doi.org/10.1016/j.celrep.2021.109914

Passmore, L. A., & Coller, J. (2022). Roles of mRNA poly(A) tails in regulation of eukaryotic gene expression. *Nature Reviews Molecular Cell Biology*, *23*(2), Article 2. https://doi.org/10.1038/s41580-021-00417-y

Patapoutian, A., Tate, S., & Woolf, C. J. (2009). Transient receptor potential channels: Targeting pain at the source. *Nature Reviews. Drug Discovery*, *8*(1), 55–68. https://doi.org/10.1038/nrd2757

Peeraer, E., Van Lutsenborg, A., Verheyen, A., De Jongh, R., Nuydens, R., & Meert, T. F. (2011). Pharmacological evaluation of rat dorsal root ganglion neurons as an in vitro model for diabetic neuropathy. *Journal of Pain Research*, *4*, 55–65. https://doi.org/10.2147/JPR.S15452

Perry, R. B.-T., Doron-Mandel, E., Iavnilovitch, E., Rishal, I., Dagan, S. Y., Tsoory, M., Coppola, G., McDonald, M. K., Gomes, C., Geschwind, D. H., Twiss, J. L., Yaron, A., & Fainzilber, M. (2012). Subcellular Knockout of Importin β1 Perturbs Axonal Retrograde Signaling. *Neuron*, *75*(2), 294–305. https://doi.org/10.1016/j.neuron.2012.05.033

Persson, A.-K., Kim, I., Zhao, P., Estacion, M., Black, J. A., & Waxman, S. G. (2013). Sodium Channels Contribute to Degeneration of Dorsal Root Ganglion Neurites Induced by Mitochondrial Dysfunction in an In Vitro Model of Axonal Injury. *The Journal of Neuroscience*, *33*(49), 19250–19261. https://doi.org/10.1523/JNEUROSCI.2148-13.2013

Pitale, P. M., Gorbatyuk, O., & Gorbatyuk, M. (2017). Neurodegeneration: Keeping ATF4 on a Tight Leash. *Frontiers in Cellular Neuroscience*, *11*, 410. https://doi.org/10.3389/fncel.2017.00410

Poon, M. M., Choi, S.-H., Jamieson, C. A. M., Geschwind, D. H., & Martin, K. C. (2006). Identification of Process-Localized mRNAs from Cultured Rodent Hippocampal Neurons. *The Journal of Neuroscience*, *26*(51), 13390–13399. https://doi.org/10.1523/JNEUROSCI.3432-06.2006

Price, T. J., & Géranton, S. M. (2009). Translating nociceptor sensitivity: The role of axonal protein synthesis in nociceptor physiology. *The European Journal of Neuroscience*, *29*(12), 2253–2263. https://doi.org/10.1111/j.1460-9568.2009.06786.x

Price, T. J., & Inyang, K. E. (2015). Commonalities Between Pain and Memory Mechanisms and Their Meaning for Understanding Chronic Pain. In *Progress in Molecular Biology and Translational Science* (Vol. 131, pp. 409–434). Elsevier. https://doi.org/10.1016/bs.pmbts.2014.11.010

Price, T. J., Rashid, M. H., Millecamps, M., Sanoja, R., Entrena, J. M., & Cervero, F. (2007). Decreased nociceptive sensitization in mice lacking the fragile X mental retardation protein: Role of mGluR1/5 and mTOR. *The Journal of*

Neuroscience: The Official Journal of the Society for Neuroscience, *27*(51), 13958–13967. https://doi.org/10.1523/JNEUROSCI.4383-07.2007

Pulido-Salgado, M., Vidal-Taboada, J. M., & Saura, J. (2015). C/EBPβ and C/EBPδ transcription factors: Basic biology and roles in the CNS. *Progress in Neurobiology*, *132*, 1–33. https://doi.org/10.1016/j.pneurobio.2015.06.003

Qi, J., Buzas, K., Fan, H., Cohen, J. I., Wang, K., Mont, E., Klinman, D., Oppenheim, J. J., & Howard, O. M. Z. (2011). Painful Pathways Induced by Toll-like Receptor Stimulation of Dorsal Root Ganglion Neurons. *Journal of Immunology (Baltimore, Md. : 1950)*, *186*(11), 6417–6426. https://doi.org/10.4049/jimmunol.1001241

Radhi, M., Ashraf, S., Lawrence, S., Tranholm, A. A., Wellham, P. A. D., Hafeez, A., Khamis, A. S., Thomas, R., McWilliams, D., & de Moor, C. H. (2021). A Systematic Review of the Biological Effects of Cordycepin. *Molecules*, *26*(19), 5886. https://doi.org/10.3390/molecules26195886

Radulovic, J., & Tronson, N. C. (2008). Protein synthesis inhibitors, gene superinduction and memory: Too little or too much protein? *Neurobiology of Learning and Memory*, *89*(3), 212–218. https://doi.org/10.1016/j.nlm.2007.08.008

Raghavan, M., Fee, D., & Barkhaus, P. E. (2019). Chapter 1—Generation and propagation of the action potential. In K. H. Levin & P. Chauvel (Eds.), *Handbook of Clinical Neurology* (Vol. 160, pp. 3–22). Elsevier. https://doi.org/10.1016/B978-0-444-64032-1.00001-1

Raghupathy, N., Choi, K., Vincent, M. J., Beane, G. L., Sheppard, K. S., Munger, S. C., Korstanje, R., Pardo-Manual de Villena, F., & Churchill, G. A. (2018). Hierarchical analysis of RNA-seq reads improves the accuracy of allele-specific expression. *Bioinformatics*, *34*(13), 2177–2184. https://doi.org/10.1093/bioinformatics/bty078

Rana, T., Shinde, V. M., Starr, C. R., Kruglov, A. A., Boitet, E. R., Kotla, P., Zolotukhin, S., Gross, A. K., & Gorbatyuk, M. S. (2014). An activated unfolded protein response promotes retinal degeneration and triggers an inflammatory response in the mouse retina. *Cell Death & Disease*, *5*(12), e1578. https://doi.org/10.1038/cddis.2014.539

Rangaraju, V., tom Dieck, S., & Schuman, E. M. (2017). Local translation in neuronal compartments: How local is local? *EMBO Reports*, *18*(5), 693–711. https://doi.org/10.15252/embr.201744045

Rao, D. D., Vorhies, J. S., Senzer, N., & Nemunaitis, J. (2009). siRNA vs. shRNA: Similarities and differences. *Advanced Drug Delivery Reviews*, *61*(9), 746–759. https://doi.org/10.1016/j.addr.2009.04.004

Ray, P., Shiers, S., Ferreira, D. T., Sankaranarayanan, I., Uhelski, M. L., Li, Y., North, R. Y., Tatsui, C. E., Dussor, G., Burton, M. D., Dougherty, P. M., & Price, T. J. (2021). *RNA Profiling of Neuropathic Pain-Associated Human DRGs Reveal*

Sex-differences in Neuro-immune Interactions Promoting Pain (p. 2021.11.27.470190). https://doi.org/10.1101/2021.11.27.470190

Ray, P., Torck, A., Quigley, L., Wangzhou, A., Neiman, M., Rao, C., Lam, T., Kim, J.-Y., Kim, T. H., Zhang, M. Q., Dussor, G., & Price, T. J. (2018). Comparative transcriptome profiling of the human and mouse dorsal root ganglia: An RNA-seq-based resource for pain and sensory neuroscience research. *Pain*, *159*(7), 1325–1345. https://doi.org/10.1097/j.pain.0000000000001217

Ren, M.-Y., & Sui, S.-J. (2012). The role of TWEAK/Fn14 in cardiac remodeling. *Molecular Biology Reports*, *39*(11), 9971–9977. https://doi.org/10.1007/s11033-012-1867-6

Renthal, W., Tochitsky, I., Yang, L., Cheng, Y.-C., Li, E., Kawaguchi, R., Geschwind, D. H., & Woolf, C. J. (2020). Transcriptional reprogramming of distinct peripheral sensory neuron subtypes after axonal injury. *Neuron*, *108*(1), 128-144.e9. https://doi.org/10.1016/j.neuron.2020.07.026

Rexed, B. (1952). The cytoarchitectonic organization of the spinal cord in the cat. *The Journal of Comparative Neurology*, *96*(3), 415–495. https://doi.org/10.1002/cne.900960303

Reynders, A., Mantilleri, A., Malapert, P., Rialle, S., Nidelet, S., Laffray, S., Beurrier, C., Bourinet, E., & Moqrich, A. (2015). Transcriptional Profiling of Cutaneous MRGPRD Free Nerve Endings and C-LTMRs. *Cell Reports*, *10*(6), 1007–1019. https://doi.org/10.1016/j.celrep.2015.01.022

Rienecker, K. D. A., Poston, R. G., & Saha, R. N. (2020). Merits and Limitations of Studying Neuronal Depolarization-Dependent Processes Using Elevated External Potassium. *ASN NEURO*, *12*, 1759091420974807. https://doi.org/10.1177/1759091420974807

Rotem, N., Magen, I., Ionescu, A., Gershoni-Emek, N., Altman, T., Costa, C. J., Gradus, T., Pasmanik-Chor, M., Willis, D. E., Ben-Dov, I. Z., Hornstein, E., & Perlson, E. (2017). ALS Along the Axons – Expression of Coding and Noncoding RNA Differs in Axons of ALS models. *Scientific Reports*, *7*, 44500. https://doi.org/10.1038/srep44500

Roux, P. P., Shahbazian, D., Vu, H., Holz, M. K., Cohen, M. S., Taunton, J., Sonenberg, N., & Blenis, J. (2007). RAS/ERK Signaling Promotes Site-specific Ribosomal Protein S6 Phosphorylation via RSK and Stimulates Cap-dependent Translation. *The Journal of Biological Chemistry*, *282*(19), 14056–14064. https://doi.org/10.1074/jbc.M700906200

Rush, A. M., & Waxman, S. G. (2004). PGE2 increases the tetrodotoxin-resistant Nav1.9 sodium current in mouse DRG neurons via G-proteins. *Brain Research*, *1023*(2), 264–271. https://doi.org/10.1016/j.brainres.2004.07.042

Saal, L., Briese, M., Kneitz, S., Glinka, M., & Sendtner, M. (2014). Subcellular transcriptome alterations in a cell culture model of spinal muscular atrophy point to widespread defects in axonal growth and presynaptic

differentiation. *RNA*, *20*(11), 1789–1802. https://doi.org/10.1261/rna.047373.114

Sahoo, P. K., Smith, D. S., Perrone-Bizzozero, N., & Twiss, J. L. (2018). Axonal mRNA transport and translation at a glance. *Journal of Cell Science*, *131*(8). https://doi.org/10.1242/jcs.196808

Sahraeian, S. M. E., Mohiyuddin, M., Sebra, R., Tilgner, H., Afshar, P. T., Au, K. F., Bani Asadi, N., Gerstein, M. B., Wong, W. H., Snyder, M. P., Schadt, E., & Lam, H. Y. K. (2017). Gaining comprehensive biological insight into the transcriptome by performing a broad-spectrum RNA-seq analysis. *Nature Communications*, *8*, 59. https://doi.org/10.1038/s41467-017-00050-4

Sapio, M. R., Goswami, S. C., Gross, J. R., Mannes, A. J., & Iadarola, M. J. (2016). Transcriptomic Analyses of Genes and Tissues in Inherited Sensory Neuropathies. *Experimental Neurology*, *283*(Pt A), 375–395. https://doi.org/10.1016/j.expneurol.2016.06.023

Sasaki, Y., Gross, C., Xing, L., Goshima, Y., & Bassell, G. J. (2014). Identification of Axon-Enriched MicroRNAs Localized to Growth Cones of Cortical Neurons. *Developmental Neurobiology*, *74*(3), 397–406. https://doi.org/10.1002/dneu.22113

Sasaki, Y., Vohra, B. P. S., Lund, F. E., & Milbrandt, J. (2009). Nicotinamide Mononucleotide Adenylyl Transferase-Mediated Axonal Protection Requires Enzymatic Activity But Not Increased Levels of Neuronal Nicotinamide Adenine Dinucleotide. *The Journal of Neuroscience*, *29*(17), 5525–5535. https://doi.org/10.1523/JNEUROSCI.5469-08.2009

Schaarschmidt, S., Fischer, A., Zuther, E., & Hincha, D. K. (2020). Evaluation of Seven Different RNA-Seq Alignment Tools Based on Experimental Data from the Model Plant Arabidopsis thaliana. *International Journal of Molecular Sciences*, *21*(5), 1720. https://doi.org/10.3390/ijms21051720

Schena, M., Shalon, D., Davis, R. W., & Brown, P. O. (1995). Quantitative Monitoring of Gene Expression Patterns with a Complementary DNA Microarray. *Science*, *270*(5235), 467–470. https://doi.org/10.1126/science.270.5235.467

Schindelin, J., Arganda-Carreras, I., Frise, E., Kaynig, V., Longair, M., Pietzsch, T., Preibisch, S., Rueden, C., Saalfeld, S., Schmid, B., Tinevez, J.-Y., White, D. J., Hartenstein, V., Eliceiri, K., Tomancak, P., & Cardona, A. (2012). Fiji—An Open Source platform for biological image analysis. *Nature Methods*, *9*(7), 10.1038/nmeth.2019. https://doi.org/10.1038/nmeth.2019

Schmelz, M., Mantyh, P., Malfait, A.-M., Farrar, J., Yaksh, T., Tive, L., & Viktrup, L. (2019). Nerve growth factor antibody for the treatment of osteoarthritis pain and chronic low-back pain: Mechanism of action in the context of efficacy and safety. *Pain*, *160*(10), 2210–2220. https://doi.org/10.1097/j.pain.0000000000001625

Schneider, C. A., Rasband, W. S., & Eliceiri, K. W. (2012). NIH Image to ImageJ: 25 years of Image Analysis. *Nature Methods*, *9*(7), 671–675.

Scholz, J., Finnerup, N. B., Attal, N., Aziz, Q., Baron, R., Bennett, M. I., Benoliel, R., Cohen, M., Cruccu, G., Davis, K. D., Evers, S., First, M., Giamberardino, M. A., Hansson, P., Kaasa, S., Korwisi, B., Kosek, E., Lavand'homme, P., Nicholas, M., … Treede, R.-D. (2019). The IASP classification of chronic pain for ICD-11: Chronic neuropathic pain. *Pain*, *160*(1), 53–59. https://doi.org/10.1097/j.pain.0000000000001365

Scholz, J., & Woolf, C. J. (2007). The neuropathic pain triad: Neurons, immune cells and glia. *Nature Neuroscience*, *10*(11), Article 11. https://doi.org/10.1038/nn1992

Schou, W. S., Ashina, S., Amin, F. M., Goadsby, P. J., & Ashina, M. (2017). Calcitonin gene-related peptide and pain: A systematic review. *The Journal of Headache and Pain*, *18*(1), 34. https://doi.org/10.1186/s10194-017-0741-2

Schroeder, A., Mueller, O., Stocker, S., Salowsky, R., Leiber, M., Gassmann, M., Lightfoot, S., Menzel, W., Granzow, M., & Ragg, T. (2006). The RIN: An RNA integrity number for assigning integrity values to RNA measurements. *BMC Molecular Biology*, *7*(1), 3. https://doi.org/10.1186/1471-2199-7-3

Scott, B. S. (1977). Adult mouse dorsal root ganglia neurons in cell culture. *Journal of Neurobiology*, *8*(5), 417–427. https://doi.org/10.1002/neu.480080503

Segond von Banchet, G., Kiehl, M., & Schaible, H.-G. (2005). Acute and long-term effects of IL-6 on cultured dorsal root ganglion neurones from adult rat. *Journal of Neurochemistry*, *94*(1), 238–248. https://doi.org/10.1111/j.1471-4159.2005.03185.x

Segond von Banchet, G., Pastor, A., Biskup, C., Schlegel, C., Benndorf, K., & Schaible, H.-G. (2002). Localization of functional calcitonin gene-related peptide binding sites in a subpopulation of cultured dorsal root ganglion neurons. *Neuroscience*, *110*(1), 131–145. https://doi.org/10.1016/S0306-4522(01)00547-4

Sharma, N., Flaherty, K., Lezgiyeva, K., Wagner, D. E., Klein, A. M., & Ginty, D. D. (2020). The emergence of transcriptional identity in somatosensory neurons. *Nature*, *577*(7790), 392–398. https://doi.org/10.1038/s41586-019-1900-1

Sharma, V., Sood, R., Khlaifia, A., Eslamizade, M. J., Hung, T.-Y., Lou, D., Asgarihafshejani, A., Lalzar, M., Kiniry, S. J., Stokes, M. P., Cohen, N., Nelson, A. J., Abell, K., Possemato, A. P., Gal-Ben-Ari, S., Truong, V. T., Wang, P., Yiannakas, A., Saffarzadeh, F., … Sonenberg, N. (2020). EIF2α controls memory consolidation via excitatory and somatostatin neurons. *Nature*, *586*(7829), 412–416. https://doi.org/10.1038/s41586-020-2805-8

Shiers, S., Klein, R. M., & Price, T. J. (2020). Quantitative differences in neuronal subpopulations between mouse and human dorsal root ganglia

demonstrated with RNAscope in situ hybridization. *Pain*, *161*(10), 2410–2424. https://doi.org/10.1097/j.pain.0000000000001973

Shigeoka, T., Jung, H., Jung, J., Turner-Bridger, B., Ohk, J., Lin, J. Q., Amieux, P. S., & Holt, C. E. (2016). Dynamic Axonal Translation in Developing and Mature Visual Circuits. *Cell*, *166*(1), 181–192. https://doi.org/10.1016/j.cell.2016.05.029

Shigeoka, T., Jung, J., Holt, C. E., & Jung, H. (2018). Axon-TRAP-RiboTag: Affinity Purification of Translated mRNAs from Neuronal Axons in Mouse In Vivo. In I. Gaspar (Ed.), *RNA Detection: Methods and Protocols* (pp. 85–94). Springer. https://doi.org/10.1007/978-1-4939-7213-5_5

Shinotsuka, N., & Denk, F. (2022). Fibroblasts: The neglected cell type in peripheral sensitisation and chronic pain? A review based on a systematic search of the literature. *BMJ Open Science*, *6*(1), e100235. https://doi.org/10.1136/bmjos-2021-100235

Shrestha, N., Bahnan, W., Wiley, D. J., Barber, G., Fields, K. A., & Schesser, K. (2012). Eukaryotic Initiation Factor 2 (eIF2) Signaling Regulates Proinflammatory Cytokine Expression and Bacterial Invasion. *The Journal of Biological Chemistry*, *287*(34), 28738–28744. https://doi.org/10.1074/jbc.M112.375915

Sinnamon, J. R., & Czaplinski, K. (2011). mRNA trafficking and local translation: The Yin and Yang of regulating mRNA localization in neurons. *Acta Biochimica et Biophysica Sinica*, *43*(9), 663–670. https://doi.org/10.1093/abbs/gmr058

Skyba, D. A., Radhakrishnan, R., Bement, M. K. H., & Sluka, K. A. (2004). The cAMP pathway and pain: Potential targets for drug development. *Drug Discovery Today: Disease Models*, *1*(2), 115–119. https://doi.org/10.1016/j.ddmod.2004.07.003

Sleigh, J. N., Weir, G. A., & Schiavo, G. (2016). A simple, step-by-step dissection protocol for the rapid isolation of mouse dorsal root ganglia. *BMC Research Notes*, *9*, 82. https://doi.org/10.1186/s13104-016-1915-8

Smith-Anttila, C. J. A., Mason, E. A., Wells, C. A., Aronow, B. J., Osborne, P. B., & Keast, J. R. (2020). Identification of a Sacral, Visceral Sensory Transcriptome in Embryonic and Adult Mice. *ENeuro*, *7*(1), ENEURO.0397-19.2019. https://doi.org/10.1523/ENEURO.0397-19.2019

Southall, M. D., & Vasko, M. R. (2001). Prostaglandin Receptor Subtypes, EP3C and EP4, Mediate the Prostaglandin E2-induced cAMP Production and Sensitization of Sensory Neurons. *Journal of Biological Chemistry*, *276*(19), 16083–16091. https://doi.org/10.1074/jbc.M011408200

Starobova, H., A, H. S. W., Lewis, R. J., & Vetter, I. (2018). Transcriptomics in pain research: Insights from new and old technologies. *Molecular Omics*, *14*(6), 389–404. https://doi.org/10.1039/C8MO00181B

Stein, C., Clark, J. D., Oh, U., Vasko, M. R., Wilcox, G. L., Overland, A. C., Vanderah, T. W., & Spencer, R. H. (2009). Peripheral Mechanisms of Pain and Analgesia. *Brain Research Reviews*, *60*(1), 90–113. https://doi.org/10.1016/j.brainresrev.2008.12.017

Steward and Levy, B. (1981). BASE OF DENDRITIC SPINES IN GRANULE CELLS OF THE DENTATE GYRUSl. *The Journal of Neuroscience*, 8.

St-Jacques, B., & Ma, W. (2011). Role of prostaglandin E2 in the synthesis of the pro-inflammatory cytokine interleukin-6 in primary sensory neurons: An in vivo and in vitro study. *Journal of Neurochemistry*, *118*(5), 841–854. https://doi.org/10.1111/j.1471-4159.2011.07230.x

St-Jacques, B., & Ma, W. (2014). Peripheral prostaglandin E2 prolongs the sensitization of nociceptive dorsal root ganglion neurons possibly by facilitating the synthesis and anterograde axonal trafficking of EP4 receptors. *Experimental Neurology*, *261*, 354–366. https://doi.org/10.1016/j.expneurol.2014.05.028

Sugimoto, Y., & Narumiya, S. (2007). Prostaglandin E Receptors. *Journal of Biological Chemistry*, *282*(16), 11613–11617. https://doi.org/10.1074/jbc.R600038200

Sutton, M. A., & Schuman, E. M. (2005). Local translational control in dendrites and its role in long-term synaptic plasticity. *Journal of Neurobiology*, *64*(1), 116–131. https://doi.org/10.1002/neu.20152

Taliaferro, J. M., Vidaki, M., Oliveira, R., Olson, S., Zhan, L., Saxena, T., Wang, E. T., Graveley, B. R., Gertler, F. B., Swanson, M. S., & Burge, C. B. (2016). Distal Alternative Last Exons Localize mRNAs to Neural Projections. *Molecular Cell*, *61*(6), 821–833. https://doi.org/10.1016/j.molcel.2016.01.020

Tanabe, K., Bonilla, I., Winkles, J. A., & Strittmatter, S. M. (2003). Fibroblast Growth Factor-Inducible-14 Is Induced in Axotomized Neurons and Promotes Neurite Outgrowth. *The Journal of Neuroscience*, *23*(29), 9675–9686. https://doi.org/10.1523/JNEUROSCI.23-29-09675.2003

Tanaka, S., Imaeda, A., Matsumoto, K., Maeda, M., Obana, M., & Fujio, Y. (2020). B2-adrenergic stimulation induces interleukin-6 by increasing Arid5a, a stabilizer of mRNA, through cAMP/PKA/CREB pathway in cardiac fibroblasts. *Pharmacology Research & Perspectives*, *8*(2), e00590. https://doi.org/10.1002/prp2.590

Tavares-Ferreira, D., Ray, P. R., Sankaranarayanan, I., Mejia, G. L., Wangzhou, A., Shiers, S., Uttarkar, R., Megat, S., Barragan-Iglesias, P., Dussor, G., Akopian, A. N., & Price, T. J. (2022). Sex Differences in Nociceptor Translatomes Contribute to Divergent Prostaglandin Signaling in Male and Female Mice. *Biological Psychiatry*, *91*(1), 129–140. https://doi.org/10.1016/j.biopsych.2020.09.022

Tavares-Ferreira, D., Shiers, S., Ray, P. R., Wangzhou, A., Jeevakumar, V., Sankaranarayanan, I., Cervantes, A. M., Reese, J. C., Chamessian, A., Copits, B. A., Dougherty, P. M., Gereau, R. W., Burton, M. D., Dussor, G., & Price, T. J. (2022). Spatial transcriptomics of dorsal root ganglia identifies molecular signatures of human nociceptors. *Science Translational Medicine*, *14*(632), eabj8186. https://doi.org/10.1126/scitranslmed.abj8186

Taylor, A. M., Berchtold, N. C., Perreau, V. M., Tu, C. H., Li Jeon, N., & Cotman, C. W. (2009). Axonal mRNA in Uninjured and Regenerating Cortical Mammalian Axons. *The Journal of Neuroscience*, *29*(15), 4697–4707. https://doi.org/10.1523/JNEUROSCI.6130-08.2009

Taylor, A. M., Blurton-Jones, M., Rhee, S. W., Cribbs, D. H., Cotman, C. W., & Jeon, N. L. (2005). A microfluidic culture platform for CNS axonal injury, regeneration and transport. *Nature Methods*, *2*(8), 599–605. https://doi.org/10.1038/nmeth777

Tennyson, V. M. (1970). THE FINE STRUCTURE OF THE AXON AND GROWTH CONE OF THE DORSAL ROOT NEUROBLAST OF THE RABBIT EMBRYO. *The Journal of Cell Biology*, *44*(1), 62–79.

Terenzio, M., Koley, S., Samra, N., Rishal, I., Zhao, Q., Sahoo, P. K., Urisman, A., Marvaldi, L., Oses-Prieto, J. A., Forester, C., Gomes, C., Kalinski, A. L., Di Pizio, A., Doron-Mandel, E., Perry, R. B.-T., Koppel, I., Twiss, J. L., Burlingame, A. L., & Fainzilber, M. (2018). Locally translated mTOR controls axonal local translation in nerve injury. *Science (New York, N.Y.)*, *359*(6382), 1416–1421. https://doi.org/10.1126/science.aan1053

Thakur, M., Crow, M., Richards, N., Davey, G. I. J., Levine, E., Kelleher, J. H., Agley, C. C., Denk, F., Harridge, S. D. R., & McMahon, S. B. (2014). Defining the nociceptor transcriptome. *Frontiers in Molecular Neuroscience*, *7*. https://doi.org/10.3389/fnmol.2014.00087

The 3Rs | NC3Rs. (n.d.). Retrieved 17 January 2022, from https://www.nc3rs.org.uk/the-3rs

Thomas, D., Tovey, S. C., Collins, T. J., Bootman, M. D., Berridge, M. J., & Lipp, P. (2000). A comparison of fluorescent Ca2+indicator properties and their use in measuring elementary and global Ca2+signals. *Cell Calcium*, *28*(4), 213–223. https://doi.org/10.1054/ceca.2000.0152

Tóth, E. N., Lohith, A., Mondal, M., Guo, J., Fukamizu, A., & Pourmand, N. (2018). Single-cell nanobiopsy reveals compartmentalization of mRNAs within neuronal cells. *The Journal of Biological Chemistry*, *293*(13), 4940–4951. https://doi.org/10.1074/jbc.M117.800763

Toulme, E., Tsuda, M., Khakh, B. S., & Inoue, K. (2010). On the Role of ATP-Gated P2X Receptors in Acute, Inflammatory and Neuropathic Pain. In L. Kruger & A. R. Light (Eds.), *Translational Pain Research: From Mouse to Man*. CRC Press/Taylor & Francis. http://www.ncbi.nlm.nih.gov/books/NBK57271/

Touska, F., Marsakova, L., Teisinger, J., & Vlachova, V. (2011). A “Cute” Desensitization of TRPV1. *Current Pharmaceutical Biotechnology*, *12*(1), 122–129.

Tsantoulas, C., & McMahon, S. B. (2014). Opening paths to novel analgesics: The role of potassium channels in chronic pain. *Trends in Neurosciences*, *37*(3), 146–158. https://doi.org/10.1016/j.tins.2013.12.002

Ugarte, G. D., Diaz, E., Biscaia, M., Stehberg, J., Montecino, M., & van Zundert, B. (2013). Transcription of the pain-related TRPV1 gene requires Runx1 and C/EBPβ factors. *Journal of Cellular Physiology*, *228*(4), 860–870. https://doi.org/10.1002/jcp.24236

Ugarte, G. D., Opazo, T., Leisewitz, F., van Zundert, B., & Montecino, M. (2012). Runx1 and C/EBPβ transcription factors directly up-regulate P2X3 gene transcription. *Journal of Cellular Physiology*, *227*(4), 1645–1652. https://doi.org/10.1002/jcp.22882

Unsain, N., Heard, K. N., Higgins, J. M., & Barker, P. A. (2014). Production and Isolation of Axons from Sensory Neurons for Biochemical Analysis Using Porous Filters. *Journal of Visualized Experiments : JoVE*, *89*. https://doi.org/10.3791/51795

Usoskin, D., Furlan, A., Islam, S., Abdo, H., Lönnerberg, P., Lou, D., Hjerling-Leffler, J., Haeggström, J., Kharchenko, O., Kharchenko, P. V., Linnarsson, S., & Ernfors, P. (2015). Unbiased classification of sensory neuron types by large-scale single-cell RNA sequencing. *Nature Neuroscience*, *18*(1), 145–153. https://doi.org/10.1038/nn.3881

Uttam, S., Wong, C., Amorim, I. S., Jafarnejad, S. M., Tansley, S. N., Yang, J., Prager-Khoutorsky, M., Mogil, J. S., Gkogkas, C. G., & Khoutorsky, A. (2018). Translational profiling of dorsal root ganglia and spinal cord in a mouse model of neuropathic pain. *Neurobiology of Pain*, *4*, 35–44. https://doi.org/10.1016/j.ynpai.2018.04.001

Vagnoni, A., Perkinton, M. S., Gray, E. H., Francis, P. T., Noble, W., & Miller, C. C. J. (2012). Calsyntenin-1 mediates axonal transport of the amyloid precursor protein and regulates Aβ production. *Human Molecular Genetics*, *21*(13), 2845–2854. https://doi.org/10.1093/hmg/dds109

van Belle, T. L., Coppieters, K. T., & von Herrath, M. G. (2011). Type 1 diabetes: Etiology, immunology, and therapeutic strategies. *Physiological Reviews*, *91*(1), 79–118. https://doi.org/10.1152/physrev.00003.2010

Van Buren, J. J., Bhat, S., Rotello, R., Pauza, M. E., & Premkumar, L. S. (2005). Sensitization and translocation of TRPV1 by insulin and IGF-I. *Molecular Pain*, *1*, 17. https://doi.org/10.1186/1744-8069-1-17

Van den Berge, K., Hembach, K. M., Soneson, C., Tiberi, S., Clement, L., Love, M. I., Patro, R., & Robinson, M. D. (2019). RNA Sequencing Data: Hitchhiker’s

Guide to Expression Analysis. *Annual Review of Biomedical Data Science*, *2*(1), 139–173. https://doi.org/10.1146/annurev-biodatasci-072018-021255

Van Driesche, S. J., & Martin, K. C. (2018). New frontiers in RNA transport and local translation in neurons. *Developmental Neurobiology*, *78*(3), 331–339. https://doi.org/10.1002/dneu.22574

van Hecke, O., Austin, S. K., Khan, R. A., Smith, B. H., & Torrance, N. (2014). Neuropathic pain in the general population: A systematic review of epidemiological studies. *PAIN*, *155*(4), 654–662. https://doi.org/10.1016/j.pain.2013.11.013

Verma, P., Chierzi, S., Codd, A. M., Campbell, D. S., Meyer, R. L., Holt, C. E., & Fawcett, J. W. (2005). Axonal Protein Synthesis and Degradation Are Necessary for Efficient Growth Cone Regeneration. *The Journal of Neuroscience*, *25*(2), 331–342. https://doi.org/10.1523/JNEUROSCI.3073-04.2005

Vicario, A., Colliva, A., Ratti, A., Davidovic, L., Baj, G., Gricman, Ł., Colombrita, C., Pallavicini, A., Jones, K. R., Bardoni, B., & Tongiorgi, E. (2015). Dendritic targeting of short and long 3′ UTR BDNF mRNA is regulated by BDNF or NT-3 and distinct sets of RNA-binding proteins. *Frontiers in Molecular Neuroscience*, *8*. https://doi.org/10.3389/fnmol.2015.00062

Vincent, A. M., Mclean, L. L., Backus, C., & Feldman, E. L. (2005). Short-term hyperglycemia produces oxidative damage and apoptosis in neurons. *The FASEB Journal*, *19*(6), 638–640. https://doi.org/10.1096/fj.04-2513fje

Vogelaar, C. F., Gervasi, N. M., Gumy, L. F., Story, D. J., Raha-Chowdhury, R., Leung, K.-M., Holt, C. E., & Fawcett, J. W. (2009). Axonal mRNAs: Characterisation and role in the growth and regeneration of dorsal root ganglion axons and growth cones. *Molecular and Cellular Neurosciences*, *42*(2), 102–115. https://doi.org/10.1016/j.mcn.2009.06.002

von Kügelgen, N., & Chekulaeva, M. (2020). Conservation of a core neurite transcriptome across neuronal types and species. *WIREs RNA*, *11*(4), e1590. https://doi.org/10.1002/wrna.1590

Vuppalanchi, D., Willis, D. E., & Twiss, J. L. (2009). Regulation of mRNA Transport and Translation in Axons. In E. Koenig (Ed.), *Cell Biology of the Axon* (Vol. 48, pp. 293–304). Springer Berlin Heidelberg. https://doi.org/10.1007/400_2009_16

Vyklický, L., & Knotková-Urbancovä, H. (1996). Can sensory neurones in culture serve as a model of nociception? *Physiological Research*, *45*(1), 1–9.

Walters, J. N., Bickford, J. S., Newsom, K. J., Beachy, D. E., Barilovits, S. J., Herlihy, J.-D., & Nick, H. S. (2012). Regulation of human microsomal prostaglandin E synthase-1 by IL-1β requires a distal enhancer element with a unique role for C/EBPβ. *Biochemical Journal*, *443*(2), 561–571. https://doi.org/10.1042/BJ20111801

Wang, C., Li, G.-W., & Huang, L.-Y. M. (2007). Prostaglandin E2 potentiation of P2X3 receptor mediated currents in dorsal root ganglion neurons. *Molecular Pain*, *3*(1), 22. https://doi.org/10.1186/1744-8069-3-22

Wang, M., Xie, Z., Xu, J., & Feng, Z. (2020). TWEAK/Fn14 axis in respiratory diseases. *Clinica Chimica Acta*, *509*, 139–148. https://doi.org/10.1016/j.cca.2020.06.007

Wang, X., & Cairns, M. J. (2013). Gene set enrichment analysis of RNA-Seq data: Integrating differential expression and splicing. *BMC Bioinformatics*, *14*(Suppl 5), S16. https://doi.org/10.1186/1471-2105-14-S5-S16

Wang, Z., Gerstein, M., & Snyder, M. (2009). RNA-Seq: A revolutionary tool for transcriptomics. *Nature Reviews. Genetics*, *10*(1), 57–63. https://doi.org/10.1038/nrg2484

Wangzhou, A., McIlvried, L. A., Paige, C., Barragan-Iglesias, P., Shiers, S., Ahmad, A., Guzman, C. A., Dussor, G., Ray, P. R., Gereau, R. W., & Price, T. J. (2020). Pharmacological target-focused transcriptomic analysis of native versus cultured human and mouse dorsal root ganglia. *Pain*, *161*(7), 1497–1517. https://doi.org/10.1097/j.pain.0000000000001866

Watanabe, T., Ito, T., Inoue, G., Ohtori, S., Kitajo, K., Doya, H., Takahashi, K., & Yamashita, T. (2008). The p75 receptor is associated with inflammatory thermal hypersensitivity. *Journal of Neuroscience Research*, *86*(16), 3566–3574. https://doi.org/10.1002/jnr.21808

Wei, S., Qiu, C.-Y., Jin, Y., Liu, T.-T., & Hu, W.-P. (2021). TNF-α acutely enhances acid-sensing ion channel currents in rat dorsal root ganglion neurons via a p38 MAPK pathway. *Journal of Neuroinflammation*, *18*, 92. https://doi.org/10.1186/s12974-021-02151-w

Weng, X., Smith, T., Sathish, J., & Djouhri, L. (2012). Chronic inflammatory pain is associated with increased excitability and hyperpolarization-activated current (Ih) in C- but not Aδ-nociceptors. *PAIN*, *153*(4), 900–914. https://doi.org/10.1016/j.pain.2012.01.019

Willis, D. E., & Twiss, J. L. (2011). Profiling axonal mRNA transport. *Methods in Molecular Biology (Clifton, N.J.)*, *714*, 335–352. https://doi.org/10.1007/978-1-61779-005-8_21

Willis, D. E., van Niekerk, E. A., Sasaki, Y., Mesngon, M., Merianda, T. T., Williams, G. G., Kendall, M., Smith, D. S., Bassell, G. J., & Twiss, J. L. (2007). Extracellular stimuli specifically regulate localized levels of individual neuronal mRNAs. *Journal of Cell Biology*, *178*(6), 965–980. https://doi.org/10.1083/jcb.200703209

Wise, B. L., Seidel, M. F., & Lane, N. E. (2021). The evolution of nerve growth factor inhibition in clinical medicine. *Nature Reviews. Rheumatology*, *17*(1), 34–46. https://doi.org/10.1038/s41584-020-00528-4

Wong, C., Barkai, O., Wang, F., Pérez, C. T., Lev, S., Cai, W., Tansley, S., Yousefpour, N., Hooshmandi, M., Lister, K. C., Latif, M., Cuello, A. C., Prager-Khoutorsky, M., Mogil, J. S., Séguéla, P., Koninck, Y. D., Ribeiro-da-Silva, A., Binshtok, A. M., & Khoutorsky, A. (2022, May 17). *MTORC2 mediates structural plasticity in distal nociceptive endings that contributes to pain hypersensitivity following inflammation*. American Society for Clinical Investigation. https://doi.org/10.1172/JCI152635

Wood, J. N., Winter, J., James, I. F., Rang, H. P., Yeats, J., & Bevan, S. (1988). Capsaicin-induced ion fluxes in dorsal root ganglion cells in culture. *Journal of Neuroscience*, *8*(9), 3208–3220. https://doi.org/10.1523/JNEUROSCI.08-09-03208.1988

Wu, S., Marie Lutz, B., Miao, X., Liang, L., Mo, K., Chang, Y.-J., Du, P., Soteropoulos, P., Tian, B., Kaufman, A. G., Bekker, A., Hu, Y., & Tao, Y.-X. (2016). Dorsal root ganglion transcriptome analysis following peripheral nerve injury in mice. *Molecular Pain*, *12*, 1744806916629048. https://doi.org/10.1177/1744806916629048

Xing, H., Chen, M., Ling, J., Tan, W., & Gu, J. G. (2007). TRPM8 Mechanism of Cold Allodynia after Chronic Nerve Injury. *Journal of Neuroscience*, *27*(50), 13680–13690. https://doi.org/10.1523/JNEUROSCI.2203-07.2007

Xu, Q., & Yaksh, T. L. (2011). A brief comparison of the pathophysiology of inflammatory versus neuropathic pain. *Current Opinion in Anaesthesiology*, *24*(4), 400–407. https://doi.org/10.1097/ACO.0b013e32834871df

Xu, W.-D., Zhao, Y., & Liu, Y. (2016). Role of the TWEAK/Fn14 pathway in autoimmune diseases. *Immunologic Research*, *64*(1), 44–50. https://doi.org/10.1007/s12026-015-8761-y

Yam, M. F., Loh, Y. C., Tan, C. S., Khadijah Adam, S., Abdul Manan, N., & Basir, R. (2018). General Pathways of Pain Sensation and the Major Neurotransmitters Involved in Pain Regulation. *International Journal of Molecular Sciences*, *19*(8), 2164. https://doi.org/10.3390/ijms19082164

Yan, C., Cao, J., Wu, M., Zhang, W., Jiang, T., Yoshimura, A., & Gao, H. (2010). Suppressor of Cytokine Signaling 3 Inhibits LPS-induced IL-6 Expression in Osteoblasts by Suppressing CCAAT/Enhancer-binding Protein β Activity. *The Journal of Biological Chemistry*, *285*(48), 37227–37239. https://doi.org/10.1074/jbc.M110.132084

Yang, F., Sun, W., Luo, W.-J., Yang, Y., Yang, F., Wang, X.-L., & Chen, J. (2017). SDF1-CXCR4 Signaling Contributes to the Transition from Acute to Chronic Pain State. *Molecular Neurobiology*, *54*(4), 2763–2775. https://doi.org/10.1007/s12035-016-9875-5

Yang, F., & Zheng, J. (2014). High temperature sensitivity is intrinsic to voltage-gated potassium channels. *ELife*, *3*, e03255. https://doi.org/10.7554/eLife.03255

Yepes, M. (2007). TWEAK and the Central Nervous System. *Molecular Neurobiology*, *35*(3), 255–265. https://doi.org/10.1007/s12035-007-0024-z

Yin, K., Deuis, J. R., Lewis, R. J., & Vetter, I. (2016). Transcriptomic and behavioural characterisation of a mouse model of burn pain identify the cholecystokinin 2 receptor as an analgesic target. *Molecular Pain*, *12*, 1744806916665366. https://doi.org/10.1177/1744806916665366

Zappulo, A., van den Bruck, D., Ciolli Mattioli, C., Franke, V., Imami, K., McShane, E., Moreno-Estelles, M., Calviello, L., Filipchyk, A., Peguero-Sanchez, E., Müller, T., Woehler, A., Birchmeier, C., Merino, E., Rajewsky, N., Ohler, U., Mazzoni, E. O., Selbach, M., Akalin, A., & Chekulaeva, M. (2017). RNA localization is a key determinant of neurite-enriched proteome. *Nature Communications*, *8*, 583. https://doi.org/10.1038/s41467-017-00690-6

Zeisel, A., Hochgerner, H., Lönnerberg, P., Johnsson, A., Memic, F., van der Zwan, J., Häring, M., Braun, E., Borm, L. E., La Manno, G., Codeluppi, S., Furlan, A., Lee, K., Skene, N., Harris, K. D., Hjerling-Leffler, J., Arenas, E., Ernfors, P., Marklund, U., & Linnarsson, S. (2018). Molecular Architecture of the Mouse Nervous System. *Cell*, *174*(4), 999-1014.e22. https://doi.org/10.1016/j.cell.2018.06.021

Zhang, F., Wang, H., Zhou, Y., Yu, H., Zhang, M., Du, X., Wang, D., Zhang, F., Xu, Y., Zhang, J., & Zhang, H.-T. (2022). Inhibition of phosphodiesterase-4 in the spinal dorsal horn ameliorates neuropathic pain via cAMP-cytokine-Cx43 signaling in mice. *CNS Neuroscience & Therapeutics*, *28*(5), 749–760. https://doi.org/10.1111/cns.13807

Zhang, J.-M., & An, J. (2007). Cytokines, Inflammation and Pain. *International Anesthesiology Clinics*, *45*(2), 27–37. https://doi.org/10.1097/AIA.0b013e318034194e

Zhang, M., Wang, Y., Geng, J., Zhou, S., & Xiao, B. (2019). Mechanically Activated Piezo Channels Mediate Touch and Suppress Acute Mechanical Pain Response in Mice. *Cell Reports*, *26*(6), 1419-1431.e4. https://doi.org/10.1016/j.celrep.2019.01.056

Zhao, E. Y., Jones, M., & Jones, S. J. M. (2019). Whole-Genome Sequencing in Cancer. *Cold Spring Harbor Perspectives in Medicine*, *9*(3), a034579. https://doi.org/10.1101/cshperspect.a034579

Zheng, J.-Q., Kelly, T. K., Chang, B., Ryazantsev, S., Rajasekaran, A. K., Martin, K. C., & Twiss, J. L. (2001). A Functional Role for Intra-Axonal Protein Synthesis during Axonal Regeneration from Adult Sensory Neurons. *Journal of Neuroscience*, *21*(23), 9291–9303. https://doi.org/10.1523/JNEUROSCI.21-23-09291.2001

Zheng, Y., Liu, P., Bai, L., Trimmer, J. S., Bean, B. P., & Ginty, D. D. (2019). Deep sequencing of somatosensory neurons reveals molecular determinants of

intrinsic physiological properties. *Neuron*, *103*(4), 598-616.e7. https://doi.org/10.1016/j.neuron.2019.05.039